UNIVERSITY OF MILANO-BICOCCA

DOCTORATE SCHOOL

Cerebral Collateral Circulation in Experimental Ischemic Stroke: From Molecular Penumbra to Collateral Therapeutics

PhD Student:

Elisa CUCCIONE

Matr. 701836

Supervisor:

Prof. Carlo FERRARESE

Co-Supervisor:

Dr. Simone BERETTA

Laboratory of Experimental Stroke Research

Department of Surgery and Translational Medicine

PhD Program in Neuroscience - Cycle XXVIII

Coordinator: Prof. Guido CAVALETTI

Academic Year 2014-2015

Abstract

Cerebral Collateral Circulation in Experimental Ischemic Stroke: From Molecular Penumbra to Collateral Therapeutics

Collateral circulation is a subsidiary vascular network which is dynamically recruited after acute ischemic stroke and may provide residual blood flow to the affected areas, slowing down the progression of ischemic penumbra to irreversible ischemic damage. The anatomy and functional performance of the collateral circulation varies among individuals, both humans and rodents, and is emerging as a strong prognostic factor in patients. Nonetheless, collateral circulation in experimental ischemic stroke is frequently neglected. In the present work, ischemic stroke was modelled by 90-minutes transient occlusion of the middle cerebral artery (MCA) in Wistar rats, followed by 24 hours of reperfusion. During surgery, multi-site laser Doppler flowmetry (LDF) was used for real-time monitoring of cerebral blood flow (CBF) both in the lateral MCA territory and in the borderzone between the MCA and anterior cerebral artery (ACA) territories, where the collateral circulation is connecting these two different vascular territories.

The relationship between collateral flow, evaluated by multi-site LDF in the collaterals territory, and the post-reperfusion molecular penumbra, defined by protein expression of Heat Shock Protein 70kDa (HSP70), was investigated. Good collateral flow was associated with reduced extent of both molecular penumbra and ischemic core and increased extent of intact tissue, suggesting a complete protection from ischemic injury in variable areas of the cortex and striatum, if reperfusion is achieved. Conversely, poor collateral status was associated with a greater extent of both ischemic core and molecular penumbra.

High variability in infarct size is common in experimental stroke models and highly affects statistical power and validity of preclinical neuroprotection trials. Cerebral collateral flow was explored as a stratification factor for the prediction of ischemic outcome, using magnetic resonance imaging (MRI) as a reference. Multi-site LDF monitoring for collateral flow assessment was able to predict ischemic outcome and infarct typology and reflected perfusion deficit in good agreement with acute MRI. These results support the additional value of cerebral collateral flow monitoring for outcome prediction in experimental ischemic stroke, especially when acute MRI facilities are not available.

Modulating collateral blood flow in order to augment or maintain perfusion to the ischemic penumbra could represent a new therapeutic strategy for the hyperacute (even pre-hospital) phase, particularly if

applied before recanalization therapies. Four therapeutic strategies were subministated 30 minutes after ischemia onset: acetazolamide (selective cerebral vasodilation), polygeline (intravascular volume load), phenylephrine (induced hypertension) and head-down tilt (cerebral flow diversion). Globally, the treated animals showed better tissue and functional outcomes at 24 hours post reperfusion and an augmentation of cerebral perfusion, mainly in the collaterals territory, after treatment subministration. These results prompt further study of strategies aiming at modulating the cerebral collateral circulation.

In conclusion, the cerebral collateral circulation and its functional performance determined both ischemic outcome and penumbra evaluated at 24 hours post-reperfusion in the experimental model considered. Monitoring collateral flow by multi-site LDF predicts ischemic outcome and allows for animals stratification, helping to control experimental ischemic outcome variability in neuroprotection studies. Moreover, monitoring collateral flow while testing therapeutic strategies provides insight about their mechanism of action and may contribute to the development of new therapeutic strategies for the hyper-acute phase of ischemic stroke.

Contents

List of Figures

List of Tables

Abbreviations

ACA	**A**nterior **C**erebral **A**rtery
AComA	**A**nterior **Com**municating **A**rtery
APAF-1	**A**poptotic **P**rotease **A**ctivating **F**actor**-1**
ADC	**A**pparent **D**iffusion **C**oefficient
AMPA	alpha-**A**mino-3-hydroxy-5-**M**ethyl-isoxazole**P**ropionic **A**cid
ASL	**A**rterial **S**pin **L**abeling
ATP	**A**denosine **T**ri**P**hosphate
BBB	**B**lood **B**rain **B**arrier
BT	**B**asilar **A**rtery
CBF	**C**erebral **B**lood **F**low
CBV	**C**erebral **B**lood **V**olume
CCA	**C**ommon **C**arotid **A**rtery
CCA	**C**ommon **C**arotid **A**rtery **O**cclusion
CMRO$_2$	**C**erebral **M**etabolism **R**ate of **O**xygen
CT	**C**omputer **T**omography
CTA	**C**omputer **T**omography **A**giography
CTP	**C**omputer **T**omography **P**erfusion
DAB	3,30-**D**i**A**amino**B**enzidine tetra hydrochloride
DALYs	**D**isability-**A**djusted **L**ife-**Y**ears
DPX	**D**ibutyl **P**hthalate **X**ylene
DSC	**D**ynamic **S**usceptibility **C**ontrast
DWI	**D**iffusion **W**eighted **I**maging
ECA	**E**xternal **C**arotid **A**rtery
eNOS	**e**ndotelial **N**itric **O**xide **S**ynthase
EPI	**E**cho **P**lanar **I**maging

ER	**E**ndoplasmic **R**eticulum
ET-1	**E**ndo**T**helin**-1**
FDA	**F**ood and **D**rug **A**dministration
FLAIR	**FL**uid **A**ttenuated **I**nversion **R**ecovery
FOV	**F**ield **O**f **V**iew
GABA	**G**amma-**A**mino**B**utyric **A**acid
G-SCF	**G**ranulocyte-**C**olony **S**timulating **F**actor
GM-SCF	**G**ranulocyte-**M**acrophage **C**olony **S**timulating **F**actor
IF	**G**radient **E**cho
H&E	**H**ematoxylin **&** **E**osin
HIF-1	**H**ypoxia **I**nducible **F**actor**-1**
HSP70	**H**eat **S**hock **P**rotein **70** (kDa)
5HT1D	**5**-**H**ydroxy**T**ryptamine**1D** receptor
ICA	**I**nternal **C**arotid **A**rtery
ICAM	**I**nter**C**ellular **A**dhesion **M**olecule-1
IF	**I**mmuno**F**luorescence
IgG	**I**mmuno**G**lobuline **G**
IHC	**I**mmuno- **H**isto- **C**hemistry
IL-1β	**I**nter**L**eukin**-1**β
LDF	**L**aser **D**oppler **F**lowmetry
LMAs	**L**epto**M**eningeal **A**nastomoses
LSCI	**L**aser **S**peckle **C**ontrast **I**maging
MAP	**M**ean **A**rterial **P**ressure
MCA	**M**iddle **C**erebral **A**rtery
MCAO	**M**iddle **C**erebral **A**rtery **O**cclusion
MCP-1	**M**onocyte **C**hemoattractant **P**rotein**-1**
MRI	**M**agnetic **R**esonance **A**ngiography
MRI	**M**agnetic **R**esonance **I**maging
MTT	**M**ean **T**ransit **T**ime
NGS	**N**ormal **G**oat **S**erum
NeuN	**Neu**ronal **N**uclei
NMDA	**N**-**M**ethyl-**D**-**A**spartate
NO	**N**itric **O**xide

OEF	**O**xygen **E**xtraction **F**raction
PAF	**P**latelet **A**ctivating **F**actor
PBS	**P**hosphate-**B**uffered **S**aline
PET	**P**ositron **E**mission **T**omography
PID	**P**eri-**I**nfarct **D**epolarization
PPA	**P**terigo**P**alatine **A**rtery
PCA	**P**osterior **C**erebral **A**rtery
PComA	**P**osterior **Com**municating **A**rtery
PWI	**P**erfusion **W**eighted **I**maging
ROI	**R**egion **O**f **I**nterest
RT	**R**oom **T**emperature
rtPA	**r**ecombinant **t**issue **P**lasminogen **A**ctivator
SAH	**S**ub**A**rachnoid **H**aemorrhage
SD	**S**tandard **D**eviation
SHR	**S**pontaneuos **H**ypertensive **R**at
spSHR	**s**troke **p**rone **S**pontaneuos **H**ypertensive **R**at
SPG	**S**pheno**P**alatine **G**anglion
TE	**E**cho **T**ime
TCD	**T**rans **C**ranial **D**oppler Ultrasonography
TNFα	**T**umour **N**ecrosis **F**actor α
TPLSM	**T**wo-**P**hoton **L**aser **S**canning **M**icroscopy
TR	**R**epetition **T**ime
TUNEL	**T**dT-mediated d**U**TP **N**ick-**E**nd **L**abeling
TTC	2,3,5-**T**riphenyl **T**etrazolium **C**hloride
TTP	**T**ime **T**o **P**eak
VCAM-1	**V**ascular **C**ell **A**dhesion **M**olecule-**1**
VEGF	**V**ascular **E**ndothelial **G**rowth **F**actor
WHO	**W**orld **H**ealth **O**rganization

Ai miei genitori

Chapter 1

Introduction

1.1 Ischemic Stroke: The Pathology

1.1.1 Stroke: an Overview

Definition

Stroke is defined by the World Health Organization (WHO) as a rapid and progressive development of neurological symptoms associated with a focal or global loss of cerebral function, originating from a cerebral vasculopathy and persisting beyond 24 hours or leading to fatal outcome.

The arbitratry 24 hours time window allows for distinction between stroke and transient ischemic attack, in which the neurological symptoms resolve within the 24 hours (Donnan *et al.*, 2008). However, TIA presents a high risk of subsequent stroke (Giles and Rothwell, 2007).

Epidemiology

Stroke is a common neurological disorder, representing a social and economical burden, as the second most common cause of death (Lozano *et al.*, 2012) and third most common cause of stroke disability-adjusted life-years (DALYs) (Murray *et al.*, 2012) worldwide in 2010. In addition, although age-standardized stroke mortality rates have decreased worldwide, the absolute number of people who have a stroke every year and stroke survivors are increasing, together with the global burden of stroke (Feigin *et al.*, 2014).

Risk Factors

Several factors play a role in risk for stroke. The INTERSTROKE study identified 10 potentially modifiable risk factors explaining 90% of the risk of stroke (O'Donnell *et al.*, 2010). Risk factors

can be non modifiable, well-documented and modifiable or less well-documented and potentially modifiable (Meschia *et al.*, 2014).

The major unmodifiable risk factor for stroke is represented by increasing age. The combined risk of fatal and non fatal stroke resulted increased by 9%/year and 10%/year in men and women, respectively, in a study including data from 8 European countries (Asplund *et al.*, 2009). Hypertension represents the most important modifiable risk factor: its treatment is among the most effective prevention strategies for stroke. Other modifiable factors are represented by diabetes mellitus and dyslipidemia, together with lifestyle factors, including diet and nutrition, cigarette smoking and excessive alcohol consumption.

1.1.2 Etiology and Classification

The reduction in cerebral blood flow causing neurological symptoms is due to hemorrhage or abrupt occlusion of a vessel providing flow to the brain. We talk about hemorrhagic and ischemic stroke, respectively. Ischemic stroke represents the majority of stroke cases, accounting for 80% of them, while the less common hemorrhagic stroke represents the remaining 20% (Figure 1.1, Warlow *et al.* (2003)).

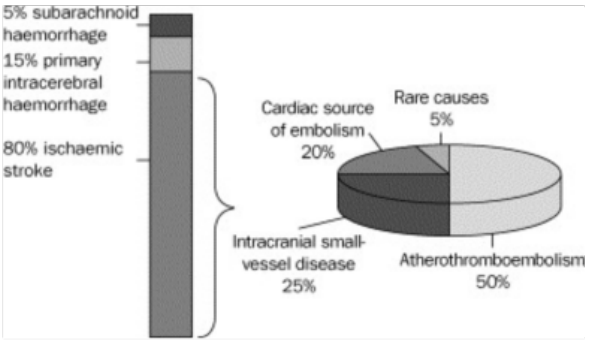

Figure 1.1: Approximate frequency of three main pathological types of stroke (in Caucasian populations) and of the main subtypes of ischemic stroke. Reproduced from Warlow *et al.* (2003)

1.1.2.1 Hemorrhagic Stroke

Hemorrhagic stroke can arise as a consequence of primary intracranial hemorrhage or subarachnoid hemorrhage. Hemorrhagic stroke caused by primary intracranial hemorrhage are more common,

representing the 15% of the main types of stroke, whereas a 5% of them is associated to subarachnoid hemorrhage (Figure 1.1, Warlow *et al.* (2003)).

Hemorragic stroke incidence is strongly correlated with hypertension. Hypertensive small-vessel disease represents the most common mechanism for hemorragic stroke, caused by the formation and subsequent rupture of small lipohyalinotic aneurysms (Auer and Sutherland, 2005). Hypertension is seen in two thirds of patients presenting with primary cerebral hemorrhage (Thrift *et al.*, 1995). Other causes of cerebral hemorrhage include intracranial vascular malformation and cerebral amyloid angiopathy, together with the development of secondary hemorrhage due to hemorrhagic transformation of ischemia. Subarachnoid hemorrhage is a bleeding in the subarachnoid space, which is situated between the arachnoid and pia mater meningeal layers, caused by the rupture of an aneurysm.

1.1.2.2 Ischemic Stroke

Ischemic stroke results from an abrupt occlusion of a cerebral artery, which leads to ischemia of the cerebral parenchyma. Neurological symptoms related to this stroke typology are strongly variable, reflecting the general heterogeneity characterizing this pathology. To start, different mechanisms can lead to ischemic stroke (Figure 1.1, Warlow *et al.* (2003)).

Modifications in the vessel wall can cause obstruction of blood flow by interacting with blood constituents. This may cause formation of a blood clot (thrombus) and consequent blockade of blood flow in the vessel itself. The main cause of vessel wall changing is the formation and presence of atherosclerotic plaques, which can change morphologically and finally lead to narrowing of the vascular lumen. In unstable plaques, the endothelial disruption causes platelets to affix to the plaque, leading to thrombus formation and lumen occlusion. In this case, we talk about *thrombotic* stroke. Atherothrombotic disease of the extra or intracranial vessels represent the cause of 50% of ischemic strokes, although the large intracranial vessels are less commonly the source of the thrombus.

A stroke is otherwise defined as *embolic* when an a moving intravascular mass (i.e. embolous), such as a blod clot, travels from where it originated to a different site, where it causes vascular occlusion. Cardiac embolism accounts for 20% of ischemic strokes, most commonly arising from atrial fibrillation.

Lacunar strokes represent instead the 25% of ischemic stroke subtypes and arise as a result of the occlusion of small intracranial arterioles. The remaining 5% of ischemic stroke are associated with several rare causes, such as vasculitis and arterial dissection.

A clinical classification divides ischemic stroke into 5 main groups, relying on their etiology (TOAST classification) (Adams *et al.*, 1993):

1. Large artery atherosclerosis
2. Cardiac embolus
3. Small vessel occlusion
4. Stroke of other determined etiology
5. Stroke of undetermined etiology

As mentioned before, ischemic stroke is a pathology characterized by a strong heterogeneity. The neurological symptoms exhibited by the patients are strongly variable and reflect the specific brain region affected by ischemia. Beyond the different the mechanisms of arterial occlusion, the location and size of the ischemic lesion in the brain parenchyma are determined by the size of the occluded vessel (occlusion level) and the compensatory capacity of the cerebral subsidiary vascular network, known as *cerebral collateral circulation*. To better explain, the occlusion of an artery supplying a defined brain region (such as the middle cerebral artery, MCA) can lead to an infarction of variable extension: if the artery is proximally occluded, the infarct might be large and include the whole territory supplied by the cerebral artery; infarct might instead be smaller, in case the vessel occlusion affects only branch of the cerebral artery (distal occlusion) or if compensatory collateral perfusion -via the Circle of Willis or leptomeningeal anastomoses- is efficient in reducing the area of critically reduced blood flow. The collateral circulation represent the core of this thesis and is extensively addressed in Section 1.2.

1.1.3 Pathophysiology of Ischemic Stroke: the Ischemic Cascade

Regardless of the etiological mechanism, the common event in ischemic stroke is the permanent or transient reduction of cerebral blood flow in the vascular territory of the occluded cerebral artery.

Because of the inability of cerebral cells to store energy supplies, the brain is constantly demanding for oxygen and glucose delivery via blood flow. When the normal cerebral blood flow is reduced as a result of the arterial occlusion, the cellular energy production via oxidative phosphorylation and, consequently, all the energy-dependent process of the neurovascular unit are compromised. The

neurovascular unit consists of neuronal, glial and vascular cell types, which interaction contributes to normal brain function.

However, in focal ischemic stroke, the reduction in the vascular territory affected is not uniform and results in a spatial gradient of hypoperfusion. Cerebral regions suffering the most severe hypoperfusion progress most rapidly to irreversible damage, while other regions with more modest blood flow reductions may become infarcted at later time points. The areas which are irreversibly damaged are referred to as *ischemic core*, while the remaining hypoperfused areas, which can be potentially saved if blood flow is timely restored, are defined as *ischemic penumbra* (see §1.1.4).

Vascular occlusion triggers a succession of ionic, biochemical and cellular pathophysiological events, ultimately leading to irreversible tissue damage, which are referred to as '*ischemic cascade*' (for detailed reviews see Dirnagl *et al.* (1999); Moskowitz *et al.* (2010)). These pathophysiological processes include primary pathogenic mechanisms, such as energy failure, anoxic depolarization, increased intracellular calcium and related events, and secondary pathogenic mechanisms, such as peri-infarct depolarisations, inflammation and apoptosis. An overview of the ischemic cascade and the evolution of the pathophysiological mechanisms over time are illustrated in Figure 1.2 and 1.3, respectively.

Energy Failure and Anoxic Depolarization

The reduction in blood flow results in a severe reduction of oxygen and glucose delivery to the neurovascular unit. Cells are therefore unable to produce energy via oxidative phosphorylation and, as a result, the energy-dependent processes together with the neuronal electrical activity are compromised. ATP levels are reduced and neurons are consequently unable to maintain their normal resting membrane potential, since adenosine triphosphate (ATP) is required for the Na^+/K^+ ATPase to function and preserve a high intracellular concentration of K^+ and low intracellular concentration of Na^+. Inactivity of the pump allows intracellular Na^+ levels to rise, leading to depolarization of the membrane potential. This in turn triggers the opening of voltage-gated calcium channels and the reversal of the Na^+/Ca^{2+} exchanger, leading to a a massive Ca^{2+} influx into the cell and its accumulation. Consequently, aminoacids such as excitatory neurotransmitters are released from the active zone of the pre-synaptic region into the synaptic cleft via calcium-mediated exocytosis. The major neurotransmitter of the central nervous system is glutamate, and a pathological lack of balance in its release and up-take in the intersynaptic space largely contributes to excitotoxic events.

Excitotoxicity

In normal conditions, energy-dependent processes remove glutamate from the extracellular space and

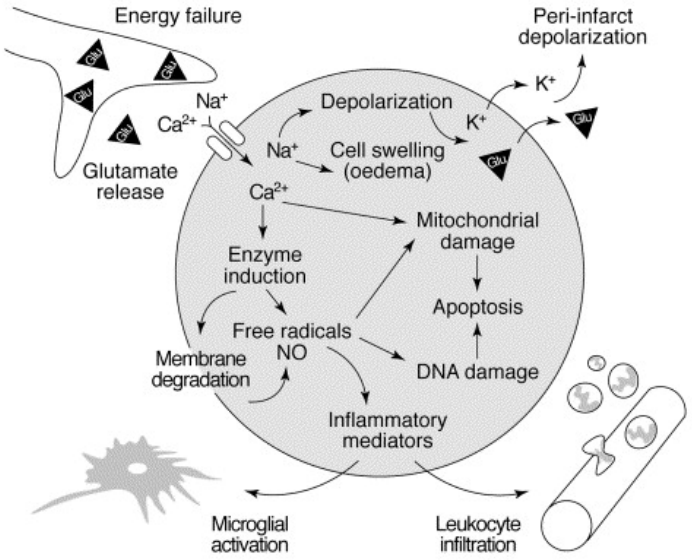

Figure 1.2: Overview of pathophysiological mechanisms during cerebral focal ischemia. The oxygen and glucose deprivation lead to energy failure, causing anoxic depolarization of neurons. Activation of specific glutamate receptors increases intracellular Ca^{2+}, Na^{+}, Cl^{-} levels whereas K^{+} is released into the extracellular space. Diffusion of glutamate (Glu) and K^{+} in the extracellular space causes a series of spreading waves of depolarization (peri-infarct depolarizations). Osmotic gradients make water enter the cell passively, causing cellular swelling (edema). The second messenger Ca^{2+} overactivates numerous enzyme pathways (proteases, lipases, endonucleases, etc.). Free radicals are generated, which damage membranes (lipolysis), mitochondria and DNA, in turn triggering caspase-mediated cell death (apoptosis). Free radicals also induce the formation of inflammatory mediators, which activate microglia and lead to the leukocyte infiltration via upregulation of endothelial adhesion molecules. Reproduced from Dirnagl *et al.* (1999).

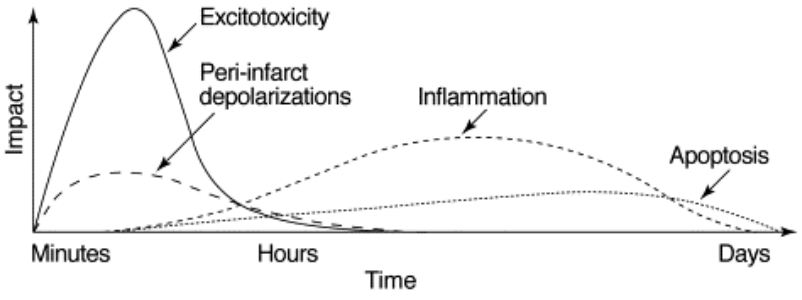

Figure 1.3: Pathophysiological mechanisms in focal cerebral ischemia: evolution of time and impact on final oucome. Excitotoxicity strongly damages neuronal and glial cells very early after ischemia onset. Secondary effects further contribute to tissue damage: peri-infarct depolarizations and the more-delayed mechanisms of inflammation and apoptosis. On the x-axis, the evolution of these events over time is represented, while the y-axis illustrate the impact of each mechanism on final outcome. Reproduced from Dirnagl *et al.* (1999).

store it in the synaptic terminal. Because of energy failure, the glutamate up-take is compromised and therefore this excitatory aminoacid accumulates in the extracellular space, leading to an increased activation of postsynaptic glutamate receptors. The activation of ionotropic receptors such as alpha-amino-3-hydroxy-5-methyl-4-isoxazolepropionate (AMPA) and Kainate lead to the influx of Na^+ and Cl^- and efflux of K^+, causing a local depolarization which in turn displaces the voltage-dependent magnesium block from another class of ionotropic receptors, the N-methyl-D-aspartate (NMDA), which allow entry of Na^+ and Ca^{2+} and the efflux of K^+. As a result, water enters passively the cell leading to *cytotoxic edema* and, ultimately, cellular lysis. Cerebral edema may affect the perfusion of the regions surrounding the infarct and also cause a rise in intracranial pressure, vascular compression and herniation. Metabotropic glutamate receptor are also activated leading in turn to activation of Phospholipase C and a signaling cascade which ultimately leads to a further stimulation of voltage-gated Ca^{2+} channels and the release into the cytosol of Ca^{2+} stored in the endoplasmic reticulum (ER), which represent the major source of Ca^{2+} in physiologic conditions. Moreover, re-storage of Ca^{2+} in ER lumen is reduced since it is an energy-dependent process.

Ca^{2+} Activation of The Ischemic Cascade

It is evident that multiple pathways are causing a rise in cytosolic Ca^{2+}, which triggers a cascade of events leading to cell damage. A variety of enzymes, including endonucleases as well as proteases and lipases are activated. These enzymes damage cell structures such as cytoskeleton, mitochondria, ER, plasma membrane, DNA and RNA, consequently affecting cellular function. Additionally, free radicals, including nitric oxide (NO), are produced and cause further cellular structures damage, ultimately leading to cell death. Free radicals also act as signalling molecules to induce an inflammatory response and trigger apoptosis (Brouns and De Deyn, 2009).

Spreading Depolarizations

While in the ischemic core cells are permanently depolarized, in less severely hypoperfused regions cells can still repolarize at expense of further energy and oxygen consumption, to compensate for the reduced blood flow. After repolarization, these cells can again depolarize in response to high glutamate and K^+ extracellular levels. Repetitive depolarizations are termed peri-infarct depolarizations (PID) and have been shown to occur spontaneously over several days after stroke both in preclinical models (Hartings *et al.*, 2003) and patients (Dohmen *et al.*, 2008). These events can contribute to the growth of the infarct with time. In a rat MCA occlusion (MCAO) model, a higher PID frequency was associated with a greater number of penumbral cells to become incorporated into the ischemic core (Mies *et al.*, 1993). Delayed ischemic brain damage was associated with PID in stroke patients

(Dreier *et al.*, 2006).

Inflammatory Response

The synthesis of transcription factors, like NFκB and hypoxia inducible factor 1 (HIF1), which promote expression of pro-inflammatory genes to produce inflammatory mediators like tumour necrosis factor α (TNFα), interleukin-1β (IL-1β) and platelet activating factor (PAF) is triggered by free radicals and Ca^{2+} mediated pathways, among other factors. These mediators induces cell surface expression of adhesion molecules like intercellular adhesion molecule 1 (ICAM-1), vascular cell adhesion molecule 1 (VCAM-1) and E-selectin, which interact with complementary receptors located on the surface of neutrophils, allowing their passage across the blood-brain barrier (BBB). Macrophages and monocytes migrate to the brain guided by chemokine signals produced by cells in the lesion region. Microglia also becomes activated, assumes an ameboid appearance, proliferates and produces both neurotoxic and neuroprotective substances. Microglia is attracted in the lesion site by monocyte chemoattractant protein 1 (MCP-1), which is activated by plasmin following opening of the BBB due to death of endothelial cells in response to ischemia. This whole inflammatory response after ischemia can further contribute to cell damage by different mechanisms: by direct toxin production, via microvascular obstruction by neutrophils (del Zoppo *et al.*, 1991) and also by induction of apoptotic pathways (Chopp *et al.*, 1996).

Cell death

Cell death may occur either by necrosis or by apoptosis, depending on the strength of the insult and the cell type (Leist and Nicotera, 1998). In the ischemic core, where perfusion is most severely affected and tissue is irreversibly damaged, cell death occurs by *necrosis* and is accompanied by the release of glutamate and toxic mediators into the extracellular space, affecting surrounding cells (Brouns and De Deyn, 2009).

In contrast, *apoptotis* is occurring in less severely damaged cells, since it is a programmed and energy-dependent process (Dirnagl *et al.*, 1999). Apoptosis is responsible for delayed death of cells that could have been potentially saved in the hyperacute phase and is therefore responsible for late lesion expansion. Apoptosis can either be caspase dependent or independent (Broughton *et al.*, 2009). The former pathway is mediated by the release of cytochrome c from the mitochondrial intermembrane space into the cytosol, due to mitochondrial dysfunction and free radicals production. Cytochrome c interacts and combine with apoptotic protease activating factor-1 (APAF-1) and pro-caspase 9, forming an apoptosome complex which in turn activates a cascade of endonucleases and caspases, which cleave DNA and structural and cellular proteins, respectively. Effector caspase 3 activation is known as one

of the critical steps in apoptosis execution. Caspase independent apoptosis is in contrast triggered by the release of apoptosis inducing factor (AIF) from the inner mitochondrial membrane, which induces DNA degradation in the nucleus. Apoptosis can also be extrinsically triggered by the activation of death receptors on the cell surface. Initiator caspase 8 is this way activated and, in turn, activates effector caspase 3 (Broughton *et al.*, 2009).

All of these pathophysiological mechanisms ultimately leading to cerebral tissue damage evolve in both time and space after the onset of ischemia. The evolution and growth of the ischemic lesion will depend on several factors, including the severity of the cerebral blood flow reduction, its duration and also the extent of collateral perfusion provided during occlusion.

1.1.4 The Ischemic Penumbra: Definition and Multi-modal Identification

1.1.4.1 Ischemic Core and Penumbra

As mentioned above, focal ischemic stroke causes a not uniform blood flow reduction in the affected vascular territory, which results in a spatial gradient of hypoperfusion. For this reason, the pathogenic mechanisms do not occur homogeneously in the hypoperfused regions. The most severly hypoperfused areas are defined as the *ischemic core*, where the ischemic cascade will rapidly lead to irreversible tissue damage. Other regions with more modest blood flow reductions may become infarcted at later time points and are referred to as the *ischemic penumbra*.

The concept of ischemic penumbra dates back to 1970s, when the group of Lyndsay Symon performed electrophysiological experiments to study the consequences of progressive reduction of cerebral blood flow (CBF) in baboons undergoing focal ischemia (Astrup *et al.*, 1977; Branston *et al.*, 1977, 1974; Symon *et al.*, 1977). The reduction in CBF required to abolish electrical activity and ion impairment, leading to cell death, were studied. In 1977, Astrup and colleagues (Astrup *et al.*, 1977) demonstrated that a CBF reduction to around 40% of the original level produced electrical dysfunction, measured by evoked somatosensory potentials. Electrical failure became complete when CBF was reduced around 30%, whereas release of potassium, with subsequent cell death, occurred at reduction to 10% (Figure1.4). Importantly, they showed that reperfusion restored electrical function and thus demonstrated the potentially salvageable nature of the ischemic penumbra as electrically silent tissue.

More generally, different tissue compartments during focal ischemia could be defined:

1. *oligemia*: brain areas characterized by a reduced CBF but preserved electrical activity (evoked cortical potentials);

2. *ischemic penumbra*: brain areas characterized by a reduced CBF (<20mL/100g/min) but electrical disfunction or inactivity;

3. *ischemic core*, where CBF is reduced around 8-10mL/100g/min and potassium is released, leading to cellular death.

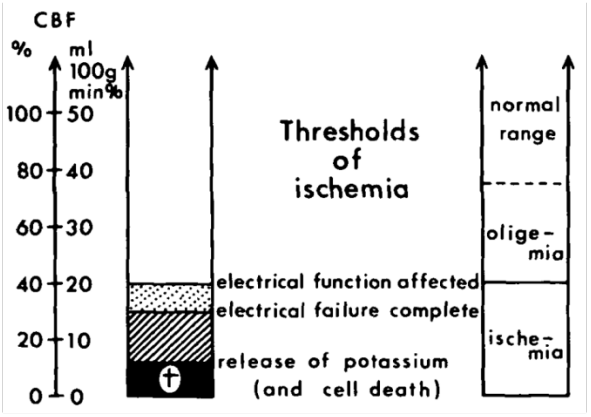

Figure 1.4: Different cerebral blood flow threshold in a baboon model of cerebral focal ischemia. Repreduced from Astrup *et al.* (1977).

Several operational definitions of ischemic penumbra have been proposed over the years (Donnan *et al.*, 2007), as a result of the different methodologies used for its assessment and especially with the emergence of neuroimaging techniques. However, the main thrust of penumbra's concept is preserved. In this regard, many of the proposed definitions are encompassed by the following (Donnan *et al.*, 2007):

> "The ischemic penumbra is ischemic tissue which is functionally impaired and is at risk of infarction but has the potential to be salvaged by reperfusion and/or other strategies. If not salvaged this tissue is progressively recruited into the infarct core, which will expand with time into the maximal volume originally at risk."

The identification of the ischemic penumbra is of utmost importance, both in clinical and preclinical settings, since therapeutic strategies for acute ischemic stroke aim at preserving this potentially salvageable areas from evolving into irreversibly ischemic damage (see §1.1.5). From a clinical point of view, assessing the presence of an extended ischemic penumbra in acute ischemic stroke patients

can be used to identify and select those who may benefit from thrombolytic therapy. In clinical trials, patients may be stratified into groups with homogenous penumbra extension and location, allowing for a the evaluation of a therapy in comparable groups of patients. In experimental stroke, the assessment of the ischemic penumbra would provide insights into the its evolution and the efficacy of a neuroprotective therapy.

The ischemic penumbra can be visualized using different imaging techniques, such as Positron Emission Tomography (PET), Magnetic Resonance Imaging (MRI) and Computerized Tomography (CT) (Ebinger *et al.*, 2009). Although PET is considered as the "gold standard" for the penumbra imaging, its clinical use is currently limited to research. MRI is instead becoming the method of choice for the evaluation of the penumbra in clinical research. Nonetheless, CT perfusion is being increasingly used.

It should be kept in mind that the ischemic penumbra is not fixed in time: it is dynamically evolving and progressively becoming part of the ischemic core because of pathophysiological mechanisms ongoing during vascular occlusion. Thus, imaging techniques provide a snapshot of this dynamic process.

1.1.4.2 Positron Emission Tomography

PET is considered as the "gold standard" for penumbra assessment, because of its capability to quantitatively measure CBF and oxygen metabolism of cerebral tissue *in vivo* after ischemia. This technique relies on the use of ligands to which a positron-emitting radioisotope is attached. These ligands are injected intravenously and a tomographic reconstruction of the emitted radioactivity is performed. Several parameters can be quantified using $C^{15}O_2$ and $^{15}O_2$ ligands, including not only CBF, but also cerebral metabolism rate of oxygen ($CMRO_2$) and cerebral oxygen extraction fraction (OEF). The ischemic penumbra can be identified as the hypoperfused areas in which cerebral metabolism is preserved and oxygen extraction is increased, to compensate for reduced CBF. In 1980 and 1981, Baron and colleagues first defined the condition of reduced CBF with preserved $CMRO_2$ as "misery perfusion" (Baron *et al.*, 1981). In humans, $CMRO_2 < 65$ μmol/100g/min and CBF$<$12 mL/100g/min define the core of irreversibly damaged tissue (Heiss, 2003). The ischemic penumbra can be instead defined by a CBF decreased to the range 12-22 mL/g/min, a $CMRO_2$ above 65mmol/100g/min and also an OEF increased to 50-90% (Heiss, 2000), against the physiological OEF around 30%.

Since the assessment of these parameters using $^{15}O_2$ requires arterial catheterisation for blood sampling, alternative non perfusion-based tracers are preferable. ^{18}Flumazenil is a marker for neuronal

integrity, thus presents affinity for γ-aminobutyric acid (GABA) receptors, which are abundant in the cerebral cortex and are sensitive to ischemia. Firstly validated in the MCAO cat model, it predicted final infarct size of acute stroke patients and showed thrombolytic efficacy (Heiss, 2000). ^{18}F-fluoromisonidazol is a marker of viable hypoxic tissue (Takasawa *et al.*, 2007). In early stroke patients, increased ^{18}F-fluoromisonidazol uptake surrounded the core, and an association between the extent of ^{18}F-fluoromisonidazol-binding surviving tissue and functional outcome was found (Markus *et al.*, 2003).

Although PET provides accurate and quantitative measure of both perfusion and metabolic parameters, its clinical use is limited for many reasons (Muir and Santosh, 2005; Schellinger *et al.*, 2003). First, radioactive tracers are administered, exposing the patients to a radiation dose and therefore preventing multiple imaging sessions. Furthermore, invasive arterial catheterisation is required. More generally, PET is expensive and of limited availability, and experienced chemists to synthesize short half-life radioisotopes are required. The use of PET in preclinical setting is also limited. In addition to its costs, it provides a poor resolution in small rodent brains. As a consequence, MRI is more widely utilized in the preclinical experimental setting.

1.1.4.3 Perfusion Computerized Tomography

Unlike PET, CT is the most accessible imaging technique in the clinical setting. It is widely utilized in stroke routine thanks to its speed in image acquisition and it practicality (Ebinger *et al.*, 2009). Perfusion CT (CTP) represent the modality for the assessment of the ischemic penumbra and requires the intravenous injection of a bolus of iodinated contrast agent. The bolus first pass is tracked in the cerebral circulation using dynamic imaging before, during and after the contrast agent injection. Parametric maps of cerebral blood volume (CBV), CBF and mean transit time (MTT, the time taken from the contrast agent to pass from the arterial to the venous circulation) can be computed and analyzed using post-processing software.

The reduction in tissue perfusion leads to vasodilation in the penumbra areas, in an attempt to compensate for the reduction in cerebral blood flow. For this reason, the CBV in the penumbra is increased compared to the infarct core, where vascular autoregulation is lost and CBV is consequently decreased. As emerged by a systematic evaluation (Wintermark *et al.*, 2006), the ischemic penumbra on CTP can be define as a relative MTT $\geq$145% compared to the contralateral hemisphere, whereas an absolute CBV of $\leq$ 2ml/100g accurately defines the ischemic core. Penumbra was assessed by CTP and PWI-DWI mismatch on MRI and a significant correlation emerged between the two techniques

(Schaefer *et al.*, 2008). More recently, the identification of core and critically hypoperfused tissue on CTP were validated using MRI as a reference (Bivard *et al.*, 2011).

However, standardization of CTP definitions for core and penumbra, also for differentiation between penumbra and oligemia, is required. Moreover, an agreement regarding quantification of the perfusion CT parameters is currently lacking and whole brain coverage is not yet readily available. Regarding health concerns, radiation exposure may prevent serial acquisition and iodinated contrast agent administration may cause nephropathy and allergy.

Nonetheless, CTP presents a great potential, in the view of a wide use of this technique for penumbra imaging. Multi-modal CT approaches could be in fact used for the selection of patients for therapy.

1.1.4.4 Magnetic Resonance Imaging

MRI is based on the electromagnetic activity of atomic nuclei, specifically of hydrogen atoms. A hydrogen nucleus is the nucleus of choice in the biomedical field and consists of a single positively charged proton which rotates around its axis (spin) and behaves like a small magnet. In normal conditions, the axes of the hydrogen nuclei are randomly oriented. When performing MRI, an external magnetic field is applied and causes the axes to align in parallel to the applied field. An electromagnetic radiation of a specific radio frequency (RF) is then also applied and excites the protons from a low to a high energy state, causing a deflection of the magnetization vector. The time for the protons to return to equilibrium (steady state) can be measured and occurs through two independent but almost simultaneous processes, known as T_1 (spin-lattice) and T_2 (spin-spin) relaxation. When T_1 or T_2 relaxation mechanisms are exploited to produce an image, we talk about T_1- and T_2-weighted imaging, respectively.

Other common MRI sequences are diffusion and perfusion-weighted imaging (DWI and PWI), which are relevant in the field of acute ischemic stroke and for the identification of the ischemic penumbra.

Diffusion Weighted Imaging

DWI shows MR signal changes depending on the diffusion of water protons in the biological tissue, e.g. brain. The diffusion constant quantifies the diffusion of water protons and varies with the direction of movement. In the cerebral tissue water molecules can't diffuse randomly in all directions (isotropic diffusion), but their movement is instead guided by the presence of natural barriers such as cell membranes or macromolecules structures (anisotropic diffusion). On native images, regions with pathological restricted diffusion appear as an augmented signal intensity compared to areas with

normal restricted diffusion when the sequence is strongly diffusion weighted (b-value of 1000). The diffusion constant can be measured and is represented by the apparent diffusion coefficient (ADC), used to compute ADC maps, where the restricted diffusion appears instead as a hypointense signal. In acute ischemic stroke, diffusion of water molecules is more restricted than in normal tissue as a result of cytotoxic edema (Moseley *et al.*, 1990b), causing redistribution of water from the extracellular to the intracellular space. As a consequence, the ischemic tissue will appear as hyperintense or hypointense areas on DWI-weighted images or ADC maps, respectively. The main advantage of DWI for imaging of ischemic stroke is the capacity to identify the ischemic damage within the hyperacute phase of stroke, i.e. within the first 6 hours (Moseley *et al.*, 1990b). In animal models of stroke, DWI can be used to visualize the ischemic lesion within minutes after MCAO (Hoehn-Berlage *et al.*, 1995; Moseley *et al.*, 1990a). In stroke patients, DWI has been used to detect ischemic lesion less than 40 minutes after stroke onset (Yoneda *et al.*, 1999). If reperfusion does not occur (untreated patients, thrombolysis failure or permanent occlusion models), the diffusion lesion will expand over time. In untreated stroke patients the DWI lesion, in parallel to the ADC lesion, is increasing in size during the first 3 days after stroke and then decrease up to 7 days (Baird *et al.*, 1997; Beaulieu *et al.*, 1999; Lansberg *et al.*, 2001).

Perfusion Weighted Imaging

PWI can be used to study the cerebral blood flow, providing quantitative assessment of cerebral tissue perfusion. This modality relies on MR signal changes induced by an exogenous or endogenous tracers. Two techniques are commonly utilized in both clinical and preclinical research: contrast agent bolus tracking (Dynamic Susceptibility Contrast, DSC) and arterial spin labeling (ASL) (Calamante *et al.*, 1999).

DSC involves the intravenous injection of a bolus of gadolinium-based contrast agents, which can be tracked through the cerebral circulation using the same dynamic approach as described for CTP. These paramagnetic agents cause magnetic inhomogeneity, resulting in a decreased signal intensity as the agent is passes through the microcirculation, which is then restored as the agent is washed out of the vascular compartment. T2*-weighted 2D or 3D echo planar imaging (EPI) sequences are the most commonly used MRI sequences for PWI, allowing fast image acquisition (1 image/sec) (Weishaupt *et al.*, 2008). A signal-time curve is reconstructed based on the changes in MR signal intensity as the contrast agent passes through the circulation. Using the equation of the sequence, the signal-time curve can be converted to ΔR2*-time curve, a physical quantity that is assumed to be proportional to the concentration of the contrast agent. Several relative parameters can be calculated

from this curve, such as relative CBF, relative CBV, relative mean transit time (MTT) and time to peak (TTP). MTT is the time taken from the contrast agent to pass from the arterial to the venous circulation (ratio CBF/CBV), whereas TTP is the time required from the start to the signal intensity to be maximal. In order to obtain quantitative informations and calculate absolute CBF, CBV and MTT, it is necessary to estimate an arterial input function (Ostergaard *et al.*, 1996). However, several issues must be considered to obtain a accurate and robust estimation of perfusion parameters (Willats and Calamante, 2013).

ASL uses the blood itself as an endogenous tracer and the injection of exogenous contrast agents is therefore avoided. Briefly, the water protons are spin labeled in the blood of an artery supplying the vascular territory of interest. In other words, the longitudinal magnetization of these water protons is inverted, producing a signal decrease as the spin labeled blood is passing into the imaged areas. However, the signal decrease is weak and in order to view the contrast image substraction between two image sets is required (Weishaupt *et al.*, 2008).

ASL techniques has been widely used in preclinical stroke research to quantify the perfusion deficit after cerebral ischemia (Foley *et al.*, 2010; McCabe *et al.*, 2009; Shen *et al.*, 2003). ASL is advantagenous over DSC since it is non-invasive, repeated imaging session can be performed, exogenous contrast agent injection is not required and absolute blood flow quantification can be directly generated (Baird and Warach, 1998). However, ASL is more difficult to perform compared to DSC.

Diffusion-Perfusion Mismatch

The MRI-based concept of ischemic penumbra is represented by the diffusion-perfusion mismatch model. The diffusion lesion was observed to expand over time, gradually encompassing the region of PWI perfusion deficit in the absence of reperfusion (Baird *et al.*, 1997; Jansen *et al.*, 1999). On this basis, DWI lesion represents the ischemic core, whereas the regions of PWI perfusion deficit but normal DWI values represents an approximation of the ischemic penumbra (Schlaug *et al.*, 1999), which is incorporated into the ischemic core as time progresses.

The DWI-PWI mismatch has been frequently used in clinical research to identify the ischemic penumbra in ischemic stroke patients. In fact, the presence of a substantial mismatch 24 post stroke was shown in up to 70% of patients (Darby *et al.*, 1999). This model has been applied in clinical trials for the assessment of the efficacy of thrombolytic therapies in patients stratified relying on the presence and extension of the ischemic penumbra (see §1.1.5).

In preclinical stroke research the PWI-DWI mismatch on MRI has been used to study the evolution of

the ischemic lesion and penumbra, conforming the expansion of the diffusion lesion into the perfusion deficit as observed in humans. In Sprague-Dawley rats, the diffusion lesion fully encompassed the penumbra tissue by 2-3 hours after permanent MCAO induction, suggesting a restricted time window for penumbra salvage in this rat strain (Meng *et al.*, 2004). When a transient MCAO was performed in the same strain, infarct volumes were significantly smaller compared those resulting from permanent MCAO, suggesting that reperfusion saved penumbral tissue (Meng *et al.*, 2004). A larger PWI-DWI mismatch was instead reported after permanent MCAO in Wistar rats (Bardutzky *et al.*, 2005b). A penumbra persisting at 4 hours post-MCAO in Sprague-Dawley rats was reported in a more recent study (Foley *et al.*, 2010), in contrast with previous results (Meng *et al.*, 2004). PWI-DWI mismatch was also used to assess penumbra in animals with co-morbidities, such as hypertension in spontaneously hypertensive (SHR) (McCabe *et al.*, 2009; Reid *et al.*, 2012) and spontaneously hypertensive stroke-prone rat (SHRSP) (Letourneur *et al.*, 2011), reporting a reduced penumbra in both strains compared to the normotensive control strain, Wistar-Kyoto (WKY). The preservation of PWI-DWI mismatch, i.e. prolonged penumbral survival, has also been used and considered as and efficacy index of neuroprotective strategies tested in preclinical stroke models (Bardutzky *et al.*, 2005a; Kim *et al.*, 2005; Legos *et al.*, 2008).

The DWI-PWI mismatch model is widely used in both clinical and preclinical stroke research. Despite its potential for penumbra evaluation, this model presents limitations (Kidwell *et al.*, 2003):

1. Different post-processing methods of data from perfusion imaging are available (i.e.: intensity curve vs. arterial input function) and several perfusion parameters can be considered (see above). Accordingly, the hypoperfused volumes vary together with the different method and parameter chosen. International standardization of the optimal criteria and hemodynamic parameters for an evaluation of the penumbra is currently lacking.

2. Perfusion imaging is currently unable to unequivocally distinguish between ischemic penumbra and benign oligemia, consequently leading to a possible overestimation of the penumbra.

3. According to the model, the initial diffusion lesion is assumed to be irreversible even if reperfusion occurs. However, both preclinical and clinical studies have shown that the diffusion lesion can be fully or partially reversed if early reperfusion occurs (Kidwell *et al.*, 2000; Olivot *et al.*, 2009).

4. The penumbra assessed by the PWI-DWI model does not reliably reflect the penumbra evaluated with the 'gold standard' method PET (Zaro-Weber *et al.*, 2009).

Despite these limitations, the PWI-DWI mismatch presents a great potential for the assessment of the ischemic penumbra. This model could be potentially improved by defining the optimal methods and perfusion-diffusion thresholds to be applied to accurately define the ischemic penumbra, by distinguishing it from the ischemic core and benign oligemia.

1.1.4.5 Molecular Penumbra

Beyond the identification of penumbra based on physiological, metabolic or perfusional changes, it can also be characterized relying on biochemical and molecular alterations ongoing in the hypoperfused tissue (del Zoppo *et al.*, 2011; Sharp *et al.*, 2000), thanks to the use of preclinical models of focal cerebral ischemia and *ex-vivo* methods with higher spatial resolution.

After acute ischemic stroke, a cascade of biochemical, metabolic and molecular events is triggered in the regions affected by hypoperfusion (see §1.1.3). One of the first biochemical consequences of ischemia is the blockade of protein synthesis, which was associated with a reduction in cerebral perfusion of approximately 50% (Mies *et al.*, 1991). A stronger flow decrease around 20% was in contrast associated with energy failure as ATP depletion. The lost ability to synthesize proteins accompanied by energy failure defines the ischemic core. When ATP levels are maintained, protein synthesis recovers over time and continues in cells that survive the ischemic insult, which is the case of the ischemic penumbra (Hossmann, 1993, 1994). It has been hypothesized that the blockade of protein synthesis may represent a mechanism of protection to prevent the formation of partially or incorrectly processed proteins.

From a molecular point of view, several "molecular penumbras" were identified (Sharp *et al.*, 2000; Weinstein *et al.*, 2004). The induction of Heat Shock Proteins (Hsps) expression represents one of the major molecular responses after ischemia. The proteins of the Hsp family are expressed in every cell type and are strongly induced after a cellular stress leading to intracellular protein denaturation, including ischemia. The major Hsp family inducible protein is Hsp70 (70 kDa), which expression has been extensively explored in rodent focal stroke models. After ischemia, this protein becomes extremely abundant and directly binds to denatured proteins in the attemp to refold them, promoting cell survival, or allow for their degradation and progression to cell death (Höhfeld *et al.*, 2001).

Converging results suggest that the areas of Hsp70 protein induction following focal ischemia represent a molecular penumbra, where this protein can exert its cytoprotective effect. The occlusion of the MCA in rodents induced a cellular stress leading to the expression of Hsp70 mRNA in the whole MCA territory, both in infarct and areas outside this region (Kinouchi *et al.*, 1994, 1993a,b).

Interestingly, Hsp70 protein was expressed in neurons of peripheral regions, while no or very little protein (mostly in vascular or glial cells) was synthesized in the infarcted areas. These observation were further supported by subsequent biochemical studies (Hata *et al.*, 2000a,b, 1998). A blood flow reduction associated with decreased protein synthesis and energy failure defined areas of Hsp70 expression (mRNA) without translation into Hsp70 protein. Conversely, in regions where a milder blood flow reduction affected protein synthesis but preserved ATP, Hsp70 mRNA expression coincided with Hsp70 protein synthesis. Thus, the ischemic core corresponds to Hsp70 mRNA induction, but without translation into the Hsp70 protein, whereas the ischemic penumbra is represented by regions of both Hsp70 mRNA induction and Hsp70 protein synthesis. Moreover, these results are in agreement with a differential vulnerability of different cellular types to ischemia: endothelial cells can express Hsp70 mRNA and synthetize Hsp70 protein, surviving in the ischemic core, whereas neuron and glia encountered cell death. After 10 minutes of MCAO, Hsp70 protein was induced in neurons throughout the MCA territory at 24 hours post-reperfusion, while it was expressed in the borderzone territory between MCA and ACA after 90 minutes of ischemia (Figure 1.5, Zhan *et al.* (2008)). The broader expression of Hsp70 protein after 10 minutes compared to 90 minutes of ischemia is explained by the extended infarction, with no or little Hsp70 expression, present after a long period of ischemia. The cytoprotective effect of increased Hsp70 expression is further supported by several studies showing that transgenic overexpression or pharmacological induction protected against focal cerebal ischemia (Lu *et al.*, 2002; Matsumori *et al.*, 2006; Mohanan *et al.*, 2011; Rajdev *et al.*, 2000).

In the present work, the relationship between the post-reperfusion molecular penumbra defined by HSP70 protein expression and the cerebral collateral blood flow was evaluated in a rat model of focal cerebral ischemia (Chapter 2).

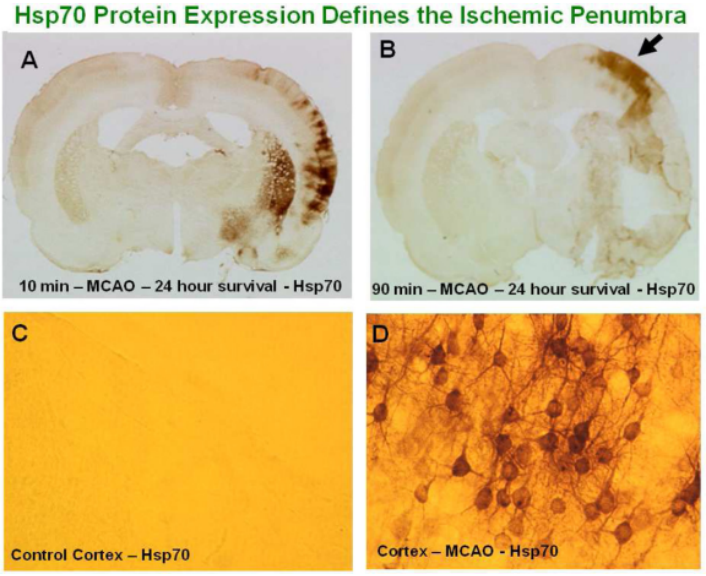

Figure 1.5: Hsp70 protein expression molecularly defines the ischemic penumbra in a rat model of MCAO. At 24 hours post-reperfusion, Hsp70 protein is induced in neurons (**D**) throughout the MCA territory after 10 minutes of ischemia (**A**), whereas after 90 minuter of ischemia Hsp70 is induced in neurons in the periphery, at the borderzone between MCA and ACA territories (B). In normal brain tissue (contralateral hemisphere), Hsp70 is espressed at very low leves. MCAO = middle cerebral artery occlusion; MCA = middle cerebral artery; ACA = anterior cerebral artery. Reproduced from Sharp *et al.* (2013)

1.1.5 Therapeutic Strategies for the Acute Phase of Ischemic Stroke

Acute ischemic stroke is caused by a sudden drop in cerebral blood perfusion caused by the occlusion of a cerebral artery or its branches. The ischemic penumbra represents the tissue at risk, which can be saved by prompt reperfusion. If hypoperfusion continues, the ischemic penumbra will progressively evolve into irreversibly damaged tissue. The goal of a therapy for acute ischemic stroke is to block this evolution and lead to salvage of cerebral tissue, hopefully accompanied by a persistent recovery from neurological symptoms. Therefore, therapeutic strategies can be primarily divided into:

- *Recanalization therapies*, aiming at restoring tissue perfusion by targeting (removing) the vascular occlusion;
- *Neuroprotective therapies*, aiming at blocking the ischemic cascade by directly targeting the pathological molecular events ongoing in the hypoperfused cerebral tissue.

1.1.5.1 Recanalization therapies

Reperfusion should be achieved in a timely manner. In other words, the therapeutic window for recanalization therapy is short. The lysis of the clot could be obtained by intra-venous (IV) or (more aggressive) intra-arterial (IA) injection of the thrombolytic drug. Alternatively, if reperfusion is not achieved, a more invasive approach by mechanical thrombectomy can be considered, which relies on the use of endovascular devices to remove the clot from the occluded artery. Combination of these strategies have also been successfully tested.

Intra-Venous Therapies

The only pharmacological therapy approved by the Food and Drug Administration (FDA) in 1996 is the IV administration of recombinant tissue plasminogen activator (rtPA), which is widely used in clinical practice. In 1999, the National Institute of Neurological Disorders and Stroke (NINDS) trial proved that fibrin-specific agents lead to both recanalization and clinical outcome improvement in all subtypes of ischemic stroke (NINDS, 1995).

A 3-hours time window for thrombolytic therapy was initially identified in the NINDS trial (NINDS, 1995). Unfortunately, this short time window is not compatible with clinical practice. In fact, the timelapse required for the patient to reach the hospital, for their neurological evaluation and for diagnosis confirmation (by primarily excluding hemorrhagic stroke on CT) easily exceeds 3 hours. For this reason, the feasibility and safety of a wider time window for therapy was investigated. A 3 to 4.5

hours time window for IV rtPA was first proven to be safe in a the European cooperative acute stroke study (ECASS-III), a placebo-controlled trial (Saver *et al.*, 2009). However, the shorter recanalization is achieved, the better the outcome: ideally, a complete symptomatic recovery could be obtained if therapy was started within 1 hour from stroke onset (Saver *et al.*, 2010).

The rtPA alteplase has a short half-life (4-6 minutes) and presents some side effects due to the activativation of a metalloproteinase and subsequent damage of the blood–brain barrier, resulting in an increased risk for intracerebral bleeding and brain edema (Micieli *et al.*, 2009). For this reason, efforts are made to identify alternative thrombolytic candidates. Agents with longer half-lives such as reteplase (Qureshi *et al.*, 2006, 2002) and tenecteplase (Haley *et al.*, 2005; Parsons *et al.*, 2009) have been tested in clinical trials with a relatively low number of patients. Desmoteplase is a more fibrin-specific, not neurotoxic agent which has been tested in Desmoteplase In Acute Stroke (DIAS) trials and Dose Escalataion of Desmoteplase for Acute Stroke (DEDAS). Unfortunately, the promising results of DIAS (Hacke *et al.*, 2005) and DEDAS (Furlan *et al.*, 2006) were not supported by the subsequent DIAS-2 (Hacke *et al.*, 2009) and 3 (Albers *et al.*, 2015) trials. To date, evidence of clinical efficacy remains stronger for alteplase. Notably, treatment was initiated 3 to 9 hours after stroke onset in these studies and, in DIAS and DIAS-2 studies, patients were selected for the presence of penumbra, evaluated by PWI-DWI mismatch on MRI or CTP.

Intra-Arterial Therapies

In case of proximal and large-vessels occlusion or non eligibility for IV therapy, a primary thrombolytic IA approach is contemplated. The IV administration of alteplase is in fact more efficient in case of distal occlusion. IA interventions are invasive, implicating a risk for vascular damage, and require the collaboration of interventional radiologists, dedicated facilities and higher costs. In the Prolyse in Acute Cerebral Thromboembolism (PROACT) I, a randomized placebo-controlled trial, patients with MCA occlusion were treated with IA recombinant pro-urokinase within 6 hours from stroke onset and recanalization rate was high for treatment group (del Zoppo *et al.*, 1998). Results of the PROACT II multicenter trial were also positive, proving treatment efficacy (Furlan *et al.*, 1999), with improved 3-months functional outcome for treatment group. However, definitive data defining the relative efficacy IA versus IV thrombolysis are still lacking (Powers *et al.*, 2015).

According to current guidelines (Jauch *et al.*, 2013), patients eligible for IV thromoblysis should receive this therapy even if endovascular treatments are being considered. In fact, a combination of IV followed by IA fibrinolysis may more efficaciously recanalize occluded major vessels compared to

IA fibrinolysis alone. The Interventional Management in Stroke (IMS) (IMS, 2004) and IMS-II (IMS-II, 2007) trials tested the feasibility and safety of IV rt-PA administration within 3 hours from stroke onset, followed by IA rtPA, if needed. IMS subjects showed significantly improved outcome at 3 months when compared to the placebo subject of the NINDS trial. However, the IMS-III trial showed similar safety outcomes and no significantly different functional outcome with combined therapy as compared with IV therapy alone and was stopped early because of reported futility (Broderick *et al.*, 2013).

Mechanical Thrombectomy

Mechanical thrombectomy may represent a primary strategy, when thrombolysis is contraindicated, or could also be combined with IV or IA thrombolysis in case of their failure. Different endovascular devices were cleared by the FDA. The MERCI (Mechanical Embolus Removal in Cerebral Ischemia) Retrieval System was the first approved by FDA in 2004, followed by the PENUMBRA System in 2007 and the Solitaire Flow Restoration Device and the Trevo Retriever in 2012. These systems for mechanical thrombectomy have been tested in several trials (Berkhemer *et al.*, 2015; Campbell *et al.*, 2015a; Goyal *et al.*, 2015). Results from these trials suggest the potential of mechanical thrombectomy in selected patients (Jauch *et al.*, 2013; Powers *et al.*, 2015). Nonetheless, direct comparison of different devices is lacking and futher clinical studies are warranted.

Imaging-Based Patients Selection for Therapy

The time from symptom onset represents the primary reference for therapy eligibility. However, due to the heterogeneity of stroke pathophysiology, salvageable penumbra may still be present in a substantial proportion of patients even beyond the reference time window.

In clinical practice, non-contrast CT imaging is performed in the emergency setting to exclude patients with hemorrhage (absolute contraindication) and non-vascular pathologies, as indicated in the current guidelines (Jauch *et al.*, 2013; Powers *et al.*, 2015). Non-invasive vascular imaging (CTA, MRA, TCD) is strongly recommended during initial imaging evaluation, if endovascular approaches are contemplated (Jauch *et al.*, 2013). Beyond these recommendations, the use of imaging techniques, such as perfusion MRI and CT, has been proposed to assess the extension of both ischemic core and (if present) penumbra to identify patient with the potential to benefit from therapy even beyond the 3-4.5 hours time window.

Therapeutic efforts beyond this timelapse may be worthwhile in patients presenting a small ischemic

lesion (core) and a large hypoperfusion (penumbra). This strategy would guide the therapeutic decision for patients in which time of onset is unknown, such as 'wake up stroke' patients, as well as for those who had a poor treatment response to IV thrombolysis and candidates for endovascular therapy.

On these basis, penumbra imaging was performed in several trials to select patients, mainly relying on PWI/DWI MRI and CTP techniques (Hillis and Baron, 2015). The use of these techniques for the evaluation of penumbra is discussed above (§1.1.4).

The DIAS and DIAS-2 trials were the first to use penumbra imaging for patients selection for inclusion (Hacke *et al.*, 2005, 2009). The echoplanar imaging thrombolysis evaluation trial (EPITHET), 101 patients were randomized for placebo vs rt-PA treatment 3–6 h after stroke. For those patients who had a significant diffusion–perfusion mismatch on MRI before the intervention (20% difference between DWI and PWI volumes), the IV rt-PA decreased the size of irreversibly damaged areas and improved clinical outcome (Davis *et al.*, 2008). In the diffusion-weighted imaging evaluation for understanding stroke evolution (DEFUSE) trial (Olivot *et al.*, 2009), 74 patients were treated with IV rt-PA within 3 to 6 hours after stroke onset. Half of the patients (54%) enrolled presented diffusion-perfusion mismatch profile. These patients benefited from treatment, while the others did not. In addition, patients with the 'malignant profile' (DWI or PWI lesion $>$ 100 mL) presented and increased risk of symptomatic intracerebral hemorrhage. The automated RAPID methodology (Straka *et al.*, 2010), allowing for a rapid estimation of thresholded PWI, DWI and PWI/DWI MRI mismatch and CTP mismatch, was used to analyze the pooled data from EPITHET and DEFUSE trials. The analysis showed that target mismatch patients (with mismatch profile and no malignant profile) benefitted from reperfusion, while the other patients didn't (Lansberg *et al.*, 2011). The EXtending the time for Thrombolysis in Emergency Neurological Deficits (EXTEND) study is a phase III randomized placebo-controlled trial testing IV rtPA within 4.5 to 9 hours after stroke onset and in wake-up stroke patients (Ma *et al.*, 2012), which design is based on the EPITHET trial, except for parameters refinement and prospective patients selection using the RAPID methodology. A threshold T_{max}>6 seconds was considered and patients with baseline DWI$\geq$70 ml were excluded.

Penumbra imaging was also performed in clinical trials for endovascular therapies. Negative results were reported by the MR RESCUE trial (Kidwell *et al.*, 2013). Baseline MRI or CT was performed before before clot retrieval (by Merci Retriever or Penumbra System) or standard care. Patients with or without a favorable penumbral pattern did not differentially benefit from endovascular therapy, nor endovascular therapy resulted superior to standard care.

Positive results were instead reported by other studies. Imaging criteria for patients selection could

explain these discrepancies (Leigh *et al.*, 2014). In the DEFUSE 2 trial from MRI predictors of therapeutic response to delayed endovascular therapy were explored (Lansberg *et al.*, 2012). Target mismatch pattern with early reperfusion was associate with more favourable clinical outcomes, whereas patients without target mismatch were not. Moreover, time to treatment did not modify the therapeutic effects in patients presenting target mismatch (Lansberg *et al.*, 2015). The EXTEND-IA trial (Campbell *et al.*, 2015b) was stopped early because efficacy was shown after 70 patients had undergone randomization (in contrast to the 100 patients planned). Patients with evidence of penumbra and a small ischemic core (<70 mL) on CTP received standard care (IV rt-PA within 4.5h) and were randomized for endovascular therapy with Solitaire FR (Flow Restoration) stent retriever or standard care alone. Early thrombectomy showed better reperfusion and both improved neurologic recovery after 3 days and functional outcome at 90 days.

Globally, these studies support the utility of imaging-based patients selection for therapy eligibility. Furthermore, identification of patients with potential to benefit from therapy would also reduce sample heterogeneity in clinical trials, which may have likely contributed to the negative results often observed in studies for new alternative therapies.

1.1.5.2 Neuroprotective Therapies

The recanalization therapies describes above aim at restoring the oxygen and glucose supply. On the other hand, neuroprotective strategies *directly* targeting molecular and biochemical events of the ischemic cascade are currently considered (Hossmann, 2006; Moskowitz *et al.*, 2010). The progression of the ischemic penumbra to infarct may be potentially limited or delayed, prolonging the time window for recanalization therapies. Many molecular targets have been indentified within the ischemic cascade (Moskowitz *et al.*, 2010). Their pharmacological manipulation may, theoretically, be neuroprotective.

Despite over 1000 putative neuroprotective agents obtained promising results in experimental stroke models (O'Collins *et al.*, 2006), no successful translation has occurred in the phase-3 stroke clinical trials performed so far (Stroke-Trials-Registry, 2015). Many reasons were advocated for this failing in translation and are discussed below in Section 1.3.2.

Interestingly, the influence of drugs on CBF has been largely neglected in preclinical research (Sutherland *et al.*, 2011). It is important to differentiate pure neuroprotective effects (acting on the ischemic

cascade) from those conditioning physiological parameters, such as CBF (Liebeskind, 2005b; Sutherland *et al.*, 2011). Monitoring CBF, including cerebral collateral flow, may help to detect indirect neuroprotective effects in preclinical studies.

In conclusion, the need for new therapeutic strategies for acute ischemic stroke is clear. The general aim of therapeutic strategies is to save the ischemic penumbra or to slow down its progression to infarction. A determinant of penumbra survival during occlusion is represented by the residual blood flow provided by collateral routes. In untreated patients, good collateral status is associated with larger baseline penumbra and reduced ischemic core (Campbell *et al.*, 2013). Modulating collateral blood flow in order to augment or maintain perfusion to the ischemic penumbra could represent a new therapeutic strategy for the hyperacute (even pre-hospital) phase (Liebeskind, 2004, 2010; Shuaib *et al.*, 2011b), particularly if applied before recanalization. Furthermore, collateral circulation may influence both thrombolytic or neuroprotective drug delivery. For this reason, the assessment of collateral blood flow may play an important role for treatment decision and patients selection, beside penumbra imaging. Nonetheless, the relevance of collateral circulation is often neglected, in both clinical trials and preclinical studies.

The next Section focuses on the cerebral collateral circulation. Its relevance in acute ischemic stroke and the current methods for its assessment in patients and preclinical stroke models are discussed, along with the most promising collateral therapeutic strategies.

1.2 Cerebral Collateral Circulation

Cerebral collateral circulation is a subsidiary vascular network which is dynamically recruited after arterial occlusion (Liebeskind, 2003) and may provide residual perfusion to ischemic areas. Cerebral collateral flow during acute ischemic stroke is highly variable among different individuals and is emerging as a strong prognostic factor either in unselected stroke patients and in patients treated with intravenous rtPA or endovascular recanalization therapy (Bang *et al.*, 2008, 2011a,b; Calleja *et al.*, 2013; Campbell *et al.*, 2013; Liebeskind, 2003; Lima *et al.*, 2010; Menon *et al.*, 2011; Miteff *et al.*, 2009).

1.2.1 Cerebral Collateral Circulation in Humans and Rodents

The main vascular network providing blood in physiological conditions is generally defined as cerebral circulation. We instead refer to cerebral *collateral* circulation when focusing on the subsidiary arterial and venous network which is dynamically recruited after arterial occlusion and includes intracranial and extracranial routes (Liebeskind, 2003).

Many similarities, with some notable differences, exist between humans and rodents in term of cerebral collateral circulation. In both humans and rodents, the cerebral circulation originates extracranially from two internal carotid arteries (ICA) and the basilar artery (BA). The principal vessels branching from this arteries are connected at the basicranium by an arterial anastomotic ring, named circle of Willis. The circle of Willis represents the primary collateral circulation.

In humans (Liebeskind, 2003), each ICA branches into a middle cerebral artery (MCA) and an anterior cerebral artery (ACA), whereas two posterior cerebral arteries (PCA) derive from the BA. An anterior communicating artery (AComA) connects the two ACA and two posterior communicating arteries (PComA) connect each PCA to the ipsilateral ICA terminus. In contrast, AComA is totally absent in rodents (Scremin, 2004), whose proximal segments of ACAs converge to form one single medial artery called Azigos ACA. Furthermore, all three cerebral arteries rise from the ICA, which is an integral part of the circle, and the PcomA connect the basilar trunk to each PCA. The structure of the circle of Willis in both humans and rodents is shown in Figure 1.6.

The circle of Willis represents the primary collateral circulation, capable of rapidly redistributing blood flow in a condition of stenosis or occlusion of upstream arteries. Its dynamic recruitment has been shown both in clinical (Hartkamp *et al.*, 1999; van Laar *et al.*, 2007) and preclinical studies

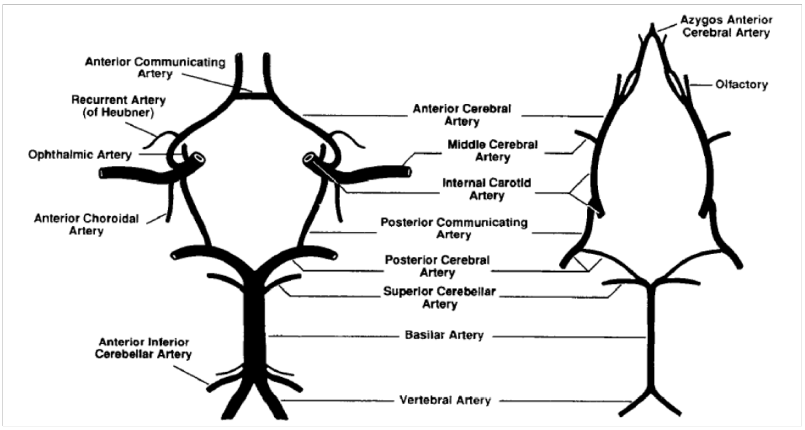

Figure 1.6: The structure of circle of Willis in humans (A) and rats (B). Reproduced from Lee (1995).

(Bonnin *et al.*, 2011; Li *et al.*, 2010). However, anatomic variability can diminish its efficiency: asymmetry is frequent and an ideal configuration is present in only a minority of cases (Iqbal, 2013).

When this primary route is inadequate or a vascular occlusion occurs downstream, the so-called secondary collateral circulaction may be recruited (Liebeskind, 2003). In humans, the ophtalmic artery (OA) connects the ICA to the external carotid artery (ECA). In case of proximal ICA occlusion, reverse blood flow via the OA provides a collateral source of blood flow from the ECA to the ICA terminus. In rodents, the pterygopalatine artery represent the collateral route between ECA and ICA (Tamaki *et al.*, 2006). It originates from the proximal ICA and provides blood flow to facial, orbital and meningeal districts via many arterial branches, including OA.

In both humans and rodents, each cerebral artery provides blood flow to its vascular territory ramifying along the cortical surface to form a pial arteriolar network. When arterioles deriving from different cerebral arteries anastomize connecting different vascular territories, they are known as leptomeningeal anastomoses (LMAs) (Brozici *et al.*, 2003; VANDER EECKEN, 1954). LMAs are mostly developed between cortical brances of MCA and ACA or MCA and PCA, in both humans and rodents. In Figure 1.7 the leptomeningeal anastomoses of a Wistar rat are shown (Coyle and Jokelainen, 1982).

In case of proximal occlusion of a cerebral artery, dynamic blood flow diversion through these anastomoses may provide residual (retrograde) blood flow to the cortical surface of the occluded artery territory, distally from the occlusion. Extension and severity of cerebral focal ischemia are critically

determined by the efficiency of this secondary collateral supply (Figure 1.8), which is highly variable among different individuals, due to differences in the diameter and number, but also in the functional performance of LMAs. Moreover, their response may need time to develop because of a different vascular resistance characterizing LMAs compared to the main arteries.

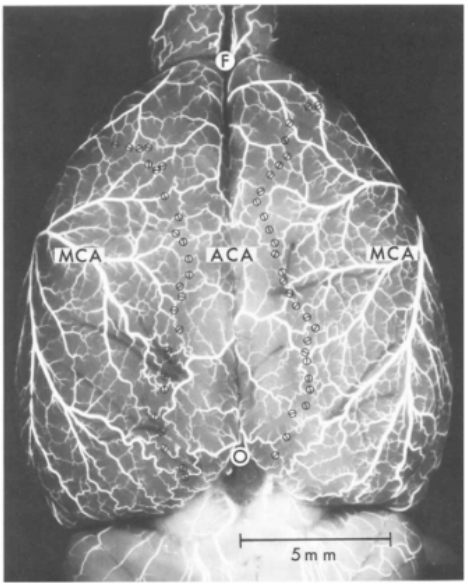

Figure 1.7: Leptomeningeal anastomoses of a Wistar rat. Cerebral arteries of a 56 days-old Wistar rat were injected with Vultex. Black circle indicate the anastomoses between branches of different cerebral arteries, characterized by and approximate bilateral simmetry and a parasaggital distribution extending over frontal (F), parietal and into occipital (O) regions. MCA = middle cerebral artery; ACA = anterior cerebral artery. Reproduced from Coyle and Jokelainen (1982).

1.2.2 Collateral Circulation in Acute Ischemic Stroke Patients

The status of collateral circulation strongly determines stroke evolution and outcome, both in treated and untreated patients, and it's emerging as a strong prognostic factor.

The status of collateral circulation is influenced by several factors. Atherosclerosis or stenosis, leading to chronic cerebral hypoperfusion, may allow for adaptative collateral development in contrast to an abrupt acute occlusion. Accordingly, the extent of collateral circulation correlates with luminal stenosis degree in intracranial atherosclerosis patients: more severe stenosis, implying a longstanding atherosclerotic disease, showed more robust collaterals than milder stenosis (Liebeskind *et al.*, 2011). In preclinical studies, chronic hypoperfusion by prolonged unilateral common carotid artery occlusion induce cerebral collateral growth (Omura-Matsuoka *et al.*, 2011; Todo *et al.*, 2008). On the other hand, advanced age (Arsava *et al.*, 2013) and chronic hypertension (Ovbiagele *et al.*, 2007) are known

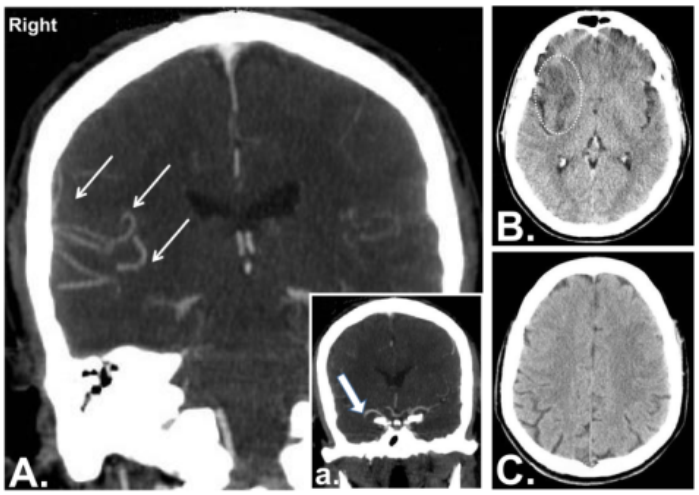

Figure 1.8: Imaging of cerebral collaterals with CT-angiography in a patient with acute ischemic stroke. Collateral vessels (**A**. small arrows) are visible in the right hemisphere. These vessels have been recruited after acute right MCA occlusion (**a**. large arrow). This patient was treated with intravenous thrombolysis and developed a small subcortical lesion (**B**), while the entire cortical territory was intact (C), due to the residual blood flow provided by the collateral circulation in the hyperacute phase, before recanalization was achieved. CT = computerized tomography; MCA = middle cerebral artery. Reproduced from Coyle and Jokelainen, 1982 (Coyle and Jokelainen, 1982)

to negatively affect the efficiency of secondary collaterals, consistent with preclinical results (Coyle, 1987; Faber *et al.*, 2011; Hecht *et al.*, 2012; Omura-Matsuoka *et al.*, 2011).

In untreated patients, good collateral status is associated with larger baseline penumbra and reduced ischemic core (Campbell *et al.*, 2013), leading to a more favourable functional outcome and reduced mortality (Bang *et al.*, 2008; Lima *et al.*, 2010; Menon *et al.*, 2011; Miteff *et al.*, 2009). After thrombolytic therapy, recanalization rate is higher in patients with more extensive pretreatment collaterals (Bang *et al.*, 2011a; Nicoli *et al.*, 2014), which may allow both for enhanced delivery of thrombolytic agents to clot and its easier dissolution. When recanalization is achieved, patients with good collaterals seem to be more protected from infarct growth and hemorrhagic transformation (Bang *et al.*, 2008, 2011b), resulting in a more favourable early and long term outcome (Calleja *et al.*, 2013).

Hence, collateral circulation may represent a valuable tool for decision making in endovascular treatment: patients with good pretreatment collaterals may be better candidate for more aggressive recanalization efforts (Bang *et al.*, 2008), with a chance of a more extended therapeutic window (Ribo *et al.*, 2011).

1.2.3 Assessment of Cerebral Collateral Flow in Acute Stroke Patients

The anatomy of cerebral collaterals in acute stroke patients can be assessed directly using conventional digital substraction angiography (DSA), CT angiography (CTA) or MR angiography (MRA), while their functional performance can be studied through tissue perfusion evaluation, via CT and MR perfusion techniques (CTP and PWI-MRI), or transcranial-doppler ultrasonography (TCD).

1.2.3.1 Digital Substraction Angiography

DSA is considered as the gold standard for collateral performance evaluation, but it is invasive and usually reserved for patients selected for endovascular procedures. Both vessel anatomy and retrograde collateral flow can be studied in a dynamic fashion (Christoforidis *et al.*, 2005; Liebeskind and Sanossian, 2012; Liebeskind *et al.*, 2014).

1.2.3.2 Multi-modal Computerized Tomography

The extent of collateral flow may be evaluated non-invasively using CTA or MRA techniques (Jäger and Grieve, 2000; Liebeskind and Alexandrov, 2012). CTA is able to visualize small vascular structures with high spatial resolution (Knauth *et al.*, 1997; Tan *et al.*, 2009) and provides direct visualization of collateral flow after arterial occlusion (Maas *et al.*, 2009) (Figure 1.8). However, if imaging acquisition is done before the contrast arrives in the leptomeningeal vessels, there is a risk to underestimate the real collateral extent. Recently, multi-phase CTA techniques have been developed to address this issue (Kaschka *et al.*, 2014).

CTP allows to study the performance of collateral flow, which is indicated by preserved or increased cerebral blood volume (CBV) and augmented mean transit time on CTP maps (Donahue and Wintermark, 2015). A more precise estimation of collateral flow can be obtained with CTP, thanks to the acquisition of serial scans after contrast bolus injection. Methods to obtain data insensitive to the timing of contrast arrival have been proposed (Smit *et al.*, 2013).

1.2.3.3 Multi-modal Magnetic Resonance Imaging

Multimodal MRI provides a number of tools to assess collateral flow, although with some limitations. MRA can determine alterations of cerebral circulation within large arteries (Liu *et al.*, 2004), but with less spatial resolution compared to CTA and without discriminating flow direction (Kinoshita

et al., 2005). Fluid Attenuated Inversion Recovery (FLAIR) images on MRI are able to show vascular hyperintensities distal to an occluded cerebral artery, due to the presence of a slow, retrograde blood flow in collateral vessels (Azizyan *et al.*, 2011; Kim *et al.*, 2012; Sanossian *et al.*, 2009). A signal loss on T2*-weighted gradient echo (GRE) MRI sequences may identify the presence of leptomeningeal collaterals: this may be caused by the fact that blood flowing in collaterals contains lot of deoxyhemoglobin, which has particular paramagnetic effects (Hermier *et al.*, 2005). PWI-MRI could assess the performance of collateral flow, showing cerebral tissue with relatively preserved CBF and a prolonged blood transit time, due to the retrograde blood flow (Nicoli *et al.*, 2013). Arterial spin labelling MRI (ASL-MRI) measures tissue perfusion of the brain using arterial water as an endogenous contrast. It can be used to detect hypoperfusion and perfusion-diffusion mistmach in acute ischemic stroke patients (Hartkamp *et al.*, 2014). More advanced ASL-MRI tecniques could potentially identify the presence of leptomeningeal collateral routes (Wu *et al.*, 2008).

1.2.3.4 Transcranial-Doppler Ultrasonography

TCD is, at the moment, the only real-time technique. Blood flow velocity and direction can be assessed, especially concerning the circle of Willis (Baumgartner *et al.*, 1997; Wessels *et al.*, 2004). Retrograde blood flow in leptomeningeal collaterals, represented by an increased velocity in ACA or PCA (compared to contralateral arteries), could be detected in patients with MCA occlusion (Kim *et al.*, 2009). TCD is a non invasive procedure and it does not require radiations or contrast agents injection. The limitations of these techniques are the lack of agreed criteria for defining leptomeningeal flow, a significant operator dependency and the absence of an adequate transtemporal bone window in some patients (Marinoni *et al.*, 1997).

Cerebral collateral imaging may be an useful tool both in establishing the prognosis in stroke patients and in selecting candidates for endovascular therapy. A general limit of imaging techniques for the assessment of collateral vessels and flow is represented by the spatial and temporal resolution they provide: a whole brain imaging, which can't be performed in real time (except for TCD). Moreover, its application is limited by a lack of consensus regarding which imaging modality should be considered, precise timing of assessment after ischemic stroke onset and which scales for grading collateral flow should be used (Liebeskind, 2013; Liebeskind and Sanossian, 2012; McVerry *et al.*, 2012). The most promising approach to improve collateral assessment in patients may be represented by new techniques combining vessels and perfusion imaging, such as multimodal CT or MR (Smit *et al.*, 2013). The methods for collateral anatomy and blood flow are summarized in Table 1.1 and 1.2.

Table 1.1: Methods for the assessment of collateral blood flow in acute ischemic stroke patients (Part 1/2). CBF = cerebral blood flow; CTA = computerized tomography angiography; CTP = computerized tomography perfusion; MRA = magnetic resonance angiography; FLAIR(MR) = fluid attenuated inversion recovery (magnetic resonance).

Technique	Temporal Resolution	Spatial Resolution	CBF Information	Risks	Logistics
Angiography	Real time	High	Gold standard for collateral performance evaluation	Invasiveness	Requires angio-suite and medical/technical expertise
CTA	Not real time	High	Large and medium-size vessels; may underestimate the real collateral extent	Contrast medium	Rapid acquisition time. Readily available in most emergency setting
CTP	Not real time	medium	Estimation of collateral performance (not influenced by a delayed contrast arrival)	Contrast medium	Rapid acquisition time. Readily available in most emergency setting
MRA	Not Real time	Medium	Limited to major arteries	No	Long acquisition time. Not available in most emergency setting
FLAIR (MR)	Not real time	Medium	Vascular hyperintensities distal to an occluded cerebral artery (retrograde blood flow in collateral vessels)	No	Long acquisition time. Not available in most emergency setting

Table 1.2: Methods for the assessment of collateral blood flow in acute ischemic stroke patients (Part 2/2). MR-PWI = magnetic resonance - perfusion-weighted imaging; ASL-MR = arterial spin labelling - magnetic resonance; TCD = transcranial Doppler ultrasonography.

Technique	Temporal Resolution	Spatial Resolution	CBF Information	Risks	Logistics
MR-PWI	Not real time	Medium	Prolonged blood transit time, expressed with time-to-peak parameter (retrograde flow in collateral routes)	No	Long acquisition time. Not available in most emergency setting
ASL-MR	Not real time	Medium	It can distinguish the blood territories from major vessels and leptomeningeal collateral routes	No	Long acquisition time. Not available in most emergency setting
TCD	Real time	Low	Retrograde blood flow in leptomeningeal collaterals represented by a blood flow diversion (increased velocity in ACA or PCA compared to contralateral arteries)	No	Bedside testing. Inexpensive. Repeatable. Highly operator-dependent.

1.2.4 Assessment of Cerebral Collateral Flow in Experimental Stroke Models

In experimental stroke models, both the site and duration of arterial occlusion are controlled. Continuous or repeated assessment of cerebral collateral flow could be performed, including pre-stroke assessment. For these reasons, preclinical research could play a crucial role for a deeper understanding of collateral response during ischemia and promote the translational development of collateral-based therapies. However, both cerebrovascular differences between different species and strains and inter-individual variability need to be meticulously considered to achieve effective results in this field of translational stroke research (Howells *et al.*, 2010; Liebeskind, 2008).

Although some techniques used in stroke patients, such as DSA, MRI or TCD, could be used in stroke models (Bonnin *et al.*, 2011; Christoforidis *et al.*, 2011; Leoni *et al.*, 2012; Sakoh *et al.*, 2000), significant limitations, including costs, logistics and low spatial resolution due to the reduced dimensions of the animals (mostly rodents) prevent their spread use. An easier assessment of collateral blood flow and anatomy with great spatial and temporal resolution can be achieved using optical imaging methods (Devor *et al.*, 2012).

1.2.4.1 Laser Speckle Contrast Imaging

Laser Speckle Contrast Imaging (LSCI) (Ayata *et al.*, 2004; Dunn, 2012; Dunn *et al.*, 2001) represents a non-expensive option for studying blood flow in LMAs. This technique provides maps of cortical blood flow, derived from the blurring of the speckle contrast pattern of a coherent light (laser), which is scattered by the motion of red blood cells (RBCs) when directed to the cortical surface (Ayata *et al.*, 2004; Dunn, 2012; Dunn *et al.*, 2001). Full-field imaging of the cortical surface and nearly real-time information about blood flow in both surface vessels and parenchyma are obtained. A cranial window is usually performed, although acquisition through intact skull is theoretically possible in mice.

LSCI was used in rodent models of MCAO to study changes in regional CBF (rCBF) and the dynamic response of LMAs to the vascular occlusion (Armitage *et al.*, 2010; Ayata *et al.*, 2004; Dunn *et al.*, 2001; Strong *et al.*, 2006; Wang *et al.*, 2012), also following treatment with collateral therapeutics (Shih *et al.*, 2009; Winship *et al.*, 2014). After thromboembolic MCAO, blood flow establishment through pial arteriolar anastomoses was immediately evident (Figure1.9), suggesting a prompt pathophysiological recruitment of the collateral circulation, also persisting after 24 hours (Armitage *et al.*, 2010). In another study (Wang *et al.*, 2012), LMAs immediately provided blood flow after permanent MCAO and were classified in persistent, impermanent and transient on the basis of their dynamic

changes. Notably, collateral dynamics were related to rCBF changes within the neighboring cortical parenchyma, suggesting a relationship between collateral flow and distribution of regional perfusion within the penumbra (Wang *et al.*, 2012).

Though the speckle contrast values are indicative of RBCs motion, they are not directly related to their speed or flow, with the exact relationship still undefined (Duncan and Kirkpatrick, 2008). For this reason, LSCI can be used to measure relative blood flow changes, rather than for its absolute quantification (Parthasarathy *et al.*, 2008).

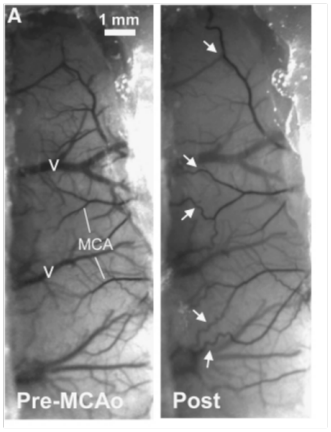

Figure 1.9: Laser Speckle Contrast Imaging map of cortical blood flow after focal stroke in rat. LSCI images showing blood flow in the surface veins (V) and branches of the MCA on the cortical surface before (**Pre-MCAo**) and after (**Post**) MCAO. Blood flows through anastomatic connections between the distal segments of the ACA and MCA is visible immediately after MCAO (arrows). LSCI = laser speckle contrast imaging; MCA = middle cerebral artery; ACA = anterior cerebral artery; MCAO = middle cerebral artery occlysion. Adapted from Armitage *et al.* (2010).

1.2.4.2 Two Photon Laser Scanning Microscopy

In contrast to LSCI, Two Photon Laser Scanning Microscopy (TPLSM) (Shih *et al.*, 2009) is an optical technique providing quantitative measure of blood flow velocity and direction in single vessels, with depth resolution up to 1 mm. Single arterioles, venules and capillaries of both surface and subsurface vasculature are resolved after intravenous injection of dextran conjugated with a fluorescent dye. A cranial window is required and scanning procedure is time-consuming, but pre-defined scanning paths may ameliorate this aspect (Shih *et al.*, 2009). Notably, TPLSM can be exploited for the study of neurovascular coupling (Shih *et al.*, 2009).

Collateral response after occlusion of both pial and penetrating arterioles were studies using TPLSM in rats (Nishimura *et al.*, 2010, 2007; Schaffer *et al.*, 2006; Shih *et al.*, 2009), also when testing collateral therapeutic strategies (Defazio *et al.*, 2012; Winship *et al.*, 2014). While collateral flow is not activated after photothrombotic occlusion of an individual penetrating arteriole (Nishimura *et al.*, 2010, 2007), it is evident after both single pial arteriole or MCA occlusion (Schaffer *et al.*, 2006): perfusion is rapidly reestablished through blood flow reversal at the first branch downstream the occlusion and approximately half of downstream distant arterioles (Schaffer *et al.*, 2006). Moreover, small pial arterioles vasodilation was observed within the ischemic penumbra after MCAO. The vasodilation persisted throughout occlusion and reperfusion period and compensated for an incomplete blood flow recovery (Shih *et al.*, 2009).

1.2.4.3 Laser-Doppler Flowmetry

Laser-Doppler Flowmetry (LDF) (Sheperd and Öberg, 1990) is a well-established technique for tissue perfusion monitoring and is recommended to confirm successful occlusion (Liu *et al.*, 2009) and exclude subarachnoid hemorrhage (SAH) (Schmid-Elsaesser *et al.*, 1998a; Woitzik and Schilling, 2002) in experimental ischemic stroke. Optical probes can be precisely located on the cerebral cortex or skull, providing an integrated reading of the underlying pial vasculature and parenchymal capillary bed in 1 mm^3 volume. Real-time relative cortical CBF values are obtained, while absolute CBF quantification cannot be achieved (Dirnagl *et al.*, 1989).

Our group developed an optimized system for multi-site LDF monitoring in rats during transient MCAO (Beretta *et al.*, 2013), which was used for monitoring of the cerebral (collateral blood flow) in the present work. A custom made holder for two probes was firmly attached to the intact skull to allow non-invasive and continuous monitoring of cerebral perfusion in the central MCA territory (Probe 1) and in the borderzone between ACA and MCA territories (Probe 2) (Figure 1.10). Although not providing a direct imaging of the LMAs, multi-site LDF monitoring allows real-time assessment of cerebral perfusion in two hemodynamically distinct territories during MCAO. Perfusion deficit recorded by Probe 2 is considered an index of the functional perfomance of LMAs, while perfusion deficit recorded by Probe 1 is used to confirm occlusion and reperfusion. Multi-site LDF may represent an easy method to quantify the functional activation of LMAs during ischemia in experimental stroke models and assess the effect of treatments.

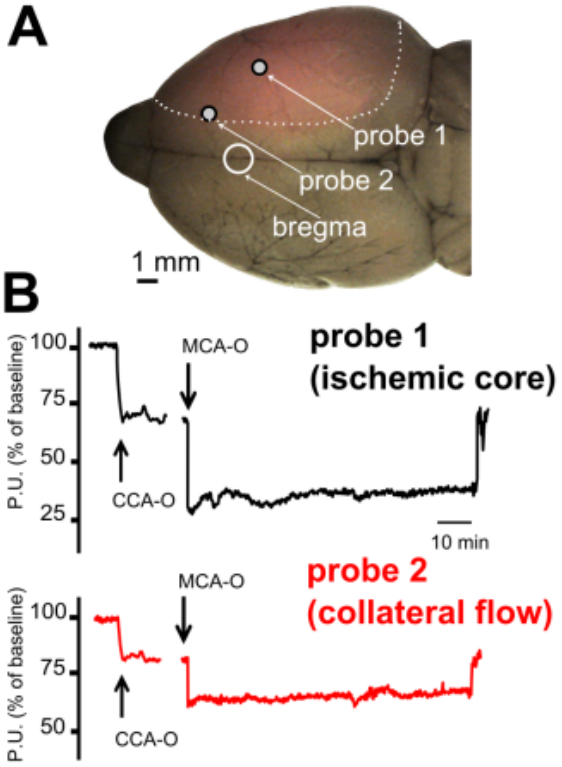

Figure 1.10: Monitoring of cerebral collateral flow in experimental ischemic stroke using multi-site laser Doppler flowmetry. **A**. The positions of the laser Doppler probes are shown, with reference to their underlying MCA territory (white dotted line) and bregma. Probe 1 = central MCA territory (ischemic core; -1 mm from bregma, 5 mm from midline); Probe 2 = MCA-ACA borderzone territory (collateral flow; +2 mm from bregma, 2 mm from midline). **B**. Laser Doppler tracings are shown from a representative animal showing a larger perfusion deficit in Probe 1 compared to Probe 2 during MCAO, suggesting functionally active intracranial collaterals under ischemic conditions. MCA = middle cerebral artery; ACA = anterior cerebral artery; MCA-O= middle cerebral artery occlusion; CCA-O= common carotid artery occlusion; P.U. = perfusion units.

The use of any of these methods (or a combination of them) to monitor arterial occlusion and collateral perfusion should be considered to improve accuracy of preclinical stroke research. Moreover, assessing collateral blood flow may clarify its dynamic response to acute vascular occlusion and may be used to study therapeutic strategies acting on the collateral circulation itself in experimental stroke models.

Advantages and drawbacks, in terms of temporal and spatial resolution, invasiveness and affordability of each technique are shown in Table 1.3.

Table 1.3: Methods for the assessment of collateral blood flow in experimental stroke models. MRI = magnetic resonance imaging; LSCI = laser speckle contrast imaging; TPLSM = two-photon laser scanning microscopy; LDF = laser Doppler flowmetry.

Technique	**Temporal Resolution**	**Spatial Resolution**	**CBF Information**	**Invasiveness**	**Cost**
MRI	Not real-time	Whole brain with low resolution	Perfusion maps	None	High
LSCI	Almost real-time	Stricktly surface reading	Relative CBF values	Craniotomy may be necessary	Moderate
TPLSM	Repetitive scanning required	Depth resolution	Quantitive CBF velocity and direction in single vessels	Craniotomy necessary	High
LDF	Real-time monitoring	Integrated reading in 1 mm^3 cortical volume	Relative CBF values	Craniotomy not necessary	Moderate

1.2.5 Collateral Therapeutics

At present, therapeutic strategies for acute stroke are focused on vascular occlusion with the aim to obtain early recanalization with acceptable risks (see §1.1.5). Intravenous thrombolysis with rtPA (Alteplase) within 4.5 hours from symptom onset (for any vessel occlusion) and endovascular thrombectomy with recanalization devices within 6 hours from symptom onset (for large vessel occlusion) are currently the best therapeutic options (Jauch *et al.*, 2013; Powers *et al.*, 2015), while intra-arterial thrombolysis is reserved for selected cases. Unfortunately, most patients are not eligible for recanalization therapies, because of its restricted time-window (Ingall, 2009; Lansberg *et al.*, 2009) and the risk of hemorrhagic transformation. Furthermore, recanalization is not always successful and, even when achieved, may be futile because of delayed reperfusion, hemorrhagic transformation, reocclusion or vascular collapse downstream (Espinosa de Rueda *et al.*, 2015; Gomis and Dávalos,

2014).

Vascular aspects beyond the occlusion are often neglected (Liebeskind, 2005a, 2010). Nonetheless, modulating collateral blood flow in order to augment or maintain perfusion to the ischemic penumbra could represent a new therapeutic strategy for the hyperacute (even pre-hospital) phase (Liebeskind, 2004, 2010; Shuaib *et al.*, 2011b), particularly if applied before recanalization or neuroprotective therapies.

Althought different strategies could be used to modulate cerebral collateral flow during acute ischemic stroke (summarized in Table 1.4 - 1.6), extensive research is needed in both animal models and stroke patients to establish the best approach in terms of benefit-to-risk ratio.

1.2.5.1 Strategies for the Acute Modulation of Collateral Blood Flow

Pressure Load

Increasing systemic blood pressure represents a first strategy. Despite chronic hypertension represents a well-established risk factor for ischemic stroke and is also associated with a worse collateral circulation status in both humans and rodents (Coyle, 1987; Lima *et al.*, 2010), the induction of hypertension in the hyperacute phase of an ischemic event has been proposed as a collateral therapeutic approach.

Phenylephrine, a selective α1-adrenergic receptor agonist, causes systemic vasoconstriction with very limited effects on cerebral vessels. A 30% augmentation of blood pressure obtained through phenylephrine infusion 10 or 60 minutes after distal MCAO induction in mice enhanced cortical CBF both in core and penumbra (Shin *et al.*, 2008). Notably, LSCI demonstrated the involvement of LMAs, with augmented blood flow visible in PCA and ACA branches but not in MCA proximal to the occlusion (Shin *et al.*, 2008). In small clinical studies, norepinephrine- o phenylephrine-induced hypertension improved outcome after stroke (Hillis *et al.*, 2003; Koenig *et al.*, 2006; Marzan *et al.*, 2004; Rordorf *et al.*, 2001), but collateral circulation was not directly assessed, leaving its contribution unclear.

Intravascular Volume Load

Increasing intravascular volume may represent a second strategy. Cerebral blood volume augmentation by plasma expansion and hemodiluition could improve cerebral perfusion in experimental stroke models (Heros and Korosue, 1989). However, in acute ischemic stroke trials performed in the 1990s, plasma expansion by dextran 40 and hydroxyethyl starch showed no benefit on neurological outcome or mortality reduction (Chang and Jensen, 2014). Notably, all these early clinical studies were

performed in the pre-thrombolysis era and outside a meaningful therapeutic window (patients were enrolled many hours or even days after symptom onset) and cerebral collateral flow was not assessed.

Albumin administration has been hypothesized to enhance cerebral perfusion through plasma expansion and inhibition of platelets aggregation. Intravenous albumin administration has been reported to enhance cerebral perfusion (Huh *et al.*, 1998; Nimmagadda *et al.*, 2008; Park *et al.*, 2008) and provide neuroprotection (Belayev *et al.*, 1997, 1998; Liu *et al.*, 2001) in several preclinical works. Regional CBF was augmented in both core and penumbra (Huh *et al.*, 1998) and arteriolar blood flow velocity distal to occlusion was increased (Nimmagadda *et al.*, 2008), enhancing the effect of thrombolytic drug (Park *et al.*, 2008). Subministration of 25% albumin 30 minutes after distal MCAO induction enhanced perfusion in both core and penumbra through cortical collateral vessels, reducing infarction in the mouse strain with insufficient collateralization (Defazio *et al.*, 2012). Promising results were also reported in a pilot clinical trial (Hill *et al.*, 2011). However, a subsequent large randomized clinical trial showed no clinical benefit of intravenous albumin solution 25% in ischemic stroke patients compared to standard treatment (Ginsberg *et al.*, 2013). Notably, 85% of these patients were treated with rtPA and intravenous albumin was administered on average 60 minutes after (not before) recanalization therapy.

Cerebral Vasodilation

Induction of cerebral vasodilation is a third strategy. Its major limit is represented by the necessity to achieve vasodilation selectively in the collateral circulation. Indeed, during acute occlusion, the vasculature in the ischemic area is immediately activated to a dilated state and a vasodilation outside the hypoperfused area may potentially lead to a vascular steal phenomenon (Bremer *et al.*, 1980; Kuwabara *et al.*, 1995).

Nitric oxide (NO) is a strong endogenous vasodilator with therapeutic potential for ischemic stroke (Terpolilli *et al.*, 2012b). NO inhalation following MCAO in adult mice induced a selective arteriolar vasodilation within the ischemic penumbra. Cortical blood flow was consequently enhanced, likely through collateral arterioles, leading to decreased brain damage and improved functional outcome (Terpolilli *et al.*, 2012a). No results are available for inhaled nitric oxide in acute stroke patients.

Sphenopalatine ganglion (SPG) electrostimulation activates parasympathetic fibers innervating intracranial vessels leading to their vasodilation. In a preclinical study, SPG-stimulation started 60 minutes after MCAO preserved DWI-PWI mismatch up to 180 minutes and reduced infarct size (Bar-Shir *et al.*, 2010). A better tissue and functional outcome was obtained even if treatment was started

many hours after occlusion onset (Henninger and Fisher, 2007). A stimulation started 15 minutes or 24 hours after photothrombotic MCAO lead to intensity- and duration-dependent increased CBF and to cortical arterioles vasodilation (Levi *et al.*, 2012). This treatment could extend the therapeutic window for conventional approaches. SPG electrostimulation in ischemic stroke patients has been demonstrated to be safe (Khurana *et al.*, 2009).

Stimulating cerebral function during ischemia could non-invasively enhance collateral perfusion of affected regions through neurovascular coupling mechanisms. An increase of blood flow to cerebral functionally-active regions derives from a coordinated interaction of neurons, glia and vasculature (i.e. functional hyperaemia) (Attwell *et al.*, 2010). Mild sensory cortical activation induced by whiskers stimulation in rats lead to a gradual reperfusion via MCA distal collaterals and to cortical function recovery, when the treatment was initiated within a critical time window from MCAO onset (Lay *et al.*, 2010, 2011). Notably, a complete protection from ischemic damage in most animals was obtained (Lay *et al.*, 2010, 2011).

Selective arteriolar vasodilation could be obtained using acetazolamide, which pharmacologically inhibits carbonic anhydrase and consequently augments CO_2 levels (Sullivan *et al.*, 1987). Its administration caused pial arteriolar vasodilation and increased cortical perfusion in piglets (Domoki *et al.*, 2008). In clinical practice, acetazolamide is used to test hemispheric cerebrovascular reactivity in patients with chronic cerebrovascular occlusions, in order to establish the risk of subsequent ischemic stroke (Kuroda *et al.*, 2001; Ogasawara *et al.*, 2002). The only report of acetazolamide in experimental stroke dates back to 1971 (Regli *et al.*, 1971), was performed in cats undergoing permanent MCAO (without reperfusion) and the drug was administered outside a meaningful time window (48-54 hours after the onset ischemia). No results are available for acetazolamide in acute stroke patients.

Cerebral Flow Diversion

Cerebral flow diversion is a fourth strategy. Gravitational influences of head positioning after acute vascular occlusion may affect pressure gradients in cerebral circulation, which enhancement may promote leptomeningeal recruitment. Augmentation of cerebral perfusion and increased MCA blood flow velocity has been reported in stroke patients after flat head positioning (Schwarz *et al.*, 2002; Wojner *et al.*, 2002; Wojner-Alexander *et al.*, 2005) and after 5° head-down tilt following bilateral CCAO in mice (Nagatani *et al.*, 2012). An increase in the collateral blood flow from posterior to anterior circulation is hypothesized (Nagatani *et al.*, 2012).

A temporary partial occlusion of the abdominal aorta may divert flow from the splanchnic circulation. Transient aortic occlusion reduced perfusion deficit and 24-hours infarct size after thromboembolic MCAO in rats (Noor *et al.*, 2010). Risk of hemorrhagic transformation wasn't increased and infarct size was further reduced when combined with thrombolysis, suggesting a synergistic interaction between the two treatments (Noor *et al.*, 2010). The same procedure also showed an increased blood flow through ACA-MCA leptomeningeal anastomoses after thromboembolic MCAO in rats, restoring it to baseline levels and maintaining stroke-induced vasodilation (Winship *et al.*, 2014). CBF increase persisted for at least 75 minutes after catheter and balloon removal, according with a previous study in a non-stroke porcine model (Hammer *et al.*, 2009). A randomized clinical trial of this procedure in acute ischemic stroke patients demonstrated an acceptable safety profile and suggested efficacy in post-hoc subgroup analysis (Shuaib *et al.*, 2011a). Tretment appeared safe also in association with thrombolysis (Emery *et al.*, 2011).

External counterpulsation diverts blood flow from lower limbs to the brain using antigravity suits or leg air cuffs. This procedure resulted safe in ischemic stroke patients (Han and Wong, 2008; Lin *et al.*, 2012), but an improvement in clinical outcome has been shown only in few patients (Berthet *et al.*, 2010). No results are available for this strategy in preclinical models.

A selective vasoconstriction of the hemisphere controlateral to the occlusion may divert flow to ipsilateral hemisphere through a mechanism known as "reverse steal phenomenon". This is based on the assumption that vessels in the ischemic areas will not respond to vasoconstrictor stimuli (being in a forced vasodilated state) and could be considered a subtype of flow diversion. Intravenous administration of a 5-HT1D receptor agonist, sumatriptan, 5 minutes after permanent MCAO in rats enhanced cortical perfusion in penumbral regions at 2 hours post-occlusion, which further improved at 3 hours. This perfusion enhancement was accompanied by an inhibition of spreading depression-like depolarizations and a reduction of ischemic volume by more than 70% (Mies, 1998).

In the present work, different strategies for the therapeutic modulation of collateral blood flow in the acute phase of ischemic stroke were tested and multi-site LDF for the assessment of collateral blood flow was used (Chapter 4).

Table 1.4: Strategies for acute modulation of cerebral collateral flow in ischemic stroke (Part 1/3). CBF = cerebral blood flow; LMAs = leptomeningeal anastomoses; MCAO = middle cerebral artery occlusion.

Strategies		**Risks**	**Cost**	**Results in preclinical stroke models**	**Results and feasibility in human stroke**
Pressure Load	Induced Hypertension	Haemorrhagic transformation, cardiac arrhythmias, myocardial ischemia. Minimally invasive (intravenous drug).	Low	Core and penumbra CBF augmentation through LMAs after distal MCAO in mice. (Shin *et al.*, 2008)	Preliminary results indicate efficacy (small clinical studies) (Hillis *et al.*, 2003; Marzan *et al.*, 2004). High feasibility.
Intravascular Volume Load	Dextran and hydroxyethyl starch	Anaphylaxis, pulmonary edema, platelet dysfunction. Minimally invasive (intravenous drug).	Low	CBF augmentation and improved outcome in various stroke models (Heros and Korosue, 1989).	No benefit in early clinical trials (before introduction of recanalization therapies) (Chang and Jensen, 2014). High feasibility.
	Albumin	Pulmonary edema, allergic reactions. Minimally invasive (intravenous drug).	Moderate	Cerebral perfusion enhancement through LMAs after distal MCAO in mice (Defazio *et al.*, 2012).	No benefit in a large random controlled trial (administered after recanalization therapy) (Ginsberg *et al.*, 2013). High feasibility.

Table 1.5: Strategies for acute modulation of cerebral collateral flow in ischemic stroke (Part 2/3). CBF = cerebral blood flow; MCAO = middle cerebral artery occlusion.

Strategies		**Risks**	**Cost**	**Results in preclinical stroke models**	**Results and feasibility in human stroke**
Cerebral Vasodilation	Nitric Oxide Inhalation	Pulmonary irritation. Non invasive (inhalation).	Moderate	Selective arteriolar vasodilation in the penumbra and cortical CBF enhancement after MCAO in mice (Terpolilli *et al.*, 2012a).	No results available in human stroke. Moderate feasibility (inhalation delivery equipement needed).
	Sphenopalatine Ganglion Stimulation	Invasive (minor surgery).	High	Cortical arterioles vasodilation and CBF augmentation after photothrombosis (Levi *et al.*, 2012).	Ongoing clinical trial (Khurana *et al.*, 2009). Moderate feasibility (surgery needed).
	Sensory-induced Vasodilation	No risks known.	Low	Gradual reperfusion through collaterals after MCAO in rats (Lay *et al.*, 2010).	No results available in human stroke. High feasibility.
	Pharmacolo-gically-induced selective vasodilation	Acetazolamide may cause paraesthesia, nausea, metabolic acidosis. Minimally invasive (intravenous drug).	Low	Pial arteriolar vasodilation and cortical perfusion enhancement in piglets (Domoki *et al.*, 2008)	No results available in human acute stroke. Clinically used as diagnostic tool in chronic stroke. High feasibility.

Table 1.6: Strategies for acute modulation of cerebral collateral flow in ischemic stroke (Part 3/3). CCAO = common cerebral artery occlusion; LMAs = leptomeningeal anastomoses; MCAO = middle cerebral artery occlusion.

Strategies		**Risks**	**Cost**	**Results in preclinical stroke models**	**Results and feasibility in human stroke**
Cerebral Flow Diversion	Head down tilt	Increase in intracranial venous pressure. Non invasive.	Low	Cerebral perfusion augmentation after bilateral CCAO in mice (Nagatani *et al.*, 2012)	Increase in cerebral perfusion and blood flow velocity by flat head positioning (case series) (Schwarz *et al.*, 2002; Wojner-Alexander *et al.*, 2005). High feasibility.
	Partial aortic occlusion	Invasive (endovascular surgery).	High	Blood flow enhancement through LMAs after thromboembolic MCAO in rats (Winship *et al.*, 2014).	Clinical trial suggest efficacy in post-hoc subgroup analysis (further confirmation required) (Shuaib *et al.*, 2011a). Moderate feasibility (endovascular procedure needed).
	External Counterpulsation	No risks known. Non invasive (external device).	Intermediate-high	No results available in preclinical stroke models.	Possible improvement of cerebral perfusion and collateral supply (Lin *et al.*, 2012). Intermediate feasibility.
	Reverse Steal Phenomenon	Sumatriptan may cause myocardial ischemia, ventricular tachycardia. Minimally invasive (intravenous drug).	Low	Cortical perfusion enhancement in the penumbra after MCAO in rats (Mies, 1998).	No results available in human stroke. High feasibility.

1.2.5.2 Strategies for the Chronic Modulation of Collateral Blood Flow

Chronic brain hypoperfusion, due to atherosclerotic disease or stenosis, augments risk of acute stroke in patients (Grubb *et al.*, 1998; Yamauchi *et al.*, 1996). On the other hand, chronic hypoperfusion is associated with a better collateral status (Liebeskind *et al.*, 2011), which may derive from an arteriogenic compensatory mechanism and could be protective during an acute occlusion.

Arteriogenesis is a process of remodeling and caliber enlargement of pre-existing vessels (Troidl and Schaper, 2012). A mechanical stimuli, as fluid shear stress, arising after a sudden vessel occlusion or a progressive stenosis, induces this process. Endothelium is activated and inflammatory circulating cells infiltrate the vascular structure, leading to remodeling.

Enhancing arteriogenesis of pre-existing collateral vasculature may represent a preventive therapy to chronically modulate collateral blood flow, ameliorating collateral functional performance during both chronic hypoperfusion and acute vascular occlusion. Various chemokines or growth factors secreted by inflammatory infiltrating cells during the arteriogenic process (Buschmann *et al.*, 2003a; Schirmer *et al.*, 2009) can be considered. Granulocyte-macrophage and granulocyte-colony stimulating factor (GM-CSF and G-CSF) have been extensively studied in preclinical models of cerebral hypoperfusion (Buschmann *et al.*, 2003b; Duelsner *et al.*, 2012; Sugiyama *et al.*, 2011; Todo *et al.*, 2008), showing an enhancement of collateral vessels growth, both at the circle of Willis (Buschmann *et al.*, 2003b; Duelsner *et al.*, 2012; Sugiyama *et al.*, 2011) and leptomeningeal anastomoses (Schneider *et al.*, 2007; Sugiyama *et al.*, 2011; Todo *et al.*, 2008). Chronic GM-CSF or G-CSF administration after unilateral CCAO in mice lead to collateral vessels growth and restored cerebrovascular reverse capacity, with a reduction of infarct volume in animals additionally subjected to ipsilater MCAO (Duelsner *et al.*, 2012; Sugiyama *et al.*, 2011; Todo *et al.*, 2008).

Statins may represent another preventive therapy: a better angiography-assessed collateral status is associated with their pre-morbid administration in acute ischemic stroke patients (Lee *et al.*, 2014; Ovbiagele *et al.*, 2007; Sargento-Freitas *et al.*, 2012), with a reduced infarct volume and a clinical improvement (Sargento-Freitas *et al.*, 2012). A number of pleiotropic cholesterol-independent effects have been demonstrated for statins, such as improvement of cerebral vasoreactivity through upregulation of endothelial nitric oxide synthase (eNOS) and enhanced NO bioavailability (Giannopoulos *et al.*, 2012), but also arteriogenic (Zacharek *et al.*, 2009) and angiogenic mechanisms (Elewa *et al.*, 2010; Lee *et al.*, 2014; Ovbiagele *et al.*, 2007).

Angiogenesis is a process distinct from arteriogenesis (Troidl and Schaper, 2012). It leads to the formation of new vessels and proliferation of endothelial cells (Troidl and Schaper, 2012) and may contribute to vascular remodeling and functional recovery during the chronic phase after stroke (Arai *et al.*, 2009). Angiogenesis is driven by an hypoxic environment and mediated by a number of angiogenic factors, including vascular endothelial growth factor (VEGF), which plays a role in the development of collateral circulation during perinatal period in transgenic mice: mice expressing low levels of VEGF presented fewer collaterals and an increased infarct volume after MCAO compared to mice expressing higher VEGF levels (Clayton *et al.*, 2008). Angiogenic response after ischemic stroke has been studied in clinical (Krupiński *et al.*, 1993; Krupinski *et al.*, 1994, 2003) and preclinical (Krupinski *et al.*, 2003; Wei *et al.*, 2001) settings and therapeutic approaches based on its enhancement have been considered (Lu *et al.*, 2012; Shen *et al.*, 2008). These approaches may also enhance cerebral collateralization. However, since the formation of new functional collateral vessels requires time, these therapies should be considered either in a premorbid phase, as a primary or secondary prevention in patients at high-risk for (first or recurrent) ischemic stroke.

A limited number of clinical and preclinical stroke studies focused on cerebral collateral circulation. Generally, neuroprotective effects are being sought, whereas the contribution of collateral blood flow is rarely considered or just inferred.

Preclinical stroke research has the potential to directly study the adaptive capacity and modulatory mechanisms of cerebral collateral flow during focal cerebral ischemia, using different methods and in different experimental conditions. These preclinical efforts are likely to be worthwhile and may produce useful translational concepts and direct comparisons of the different strategies to enhance cerebral collateral flow, including some therapeutic approaches which did not prove successful in past clinical trials conducted in the pre-thrombolysis era. Importantly, collateral therapeutics may have a role in the hyperacute (even pre-hospital) phase of ischemic stroke, prior to recanalization therapies.

In the next Section, a general view on preclinical stroke research is provided. In particular, the relevance of cerebral collateral perfusion assessment in the context of neuroprotection studies is discussed.

1.3 Preclinical Stroke Research

Preclinical stroke research relies on the use of experimental models to reproduce the pathophysiological events following cerebral ischemia. *In vitro* models of ischemia include cell cultures or *ex-vivo* preparations, which are deprived of oxygen and glucose or are exposed to excitotoxic stimuli. These models are suitable for the study of molecular mechanisms in individual cell types (neuronal, glial, vascular or immune cells) and allow for a greater control of the experimental variables compared to the *in vivo* models. On the other hand, *in vivo* models are certainly more closely mimicking the pathophysiological conditions of cerebral ischemia within the context of a living organism.

Collectively, preclinical stroke models are contributing to the study and understanding of the complex pathophysiology underlying ischemia and testing different therapeutic strategies, elucidating and providing proof-of-concept for their mechanisms of action. The translation of these findings into a clinical research context ultimately relies on the use of different *in vivo* models of cerebral ischemia. The main models, their features and limitations to their translational impact are discussed.

1.3.1 *In Vivo* Models of Cerebral Ischemia

1.3.1.1 Animal Species

The main features of ischemic stroke pathology can be modelled in different animal species by inducing a vascular occlusion, which is blocking blood flow to the brain. The species considered for preclinical stroke research vary from rodents to non-human primates and other higher-order mammals, among which the former are the most frequently considered (Howells *et al.*, 2010).

Reproducing ischemic stroke in non-human primates and other higher-order mammals (e.g. cats, pigs) is of strong relevance because of their similarity to humans for several aspects, including being gyrencephalic species with a similar grey/white matter proportion. Differently, rodents are lissencephalic and also present a different grey/white matter proportion, as white matter is more abundant in the human brain compared to the rodent brain. Non-human primates are also relevant for neurobehavioral outcome studies. On the other hand, ethical considerations, maintenance costs and the requirement for dedicated facilities must be taken into account. For these reasons, most of the preclinical studies are initially performed in small animals such as rodents, to establish the drug efficacy in different strains. Positive results should be then replicated in non-human primates or higher-order mammals, before proceeding to clinical trials (STAIRs, 1999).

The ordinary use of rodents for preclinical research and the similarities between human and rodent cerebral circulation (see §1.2.1) promoted their widespread use in the field of stroke research. In addition, rodent neuroanatomy and ischemic pathophysiology are well characterized. Since genetic modification can be relatively easily introduced in mice, they represent the first choice for the study of molecular pathophysiology. On the other hand, the greater size of rats makes them more appropriate for physiological parameters monitoring and application of neuroimaging techniques. In both mice and rats, histological analysis and neurobehavioral tests can be performed to evaluate the structural and functional effects of ischemic stroke, respectively.

1.3.1.2 Models of Focal Cerebral Ischemia

Given the heterogeneity and complexity of ischemic stroke in humans, different models of cerebral ischemia are considered but none of them is encompassing all of the features of human stroke. For this reason, a precise model should be carefully chosen relying on the aim of the specific study and the hypothesized mechanism of action of the analyzed drug. However, before translating to clinical trials, a given drug should prove efficient in different models and animal species.

Since the vascular territory of the MCA is the most commonly involved in ischemic stroke in humans, accounting for approximately 70% of infarcts, occlusion of the MCA is usually contemplated in preclinical stroke models. The artery can be temporary or permanently occluded (transient vs. permanent model). Permanent models are relevant when prospecting a scenario in which recanalization is not occuring, whereas transient occlusions are mimicking recanalization and associated reperfusion injury. Moreover, occluding the MCA at different site would differentially model a proximal or distal occlusion. Both occlusion site and duration of ischemia determine the infarct size, leading to lesions ranging from large hemispheric to small cortical infarcts. The induction of large infarct mimicks a malignant profile in humans.

The most common MCAO models are hereby described and their advantages and disadvantages summarized (for detailed reviews see Durukan and Tatlisumak (2007); Fluri *et al.* (2015); Macrae (2011)).

Intraluminal Suture MCAO Model

The most widely used method to induce cerebral ischemia is the intraluminal model of MCAO, first described by Koizumi and collegues (Koizumi *et al.*, 1986) and later modified (Belayev *et al.*, 1996; Longa *et al.*, 1989). A filament is inserted into the CCA or ECA, subsequently introduced into the ICA and then advanced to block the origin of the MCA (Figure1.11). A proximal occlusion is obtained and

can be either permanent (by leaving the filament in place) or transient (by withdrawing it, allowing for reperfusion). For transient occlusion, the ECA access approach is recommended, since preserving the CCA integrity for reperfusion. Occlusion of 60, 90 or 120 minutes are usually performed, reproducing a reperfusion-associated scenario. In rats, the ischemic lesion involves the striatum, the occipital, frontoparietal and temporal cortex, associated with a robust neurological deficit. Although considered as one of the most reproducible models of ischemia, infarct variability after suture MCAO has been reported and represents a limitation, in particular for neuroprotection studies. The reproducibility of the intraluminal occlusion model is affected by different factors, discussed in Section 1.3.2.2. The collateral circulation may represent an endogenous factor associated with outcome variability. A differential compensation provided by cortical collateral vessels after MCAO may in fact lead to a variable involvement of the cortical areas. In contrast, striatal regions are constantly infarcted in this model, since the the MCA end branches vascularizing these regions do not form collaterals with adjacent vascular territories (Zülch, 1981).

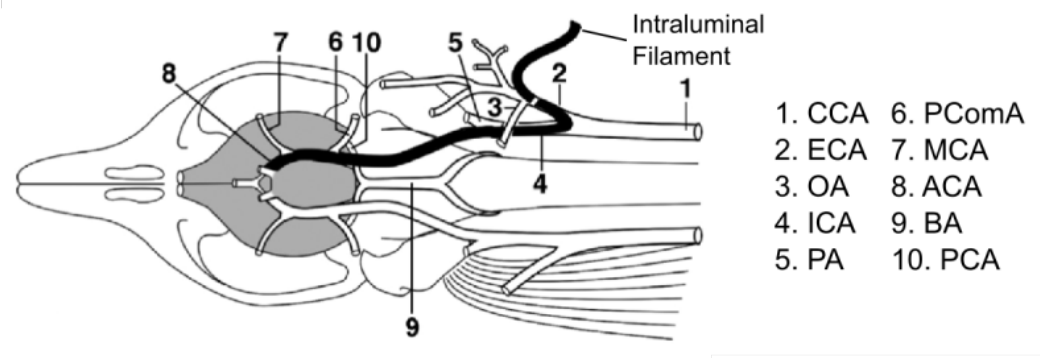

Figure 1.11: Schematic representation of the intraluminal suture model of MCAO. The filament is inserted in the ECA (ECA access approach), introduced into the ICA and advanced to block the origin of the MCA. CCA = common carotid artery; ECA = external carotid artery; OA = ophtalmic artery; ICA = internal carotid artery; PA = pterygopalatine artery; PComA = posterior communicating artery; MCA = middle cerebral artery; ACA = anterior cerebral artery; BA = basilar artery; PCA = posterior cerebral artery. Adapted from Durukan and Tatlisumak (2009).

The intraluminal suture model presents different advantages. Similarly to humans, a penumbra is present and makes this model suitable for neuroprotection studies. A craniotomy is not required and thus related brain damage can be avoided. Finally, the duration of ischemia and reperfusion can be precisely controlled. On the other hand, inadequate MCAO may occur and the risk of vessel rupture and subarachnoid haemorrage must be taken into account. Moreover, occlusion of the hypothalamic

artery leads to hypothalamic ischemia, in turn causing spontaneous hyperthermia that was shown to persist for at least one day in rats (Li *et al.*, 1999) and may affect further analysis.

In the present study, the intraluminal MCAO was considered to model a focal cerebral ischemia in Wistar rats. In particular, the ischemic outcome variability was studied in relation to the collateral blood flow (Chapter 3).

MCA Electrocoagulation or Occlusion by Other Devices

Robinson and collegues (Robinson *et al.*, 1975) firstly proposed a model based on MCA elettrocoagulation, subsequently modified by Tamura and colleagues (Tamura *et al.*, 1981). After craniotomy, the proximal region of the MCA is exposed and can be coagulated and cut at the origin of the lenticostriatal branches (Tamura *et al.*, 1981) or more distally (Bederson *et al.*, 1986), inducing corticostriatal or cortical damage only, respectively. Differently from MCAO suture model, the hypothalamic, hippocampal and midbrain areas are spared and related hyper/hypothermia is avoided. The effective occlusion of the MCA is visually confirmed in this model, which is characterized by a good reproducibility, low mortality and a neurological deficit. Moreover, performing a craniotomy diminishes the mortality associated with brain swelling following ischemia, preventing the rise in intracranial pressure. On the other hand, this model is technically demanding and only permanent ischemia is reproduced. However, occlusion by other devices such as microclips (Shigeno *et al.*, 1985) and ligature (Buchan *et al.*, 1992) allow for control over the duration of the ischemia and reperfusion. Reproducibility of these models can be improved by tandem vessel occlusion techniques, combining MCAO to unilateral (Brint *et al.*, 1988) or bilateral (Chen *et al.*, 1986) CCAO.

Embolic Models

Embolic models rely on the introduction of emboli into the cerebrovasculature in order to occlude a cerebral artery. They can be divided into two main categories, depending on the emboli nature: thromboembolic clot models and artificial microsphere-/macrosphere-induced stroke models.

The thromboembolic model was first described by Longa and colleagues (Longa *et al.*, 1989). Animal's blood is drawn and used to form autologous clots of specific size and composition, which are then introduced into the ICA and advanced to occlude the MCA. Another method is to inject thrombin directly into the intracranial ICA (Zhang *et al.*, 1997) or into the MCA (Orset *et al.*, 2007). Alternatively, thrombus formation can be induced *in situ* by application of $FeCl_3$ on the distal portion of the MCA (Karatas *et al.*, 2011). Thrombi represent a frequent cause of stroke in humans and the thromboembolic model is particularly relevant for testing thrombolytic or combination therapies. For

this model, craniectomy is not required and, when the clot is correctly positioned, large corticostriatal infarcts and related neurological deficits are induced. However, infarcts are less reproducible compared to the suture model and can result in multi-focal ischemia (with variable size and location) as well as spontaneous early autolysis of the clot (Beech *et al.*, 2001; Busch *et al.*, 1997), making this model unappropriate for neuroprotective effects validation. Moreover, hemorrhage and mortality rate are high (Ansar *et al.*, 2014).

The artificial microsphere model relies on the injection of spheres with a diameter of 20–50 μm of different materials (e.g. dextran, supraparamagnetic iron oxide, TiO2, ceramic) (Hossmann, 2008). Microspheres are injected into the ICA or MCA using a microcatheter and cause multifocal and heterogeneous infarcts (Gerriets *et al.*, 2003). Microspheres size and dose can regulate the extent of the infarct (Fukuchi *et al.*, 1999). Spheres of 100-400 μm diameter are instead injected in the ICA in the macrosphere model, causing an MCA occlusion and an infarct similar to MCAO suture model (Gerriets *et al.*, 2003). In contrast to the MCAO model, hypothalamus is spared from ischemia. Differently from the thromboembolic model, a permanent occlusion is induced and no induced or spontaneous reperfusion can occur.

Photothrombotic Model

In the photothrombotic model a photoactive dye (e.g. Rose bengal, erythrosin B) is injected intraperitoneally in mice (Kleinschnitz *et al.*, 2008) or intravenously in rats (Watson *et al.*, 1985) and the intact skull is irradiated by a laser light at a specific wavelength, which causes the generation of free radicals and subsequent endothelial damage and platelet activation and aggregation in the vessels within the irradiated area (Watson *et al.*, 1985). The region of cerebral ischemia can be precisely determined by irradiation based on stereotactical coordinates. The minimal surgery, high reproducibility and the low mortality represent further advantages of this model. On the other and, the induced end-arterial occlusion and the little or lack of ischemic penumbra represent disadvantages.

Endothelin-1 Model

The endothelin-1 (ET-1) model is based on the application of this potent and long-acting vasoconstrictive peptide (Yanagisawa *et al.*, 1988), which can be applied on the exposed MCA (Robinson *et al.*, 1990) or by intracerebral stereotactic injection (Hughes *et al.*, 2003), inducing a lesion comparable to that induced by permanent MCAO. A cortical lesion is induced when ET-1 is applied onto the cortical surface (Fuxe *et al.*, 1997). The ischemic lesion is dependent on the dose injected, with reperfusion

occurring over several hours (Biernaskie *et al.*, 2001). This model is characterized by low mortality but the expression of the ET-1 receptors and converting enzyme also by neurons and astrocytes (Nakagomi *et al.*, 2000) may interfere with the study of neuronal repair (Carmichael, 2005).

1.3.1.3 Ischemic Outcome Measures

In preclinical stroke research, evaluation of the ischemic outcome is extremely important in order to assess the efficacy of therapeutic strategies. The two major outcomes considered are the final infarct size and the neurological deficits.

Final infarct volumes are more frequently quantified by histological staining of coronal brain sections by techniques such as hematoxylin and eosin (H&E), cresyl violet or 2,3,5-triphenyltetrazolium chloride (TTC). Healthy cerebral tissue and necrotic areas are differentially stained by H&E and cresyl violet, with the infarct resulting unstained compared to the healthy tissue (see Figure 1.12). This allows for a clear demarcation between healthy and infarcted tissue. Morphological changes in the tissue and cellular structure can also be seen with these techniques. TTC is processed by mitochondrial enzymes into a red substance, staining therefore the healthy tissue and also delineating the (unstained) ischemic area. Alternatively, infarct can be quantified non invasively using imaging techniques such as MRI, e.g. T2-weighted imaging at 24 hours (see Figure 1.12). The area of infarct on each brain section can be quantified manually or semi-automatically on a sufficient number of coronal sections to allow accurate determination of infarct volume. Moreover, infarct volume should be corrected for cerebral edema, using published formulas (e.g. Swanson *et al.* (1990), Leach *et al.* (1993)). In fact, cerebral edema is present after a few hours and is developed over the first 2-3 days after occlusion. The related brain swelling may lead to overestimation of the infarct volume. Infarct size should be expressed as mean and standard deviation, either as an absolute volume (mm^3) or as a relative value (e.g. % of the contralateral hemisphere, or brain volume), although relative values allow more straightforward comparison between different studies.

The assessment of neurological deficits and outcome is essential for the preclinical evaluation of therapeutic strategies, and represent the most relevant outcome from a clinical point of view. Several neurobehavioural tests have been developed for the quantification of the sensimotor deficit and recovery (Metz, 2010; Schallert, 2006). However, neurological assessment is extremely challenging and time-consuming. The main weakness is the lack of consensus and guidelines on the typologies, number and frenquency of the neurological tests, also linked to the continuous development of new

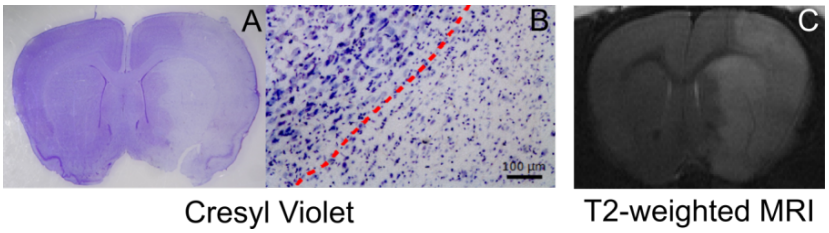

Figure 1.12: Infarct volume assessment. A clear demarcation between infarct and healthy tissue can be visualized on tissue section histologically stained using Cresyl violet (**A**, **B** for higher magnification) and non-invasively on T2-weighted MRI images (**C**).

tests and modification of the existing ones. Neurobehavioural testing ranges from specific tests to more general scoring system. Examples of specific tests are the Morris water maze (to determine cognitive deficits, D'Hooge and De Deyn (2001)), sticky label or dot test (to test sensimotor asymmetry, Sughrue *et al.* (2006)), cylinder test, horizontal ladder and tapered beam walking task (to test fore/hindlimb use). Scoring systems on the other hand provide an overall evaluation of the rodent's condition. They range from simple (e.g. 0-3 point scores, Bederson *et al.* (1986)) to more detailed scoring (e.g. 3-18 or 21 point scores, Garcia *et al.* (1995); Hunter *et al.* (2000)). Neurobehavioral testing in rodents is challenging for different reasons: first, animal's compliance to undertake the tasks cannot be taken for granted; moreover, neurological deficits may not be overt (even for large infarcts) or rapidly regress (for small cortical infarcts). As for the evaluation of the infarct volume, time from stroke onset should be taken into account when evaluating and interpreting the neurobehavioral outcome.

In the present work, ischemic outcome was evaluated at 24 hours post-reperfusion after 90 minutes of MCAO induced by intraluminal suture insertion. Cresyl violet staining (Chapter 2 and 4) and MRI T2-weighted imaging (Chapter 3) were used for the evaluation of the cerebral infarct (Figure 1.12) and the scoring system by Garcia *et al.* (1995) for the neurobehavioral evaluation.

1.3.2 Limitations to Translational Stroke Research

1.3.2.1 The STAIRs Recommedations

Despite successful neuroprotection has been reported in numerous experimental studies, it has failed to translate into clinical positive results (O'Collins *et al.*, 2006; Stroke-Trials-Registry, 2015) (see §1.1.5.2). The causes of this "translational roadblock" have been investigated and, among these, the quality of experimental stroke research has been questioned.

Intrinsic limitations to the translational potential of preclinical stroke research should also be taken into account. Firstly, none of the stroke models available is precisely mimicking the human stroke (see above §1.3.1). For this reason, it is fundamental to choose the most appropriate model, depending on the specific aim of the study. In addition to this, it should be kept in mind that the consistency of ischemic stroke models is in contrast to the heterogeneity of human stroke: while in ischemic stroke models the vascular occlusion duration and location are controlled and its time of onset are known, in humans this factors are extremely variable or not controlled.

In 1999, the Stroke Therapy Academic Industry Roundtable (STAIRs, 1999) tried to explain the potential reasons behind this traslational failure and consequently reported recommendations for improving the quality of preclinical stroke research, which were updated in 2009 (Fisher *et al.*, 2009). These aspects have been extensively discussed (Dirnagl, 2006; Fisher *et al.*, 2009; Kahle and Bix, 2012; Liu *et al.*, 2009; STAIRs, 1999) and are hereby briefly summarized:

- **Animal and stroke model.**

  The choice of the specific stroke models (i.e. proximal/distal occlusion, permanent/transient occlusion, occlusion duration, method for occlusion induction) is fundamental and should be driven by the specific aim of the study (see §1.3.1). The results should be replicated in *different species* (i.e. from rodents to non-human primates). After initial studies have confirmed positive effects of a therapeutic strategy in young healthy animals, subsequent studies should incorporate *aged animals* and/or with stroke *co-morbidities*, such as hypertension, diabetes and hypercholesterolemia. Moreover, efficacy should be tested in both male and female animals.

- **Therapeutic strategy administration**.

  After a pharmacological strategy has proven effective, *pharmacokinetic* and *pharmacodynamic* analysis should be performed, including dose-response curves. The minimum dose of effectiveness and maximum dose tolerated should be identified.

  A "*polypharmacological*" approach, where different treatments with different targets or mechanisms of action are combined, should be considered. The interactions between new treatments and the thrombolytic drug rtPA are of foremost importance, together with the their interactions with co-morbidity drugs. Potential synergic, neutralizing or harmful effects should be investigated.

  Clinically relevant *routes of drug administration* (i.e. intravenous, intraperitoneal, intramuscolar) should be considered rather than less feasible intracerebroventricular or intrathecal routes. Furthermore, the effective drug delivery to the brain should be verified.

Finally, the *timing* of administration is extremely important and should match with a clinically feasible therapeutic window. Moreover, penumbra imaging could be considered for the investigation of the therapeutic window.

- **Monitoring of physiological parameters.**

  Physiological parameters such as arterial pressure, temperature, blood gases and glucose should be monitored. *CBF monitoring* is particularly relevant and can be performed real-time by LDF, which is recommended to confirm successful occlusion. Importantly, monitoring physiological parameters would permit to discriminate between pure neuroprotective effects or neuroprotection related to physiological parameters modification (e.g. hypothermia, augmented CBF).

- **Anesthetics.**

  Some anesthetics are associated with neuroprotective effects. Therefore, the mechanism of action of the anesthetic should be taken into account and eventual interaction between the therapeutic strategy tested and the anesthetic should be considered.

- **Endpoints evaluation.**

  Measurement of infarct size and neurobehavioral testing are the two most relevant and most common outcome evaluations. *Infarct size* can be determined with several methods, among which histology (e.g. cresyl violet, hematoxylin and eosin, nissl), triphenyl tetrazolium chloride (TTC) or imaging (MRI). Importantly, factors for the correction of cerebral swelling due to edema should be applied.

  Depending on the stroke models used, stroke-related dysfunctions should be assessed by *behavioral, sensorial and motor tests*, perfomed by the same trained tester. Tasks minimizing animals anxiety or fear should be considered. Furthermore, long term assessment should also be considered (beyond 24 hours and up to 2-3 week or longer) in order to ensure outcome stability.

- **Fundamental standards for quality.**

  Recommendations for high studies quality include sample size calculation, statement of inclusion/exclusion criteria (and subsequent report of excluded animals), randomization, allocation concelament, blind outcome assessment and report of eventual conflict of interest. These points are briefly explained in Table 1.7.

Table 1.7: Fundamental standards for quality. Adapted from Fisher *et al.* (2009).

Sample size calculation	How the size of the experiment was planned should be described, reporting details including the expected variance, the desired statistical power, and the sample size calculated.
Inclusion and exclusion criteria	Criteria should be applied before the allocation to experimental groups and reported in details. For instance, the CBF values detected by LDF or the devel development of neurological impairment of a given severity may represent exclusion/inclusion criteria.
Randomization	The method by which animals were allocated to experimental group should be described and, if by randomization, the speficic method should be stated (e.g. computer-generated randomization schedules).
Allocation concealment	Allocation is concealed if the investigator responsible for the induction, maintenance, and reversal of ischaemia and for decisions regarding the care of (including the early sacrifice of) experimental animals has no knowledge of the experimental group to which an animal belongs. The method of allocation concealment should be described.
Reporting of animals excluded from analysis	The criteria for for exclusion of animals should be determined *a priori* and described. The animals excluded and the circumstances under which this exclusion will occur should be reported.
Blinded assessment of outcome	The assessment of outcome is blinded if the investigator responsible for measuring infarct volume, for scoring neurobehavioral outcome or for determining any other outcome measures has no knowledge of the experimental group to which an animal belongs. The method of blinding the assessment of outcome should be described.
Reporting potential conflicts of interest and study funding	Any potential conflict of interest should be discosed along with funding information.

1.3.2.2 Ischemic Outcome Variability

A well-recognized limitation of preclinical stroke models is outcome variability (Howells *et al.*, 2010), particularly regarding infarct size (Tudela *et al.*, 2014), which is the most commonly used primary outcome. The objective of experimental stroke models is to achieve reproducibility and minimize or control variability, in order to maximize their reliability. The variability in infarct size in different rat strains after suture MCAO is shown in Figure 1.13. In a recent meta-analysis of 502 control groups in preclinical stroke experiments, the average infarct size coefficient of variation was about 30% (ranging from 1.7% to 148%) (Ström *et al.*, 2013). The problem with high outcome variability is that a higher number of animals is needed to get an adequate statistical power, which is problematic from both an ethical and economical point of view. The main reasons of infarct size variability in stroke modes are not completely understood.

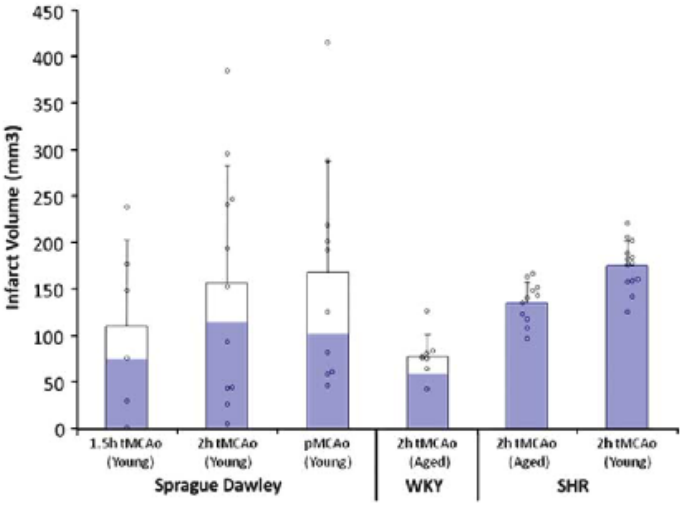

Figure 1.13: Infarct volume variability in different rat strains after suture MCAO. The infarct volumes after suture MCAO in Sprague–Dawley, Wistar Kyoto (WKY), and spontaneously hypertensive rat (SHR) under a range of experimental circumstances. Purple areas represent the proportion of animals with cortical infarction. Mean and Standard Deviation plus individual data points. Adapted from Howells *et al.* (2010).

Regarding the suture MCAO model, several factors have been demonstrated to be associated with infarct size variability (Braeuninger and Kleinschnitz, 2009; Liu *et al.*, 2009) and are hereby summarized:

- **Suture diameter**. The suture diameter (3-0 or 4-0 sutures for rats; 6-0 for mice) well correlated with infarct size in mice (Türeyen *et al.*, 2005). The insertion length also influences infarct size

and may vary from 18 to 22 mm in rats (Zarow *et al.*, 1997). In fact, when the suture is inserted 15-16 mm from the carotid bifurcation, only the hypothalamic and anterior choroidal arteries are occluded (He *et al.*, 1999).

- **Suture coating**. The suture can be uncoated or coated with silicone (Bouley *et al.*, 2007) or poly-L-lysine (Belayev *et al.*, 1996), with the coated filaments better adhering to the endothelium and thus associated with larger infarcts and reduced variability.

- **Coating length**. Different coating length account for different infarcts size: a 2.0 to 3.3 mm silicone coating is required to completely occlude the MCA in rats, while a coating length >3.3 mm results in additional occlusion of the anterior choroidal artery, hypothalamic artery and posterior cerebral artery (Guan *et al.*, 2012).

- **Rodent strain**. MCAO induction in certain rodent strains resulted in more extended infarcts (Duverger and MacKenzie, 1988; Oliff *et al.*, 1996), probably due to the differences in the collateral circulation (Oliff *et al.*, 1997). Beside final infarct size, also the penumbra dynamics seem to differ depending on the rat strain (Bardutzky *et al.*, 2005b).

- **Age and co-morbidities**. The infarct volume is likely to be affected by the age of the animals, although discrepant results were reported (Davis *et al.*, 1995; Shapira *et al.*, 2002; Wang *et al.*, 2003). However, aging was associated with reduced angiogenesis and worse functional recovery after stroke in rats (Zhang *et al.*, 2005). Co-morbidities such as hypertension may also affect infarct size. The spontaneously hypertensive rats (SHR) develop larger and less variable infarcts following MCAO (Coyle, 1986; Duverger and MacKenzie, 1988).

- **Physiological parameters**. Several physiological parameters such as temperature, blood pressure and gases and glycemia contribute to infarct variability and for this reason must be monitored during experiments. While hypothermia is associated to neuroprotection, an extension of neuronal damage is associated with hyperthermia (Krieger and Yenari, 2004; Mcilvoy, 2005). Contrasting results were reported about the effects of hyperglycemia (Ginsberg *et al.*, 1987; Huang *et al.*, 1996; Prado *et al.*, 1988). The lost capacity of autoregulation of the ischemic brain makes it more vulnerable to changes in arterial blood gases and blood pressure.

- **Anesthesia**. Experimental stroke models usually rely on the use of anesthetized animals. Anesthetic methods include intraperitoneal injection, inhalation via face-mask in spontaneously breathing animals or, less frequently inhalation via face-mask in intubated and mechanically ventilated animals. Many anesthetics used have been associated with neuroprotective effects

(Kirsch *et al.*, 1996). For this reason, its important to choose the most suitable anesthetic depending on the specific aim of the study.

For the present work, young healthy outbred Wistar rats were anesthetized with isofluorane. The intraluminal suture model was performed by insertion of a silicon-coated thread into the ECA, which is then advanced for 20 mm into ICA, occluding the origin of the MCA. During surgery, arterial blood pressure was monitored and temperature was feed-back controlled with a heating pad and kept around 37∘C.

Beside these methodological aspects, factors related to inter-individual differences in cerebrovascular anatomy (Barone *et al.*, 1993) and cerebral collateral circulation (Riva *et al.*, 2012) have been reported. Interestingly, the National Centre for the Replacement, Refinement and Reduction of Animals in Research (NC3Rs) is currently funding a project (2014-2015) entitled "Determining the source of variability within experimental stroke models", which is mostly focused on vascular anatomy and reperfusion (NC3Rs, 2015). Nevertheless, the variability of cerebral hemodynamics during ischemia has been largely neglected in preclinical research, as well as the influence of drugs on CBF (Sutherland *et al.*, 2011).

As previously mentioned, monitoring cerebral blood flow using Laser-Doppler Flowmetry (LDF) is recommended to confirm successful occlusion (Liu *et al.*, 2009) and exclude subarachnoid hemorrhage (SAH) (Schmid-Elsaesser *et al.*, 1998a; Woitzik and Schilling, 2002) in experimental ischemic stroke. In the present work, LDF was also used to monitor cerebral collateral blood flow, as explained above in Section 1.2.4.3. Our group previously showed that the functional performance of the cerebral collaterals during MCAO in rats, assessed using multi-site LDF monitoring (Beretta *et al.*, 2013), predicted infarct size and functional outcome more accurately than conventional LDF monitoring of perfusion deficit in the ischemic core alone (Riva *et al.*, 2012). Further experiments using the same method, in a series of 45 animals, confirmed a highly significant correlation of collateral flow during MCAO and stroke outcome (Figure 1.14).

In the present work collateral flow assessed by multi-site LDF and acute DWI-MRI were used for the prediction of 24 hours ischemic outcome and animal stratification based on infarct typology (Chapter 3).

Animal stratification by collateral flow during MCAO represents a promising tool to adjust for outcome variability in experimental stroke studies. Using cerebral collateral flow during MCAO as a covariate in multiple regression analysis may represent a simple method to stratify animals in term

of pre-treatment perfusion deficit, reducing the within group variability and improving efficacy analysis in preclinical neuroprotection studies. Further studies are needed to determine the more suitable method, timing and statistical tool for collateral flow assessment in pre-clinical neuroprotection trials.

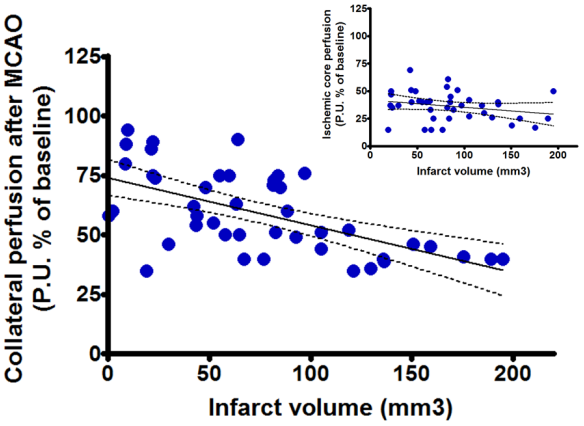

Figure 1.14: Relationship between cerebral collateral flow during MCAO and stroke outcome in rats. Linear regression between infarct volume and perfusion deficit during MCAO in the territory of leptomeningeal collaterals, measured using multi-site laser Doppler, was calculated for 45 consecutive untreated rats ($p < 0.0001$; Pearson's r = -0.59). Notably, the correlation between infarct volume and perfusion deficit in the ischemic core (central MCA territory) was not significant ($p = 0.14$, smaller graph).

1.4 Aims of the Thesis

Despite its contribution in determining ischemic outcome and its potential for the development of new therapeutic strategies, a limited number of clinical and preclinical stroke studies focused on cerebral collateral circulation. For this reason, this work generally aimed at bringing attention to this aspect:

1. The first study, presented in Chapter 2, aims at exploring the relationship between cerebral collateral flow during transient MCAO and the development of molecular penumbra and ischemic infarct after 24 hours of reperfusion.

2. The second study, presented in Chapter 3, aimed at exploring collateral flow assessed by multi-site LDF as a stratification factor for the prediction of 24h ischemic outcome, using acute magnetic resonance imaging as a reference.

3. The third and last study, presented in Chapter 4, aimed at testing different strategies for the therapeutic modulation of collateral blood flow. The effects of this strategies on the cerebral (collateral) perfusion assessed by multi-site LDF and 24h ischemic outcome were evaluated.

Chapter 2

Cerebral Collateral Flow Defines Topography and Evolution of Molecular Penumbra in Experimental Ischemic Stroke

Adapted from:

Beretta S[1*], **Cuccione E**[2*], Versace A[3], Carone D[3], Riva M[3], Padovano G[3], Dell'Era V[3], Cai R[3], Monza L[3], Presotto L[4], Rousseau D[5], Chauveau F[5], Paternò G[3], Pappadà GB[3], Giussani C[3], Sganzerla EP[3], Ferrarese C[6].

Neurobiol Dis. 2015 Feb;74:305-13. doi: 10.1016/j.nbd.2014.11.019. Epub 2014 Dec 5.

[1]Laboratory of Experimental Stroke Research, Department of Surgery and Translational Medicine, University of Milano Bicocca, Monza, Italy; Milan Center for Neuroscience (NeuroMi), Milano, Italy. Electronic address: simone.beretta@unimib.it.

[2]Laboratory of Experimental Stroke Research, Department of Surgery and Translational Medicine, University of Milano Bicocca, Monza, Italy; PhD Programme in Neuroscience, University of Milano Bicocca, Monza, Italy.

[3]Laboratory of Experimental Stroke Research, Department of Surgery and Translational Medicine, University of Milano Bicocca, Monza, Italy.

[4]Department of Nuclear Medicine, San Raffaele Scientific Institute, Milan, Italy; Institute of Bioimaging and Molecular Physiology, National Research Council, Milan, Italy.

[5]Université de Lyon, CREATIS, CNRS UMR5220, Inserm U1044, INSA-Lyon, Université Lyon 1, France.

[6]Laboratory of Experimental Stroke Research, Department of Surgery and Translational Medicine, University of Milano Bicocca, Monza, Italy; Milan Center for Neuroscience (NeuroMi), Milano, Italy.

* These authors equally contributed to this work

Abstract

Intracranial collaterals are dynamically recruited after arterial occlusion and are emerging as a strong determinant of tissue outcome in both human and experimental ischemic stroke. The relationship between collateral flow and ischemic penumbra remains largely unexplored in pre-clinical studies. The aim of the present study was to investigate the pattern of collateral flow with regard to penumbral tissue after transient middle cerebral artery (MCA) occlusion in rats.

MCA was transiently occluded (90 minutes) by intraluminal filament in adult male Wistar rats (n=25). Intracranial collateral flow was studied in terms of perfusion deficit and biosignal fluctuation analyses using multi-site laser Doppler monitoring. Molecular penumbra was defined by topographical mapping and quantitative signal analysis of Heat Shock Protein 70kDa (HSP70) immunohistochemistry. Functional deficit and infarct volume were assessed 24h after reperfusion.

The results show that functional performance of intracranial collaterals during MCA occlusion inversely correlated with HSP70 immunoreactive areas in both the cortex and the striatum, as well as with infarct size and functional deficit. Intracranial collateral flow was associated with reduced areas of both molecular penumbra and ischemic core and increased areas of intact tissue in rats subjected to MCA occlusion followed by reperfusion.

Our findings prompt the development of collateral therapeutics to provide tissue-saving strategies in the hyper-acute phase of ischemic stroke prior to recanalization therapy.

2.1 Introduction

Intracranial collateral circulation represents a multiple-level subsidiary vascular network which is dynamically recruited after occlusion of cerebral arteries to provide a source of residual blood flow (Liebeskind, 2003). In both humans and rodents, a significant supply of collateral flow after middle cerebral artery (MCA) occlusion is provided by the circle of Willis through the anterior cerebral artery (ACA) and the leptomeningeal anastomoses between the cortical branches of ACA and MCA. However, a significant degree of inter-individual variability exists in the functional performance of intracranial collaterals under ischemic conditions in humans (Liu *et al.*, 2011; Qureshi *et al.*, 2008) and rodents (Armitage *et al.*, 2010; Riva *et al.*, 2012). Cerebral collateral flow is emerging as a powerful determinant of functional and tissue outcome in unselected ischemic stroke patients (Maas *et al.*, 2009; Menon *et al.*, 2011) and in stroke patients treated with intravenous rtPA (Brunner *et al.*, 2014; Miteff *et al.*, 2009) or endovascular recanalization (Bang *et al.*, 2008, 2011a). For these reasons, an in-depth understanding of the physiology, adaptive response and modulation of intracranial collateral circulation is of foremost importance for acute stroke pathophysiology and therapy.

Ischemic penumbra was originally defined as "tissue at risk", which has been made functionally silent and metabolically metastable by ischemic injury but still has the potential for full recovery if reperfusion is timely achieved (Baron, 1999; Branston *et al.*, 1974; Hossmann, 1994). The concept of ischemic penumbra is gradually evolving, after pre-clinical and clinical studies showed a heterogeneous and variable pattern of perfusion deficit, molecular response, topographical distribution and evolution of the penumbra in relation to the ischemic core (del Zoppo *et al.*, 2011; Manning *et al.*, 2014). Hsp70 is the major inducible heat shock protein (Sharp *et al.*, 2000), whose expression after focal cerebral ischemia reflects an endogenous cell response to injury. The neuronal expression of Hsp70 is considered as a molecularly defined penumbra, where injured neurons have activated endogenous pathways for protein renaturation and protection against further ischemia.

In the present study, we investigated the relationship between intracranial collateral flow during transient MCA occlusion and the development of molecular penumbra and ischemic infarct after 24h. The hemodynamic monitoring of central and peripheral MCA territories was analyzed in terms of perfusion deficit and biosignal fluctuation. Hemodynamic data were correlated with the corresponding areas of molecular penumbra, infarct volume and functional deficit.

2.2 Material and Methods

2.2.1 Animals and Experimental Design

The experimental protocol was approved by the Committee on Animal Care of the University of Milano Bicocca, in accordance with the national guidelines on the use of laboratory animals (D.L. 116/1992) and the European Union Directive for animal experiments (2010/63/EU), under project license from the Italian Ministry of Health.

Animals were housed in single cages, exposed to 12/12 hour light/ dark cycle, at controlled room temperature, with free access to food and water, in a specific pathogen free (SPF) facility.

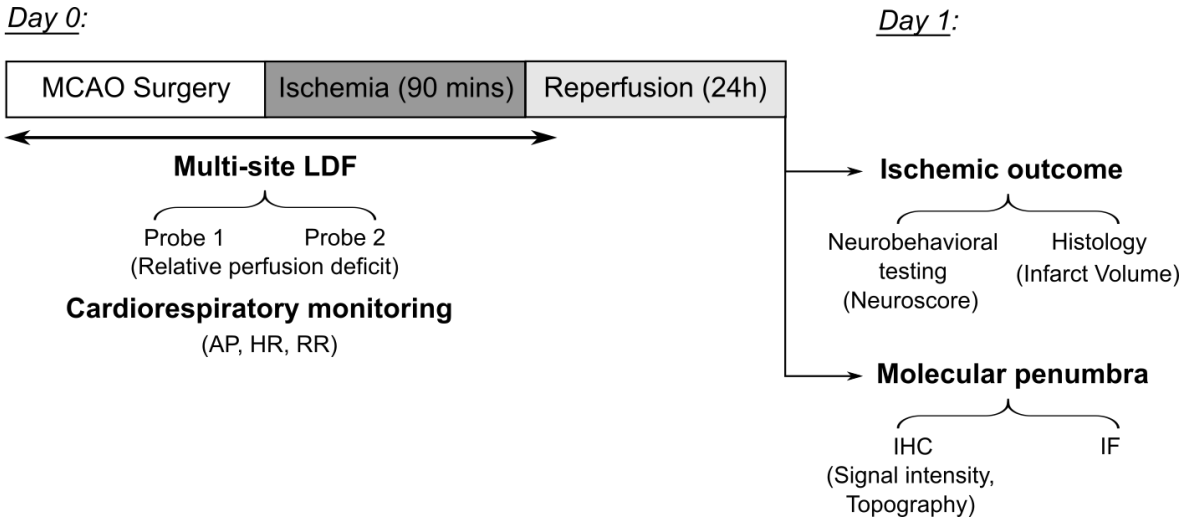

Figure 2.1: Experimental Design. On day 0, animals underwent transient MCAO and cerebral perfusion was continuously monitored by multi-site LDF for the entire period of anesthesia, including reperfusion. Cardiorespiratory parameters were also continuously monitored. After 24 hours of reperfusion (Day 1), neurological outcome was evaluated and scored according to a neurobehavioral scale. Infarct volume was calculated on histological slices stained with Cresyl Violet. Immunohistochemistry and immunofluorescence for Hsp70 (and other targets) were performed to evaluate the molecular penumbra. MCAO = middle cerebral artery occlusion; LDF = laser Doppler Flowmetry; AP = arterial pressure; HR = heart rate; BR = breath rate; IHC = immunohistochemistry; IF = immunofluorescence.

The experimental design is illustrated in Figure 2.1. On day 0, animals underwent transient MCAO. Cerebral perfusion monitoring by multi-site LDF was performed continuously during the entire period of anesthesia, including reperfusion.

On day 1, after 24 hours of reperfusion, neurological outcome was evaluated and scored according to a neurobehavioral scale. Animals were then sacrificed and brains were extracted and processed. Histological slices were stained with Cresyl Violet for the evaluation of the ischemic lesion and underwent immunohistochemistry and immunofluorescence for Hsp70 (and other targets) for the evaluation of the molecular penumbra.

A group of consecutive Adult male Wistar rats (280 $\pm$ 5% g; n = 28) undergoing successful MCA occlusion were used for this study. Three rats were excluded from the experimental series for early death occurred before successful MCA occlusion (one rat died for anesthesiological complications, two rats died for subarachnoid hemorrhage). All successfully occluded rats (n = 25) survived the 24-hours reperfusion time and were used for analysis.

2.2.2 MCAO Surgery

On Day 0, rats were anesthetized with 3% isoflurane in O_2/N_2O (1:3), and maintained with 1.5% isoflurane. A silicon-coated filament (diameter 0.39 $\pm$ 0.02 mm, Doccol Corporation, Redlands, CA, USA) was inserted into the right external carotid artery and advanced in the internal carotid artery, reaching and occluding the MCA origin. Immediately before filament insertion, the common carotid artery (CCA) was transiently occluded and subsequently re-opened during ischemia and reperfusion. The pterygopalatine artery was transiently occluded during both the surgical insertion of the filament and ischemia, then re-opened during reperfusion. After 90-minutes, the filament was withdrawn and animals were allowed to recover and had free access to food and water.

2.2.3 Physiological Parameters Monitoring

In a subset of animals (n = 12) cardiorespiratory parameters (arterial pressure, heart rate, respiratory rate) were continuously monitored using a Samba Preclin 420 transducer (Samba Sensors, Harvard Apparatus, UK) inserted in the right femoral artery before ischemia induction.

2.2.4 Multi-Site Laser Doppler Flowmetry

The induction of focal cerebral ischemia was assessed using laser Doppler (LD) perfusion monitoring (dual channel moorVMS-LDF^{TM}, Moor, Axminster, UK) using two blunt needle probes (VP12). Probes were positioned in a custom made silicon holder attached with surgical glue over the intact

skull and further secured in place using sutures to surrounding soft tissues (Beretta *et al.*, 2013). The cranial coordinates for probes positioning were based on a rat brain atlas (Paxinos and Watson, 2007). The first probe (Probe 1) was attached to the skull 1 mm posterior to the bregma and 5 mm lateral to the midline (lateral probe, corresponding to the core of the MCA territory). The second probe (Probe 2) was attached to the skull 2 mm anterior to the bregma and 2 mm lateral to the midline (medial probe, corresponding to the borderzone territory between ACA and MCA territories). Cerebral perfusion monitoring was performed continuously during the entire period of anesthesia (approximately 140 min), including reperfusion. The mean duration of cerebral perfusion monitoring after reperfusion was 7.8 (4–15) min. Three hemodynamic parameters were considered for signal analysis of each probe:

1. drop in cerebral perfusion (expressed as % of baseline) during MCA occlusion following successful filament insertion;
2. biosignal fluctuation analysis during the pre-ischemic period and during MCA occlusion (see below);
3. cerebral reperfusion (expressed as % of baseline), from the removal of the filament until the end of anesthesia.

Hemodynamic assessment was blinded to outcome data (neurobehavioral scoring, infarct volume, Hsp70 staining).

2.2.5 Biosignal Fluctuation Analysis of Cerebral Perfusion

Fluctuation analysis of blood microcirculation from LD signals or alternative laser speckle imaging signals has been undertaken with various measures (see (Humeau-Heurtier *et al.*, 2013) for a recent review). In this study, auto-correlation R(k) analysis was based on linear second order statistics (Humeau *et al.*, 2008).

We modeled the signal recorded on each probe as the realization X_i of a stationary random variable X at instant i with average μ and standard deviation σ. Let us call X_{i+k} the realization of X at instant $i + k$. We then consider the auto-correlation function $R(k)$ as follows:

$$R(k) = \frac{E[(X_i - \mu)(X_i - \mu)]}{\sigma^2} \tag{2.1}$$

We estimated the expectation in the auto-correlation function by empirical averaging over periods of 120 s. Two auto-correlation function $R(k)$ computed following this estimation procedure are plotted as a function of k in seconds between 0 and 120 seconds for the corresponding two probes. The auto-correlation function $R(k)$ is a measure of selfmemory of a random signal between instant i and instant $i + k$. It takes values between 1 if $X_i = X_{i+k}$ and -1 if $Xi = -Xi + k$. $R(k)$ is zero if X_i and X_{i+k} are independent. In $R(k)$ the auto-correlation are computed on centered variables $(X_i - \mu)$ and $(X_i - \mu)$.

In other words, the auto-correlation $R(k)$ measures the self-memory of the fluctuations around the average value and constitutes an analysis different from the record of the drop of average value between the two probes.

As shown in Figure 2.4, the two autocorrelation functions estimated for the two probes display a decrease but with a distinct characteristic time decay. To quantify this observation, we compute the time in seconds that autocorrelation $R(k)$ takes to drop from 1 to 0.9 for each probe.

2.2.6 24h Ischemic Outcome Evaluation

On Day 1, final ischemic outcome was assessed after 24 hours of reperfusion by both neurobehavioral testing and evaluation of ischemic lesion by Cresyl Violet staining of histological sections. Both neurobehavioral evaluation and infarct volume calculation on histological sections were blinded to hemodynamic data.

2.2.6.1 Neurobehavioral Testing

On Day 1, after 24-hours reperfusion, rats were evaluated for spontaneous activity, motor and sensitive function as described by Garcia and collegues (Garcia *et al.*, 1995). This functional outcome evaluation comprised 6 tasks for the assessment of spontaneous activity, symmetry in limb movement, forepaw outstretching, climbing ability, body proprioception and response to vibrissae touch. The maximum score for an individual test was 3 points, indicating no impairment. The total score scale (summation of the score of each individual test) ranged from a minimum of 3 (most severe impairment) to a maximum of 18 (no deficit). The functional tasks are described below and summarized in Table 2.1.

1. **Spontaneous Activity**

   The rat was observed for 5 minutes in its home cage after the cage top was removed. The

animal's ability to approach all four walls of the cage was observed. A score of 3 was given when the rat moved around, explored the environment, and approached at least three walls of the cage. When the rat moved about in the cage but did not approach all sides and hesitated to move the corresponding score was 2, although it eventually reached at least one upper rim of the cage. A score of 1 indicated a severely affected rat that did not rise up at all and barely moved in the cage. Finally, a score of 0 was given to rats that did not move at all.

2. **Symmetry in the Movement of Four Limbs**

   In order to assess the simmetry in the movement of the four limbs, the rat was suspended in the air by holding the base of the tail. A score of 3 indicate that all four limbs extended symmetrically; a score of 2 was given when the limbs on the contralateral side extended less or more slowly than those on the ipsilateral; a score of 1 corresponded to minimal movement of the limbs on contralateral side; a score of 0 was given when forelimb on contralateral side did not move at all.

3. **Forepaw Outstretching**

   The rat was again held by the base of the tail. While the hindlimbs were kept in the air, the rat was allowed to reach the hedge of the table with its forelimbs and then made to walk on the table's surface using its forelimbs only. The symmetry of forelimbs outstreching was observed and scored: 3 for both forelimbs outstretching and rat walking symmetrically on forepaws; 2 when contralateral forelimbs outstretched less than the ipsilateral and forepaw walking was impaired; 1 when contralateral forelimb moved minimally; and 0 when contralateral forelimb did not move.

4. **Climbing**

   The rat was placed on wire cage and the strength of attachment was observed when it was removed by pulling it off by the tail. A score of 3 was given when the animal climbed easily and gripped tightly to the wire. When contralateral side was impaired while climbing or did not grip as hard as the ispilateral side a score of 2 was given. Finally, a score of 1 indicated rat failure to climb or tendency to circle instead of climbing.

5. **Body Proprioception**

   Each side of the rat's body was tapped with a blunt stick and the reaction to this stimulus was observed. A score of 3 was given when the rat reacted by turning its head and was equally startled by the stimulus on both sides. When the rat reacted slowly to stimulus on contralateral

side, a score of 2 was given. A score of 1 indicated lack of respond to the stimulus on the contralateral side.

6. **Response to Vibrissae Touch**

   Vibrissae on each side were brushed with a blunt stick. In order to avoid entering the visual field of the rat, the stick was moved towards the wiskers from the rear of the animal. When the rat reacted by turning the head or was equally startled by the stimulus on both sides, a score of 3 was given. A score of 2 indicated a slow reaction to the stimulus on the contralateral side. Finally, a score of one indicated lack of respond to stimulus on the contralateral side.

Table 2.1: Neurobehavioral assessment after tMCAO in Wistar rats. Adapted from Garcia *et al.* (1995).

.

Test	Score			
	0	1	2	3
Spontaneous activity (in cage for 5 min)	No movement	Barely moves	Moves but does not approach at least three sides of cage	Moves and approaches at least three sides of cage
Symmetry of movements (four limbs)	Contralateral side: no movement	Contralateral side: slight movement to outreach	Contralateral side: moves and outreaches less than right side	Symmetrical outreach
Symmetry of movements (four limbs)	Contralateral side: no movement	Contralateral side: slight movement to outreach	Contralateral side: moves and outreaches less than right side	Symmetrical outreach
Climbing wall of wire cage	...	Fails to climb	Contralateral side is weak	Normal climbing
Reaction to touch on either side of trunk	...	No response on contralateral side	Weak response on contralateral side	Symmetrical response
Response to vibrissae touch	...	No response on contralateral side	Weak response on contralateral side	Symmetrical response

2.2.6.2 Cerebral Tissue Processing

After neurobehavioral testing, animals were sacrified using CO_2 overdose. Brains were carefully extracted and fixed by immersion into ice-cold 10% neutral buffer formalin and kept at 4 °C for at least 24 hours. After fixation, brains were rinsed in PBS and stored in PBS 0.05% Sodium Azide (Sigma-Aldrich, Milano, Italy).

Serial coronal tissue sections (50 μm thick) were obtained using a vibratome (Vibratome 1000 Plus-Tissue Sectioning System). Tissue sections of the brain portion ranging from Bregma +2.5 mm and Bregma -3 mm were sequentially placed in PBS 0.05% Sodium Azide in 24-well plates (1 section/well) and stored at 4 °C.

2.2.6.3 Ischemic Lesion Evaluation: Cresyl Violet Histology

Nineteen consecutive sections with 250 μm interval (bregma + 2.5 mm to - 3.0 mm) were stained with Cresyl Violet. Sections were mounted on slides using PBS and left for 24h at room temperature (RT), allowing the section to strongly adhere to the slides. Sections were first rehydrated by immersion in a series of graded alcohols (Sigma-Aldrich, Milano, Italy) followed by demineralized water and then stained in Cresyl Violet 0.1% (Bio-Optica, Milano, Italy). Afterwars, sections were rinsed in demineralized water and dehydrated by immersion in another series of graded alcohols (Sigma-Aldrich, Milano, Italy). Finally, sections were immersed in Xilene (Sigma-Aldrich, Milano, Italy) prior to mounting the slides using dibutyl phthalate xylene mounting medium (DPX; BDH Laboratory Supplies). The protocol details are illustrated in Table 2.2.

A digital camera (Nikon Coolpix P5000) adaptable to a stereomicroscope was used to obtain images of each section. Areas of contralateral hemisphere, ipsilateral hemisphere and of the ischemic lesion were measured using ImageJ (National Institute of Health, Bethesda, MD, USA).

Infarct volume corrected for inter-hemispheric asymmetries due to cerebral edema was calculated, and expressed in mm^3. Inter-hemispheric asymmetries were corrected using the formula 2.2 (Leach *et al.*, 1993):

$$\textit{Corrected infarct area} = \frac{\textit{measured infarct area} \times \textit{contralateral hemisphere area}}{\textit{ipsilateral hemisphere area}} \tag{2.2}$$

Corrected infarct volume (mm^3) was calculated using the formula 2.3:

Table 2.2: Cresyl Violet staining protocol steps. RT = room temperature.

Step	Solution	Time period (min)	Temperature
1	Ethanol 95%	15	RT
2	Ethanol 70%	1	
3	Ethanol 50%	1	
4	Demineralized water	2	
5	Demineralized water	1	
6	Cresyl Violet	12-15	50°C
7	Demineralized water	1	RT
8	Ethanol 50%	1	
9	Ethanol 70% with glacial acetic acid	1.5	
10	Ethanol 95%	1	
11	Ethanol 95%	few deeps	
12	Ethanol 100%	2	
13	Xilene	5	

$$Correctedinfarctvolume = \frac{D}{3} \cdot [A_1 + 4\sum_{i=2}^{18}(A_n) + 2\sum_{i=3}^{17}(A_m) + A_{19}] \tag{2.3}$$

Where D represents the gap between tissue sections considered (250 μm), A is the correct infarct area (espressed in μm^2) of each section *i* (i = [1;19], i $\in$ N) sequentially considered, with n being pair numbers and m odd numbers.

2.2.7 Molecular Penumbra Evaluation

2.2.7.1 Hsp70 Immunohistochemistry

Brains were processed as described in 2.2.6.2. Briefly, brains were extracted and fixed in ice-cold 10% neutral buffer formalin for at least 24 hours. Serial coronal sections (50 μm thick) were obtained using a vibratome throughout its rostro-caudal extension. For each brain, slices anatomically identified as bregma +1, -1 and -3 were immunoreacted for Hsp70. Free-floating coronal sections were pre-incubated for 10 min in 3% H_2O_2 and 30 min in blocking solution (10% normal goat serum and 0.2% Triton X-100). Sections were then incubated overnight at 4 °C with anti-Hsp70 primary antibody (1:1000, mouse anti-Hsp70, Enzo LifeScience, Farmingdale, New York, USA) and at RT for 75 min with monoclonal Horseradish Peroxidase-conjugated goat anti-mouse IgG (1:200, Millipore, Bellerica, MA, USA) diluted in PBS 1% NGS. Sections were finally incubated with 3,30-diaminobenzidine tetra hydrochloride (DAB) as chromogen.

Negative controls, to verify the specificity of the antibodies, were obtained by omitting primary antibody. Macroscopic section images were obtained using a digital camera (Nikon Coolpix P5000) adapted to optical microscope. Higher magnification images were obtained using a Nikon Eclipse E200 optical microscope and Leica Qwin V3.2.0 software.

2.2.7.2 Hsp70 Topography

Hsp70 topography was obtained by manual identification of stained cell clusters in the cortex, whose areas were superimposed to corresponding brain atlas images at bregma +1, -1 and -3 (Paxinos and Watson, 2007). Each cell cluster is represented by a single pink-colored area of variable size. A darker pink color is the result of variable overlapping degree with adjacent areas from different animals. This method of Hsp70 qualitative topography was not applied in the striatum, where Hsp70-positive cells were mostly present as single cells instead of cell clusters, because of its different cytoarchitecture compared to the cortex.

2.2.7.3 TUNEL staining, NeuN and Hsp70 Triple Co-Immunofluorescence

Triple labeling was obtained by performing TUNEL assay followed by NeuN and Hsp70 immunofluorescence on the same brain sections. The TUNEL kit was used following manufacturer instructions (DeadEnd^{TM} Fluorometric TUNEL System, Promega, Madison, WI, USA), except that the tissue permeabilization step was performed using 0.2% Triton X-100 instead of Protease K. After stopping TUNEL reaction, a further step of incubation with 0.1 M glycine in PBS for 15 min was performed. Sections were then incubated with PBS 10% NGS blocking solution at RT for 30 min and overnight at 4 °C with anti-NeuN primary antibody (1:100, mouse anti-NeuN, Merck Millipore (Chemicon), © Merck KGaA, Darmstadt, Germany) and anti-Hsp70 primary antibody (1:500, rabbit anti-Hsp70, Enzo LifeScience, Farmingdale, New York, USA) diluted in PBS 1% NGS. Afterwards sections were incubated at RT for 75 min with appropriate fluorochrome-conjugated secondary antibody diluted in PBS 1% NGS (1:200, Alexa Fluor 647 goat anti-mouse, Invitrogen, Oregon, USA and 1:200, Alexa Flour 546 goat anti-rabbit, Invitrogen, Oregon, USA). Sections were then rinsed 3 times for 5 min with PBS 0.1% Triton X-100 and 5 mg/mL BSA and finally mounted with polyvinyl alcohol with anti-fading (Polyvinyl Alcohol mounting medium with DABCO® Antifading pH 8.7, Sigma-Aldrich, Milano, Italy).

Negative controls were obtained by omitting primary antibody for Hsp70/NeuN signal or TdT enzyme for TUNEL signal. Microscopy analysis was performed with laser confocal microscopy (Radiance

2100; Biorad Laboratories, Hercules, CA, USA). Noise reduction was achieved by Kalman filtering during acquisition.

2.2.7.4 Hsp70 Signal Analysis: Evaluation of Signal Intensity

A quantitative analysis of the mathematical energy of Hsp70 signal was performed as previously described for quantitative immunohistochemistry (Matkowskyj *et al.*, 2000). An in-house program was developed using Matlab software to obtain automated signal energy difference between corresponding regions of interests (ROIs) in the control and ischemic hemisphere. Briefly, Hsp70 stained sections anatomically identified as bregma +1, -1 and -3 were considered. On each section, four regions of interests (ROIs) were identified corresponding to the entire cortical or striatal regions of each hemisphere. We assume that all information contained in the selected ROIs is of importance. In other words, the amount of antibody-generated chromogen is represented by all the information contained in the image file. After acquisition with a digital camera, the file for the experimental image is opened in the Matlab dedicated program. The ROIs are defined using a tool that allows an area of any pixel dimension to be determined by the operator. The same areas were considered for the cortex, as well as the striatum, in each hemisphere (control and ischemic). The "norm" function was used to compute a unique value of the energy from a three-color image, which represents the mathematical energy of the image file. The energy per pixel is estimated by normalizing the measured energy over the whole ROI to the number of pixels included. Finally, the normalized energy of the ischemic ROIs (cortex or striatum) is subtracted from the corresponding control ROIs (cortex or striatum respectively) and expressed as an absolute value.

2.2.8 Gelatin Ink Perfusion

In a further set of experiments, rats (n = 4) underwent a trans-cardiac perfusion 60 min after the induction of cerebral ischemia, without reperfusion (the intraluminal filament was left in place). Normal saline (200 mL) at 37 °C was infused first followed by 20 mL of gelatine-ink solution at 37 °C (gelatin 3% solution in 0.9% NaCl mixed 1:1 with black ink NSE-40BL, Nihon Kohden, Tokyo, Japan). The brains were then removed and fixed in 10% neutral buffer formalin. To enhance the contrast between ischemic and non-ischemic tissue, brains were imaged using color inversion.

2.2.9 Statistical Analysis

We planned this study with 25 animals in which we regressed their values of collateral flow perfusion against Hsp70 immunohistochemistry intensity signal. Our previous data indicated that the standard deviation of Hsp70 signal was 0.5. Aiming for a slope of the line obtained by regressing collateral flow perfusion against Hsp70 signal above 0.4 to be considered of interest and regression errors below 0.3, we were able to reject the null hypothesis that this slope equals zero with a probability (power) of 0.89. The Type I error probability associated with this test of this null hypothesis was 0.05.

Values were expressed as mean $\pm$ standard deviation (SD). For two-group analysis unpaired Student's t test was used. Correlation and linear regression analyses were computed with Pearson's *r* test. A value of $p < 0.05$ was considered significant.

2.3 Results

2.3.1 Multi-Site Cerebral Perfusion Monitoring During MCA Occlusion

Hemodynamic monitoring with two LD probes was performed during transient MCA occlusion, as shown in Figure 2.2. The position of the probes was decided according to the rat cerebral vascular territories and verified by gelatin-ink perfusion experiments (Figure 2.2-A). Probe 1 (bregma -1 mm, 5 mm from midline) was positioned within the central MCA territory, while Probe 2 (bregma +2 mm, 2 mm from midline) was positioned in the borderzone territory between the cortical branches of ACA and MCA to monitor anterior circulation leptomeningeal collaterals.

Multi-site cerebral perfusion monitoring was performed during the entire period that the animals remained under anesthesia (Figure 2.2-C and D). Mean perfusion deficit after MCA occlusion in Probe 2 was significantly lower ($p < 0.0001$) and more variable compared to Probe 1(Figure 2.2-B). Mean reperfusion values did not differ significantly between the two probes (approximately 92% of baseline, see Figure 2.2-B) and were not correlated to outcome (data not shown).

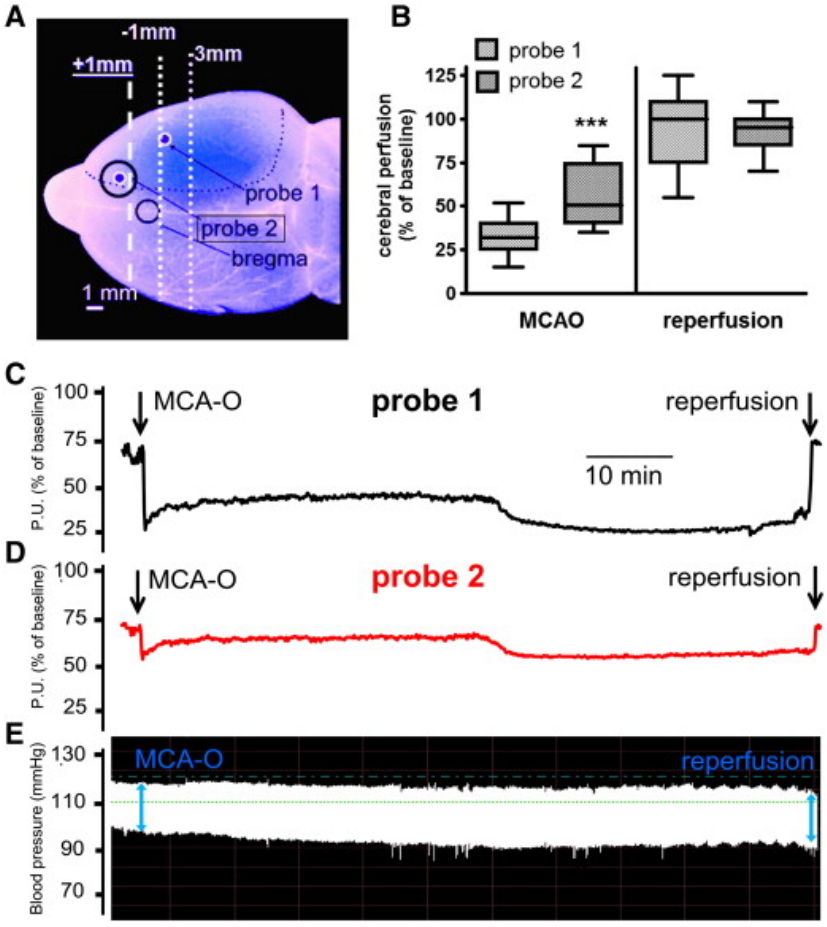

Figure 2.2: Hemodynamic monitoring of intracranial collateral flow (anterior circulation leptomeningeal collaterals) A. Representative brain perfused with gelatin-ink solution after 90 minute ischemia, without reperfusion (intraluminal filament was left in place). After color-inversion, ischemic (not-perfused) area appeared intensely blue-colored, while the rest of the brain appeared violet with white-stained vessels. The positions of the two laser Doppler probes are shown, with reference to their underlying MCA territory (blue dotted line) and bregma. Probe 1 = central MCA territory (-1 mm from bregma, 5 mm from midline); Probe 2 = medial MCA –ACA borderzone territory (+2 mm from bregma, 2 mm from midline). Levels of sections for Hsp70 immunostaining (bregma + 1, - 1 and - 3) are shown (white dotted lines). **B**. Perfusion deficit (% of baseline) in the central MCA territory (Probe 1) and in the MCA–ACA borderzone territory (Probe 2) during MCA-O and reperfusion (n = 25). Laser-Doppler tracings are shown from a representative animal showing a larger perfusion deficit in Probe 1 (**C**) compared to Probe 2 (**D**) during MCA-O, suggesting functionally active intracranial collaterals under ischemic conditions. **E**. Representative tracing of invasive blood pressure monitoring during MCA-O and reperfusion. *** $p < 0.0001$ compared to Probe 1. MCA = middle cerebral artery. MCA-O = middle cerebral artery occlusion; ACA = anterior cerebral artery; P.U. = perfusion units.

Arterial pressure was continuously monitored (Figure2.2-E) and did not show significant changes during MCA occlusion (mean arterial pressure 114 mmHg; intra-subject SD 6 mmHg; inter-subject SD 19 mmHg; see Figure 2.3).

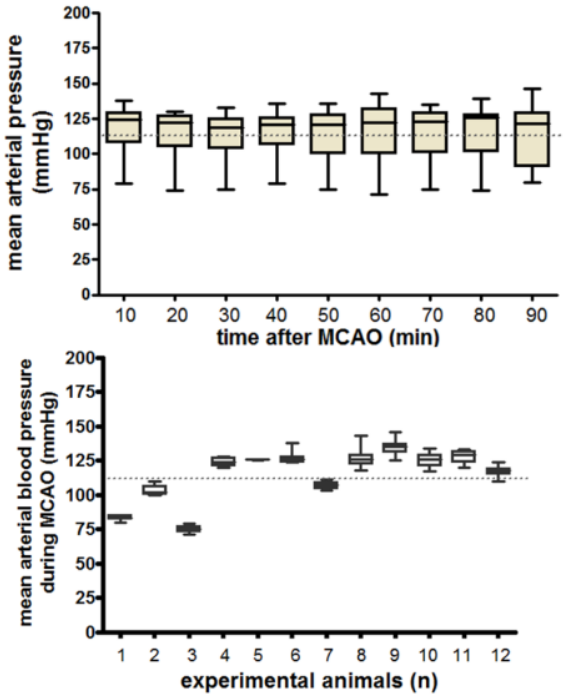

Figure 2.3: Invasive blood pressure monitoring during transient middle cerebral artery occlusion (MCAO). Upper graph shows mean blood pressure values (n = 12) every 10 minutes interval, demonstrating no significant variation of blood pressure over the ischemic period of 90 min. Lower graph shows mean blood pressure values of each animal, demonstrating small intra-subject variability of blood pressure during the entire ischemic period.

A biosignal fluctuation analysis of cerebral perfusion tracings, before and after MCA occlusion, showed that the degree of auto-correlation was similar in both probes in the pre-ischemic period, while it differed significantly during ischemia (Figure 2.4). Although the auto-correlation coefficient increased in both probes compared to the pre-ischemic period, a significantly larger increase was observed in Probe 1 (approximately tripled; $p < 0.001$ versus pre-ischemic values) compared to Probe 2 (approximately doubled; $p < 0.05$ versus pre-ischemic values) during ischemia.

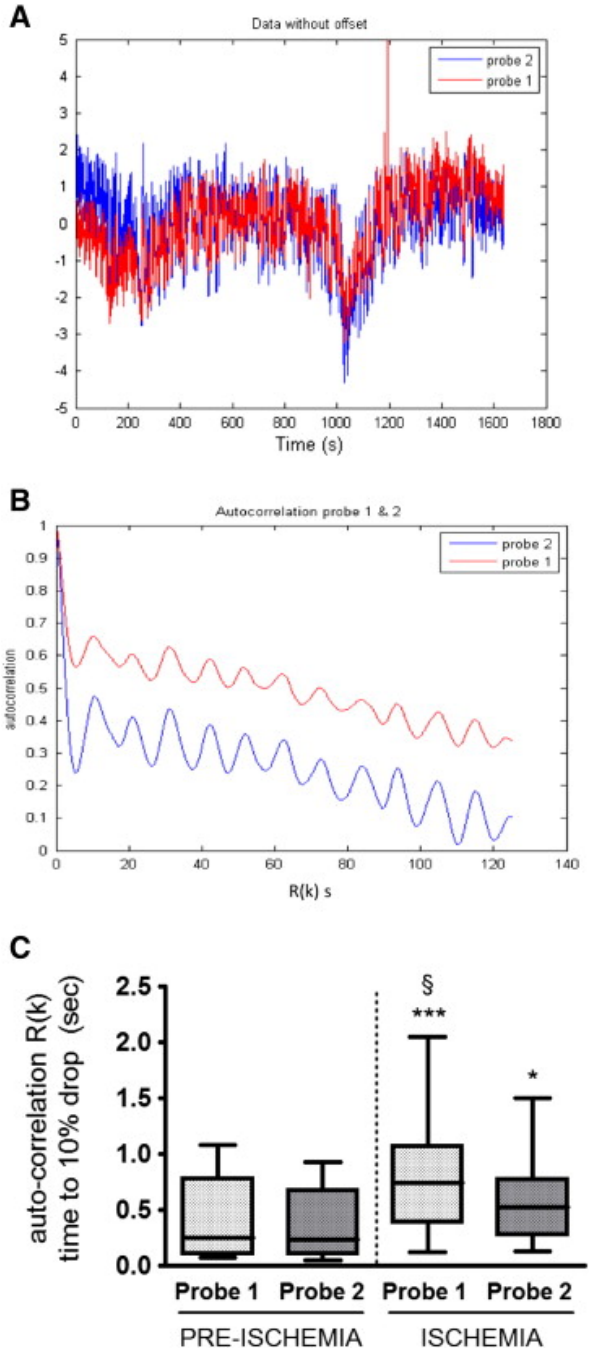

Figure 2.4: Biosignal fluctuation analysis of cerebral perfusion in the central MCA territory (Probe 1) and in the MCA–ACA borderzone territory (Probe 2) at baseline and during MCAO. Regions of interests (ROIs) of laser Doppler tracings were selected and averaged for offset (**A**). Self-memory of the signal was calculated and expressed as auto-correlation analysis over time for Probe 1 and Probe 2 (**B**). Self-memory of the signal was quantified (**C**) as the time to 10% drop in auto-correlation for Probe 1 and Probe 2, either before ischemia and during MCA-O. *** $p < 0.001$ compared to pre-ischemic Probe 1. * $p < 0.05$ compared to pre-ischemic Probe 2. § $p < 0.05$ compared to ischemic Probe 2. MCA = middle cerebral artery; ACA = anterior cerebral artery; MCAO = middle cerebral artery occlusion; R(k) = auto-correlation function.

2.3.2 Topography of the Molecular Penumbra

Hsp70 immunoreactivity was assessed 24 hours after reperfusion at sections bregma +1, -1 and -3. Immunofluorescent triple staining confirmed that neuronal Hsp70 labeling and apoptotic neuronal nuclei were mutually exclusive, confirming that Hsp70 positive cells represented surviving neurons (Figure 2.5; see Figure 2.6 for details on the transition zone between ischemic core and penumbra). The pattern of Hsp70 staining was consistently different in the cortex compared to the striatum (Figure 2.7-A). In particular, cortical staining showed discrete areas of intensely marked cell clusters (Figure 2.7-B and C), whereas sparse single stained cells were observed in the striatum (Figure 2.7-D and E). Mapping of cortical cell clusters allowed visualizing the topographical distribution of the penumbra in the cortex, which consisted in multiple areas with considerable fragmentation and variable degree of overlaps among different animals (Figure 2.7-F).

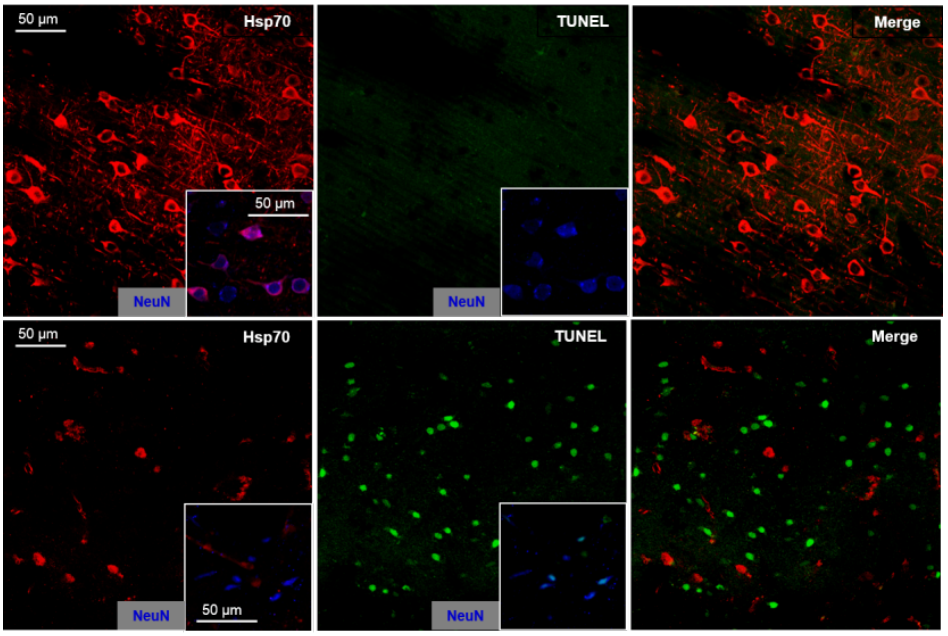

Figure 2.5: Triple staining immunohistochemical characterization of the post-reperfusion (24h) penumbra. Penumbral areas showed Hsp70-immunoreactive cells, co-labeling with the neuronal cell marker Neu-N, and absence of TUNEL-positive nuclei (**A**–**C**). Ischemic core areas showed TUNEL-positive nuclei, co-labeled with Neu-N, and absence of Hsp70-immunoreactive cells with neuronal co-labeling (**D**–**F**). Sparse Hsp70-positive non-neuronal cells were observed in the ischemic core, which did not co-localize with TUNEL-positive nuclei. Representative micrographic pictures are shown. Hsp70 = Heat Shock Protein 70 kDa.

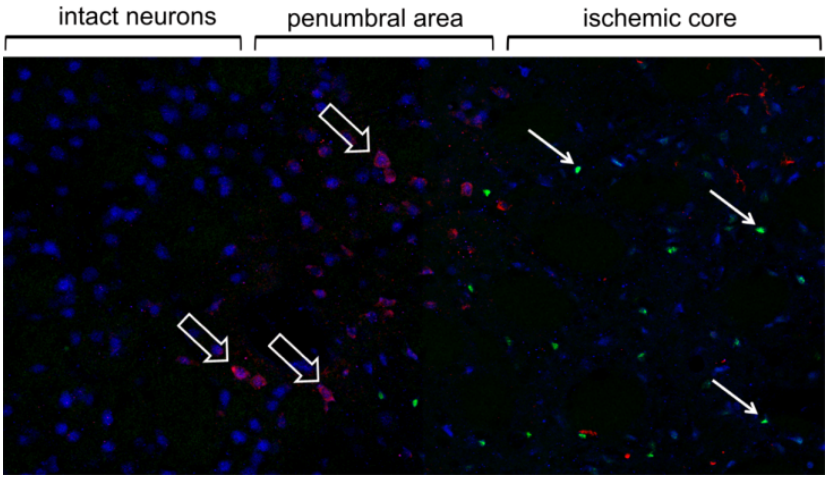

Figure 2.6: Representative view of the "transition zone" between intact and ischemic tissue 24h after transient middle cerebral artery occlusion. Brain sections were stained with triple immunofluorescence for NeuN (neuronal cells; blue), Hsp70 (penumbra; red) and TUNEL (apoptotic nuclei; green). Healthy neurons (NeuN +, Hsp70 -, TUNEL -), penumbral neurons (NeuN +, Hsp70 +, TUNEL -; open arrows) and apoptotic neurons (NeuN +, Hsp70 -, TUNEL +; small arrows) appear as separate cell populations with a clear topographical demarcation.

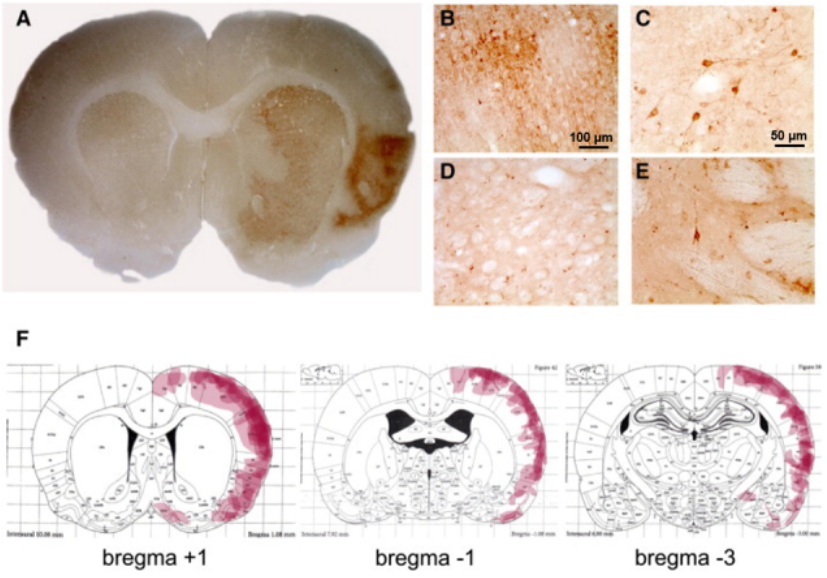

Figure 2.7: Morphology and topographic distribution of post-reperfusion penumbra. A. Representative picture of Hsp70 staining 24h after transient MCA-O (90 min) on brain section at bregma + 1. Higher magnification pictures showing Hsp70-positive cells with neuronal morphology, which were observed in clusters in the cortex (**B**. 10x; **C**. 20x) and as single cells in the striatum (**D**. 10x; **E**. 20x). **F**. Topographical mapping of Hsp70-immunoreactive cell clusters in the cortex at bregma levels + 1, - 1 and - 3. Each cell cluster is represented by a single pink-colored area of variable size. A darker pink color is the result of variable overlapping degree with adjacent areas from different animals.

2.3.3 Quantification of the Molecular Penumbra in Relation to Infarct Size and Functional Deficit

Hsp70 signal was quantified in selected ROIs in the cortex and striatum as shown in Figure 2.8-A. A positive correlation was observed between Hsp70 signal (at section bregma + 1) and infarct volume in both the cortex (Figure 2.8-A; $p < 0.001$; Pearson's r = 0.67) and the striatum (Figure 2.8-D; $p < 0.05$; Pearson's r = 0.47). This correlation was also observed at other brain sections, namely at bregma -1 and -3 (Figure 2.9). A negative correlation was observed between Hsp70 signal (at section bregma +1) and neuroscore in both the cortex (Figure 2.8-C; $p < 0.05$; Pearson's r = -0.49) and the striatum (Figure 2.8-E; $p < 0.01$; Pearson's r = -0.54).

2.3.4 Quantification of the Molecular Penumbra in Relation to Intracranial Collateral Flow

No correlation was observed between Hsp70 signal (at section bregma + 1) and cerebral perfusion in Probe 1 in both the cortex (Figure 2.10-A) and the striatum (Figure 2.10-B). Conversely, a negative correlation was observed between Hsp70 signal (at section bregma + 1) and cerebral perfusion in Probe 2 in both the cortex (Figure 2.10-C; $p < 0.01$; Pearson's r = -0.54) and the striatum (Figure 2.10-D; $p < 0.05$; Pearson's r = -0.42). Interestingly, this correlation was gradually lost in more distant brain sections, namely bregma - 1 and - 3 (Figure 2.11).

A negative correlation ($p < 0.001$; Pearson's r = -0.62) was observed between infarct volume and cerebral perfusion in Probe 2, while this was not observed in Probe 1 (Figure 2.12).

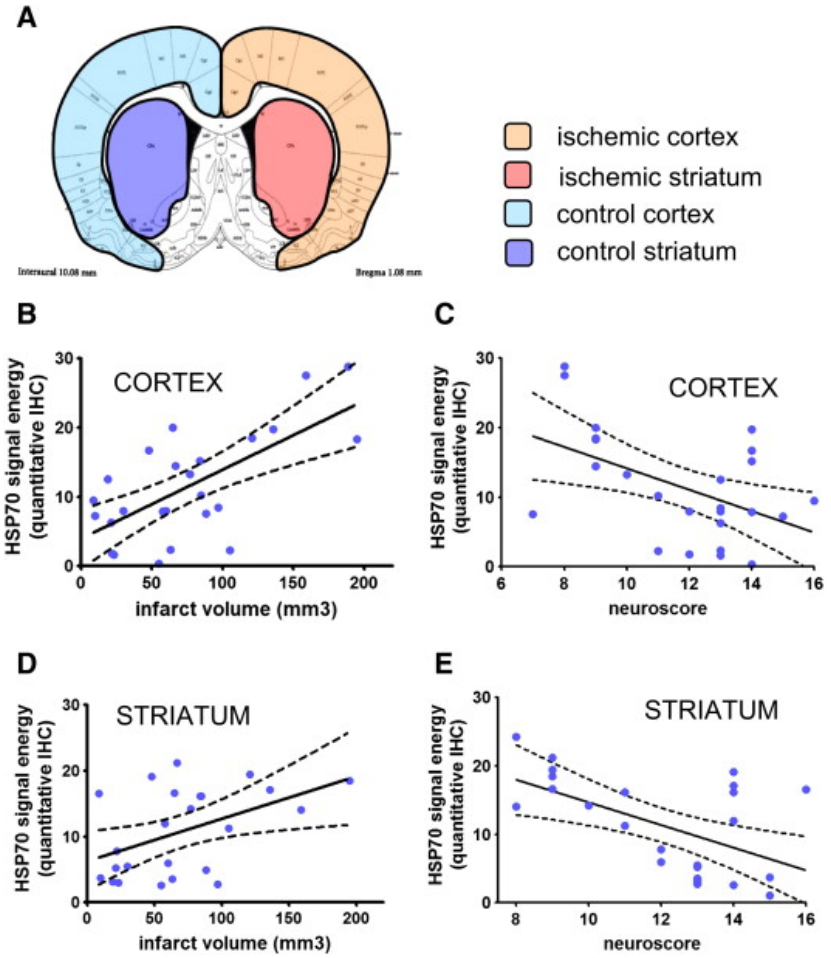

Figure 2.8: Quantitative immunohistochemistry of Hsp70 after transient MCAO in relation to structural and functional outcome. **A**. Representation of the four selected regions of interests (ROIs) in section bregma + 1, which were selected for quantification of Hsp70 immunoreactivity using a dedicated software for calculating the mathematical energy of Hsp70 signal. **B**. A positive correlation ($p < 0.001$, Pearson's $r = 0.67$) was observed between Hsp70 energy signal in the cortex (section bregma + 1) and corresponding infarct volume. **C**. A negative correlation ($p < 0.05$, Pearson's $r = -0.49$) was observed between Hsp70 energy signal in the cortex (section bregma +1) and corresponding neuroscore. **D**. A positive correlation ($p < 0.05$, Pearson's $r = 0.47$) was observed between Hsp70 energy signal in the striatum (section bregma +1) and corresponding infarct volume. **E**. A negative correlation ($p < 0.01$, Pearson's $r = -0.54$) was observed between Hsp70 energy signal in the striatum (section bregma +1) and corresponding neuroscore. IHC = immunohistochemistry.

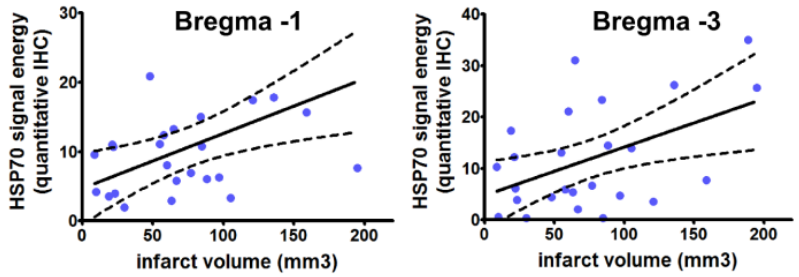

Figure 2.9: Quantitative immunohistochemistry of Hsp70 after transient MCAO in relation to infarct volume in sections bregma - 1 and - 3. A positive correlation was observed between Hsp70 energy signal in the cortex and corresponding infarct volume for brain sections at bregma -1 (left graph; $p < 0.01$, Pearson's $r = 0.52$) and bregma -3 (right graph; $p < 0.05$, Pearson's $r = 0.48$). IHC = immunohistochemistry.

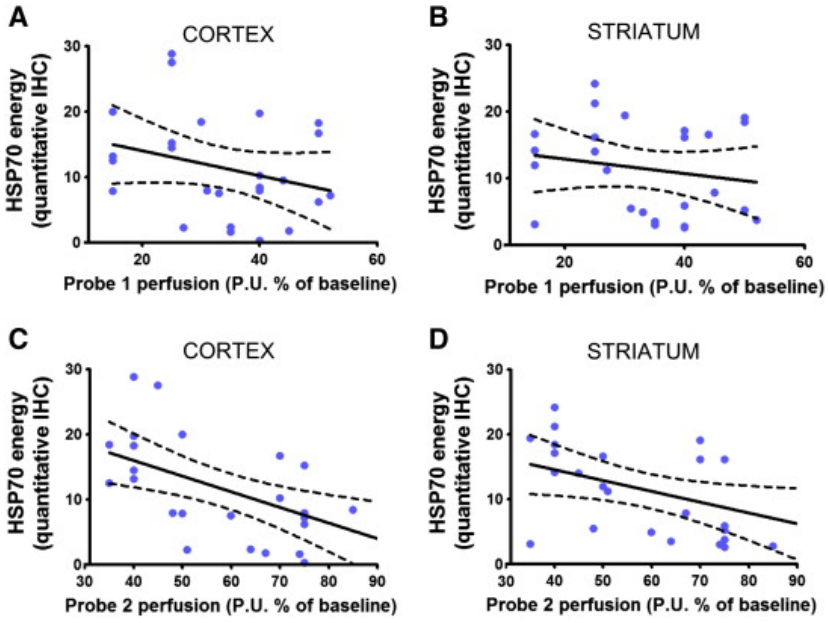

Figure 2.10: Correlation between Hsp70 energy signal and hemodynamic monitoring in Probe 1 (central MCA territory) and Probe 2 (MCA–ACA borderzone territory). A. No correlation was observed between perfusion values in Probe 1 during MCA occlusion and Hsp70 energy signal in the cortex (bregma section +1). **B**. No correlation was observed between perfusion values in Probe 1 during MCA occlusion and Hsp70 energy signal in the striatum (bregma section +1). **C**. A negative correlation ($p < 0.01$, Pearson's $r = -0.54$) was observed between perfusion values in Probe 2 during MCA occlusion and Hsp70 energy signal in the cortex (bregma section +1). **D**. A negative correlation ($p < 0.05$, Pearson's $r = -0.42$) was observed between perfusion values in Probe 2 during MCA occlusion and Hsp70 energy signal in the striatum (bregma section +1). IHC = immunohistochemistry; P.U. = perfusion units; MCA = middle cerebral artery; ACA = anterior cerebral artery.

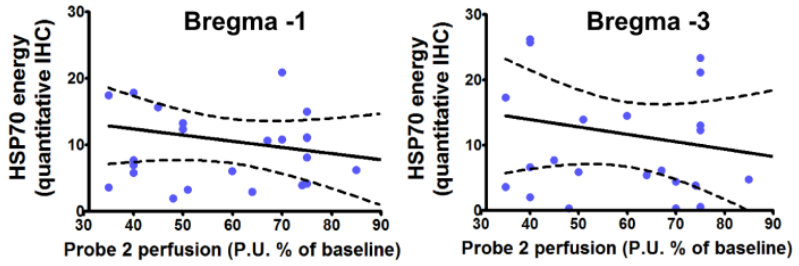

Figure 2.11: Quantitative immunohistochemistry of Hsp70 after transient MCAO in relation to cerebral collateral flow (Probe 2). No correlation was observed between Hsp70 energy signal in the cortex at bregma -1 (left graph) and bregma -3 (right graph) and cerebral collateral flow (measured at bregma +1). IHC = immunohistochemistry.

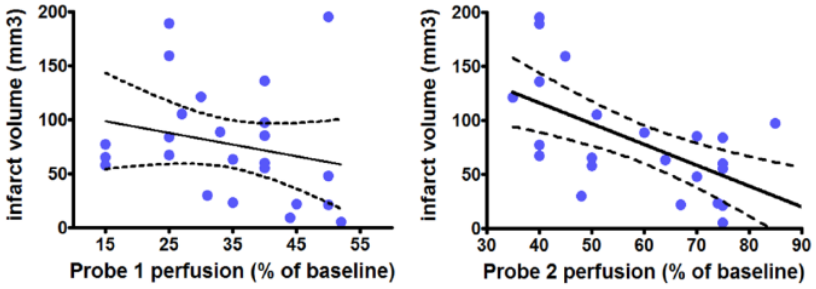

Figure 2.12: Correlation between infarct volume and cerebral perfusion in Probe 1 (central MCA territory) and Probe 2 (MCA–ACA borderzone territory) during MCA occlusion. No correlation was observed between infarct volume and cerebral perfusion in Probe 1 (left graph). A negative correlation (right graph; p = 0.001, Pearson's r = -0.62) was observed between infarct volume and cerebral perfusion in Probe 2. MCA = middle cerebral artery; ACA = anterior cerebral artery.

2.4 Discussion

The functional performance of intracranial collaterals is crucially involved in the pathophysiology of acute ischemic stroke (Liebeskind, 2012). Functionally active cerebral collaterals have been associated with reduced penumbra loss (Jung *et al.*, 2013) and better outcomes (Cortijo *et al.*, 2014) in acute stroke patients, even with delayed reperfusion. Therapeutic modulation of cerebral collateral flow is being proposed (Shuaib *et al.*, 2011b) and may be used for widening the therapeutic window for recanalization and enhancing delivery of neuroprotective drugs.

The endurance of "tissue at risk" in the setting of hypoperfusion has been postulated to be dependent on collateral flow in humans (Liebeskind, 2013). Nonetheless, the relationship between the degree of collateral perfusion and the extent and evolution of ischemic penumbra in acute ischemic stroke has not been investigated in experimental studies and remains an important unsolved issue. The definition of penumbral tissue in current stroke research mostly relies on MRI imaging in human (Schlaug *et al.*, 1999) and animal models (Reid *et al.*, 2012), applying diffusion-weighted imaging (DWI) and perfusion-weighted imaging (PWI) and calculating the PWI–DWI mismatch. This method has been demonstrated to predict clinical outcome and final infarct size in stroke patients undergoing endovascular therapy (Lansberg *et al.*, 2012; Wheeler *et al.*, 2013). Nonetheless it is recognized that PWI–DWI mismatch cannot define the penumbra with absolute accuracy in humans (Heiss, 2011) and in animals (Duong, 2012) and remains unsatisfactory for pathophysiological studies assessing tissue viability and response to injury. Moreover, the pattern of DWI lesions and PWI–DWI mismatch in the first hours after acute ischemic stroke has been shown to display significant inter-individual variability and evolve over time (Olivot *et al.*, 2009).

Our experimental study investigated the dynamic relationship between cerebral collateral flow and the development of molecular penumbra, after intraluminal proximal MCA occlusion (90 min) followed by 24-hours reperfusion. We mapped and quantified the ischemic penumbra by molecular activation of Hsp70. The extent of this "molecular penumbra" was related to the vascular perfusion deficit in the acute phase and to the structural and functional outcome at 24h.

Our findings indicate that good collateral flow during MCA occlusion reduces the molecular activation associated with penumbral tissue, providing complete protection from ischemic injury in variable areas of the cortex and striatum, if reperfusion is achieved. Conversely, poor collateral status is associated with a greater extent of both ischemic core and molecular penumbra.

This new scenario of the interplay between cerebral collateral flow and ischemic penumbra might have

potential translational applications. Therapeutic strategies aimed to enhance collateral circulation early after arterial occlusion may completely prevent the "ischemic cascade" in a significant amount of brain tissue, expanding the therapeutic effect of recanalization therapies and reducing their risks.

The study of intracranial collaterals and cerebral hemodynamic changes in experimental ischemic stroke remains largely unexplored (Sutherland *et al.*, 2011), mostly because of the technical difficulties in obtaining a quantitative assessment of the dynamic response of collateral vessels. Our group recently developed an optimized system for cerebral perfusion monitoring in rats (Beretta *et al.*, 2013), demonstrating that leptomeningeal collateral flow showed significant variability during MCAO in rats and is a strong predictor of "hard outcomes" such as infarct size and functional deficit (Riva *et al.*, 2012), while its relationship to the penumbra remained to be explored.

Our findings confirm the utility of multi-site LD monitoring in the central and peripheral MCA territories as an easy and reliable method to quantify cerebral collateral flow during proximal MCA occlusion. A gradient of severity between the two probes was observed either by relative perfusion deficit or biosignal fluctuation analysis. In particular, hemodynamic monitoring in LD Probe 2, in the territory of MCA–ACA leptomeningeal branches, showed a cortical area with a lower perfusion deficit, higher inter-individual variability and larger fluctuations of the biosignal, compared to LD Probe 1 in the central MCA territory. In most animals the topographical mapping of molecular penumbra (Hsp70 positive areas after 24 hours of reperfusion) revealed multiple patchy areas with irregular distribution, not limited to the perilesional zone; this is in contrast with the final infarct, which invariably consisted in a single lesion of variable size. Our results confirmed that Hsp70-stained neurons are a separate population from neurons undergoing selective cell death (TUNEL-stained neurons), in agreement with previous reports (del Zoppo *et al.*, 2011).

Surprisingly, we observed a striking correlation between the extent of molecular penumbra and stroke severity, in terms of both infarct volume and neuroscore. Notably, small infarcts (mostly limited to the striatum) were associated with little (if any) penumbral tissue, whereas larger infarcts involving the striatum and cortex were associated with larger areas of molecular penumbra. No animals exhibited a pattern of small ischemic core surrounded by large penumbral areas.

A strong correlation was observed between the extent of molecular penumbra and the severity of perfusion deficit in the peripheral MCA territory (Probe 2), which reflects intracranial collateral perfusion. Interestingly, no correlation was observed in the extent of molecular penumbra and perfusion deficit in the central MCA territory (Probe 1).

In other terms, the presence of good collaterals reduced the extent of both molecular penumbra and

ischemic core at 24 hours, increasing the amount of uninjured (completely "saved") cerebral tissue. Two additional results strengthen the specificity of these findings: first, the correlation between perfusion deficit in Probe 2 and Hsp70-stained areas is stronger at level bregma + 1 (the nearest to the Probe 2 position) and gradually diminishes with distance, i.e. bregma - 1 and - 3; second, arterial blood pressure neither showed significant changes during the ischemic phase (90 min) nor correlated with the final stroke outcome in our series.

The major limitation of our study is that acute penumbral MRI imaging using DWI–PWI mismatch has not been performed and molecular penumbra was assessed 24h after reperfusion, as this was necessary to obtain a useful Hsp70 staining. However, cerebral collateral flow was the main focus of the study and this can be quantified more reliably with multi-site LD monitoring than with current MRI technology in small animals. The relationship between acute penumbral MRI imaging and molecular penumbra assessed by Hsp70 staining is beyond the scope of this study and is currently being explored in new experiments. Although acute MRI-defined penumbra could be expected to be larger than molecular penumbra after 24 hours of reperfusion (due to the progressive recruitment of penumbra into infarct core), this is unlikely to change the major findings of the present study.

2.5 Conclusions

The degree of cerebral collateral perfusion inversely correlated with both ischemic core and molecular penumbra during transient proximal MCA occlusion. Our findings prompt the development of collateral therapeutics to provide tissue-saving strategies in the hyper-acute phase of ischemic stroke prior to recanalization therapy.

Chapter 3

Multi-Site Laser Doppler Flowmetry for Assessing Collateral Flow in Experimental Ischemic Stroke: Validation of Outcome Prediction with Acute MRI

Cuccione E[1], Versace A[2], Cho TH[3], Carone D[2], Ong E[3], Berner LP[3], Rousseau D[4], Cai R[2], Monza L[2], Ferrarese C[5], Sganzerla EP[5], Berthezène Y[3], Nighoghossian N[3], Wiart M[4], Beretta S[5*], Chauveau F[6*].

In preparation

[1] Laboratory of Experimental Stroke Research, School of Medicine, University of Milano Bicocca, Monza, Italy; PhD Program in Neuroscience, University of Milano Bicocca, Monza, Italy.

[2] Laboratory of Experimental Stroke Research, School of Medicine, University of Milano Bicocca, Monza, Italy.

[3] Université de Lyon, CREATIS; CNRS UMR5220; Inserm U1044; INSA-Lyon; Université Lyon 1, Lyon, France; Hospices Civils de Lyon, France.

[4] Université de Lyon, CREATIS; CNRS UMR5220; Inserm U1044; INSA-Lyon; Université Lyon 1, Lyon, France.

[5] Laboratory of Experimental Stroke Research, School of Medicine, University of Milano Bicocca, Monza, Italy; Milan Center for Neuroscience (NeuroMi), Milan, Italy.

[6] Université de Lyon, Lyon Neuroscience Research Center; CNRS UMR5292; Inserm U1028; Université Lyon 1, Lyon, France.

* These authors equally contributed to this work

Abstract

High variability in infarct size is common in experimental stroke models and highly affects statistical power and validity of preclinical neuroprotection trials. The aim of this study was to explore cerebral collateral flow as a stratification factor for the prediction of ischemic outcome, using magnetic resonance imaging (MRI) as a reference.

Transient intraluminal occlusion of the middle cerebral artery (MCA) was induced for 90 minutes in 18 rats. Cerebral collateral flow was assessed intra-procedurally using multi-site laser Doppler flowmetry (LDF) monitoring in both the lateral MCA territory and the borderzone territory between the leptomeningeal branches of MCA and anterior cerebral artery. Multi-modal MRI was used to assess acute ischemic lesion (diffusion weighted imaging, DWI), acute perfusion deficit (time to peak, TTP) and final ischemic lesion at 24 hours.

Final ischemic lesion volume and infarct typology (large hemispheric versus basal ganglia infarcts) was predicted by both intra-ischemic cerebral collateral perfusion and acute DWI lesion volume. Cerebral collateral flow assessed by multi-site LDF correlated with the corresponding acute perfusion deficit using TTP maps. Multi-site LDF monitoring for collateral flow assessment was able to predict ischemic outcome and perfusion deficit in good agreement with acute MRI.

Our results support the additional value of cerebral collateral flow monitoring for outcome prediction in experimental ischemic stroke, especially when acute MRI facilities are not available.

3.1 Introduction

The failure of promising preclinical neuroprotective therapies to translate into successful clinical results raised discussions about the quality of preclinical trials (Dirnagl, 2006; Dirnagl and Fisher, 2012). Among several aspects, attention should be addressed to the poor statistical power of most neuroprotection studies, mainly driven by small sample size and variability of lesion size in ischemic models. Several factors may account for this variability, including the collateral circulation (Riva *et al.*, 2012; Zhang *et al.*, 2010). The collateral circulation is a subsidiary vascular network virtually able to provide residual perfusion to potentially salvageable cerebral regions after occlusion of a cerebral artery (Liebeskind, 2003). It is emerging as a strong determinant of stroke outcome not only in humans (Miteff *et al.*, 2009), but also in experimental stroke models (Riva *et al.*, 2012; Zhang *et al.*, 2010).

In neuroprotection studies, predicting ischemic outcome before animal allocation would allow researchers to a priori stratify animals relying on the lesion size and consequently control the variability-related bias. Multimodal Magnetic Resonance Imaging (MRI) performed during occlusion has previously been used in neuroprotection studies (Bardutzky *et al.*, 2005a; Chauveau *et al.*, 2011; Cho *et al.*, 2013; Minematsu *et al.*, 1993). In particular, a strong correlation between acute and 24h ischemic lesion was shown (Chauveau *et al.*, 2012). While MRI provides spatial resolution, Laser Doppler Flowmetry (LDF) instead monitors cortical perfusion within a precise cortical region, where a recording probe is positioned. A single LDF probe is commonly monitoring in the lateral middle cerebral artery (MCA) territory (Esposito *et al.*, 2013; Hungerhuber *et al.*, 2006; Kläsner *et al.*, 2006; Taninishi *et al.*, 2015), but the perfusion threshold to stratify animals is not well standardized.

In the present work, two probes were used for the monitoring of cortical perfusion in two different regions (Beretta *et al.*, 2013): the lateral MCA territory and the borderzone between anterior and middle cerebral arteries (ACA-MCA) territories, in order to monitor the perfusion drop due to occlusion and the residual perfusion provided by the leptomeningeal anastomoses (i.e. collateral circulation), respectively. We previously showed a correlation between the collateral perfusion evaluated by multi-site LDF and both 24 hours outcome (Riva *et al.*, 2012) and molecular penumbra (Beretta *et al.*, 2015).

The aim of this study was to validate the predictive value of collateral flow assessment by multi-site LDF monitoring using MRI in the intraluminal MCA occlusion (MCAO) in rats. The results show the

additional value of multi-site LDF compared to single-site LDF for outcome prediction, suggesting its potential as a good alternative to MRI for controlling the variability of lesions.

3.2 Material and Methods

3.2.1 Animals and experimental design

The experimental protocol was approved by the Committee on Animal Care of the University of Milano Bicocca Italy, and of the CNRS (CREEA Rhône-Alpes, France, approval n°0274). Procedures were performed in accordance with the European Union Directive for animal experiments (2010/63/EU), the national guidelines on the use of laboratory animals (D.L. 116/1992), under project licence from the Italian Ministry of Health and French Decree 2013-118.

Adult male Wistar rats were housed at a constant temperature of 22 $\pm$ 2°C in Plexiglas cages in groups of six in a colony room maintained on a 12/12 hours light/dark cycle (07:00–19:00), and were provided with food and water ad libitum.

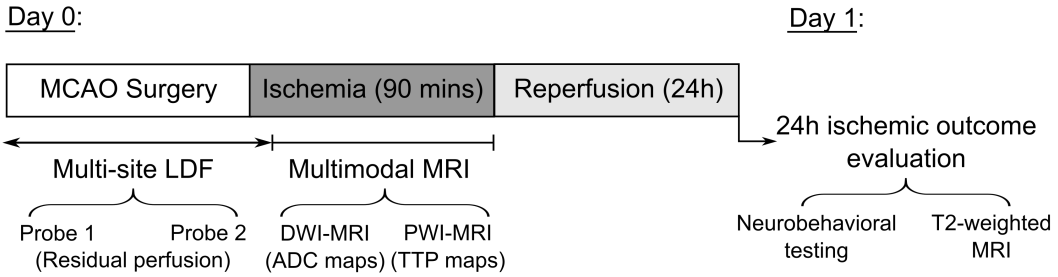

Figure 3.1: Experimental Design. On Day 0, animals (n=18) underwent 90-minutes of focal cerebral ischemia induced by intraluminal MCAO. Cerebral perfusion was monitored by multi-site LDF during surgery up to occlusion induction and for 10 minutes after. Next, animals underwent multiparametric MRI, including DWI and PWI for the respective evaluation of acute lesion and perfusion during occlusion. After 90 minutes of ischemia, animals were reperfused. On Day 1, after 24 hours of reperfusion, neurobehavioral assessment and T2-MRI imaging were performed. MCAO = middle cerebral artery occlusion; LDF = laser Doppler flowmetry; MRI = magnetic resonance imaging; DWI = diffusion weighted imaging; PWI = perfusion weighted imaging; ADC = apparent diffusion coefficient; TTP = time to peak.

Experimental design is illustrated in Figure 3.1. On Day 0, animals (250-300 g; n = 18) underwent 90-minutes of focal cerebral ischemia induced by intraluminal MCAO. Cerebral perfusion was

monitored by multi-site LDF during surgery and occlusion induction. Afterwards, LDF probes were detached and animals were immediately transferred to the scanner to undergo multiparametric MRI (T2-weighted imaging, diffusion weighted imaging or DWI and perfusion weighted imaging or PWI) for the respective evaluation of anatomy, acute lesion and perfusion during occlusion. The imaging session started approximately 40 minutes after ischemic onset. After 90 minutes of ischemic, animals were reperfused outside the magnet. On Day 1, after 24 hours of reperfusion, neurobehavioral assessment and T2-MRI imaging were performed. Animals were then euthanized under deep anesthesia.

Early death and signs of subarachnoid haemorrhage detected by MRI were used as exclusion criteria.

All investigators were blind to data obtained with other modalities than the one they performed and/or analyzed.

A total number of 18 rats were enrolled in the study. Three rats did not complete the protocol because of they died early after ischemia, likely because of anesthesiological complications or/and massive infarcts. Hence, 15 rats were included in the analysis. No signs of subarachnoid haemorrhage were detected by MRI.

3.2.2 MCAO Surgery

On Day 0, rats were anesthetized with 3% isoflurane air, and maintained with 1.5% isoflurane. Before surgery, animals received 0.05 mg/kg subcutaneous buprenorphine to alleviate pain and throughout surgical procedure, their body temperature was monitored by a rectal thermometer and maintained to $37.0 \pm 0.5^{\circ}$C by a feedback-controlled heating pad.

A silicon-coated filament (diameter 0.39 ± 0.02 mm, Doccol Corporation, Redlands, CA, USA) was inserted into the right external carotid artery and advanced in the internal carotid artery under LDF monitoring (see below), reaching and occluding the MCA origin. Immediately before filament insertion, common carotid artery (CCA) was transiently occluded and subsequently re-opened during ischemia and reperfusion.

After 90-minutes, the filament was withdrawn and animals were allowed to recover and had free access to food and water.

3.2.3 Multi-Site Laser Doppler Flowmetry

An LDF apparatus (dual channel moorVMS-LDF^{TM}, Moor, Axminster, UK) was used to continuously monitor cerebral perfusion during MCAO surgery, up to occlusion induction and for 10 minutes after. Two blunt needle probes (VP12, Moor, Axminster, UK) were firmly positioned on the intact skull surface thanks to a custom-made silicon probe holder (Beretta *et al.*, 2013). The cranial coordinates for probes positioning were based on a rat brain atlas (Paxinos and Watson, 2007). A first probe (Probe 1) monitored perfusion within the lateral MCA territory, corresponding to the core territory of MCA (1 mm posterior to the Bregma and 5 mm lateral to the midline). A second probe (Probe 2) monitored perfusion within the borderzone territory between ACA and MCA territory (2 mm anterior to the Bregma and 2 mm lateral to the midline), where leptomeningeal anastomoses are likely to provide residual perfusion after occlusion induction. For both probes, the residual perfusion after occlusion was expressed as % of pre-ischemic baseline.

3.2.4 Magnetic Resonance Imaging

MRI experiments were performed on a Bruker Biospec 7T/12 cm horizontal magnet equipped with Paravision 5.0 (Bruker, Ettlingen, Germany). A birdcage head coil of 72 mm inner diameter was used for radiofrequency transmission, and a 25 mm-diameter surface coil was used for reception. The rats were placed in a cradle equipped with a stereotaxic holder, an integrated heating system to maintain body temperature at 37 $\pm$ 1°C, and a pressure probe to monitor respiration.

3.2.4.1 MRI Sequences

During arterial occlusion, both DWI and PWI were performed. DWI echo planar imaging (EPI) spin-echo images were acquired using field of view (FOV) = 3.0 x 1.5 cm^2, fifteen contiguous slices of 1 mm thickness, with matrix = 128 x 64, echo time/repetition time (TE/TR) = 22.75/5250 ms, and six b-values (100, 200, 400, 600, 800, 1000 s/mm^2) for a total duration of 4 minutes 54 s.

PWI was performed with multislice dynamic susceptibility contrast-enhanced MRI (DSC-MRI), using an EPI gradient-echo sequence with the same FOV and slice characteristics, matrix = 80 x 40 and TE/TR 6.61/600 ms, for a total duration of 1 minute. One hundred consecutive images were acquired per slice with a time resolution of 0.6 s during before, during and after the intravenous injection of a 200-μmol/kg bolus of gadolinium (Dotarem, Guerbet Aulnay-sous-Bois, France).

After 24 hours of reperfusion, T2-weighted images were acquired using a RARE sequence with the same FOV and slice characteristics, matrix = 256 x 128, effective TE/TR = 60.28/3500 ms, RARE factor 8 and 4 averages (total duration: 2 minutes 48 s).

3.2.4.2 Maps Computation

Apparent Diffusion Coefficient (ADC) maps (in mm^2/s) were calculated from DWI images by fitting MR signal curves to a monoexponential model function on a pixel-by-pixel basis using in-house software written in Matlab 2009 (MathWorks, Natick, MA).

Time To Peak (TTP) maps (in s) were calculated from PWI images after converting the signal-time curves to concentration-time curve according to: $\Delta R_2{}^*(t) = -\frac{1}{TE} \cdot \ln \frac{S(t)}{S_0}$ as the time between the first T2*-weighted measurement and the bolus peak (Neumann-Haefelin *et al.*, 1999).

3.2.4.3 Image Analysis

Images were analyzed on MIPAV software (Medical Image Processing And Visualization, NIH, Bethesda, MD; http://mipav.cit.nih.gov/) (McAuliffe *et al.*, 2001).

For the evaluation of acute ischemic lesion, the ipsilateral regions encompassing hypointense signal (compared to contralateral hemisphere) were manually outlined on ADC maps. Subsequently, the acute ischemic lesion was segmented in these regions by applying the already reported viability threshold of 0.53×10^{-3} mm^2/s (Shen *et al.*, 2003) and lesion volume (expressed in mm^3) was calculated.

For the evaluation of cerebral perfusion, TTP maps were used. Ipsilateral and contralateral ROIs covering the upper cortex were delineated on the slices corresponding to the two regions of LDF monitoring: slice anatomically identified as Bregma -1 and Bregma +2, for Probe 1 and Probe 2, respectively. The ipsilateral and contralateral average TTP values were considered. Assuming the contralateral perfusion to be comparable to pre-ischemic perfusion (Schmid-Elsaesser *et al.*, 1998b), the difference between ipsilateral and contralateral TTP values was considered to reflect the residual perfusion monitored by LDF (relative TTP).

3.2.5 24h Ischemic Outcome Evaluation

On Day 1, ischemic outcome was assessed after 24 hours of reperfusion by both neurobehavioral testing and T2-weighted MRI for the assessement of final lesion volume.

3.2.5.1 Neurobehavioral Testing

Just before Day 1 MRI acquisitions, rats were evaluated for spontaneous activity, motor and sensitive function and scored on a scale from 3 (most severe) to 18 (no deficit) (Garcia *et al.*, 1995) (see §2.2.6.1).

3.2.5.2 Ischemic Lesion Volume

For the evaluation of 24h infarct lesion, the ipsilateral areas of hyperintense signal were manually defined on T2-weighted images and infarct volume (expressed in mm^3) was calculated and corrected for asymmetries due to cerebral edema using the formula 3.1 (Leach *et al.*, 1993):

$$Corrected\ infarct\ area = \frac{Infarct\ area \times contralateral\ hemisphere\ area}{ipsilateral\ hemisphere\ area} \tag{3.1}$$

Furthermore, the typology of the ischemic lesions was visually evaluated and animals were subsequently divided in two groups: large hemispheric lesions (corticostriatal lesions, Group A) and basal ganglia lesions (subcortical lesions, Group B).

3.2.6 Statistical Analysis

All results are expressed as mean $\pm$ standard deviation, except for neurobehavioral scores which are expressed as median [min; max]. Statistical analyses were performed using GraphPad Prism software. Unpaired Student's *t*-test was used for two-group analysis, while correlation and linear regression analysis were computed with Pearson's *r* test. A value of $p<0.05$ was considered significant.

3.3 Results

3.3.1 Evaluation of Outcome at 24h Post-Reperfusion

Animals with a large hemispheric lesion, characterized by a significant involvement of the cortex, were included in Group A (n = 9, Figure 3.2-A). Animals with a lesion restricted to basal ganglia were included in Group B (n = 6, Figure 3.2-B). In Group A, lesion volumes (208 $\pm$ 61 mm^3, n = 9) were significantly higher ($p < 0.001$, Figure 3.2-C) than in Group B (68 $\pm$ 32 mm^3, n = 6). According to these results, Group A animals showed higher deficits, resulting in significantly lower

neurobehavioral scores (9 [6; 12], n = 9, $p < 0.0001$, Figure 3.2-D) compared to Group B (17 [14; 18], n = 6).

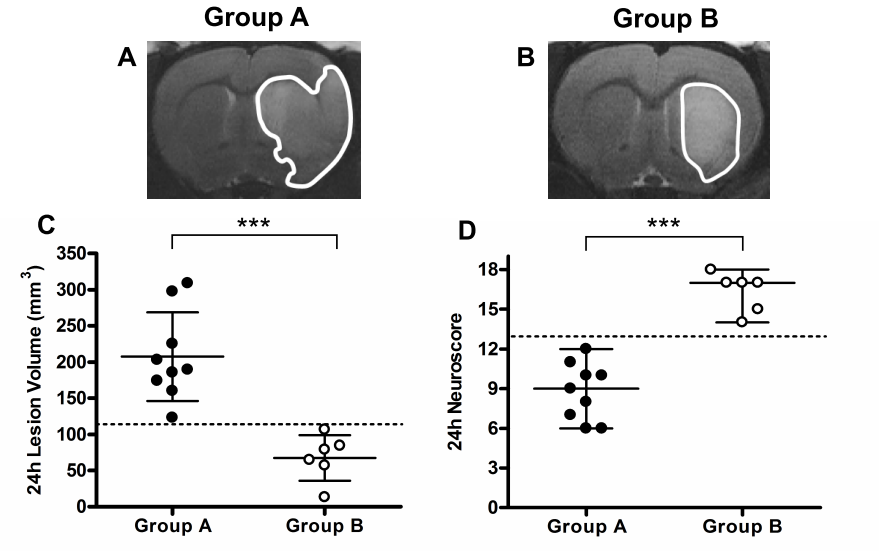

Figure 3.2: Evaluation of post-reperfusion ischemic outcome. Representative T2-weighted images showing a large hemispheric (**A**) and basal ganglia (**B**) lesion, visible as hyperintense areas (contoured). **C**. Ischemic lesion volumes of Group A were significantly higher compare to Group B and no overlap was present between the two groups (dotted line). **D**. Group A neuroscore resulted significantly lower (higher deficit) compared to Group B and no overlap was present between the two groups (dotted line). For two-group analysis unpaired Student's *t*-test was used. Black spots = Group A animals (n = 9); White spots = Group B animals (n = 6). *** $p < 0.001$.

3.3.2 Diffusion-Weighted Magnetic Resonance Imaging for the Prediction of Ischemic Outcome

Acute lesion was visually evaluated on ADC maps (Figure 3.3A-D) and, as expected, group distribution was found to exactly match that of 24h lesion. In other words, animals presenting a large hemispheric lesion (or basal ganglia lesion) acute (D0) lesion were presenting a large hemispheric lesion (or basal ganglia lesion) final (D1) lesion. In addition, acute lesion volume quantified on ADC maps positively correlates with 24h lesion volume calculated on T2-weighted images ($p < 0.0001$, Pearson's $r = 0.91$, Figure 3.3-E).

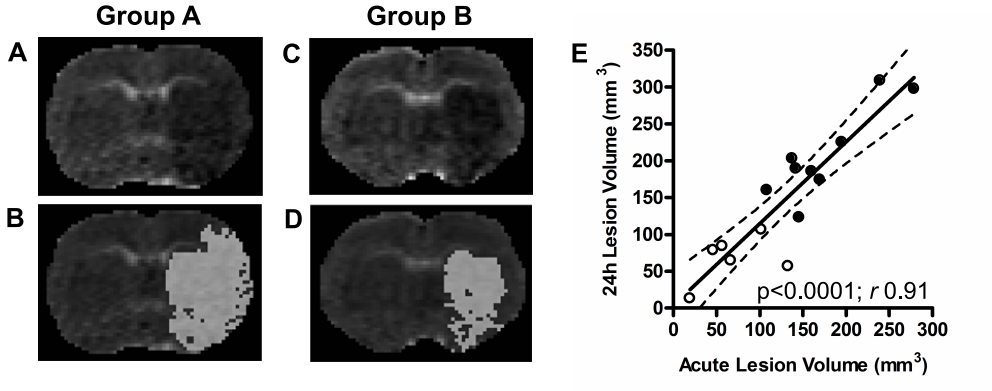

Figure 3.3: Evaluation of acute ischemic lesion on DWI-MRI and correlation with 24 hours ischemic lesion Representative ADC maps showing a large hemispheric (**A**) and basal ganglia (**C**) lesion, visible as hypointense areas (same animals as in Figure 3.2). Corresponding segmentation masks of the lesion (viability threshold value 0.53 x 10^{-3} mm^2/s) are superimposed on the ADC maps (**B** and **D**). Acute lesion volumes positively correlates with 24h lesion volumes (**E**). Dashed lines represent the 95% confidence interval of the regression line. Black spots = Group A animals (n = 9); White spots = Group B animals (n = 6). DWI = diffusion weighted imaging; MRI = magnetic resonance imaging; ADC = apparent diffusion coefficient.

3.3.3 Multi-Site Laser Doppler Flowmetry for the Prediction of Ischemic Outcome

Cerebral perfusion was monitored by two probes within two different regions of the ischemic cortex: lateral MCA territory (Probe 1) and ACA-MCA borderzone territory (Probe 2). Monitoring with Probe 2 encountered technical problems for one rat. This unreliable data was subsequently excluded from the analysis.

As expected, residual perfusion values monitored by Probe 2 correlated with the 24h ischemic outcome, both in terms of infarct volume ($p < 0.01$, Pearson's r = -0.70, Figure 3.4-D) and neuroscore ($p < 0.01$, Pearson's r = 0.68, Figure 3.4-F), while Probe 1 perfusion did not (p = 0.15, Pearson's r = -0.39 for infarct volume, Figure 3.4-C; p = 0.54, Pearson's r = 0.17 for neuroscore, Figure 3.4-E). Furthermore, residual perfusion values monitored by Probe 1 did not correlate with the acute lesion volume (p = 0.06, Pearson's r = -0.51, Figure 3.4-A), whereas Probe 2 perfusion did ($p < 0.05$, Pearson's r = -0.65, Figure 3.4-A).

Interestingly, residual perfusion values monitored by Probe 1 were not significantly different (p = 0.34) between Group A (37% $\pm$ 15%, n = 9) and B (46% $\pm$ 17%, n = 6) (Figure 3.5-A). On the contrary, residual perfusion values monitored by Probe 2 were significantly higher ($p<0.001$) in Group B (60% $\pm$ 6%, n = 6) than in Group A (45% $\pm$ 6%, n = 8) (Figure 3.5-B). In particular, a value

of 53% residual perfusion was identified as a threshold dividing the two groups, with Group A and B presenting lower and higher values, respectively (Figure 3.5-B, dotted line). In contrast, Probe 1 values between the two groups presented a wide overlap (Figure 3.5-A).

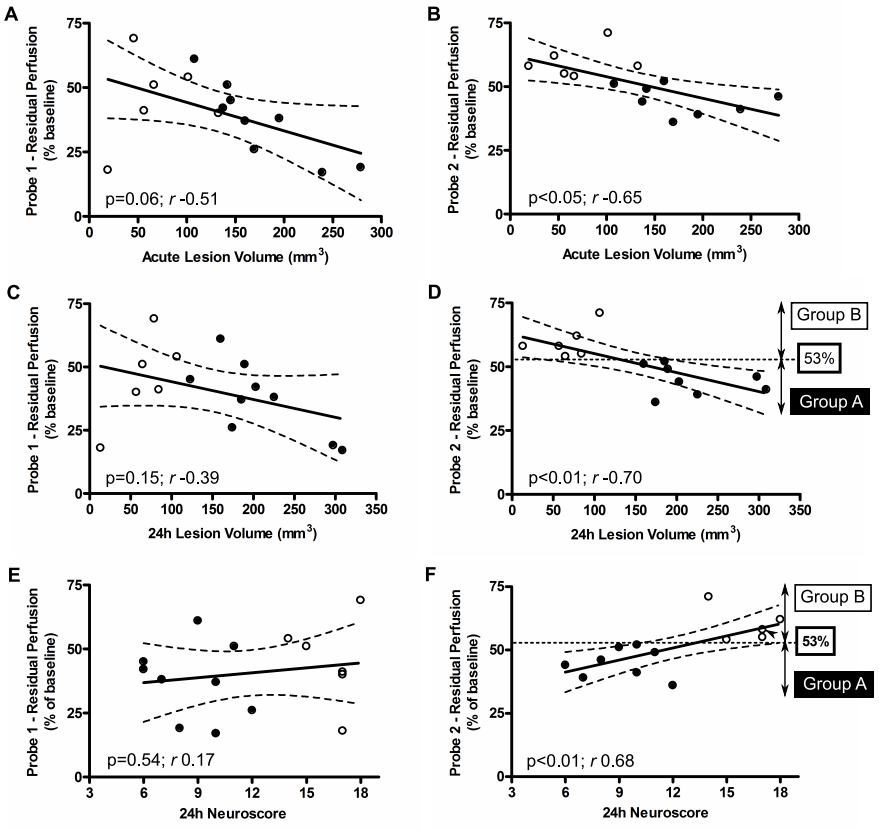

Figure 3.4: Multi-site LDF perfusion monitoring and correlation with acute lesion and 24h ischemic outcome. No significant correlation was observed between Probe 1 perfusion values and acute lesion volumes (**A**) nor 24h ischemic outcome, both in terms of ischemic lesion volumes (**C**) and neuroscores (**E**). In contrast, a negative correlation was observed between Probe 2 perfusion values and both acute lesion volumes (**B**) and 24h ischemic outcome, both in terms of ischemic lesion volumes (**D**) and neuroscores (**F**). The 53% perfusion value threshold discriminating between group A and B in shown in **D** and **F** (dotted line). Dashed lines represent the 95% confidence interval of the regression line. Black spots = Group A animals (n = 9 in **A**, **C** and **E**; n = 8 in **B**, **D** and **F**); White spots = Group B animals (n = 6). The arrowhead in **F** indicates two overlapped spots. LDF = laser Doppler flowmetry.

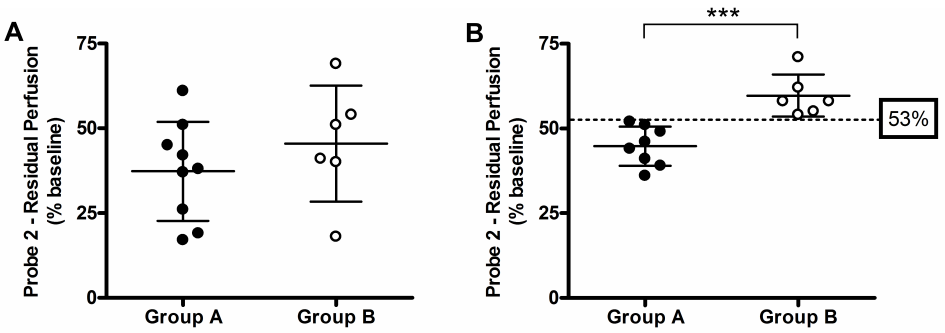

Figure 3.5: Multi-site LDF perfusion monitoring and infarct typology classification LDF perfusion monitoring and infarct typology classification. **A**. Group A (n = 9) and B (n = 6) perfusion values monitored by Probe 1 are not significantly different and are largely overlapping. **B**. Group A (n = 8) and B (n = 6) perfusion values monitored by Probe 2 are significantly different and a 53% value was identified as a threshold discriminating between the two groups (dotted line). Black spots = Group A animals; White spots = Group B animals. *** $p < 0.001$. LDF = laser Doppler flowmetry.

3.3.4 Perfusion-Weighted Magnetic Resonance Imaging and Laser Doppler Flowmetry for the Evaluation of Cerebral Perfusion

The cortical perfusion was evaluated on TTP maps within slices encompassing the two cortical regions of LDF monitoring: slices anatomically identified as Bregma -1 and Bregma +2 for Probe 1 and Probe 2, respectively. TTP values were significantly higher for Group A compared to Group B in both Bregma -1 ($p < 0.05$, Figure 3.6-A) and Bregma +2 ($p < 0.05$, Figure 3.6-B) slices. Interestingly, residual perfusion values monitored by Probe2 negatively correlated with corresponding TTP values ($p < 0.05$, Pearson's r = -0.61, Figure 3.6-D), whereas Probe 1 residual perfusion values did not correlate with corresponding TTP values (p = 0.34, Pearson's r = -0.27, Figure 3.6-C).

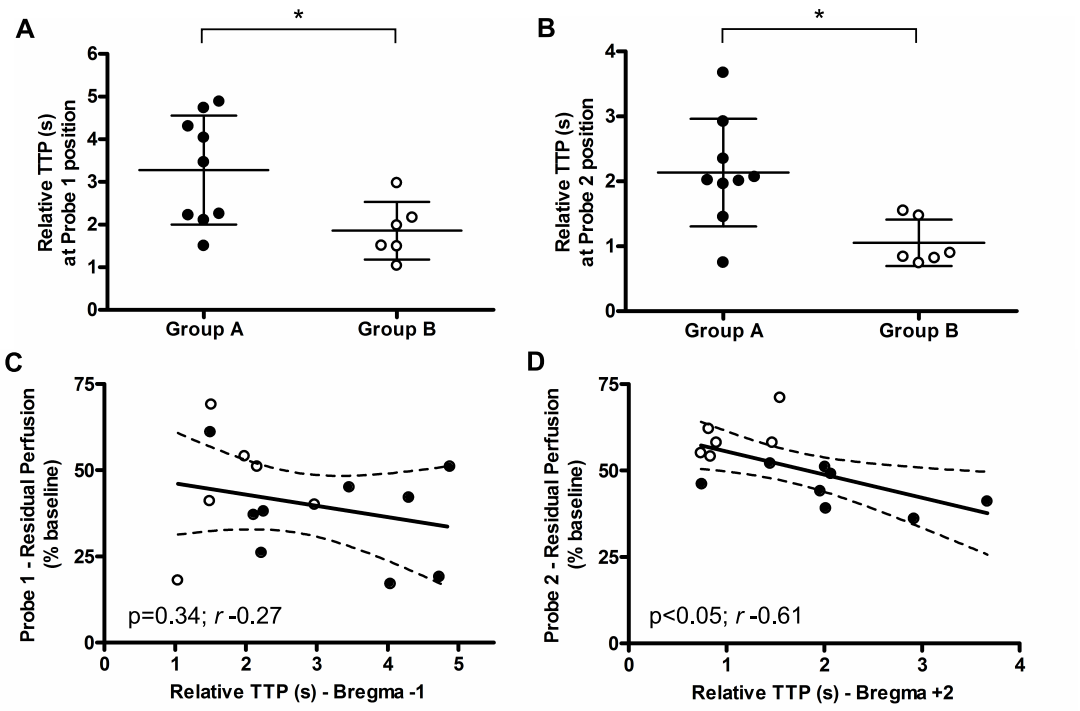

Figure 3.6: Cerebral perfusion evaluated by PWI-MRI and multi-site LDF. Cerebral perfusion evaluated by PWI-MRI and LDF. Relative TTP values (delay of bolus peak between the contralateral and ipsilateral hemisphere) were significantly different between Group A and B for both slice Bregma -1 (Probe 1 position) (**A**) and Bregma +2 (Probe 2 position) (**B**). **C**. No significant correlation was observed between Probe 1 residual perfusion values and corresponding TTP values. **D**. A negative correlation was observed between Probe 2 residual perfusion values and corresponding TTP values. Dashed lines represent the 95% confidence interval of the regression line. Black spots = Group A animals (n = 9); White spots = Group B animals (n = 6). * $p < 0.05$. TTP = time to peak. LDF = laser Doppler flowmetry; PWI = perfusion weighted imaging; MRI = magnetic resonance imaging; TTP = time to peak.

3.4 Discussion

The aim of this study was to validate collateral flow assessment by multi-site LDF for the prediction of the 24-hours ischemic outcome, using multimodal MRI. The intraluminal model of 90-minutes MCAO in rats was considered. Multi-site LDF recorded cerebral perfusion in both lateral MCA territory and ACA-MCA borderzone (collaterals territory) at MCAO induction, thanks to a custom-made probe holder allowing for a precise and stable positioning of two probes over the intact skull surface (Beretta *et al.*, 2013). As expected, cerebral perfusion evaluated by LDF in the collaterals territory correlated with ischemic outcome after 24 hours of reperfusion, both in terms of infarct volume and neuroscore, and acute lesion volumes correlated with 24 hours infarct volumes, confirming our previous results (Chauveau *et al.*, 2012; Riva *et al.*, 2012). Moreover, different 24h infarct typologies (i.e. large hemispheric or basal ganglia infarcts) were correctly a priori identified relying on both visual evaluation of the MRI acute ischemic lesion and LDF perfusion monitored in the collaterals territory (but, again, not in the lateral MCA territory).

As commonly reported by other groups (Howells *et al.*, 2010), we observed a variable lesion size after the same MCAO procedure. The presence or lack of a cortical involvement (as in large hemispheric and basal ganglia infarcts, respectively) can be influenced by exogenous (surgery, filament) and endogenous (collaterals) factors. Outcome variability of ischemic stroke models represents one of the several aspects that may participate in the translational failure of neuroprotective strategies (Dirnagl, 2006). Indeed, variability affects sample homogeneity, implying a higher number of animals required to reach an optimal statistical power.

Different methods have been used in experimental stroke research to assess correct MCAO induction. i) The presence of neurological deficits during arterial occlusion has been widely used in the past as an inclusion criteria, but was shown not predictive of final infarct (Chauveau *et al.*, 2012). ii) Imaging perfusion deficit, acute lesion or vascular occlusion on MRI (PWI-MRI, DWI-MRI and Magnetic Resonance Angiography and MRA, respectively) certainly represents the method of choice for the prediction of lesion extent (Bouts *et al.*, 2013), but it is expensive and not widely available to stroke basic scientists. However, the development of benchtop MRI systems could enable a more widespread use of imaging in the future (Caysa *et al.*, 2011). As disadvantages, MRI requires manipulation of the animal during occlusion (accompanied by the risk of thread displacement) and does not provide intra-surgical information. iii) LDF has been frequently used to monitor cerebral blood flow drop at occlusion induction in several stroke models, including the intraluminal MCA occlusion (Esposito

et al., 2013; Henninger *et al.*, 2009; Hungerhuber *et al.*, 2006; Kläsner *et al.*, 2006; Taninishi *et al.*, 2015). This simple and flexible option is probably a method of choice for multicentre neuroprotection studies, provided that its application can be standardized. Different perfusion drop values are considered to confirm intraluminal MCAO induction, varying in the range of 60-80% (Esposito *et al.*, 2013; Harada *et al.*, 2005; Hungerhuber *et al.*, 2006; Kläsner *et al.*, 2006; Taninishi *et al.*, 2015), or being not specified (Zhao *et al.*, 2008). A single monitoring probe is commonly positioned in the lateral MCA territory of the parietal cortical surface, more frequently after craniotomy (Esposito *et al.*, 2013; Hungerhuber *et al.*, 2006; Kläsner *et al.*, 2006; Taninishi *et al.*, 2015), while a less invasive approach through intact skull may be considered (Beretta *et al.*, 2013; Harada *et al.*, 2005).

Interestingly, if the perfusion threshold values reported in the literature for the identification of large hemispheric infarcts were applied to Probe 1 in this study (i.e. 60-80% residual perfusion), only 7 (for 60% threshold) to 3 (for 80% threshold) animals out of 15 would have been correctly classified (50%-70% misclassification rate). In particular, if large hemispheric infarcts were to be included and basal ganglia infarcts to be excluded, 5 to 2 animals would have been correctly included (large hemispheric infarcts, for 60% and 80% threshold, respectively) and 2 to 1 animals would have been wrongly included (basal ganglia infarcts, for 60% and 80% threshold, respectively). This misclassification may have a strong impact on the results of a neuroprotection study: if a basal ganglia infarct allocated in the treatment group is a priori misclassified as large hemispheric infarct, it will be wrongly interpreted as a result of the neuroprotective effect.

Though LDF monitoring in the lateral MCA territory is effective in detecting a perfusion drop indicative of arterial occlusion (or subarachnoid haemorrhage), we here confirm that additional LDF monitoring in a transition zone between different cerebral arteries territories provides distinct and predictive information. Indeed, Probe 2 perfusion values could discriminate between hemispheric infarcts and basal ganglia infarcts and, precisely, a threshold value of 53% residual perfusion was identified in this set of animals.

In order to confirm that LDF perfusion monitored in a restricted cortical area is reflecting the actual perfusion, the latter was evaluated on TTP maps computed from per-occlusion PWI-MRI and compared to LDF perfusion. As expected, cortical perfusion was significantly lower for the large hemispheric compared to basal ganglia infarcts, in both slices corresponding to Probe 1 and Probe 2 monitoring sites (Bregma -1 and Bregma +2, respectively). Surprisingly, TTP values correlated with LDF perfusion only for Probe 2 and not for Probe 1. The main advantages of using TTP maps to assess perfusion are that they are easy to generate, they do not require measuring an arterial input

function, and abnormal regions can be easily identified and delineated. However, there are also notable limitations to the TTP maps. The TTP is only an indirect measure of tissue perfusion, and TTP delays may occur in regions with good collaterality. This confounding effect is expected to increase in regions that are further away from the leptomeningeal collaterals (because the time for the bolus to reach these regions via the collaterals is increased and thus a long TTP might be wrongly interpreted as a low perfusion). This might explain the discrepancy between the LDF perfusion and TTP values in the slice corresponding to Probe 1 monitoring site.

Taken together, these results highlight the potential of multi-site LDF monitoring for the prediction of ischemic outcome. While monitoring in the lateral MCA territory can be useful as guidance during surgery to assess occlusion induction, monitoring in the collaterals territory provides an additional value, relevant for outcome prediction and animal stratification.

A major limitation of this study is the small sample size. Nevertheless, we were able to obtain reliable stratification based on Probe 2 perfusion value despite n=15. Further studies in independent laboratories including larger sample size are warranted. Another limitation is represented by the lack of simultaneous assessment of multi-site LDF and MRI, since this was not feasible. Nonetheless, LDF was applied for 10 minutes during MCAO immediately before transferring the same animals in the MRI scanner, making unlikely any relevant change in the extent of perfusion deficit between the two methods.

3.5 Conclusions

In this study, multi-site LDF for the monitoring of collateral flow was in agreement with multimodal acute MRI for the prediction of ischemic outcome in experimental ischemic stroke. We propose this approach to a priori stratify animals in neuroprotection studies, in order to enhance sample homogeneity. The additional value of multi-site LDF compared to single-site LDF highlights its potential for outcome prediction in experimental ischemic stroke, especially for laboratories in which MRI is not accessible.

Chapter 4

Study of Collateral Therapeutics for the Hyper-Acute Phase of Ischemic Stroke: a Randomized Controlled Preclinical Study

Beretta S[1], Stiro F[2], Versace A[2], Carone D[2], Riva M[2], **Cuccione E**[3], Cai R[2], Monza L[2], Padovano G[2], Dell'Era V[2], Pirovano S[2], Presotto L[4], Sganzerla EP[1], Ferrarese C[1].

In preparation.

[1] Laboratory of Experimental Stroke Research, School of Medicine, University of Milano Bicocca, Monza, Italy; Milan Center for Neuroscience (NeuroMi), Milan, Italy.

[2] Laboratory of Experimental Stroke Research, School of Medicine, University of Milano Bicocca, Monza, Italy.

[3] Laboratory of Experimental Stroke Research, School of Medicine, University of Milano Bicocca, Monza, Italy; PhD Program in Neuroscience, University of Milano Bicocca, Monza, Italy.

[4] Department of Nuclear Medicine, San Raffaele Scientific Institute, Milan, Italy; Institute of Bioimaging and Molecular Physiology, National Research Council, Milan, Italy.

Abstract

Cerebral collateral circulation performance is emerging as a strong outcome determinant in both human and experimental ischemic stroke. We planned this preclinical randomized controlled study to investigate and compare the efficacy and safety of four putative strategies, which might actively modulate collateral flow in the setting of acute cerebral ischemia: induced systemic hypertension using phenylpephrine, intravascular volume load using polygeline, cerebro-selective vasodilatation using acetazolamide and cerebral flow diversion by head-down tilt.

The middle cerebral artery (MCA) was transiently occluded (90 minutes) by intraluminal filament in adult male Wistar rats. According to the composite randomization, 58 rats were left untreated, whereas 60 rats were treated after 30 minutes of ischemia with intravenous administration of phenylephrine (n=14), polygeline (n=16), acetazolamide (n =16) or positioned with a 15° slope until reperfusion (head-down tilt, n=14). Cerebral blood flow was assessed using multi-site laser Doppler monitoring and after 24 hours of reperfusion functional deficit was evaluated using a sensory-motor score and infarct volume was calculated on tissue sections stained with Cresyl violet. During surgery, blood pressure, heart and respiratory rate were continuously monitored by a pressure transducer placed in femoral artery.

Collateral therapeutics significantly increased cerebral flow during MCAO, mainly in the territory of leptomeningeal collateral vessels, and reduced 24 hours infarct size as well as functional deficit when globally considered. Single strategies comparison lead to differential results: acetazolamide, polygeline and head-down tilt lead to a significant improvement of tissue outcome, although this was paralleled by a functional improvement only for head-down tilt. Phenylephrine showed no significant improvement of ischemic outcome. No significant effect on cardiorespiratory parameters was observed, except for phenylephrine. Notably, no animals died after head-down tilt.

In conclusion, therapeutic modulation of intracranial collateral flow is feasible and is associated with a better outcome after transient MCA occlusion in rats. In this study, head-down tilt emerged as the safest and most efficace among the therapies considered. “Collateral therapeutics” may represent an simple tissue-saving strategy in the hyper-acute phase of ischemic stroke prior to recanalization therapy.

4.1 Introduction

Ischemic stroke represents the second most common cause of death worldwide (Lozano *et al.*, 2012) and the leading cause of disability (Feigin *et al.*, 2003). Unfortunately, therapeutic strategies for acute phase of stroke are limited. The current approaches are focused on vascular occlusion and aim to obtain prompt recanalization. Intravenous thrombolysis with rtPA (Alteplase) and endovascular thrombectomy within 4.5 and 6 hours from symptoms onset, respectively, represent the best therapeutic options (Jauch *et al.*, 2013; Powers *et al.*, 2015). Unfortunately, most patients are not eligible for recanalization therapies, primarly because of the restricted time-window (Ingall, 2009; Lansberg *et al.*, 2009) and the risk of hemorrhagic transformation. Besides recanalization therapies, neuroprotection has been extensively explored, but success in experimental stroke has failed to translate into patients (Sutherland *et al.*, 2012). Hence, the need for new therapeutic strategies is clearly emerging.

Collateral circulation is subsidiary vascular network, which is dynamically recruited following vascular occlusion and may provide residual blood flow to the affected areas, slowing down the progression of ischemic penumbra to irreversible ischemic damage (Liebeskind, 2005a, 2010). In untreated patients, good collateral status is associated with larger baseline penumbra and reduced ischemic core (Campbell *et al.*, 2013), leading to a more favourable functional outcome and reduced mortality (Bang *et al.*, 2008; Lima *et al.*, 2010; Menon *et al.*, 2011; Miteff *et al.*, 2009). Recanalized patients with good collaterals seem to be more protected from infarct growth and hemorrhagic transformation (Bang *et al.*, 2008, 2011b), resulting in a more favourable early and long term outcome (Calleja *et al.*, 2013). We previously showed that the collateral perfusion correlated with both 24 hours outcome (Riva *et al.*, 2012) and molecular penumbra (Beretta *et al.*, 2015) after transient middle cerebral artery occlusion (MCAO) in rats.

Modulating collateral blood flow in order to augment or maintain perfusion to the ischemic penumbra could represent a new therapeutic strategy for the hyperacute phase (Liebeskind, 2004, 2010; Shuaib *et al.*, 2011b), particularly if applied before recanalization or neuroprotective therapies.

We planned this preclinical randomized controlled study to investigate and compare the efficacy and safety of four putative strategies, which might actively modulate collateral flow in the setting of acute cerebral ischemia: induced systemic hypertension using phenylpephrine, intravascular volume load using polygeline, cerebro-selective vasodilatation using acetazolamide and cerebral flow diversion by head-down tilt. Rats underwent transient MCAO of 90 minutes and treatments were administered 30 minutes after ischemia induction. Cerebral blood flow was continuously monitored by multi-site laser

Doppler (LD) (Beretta *et al.*, 2013). Blood pressure, heart and respiratory rate were continuously monitored by a pressure transducer placed in femoral artery. After 24 hours of reperfusion, tissue and functional ischemic outcomes were evaluated.

4.2 Material and Methods

4.2.1 Animals and Experimental Design

The experimental protocol was approved by the Committee on Animal Care of the University of Milano Bicocca, in accordance with the national guidelines on the use of laboratory animals (D.L. 116/1992) and the European Union Directive for animal experiments (2010/63/EU), under project license from the Italian Ministry of Health.

Animals were housed in single cages, exposed to 12/12 hour light/ dark cycle, at controlled room temperature, with free access to food and water, in a specific pathogen free (SPF) facility.

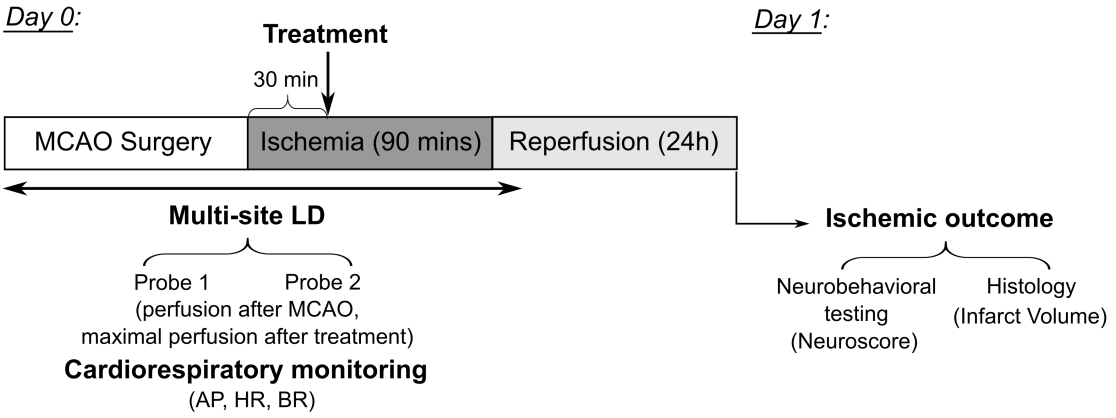

Figure 4.1: Experimental Design. On day 0, transient MCAO of 90 minutes was induced. Cerebral perfusion monitoring by multi-site LD was continuously performed during the whole surgical procedure, up to reperfusion. Treatments were administered after 30 minutes of ischemia. Residual perfusion after MCAO (before-treatment) and maximal perfusion after treatment were considered. Cardiorespiratory parameters (arterial pressure, heart rate, breath rate) were also continuously monitored. On day 1, after 24 hours of reperfusion, neurological deficits were evaluated according to a neurobehavioral score scale. Afterwards, rats were sacrificed and brains were extracted and processed. Cresyl Violet was used for istological staining of brain section for the evaluation of the ischemic lesion and calculation of infarct volume. MCAO = middle cerebral artery occlusion; LD = laser Doppler; AP = arterial pressure; HR = heart rate; BR = breath rate.

The experimental design is illustrated in Figure 4.1. On day 0, transient MCAO of 90 minutes was induced. Cerebral perfusion monitoring by multi-site LDF was performed continuously during the whole surgical procedure (approximately 140 min), including reperfusion by filament withdrawal. Treatments (see below) were administered after 30 minutes of ischemia. Cardiorespiratory parameters were also continuously monitored. On day 1, after 24 hours of reperfusion, neurological outcome of animals was assessed with a functional neuroscore. Afterwards, rats were sacrificed and brains were extracted and processed. Cresyl Violet was used for istological staining of brain section for the evaluation of the ischemic lesion.

Adult male Wistar rats (280 $\pm$ 10% g; n = 126) were globally considered for this study. Randomization and exclusion criteria are described below (§4.2.6.2). Eight rats were excluded and the remaining randomized rats (n = 118) were considered for analysis.

4.2.2 MCAO Surgery and Treatments Administration

On Day 0, rats were anesthetized with 3% isoflurane in O_2/N_2O (1:3), and maintained with 1.5% isoflurane. A silicon-coated filament (diameter 0.39$\pm$0.02 mm, Doccol Corporation, Redlands, CA, USA) was used to occlude the origin of the MCA. The surgical protocol is described in details in §2.2.2. The core temperature was monitored by a rectal thermometer and maintained to 37.0$\pm$0.5°C using a heating pad.

Therapeutic strategies (3 pharmacological strategies, 1 non-pharmacological strategy) were administred at 30 minutes post-MCAO:

- Phenylephrine (PHE group, n = 14): a 2.5 mg/ml phenylephrine solution was infused at a velocity of 2.7 ml/h to induce a rise in MAP of about 20-25%;
- Polygeline (PLG group, n = 16): 4,5 mL of polygeline solution were injected to induce a volume expansion of about 25%;
- Acetazolamide (ACZ group, n = 16): 600 μl of acetazolamide solution (50 mg/ml) were injected;
- Head Down Tilt (HDT group, n = 14, non-pharmacological): rats were positioned on a surface with a 15° slope until reperfusion.

Pharmacological treatments were infused intravenously into the right femoral vein, with a mean infusion time of 5 minutes. Control rats (CTRL group, n = 58) received no pharmacological active treatment and were maintained in horizontal position.

After 90-minutes of ischemia, animals were reperfused by filament withdrawal. They were then allowed to recover and had free access to food and water.

4.2.3 Multi-site Laser Doppler Monitoring of Cerebral Perfusion

The induction of focal cerebral ischemia was assessed using laser Doppler (LD) perfusion monitoring (dual channel moorVMS-LDF^{TM}, Moor, Axminster, UK) as described in §2.2.4. Briefly, two probes were firmly position over the intact skull surface thanks to a custom-made probes holder (Beretta *et al.*, 2013). The first probe (Probe 1) was positioned in the core of the MCA territory (1 mm posterior to the bregma and 5 mm lateral to the midline). The second probe (Probe 2) was positioned in the borderzone between ACA and MCA territories (2 mm anterior to the bregma and 2 mm lateral to the midline). Cerebral perfusion monitoring was performed continuously during the entire period of anesthesia (approximately 150-180 min) and the following parameters were considered for each probe:

1. cerebral perfusion before CCAO, which was considered as baseline value;
2. residual cerebral perfusion (expressed as % of baseline) after MCAO, following flow stabilization (excluding the early phase after filament insertion) and up to 30 minutes of ischemia, before treatment administration;
3. maximal perfusion after treatment administration (expressed as % of baseline), from 30 to 90 minutes of ischemia;
4. cerebral perfusion (expressed as % of baseline) at reperfusion, following filament withdrawal.

Hemodynamic assessment was blinded to primary (neuroscore, infarct volume) and secondary (cardiorespiratory parameters) outcome data.

4.2.4 Physiological Parameters Monitoring

Cardio-respiratory parameters (arterial pressure, heart rate, respiratory rate) were continuously monitored throughout the surgical procedure using a Samba Preclin 420 transducer (Samba Sensors, Harvard Apparatus, UK) inserted in the right femoral artery. Cardio-respiratory and cerebral perfusion recordings were synchronized using a software written in Matlab 2013 (MathWorks, Natick, MA).

Analysis of cardiorespiratory parameters was blinded to primary (neuroscore, infarct volume) and secondary (hemodynamic parameters) outcome data.

4.2.5 24h Ischemic Outcome Evaluation

On Day 1, final ischemic outcome was assessed after 24 hours of reperfusion by both neurobehavioral testing (see §2.2.6.1) and evaluation of ischemic lesion by Cresyl Violet staining of histological sections (see §2.2.6.3). Briefly, animals were tested for neurological outcome by different behavioral, motor and sensitive tasks and scored on a scale ranging from 3 (most severe) to 18 (no deficit). Rats were then sacrified by $C0_2$ overdose and brains were extracted and fixed by immersion into ice-cold 10% neutral buffer formalin. Nineteen serial coronal tissue sections (50 μm thick) of the brain portion ranging from Bregma +2.5 mm and Bregma -3 mm were obtained using a vibratome (Vibratome 1000 Plus-Tissue Sectioning System) and stained with Cresyl violet for the visualization of the ischemic lesion. Infarct volume corrected for inter-hemispheric asymmetries due to cerebral edema was calculated, and expressed in mm^3.

Both neurobehavioral evaluation and infarct volume calculation on histological sections were blinded to secondary (cardiorespiratory and hemodynamic parameters) outcome data.

4.2.6 Statistical Design and Analysis

4.2.6.1 Sample Size and Statistical Power Calculation

We planned this preclinical randomized-controlled study, in which animal allocation to a specific group was concealed and primary and secondary outcomes evaluation was blinded to animal allocation. Infarct volumes and neurological deficits evaluated at 24 hours post-reperfusion were considered as primary outcomes, whereas cerebral perfusion, cardio-respiratory parameters (mean arterial pressure, heart rate, respiratory rate) and treatment-associated mortality were considered as secondary outcomes.

The primary study was planned to compare 2 groups (control vs collateral therapeutics animals, 1:1 randomization), with a Type I error probability of 0.05 and a statistical power of 0.99. Assuming a difference of primary outcome (infarct volume) between the two groups above 30% to be considered of interest and provided a standard deviation of infarct volumes of 45% (previous results), a sample size of 60 animals per group was required.

The secondary study was planned to compare the control group to each of the four treatments considered (1:4 randomization), with a Type I error probability of 0.05 and a statistical power of 0.80. Assuming a difference of primary outcome (infarct volume) between the two groups above 40% to be considered of interest and provided a standard deviation of infarct volumes of 45% (previous results), a sample size of 13 animals per treatment group and of 52 animals for the control group was required.

4.2.6.2 Randomization and Exclusion Criteria

A number of 126 rats were globally used for this study. The randomization is illustrated in Figure 4.2. Signs of subarachnoid hemorrhage (SAH) and early death (before treatment) were used as exclusion criteria. SAH was detected by a cerebral perfusion drop $>$90% for both Probe 1 and 2 and then visually confirmed after brain extraction. Eight animals were excluded because of SAH and the remaining 118 were allocated to an experimental group according to a centralized composite randomization list. Centralized randomization was compiled until reaching 14 animals per group. The first randomization, dividing animals into control group and collateral therapeutics group, involved:

- Control (CTRL group): n = 58;
- Collateral therapeutics (COLL-THER group): n = 60.

The second randomization divided treatment group animals into 4 treatment groups, one for each therapeutic strategy considered, and involved:

- Phenylephrine (PHE group): n = 14;
- Polygeline (PLG group): n = 16;
- Acetazolamide (ACZ group): n = 16;
- Head Down Tilt (HDT group): n = 14.

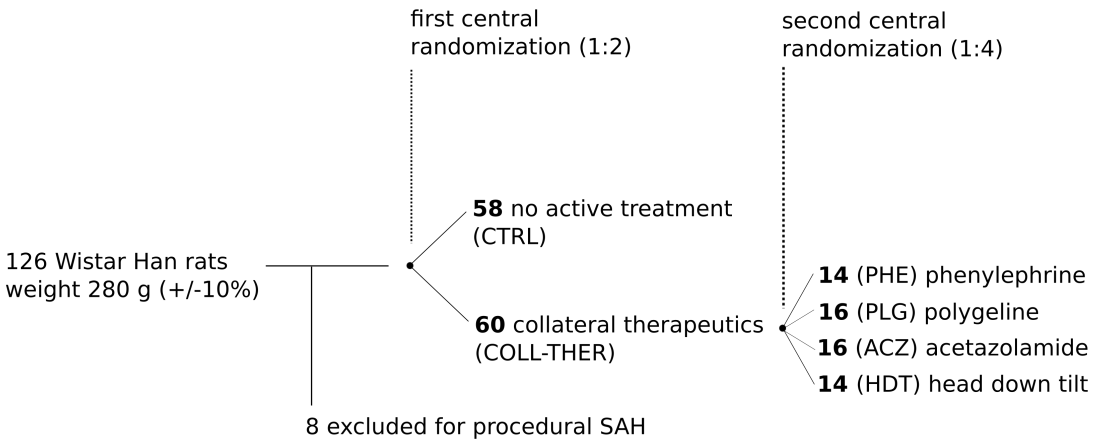

Figure 4.2: Randomization design of the study. The composite randomization of this study divided animals into CTRL (n = 58) and COLL-THERAP (n = 60) group (first randomization, 1:2). C-TH group animals were then randomized into PHE (n = 14), PLG (n = 16), ACZ (n = 16) and HDT (n = 14) groups (second randomization, 1:4).

4.2.6.3 Statistical Analysis

Values were expressed as mean $\pm$ standard deviation (SD). For two-group analysis, unpaired (or paired, where appropriate) Student's t test was used. For multi-group analysis, one-way ANOVA and Bonferroni's post-hoc test were considered. A value of $p < 0.05$ was considered significant. In order to adjust the primary outcome for cerebral perfusion, ANCOVA and Bonferroni's post-hoc test were considered. For this analysis, infarct volume was considered as dependent variable and Probe 1 and 2 residual perfusion were tested as covariates.

4.3 Results

4.3.1 Baseline Characteristics of The Experimental Sample

The baseline characteristics of the animals involved in this study are reported in Table 4.1. The parameters weight, Probe 1 and 2 perfusion deficit at MCAO, mean arterial blood pressure, mean heart rate and mean breath rate were evaluated before treatment and compared between control and treated animals. No significant differences emerged between the two groups for any parameters, except for Probe 2 residual perfusion at MCAO, which resulted about 10% higher in the treated compared to control group.

	CTRL (n=58), mean (SD)	**COLL-THER (n=60), mean (SD)**	**p-value**
Weight (grams)	289.19 (26.56)	293.80 (20.55)	0.374
Probe 1 residual perfusion at MCAO (%)	38.53 (14.33)	44.32 (17.61)	0.074
Probe 2 residual perfusion at MCAO (%)	60.26 (19.26)	70.92 (21.93)	**0.011***
Mean arterial blood pressure before treatment (mmHg)	115 (33)	113 (23)	0.895
Mean heart rate before treatment (bpm)	434 (30)	433 (38)	0.901
Mean breath rate before treatment (brpm)	57 (11)	58 (11)	0.854

Table 4.1: Baseline characteristics of the experimental sample. Baseline characteristics of CTRL (n = 58) and C-THER group (n = 60) are reported. * $p < 0.05$, unpaired Student's *t*-test. CTRL = control; COLL-THER = collateral therapeutics; SD = standard deviation; MCAO = middle cerebral artery occlusion; bpm = beats per minute; brpm = breath rate per minute.

4.3.2 Effect of Collateral Therapeutics on 24h Ischemic Outcome

Primary outcomes (infarct volume and neuroscore) were evaluated 24 hours post-reperfusion. Globally, infarct volume is reduced in collateral therapeutics ($p < 0.001$) compared to control group (Figure 4.3-A). When considering single treatments, infarct volume is reduced in animals treated with polygeline ($p < 0.01$), acetazolamide ($p < 0.01$) and head-down tilt ($p < 0.001$), while treatment with phenylephrine showed no significant infarct reduction compared to control (Figure 4.3-B).

Infarct volumes showed a wide variability among animals, with infarcts ranging from small subcortical (Figure 4.3-C) to large corticostriatal lesions (Figure 4.3-D).

Analysis of covariance (ANCOVA) was performed to adjust the tissue outcome values for the cerebral residual perfusion at MCAO recorded by Probe 1 and 2. Perfusion recorded by Probe 1 did not covary ($p = 0.101$) with the infarct volumes. On the contrary, perfusion recorded by Probe 2 significantly covaried ($p < 0.001$) with the infarct volumes. On this basis, infarct volumes were adjusted according to the Probe 2 perfusion deficit and their values resulted statistically different compared to control for animals treated with polygeline ($p < 0.001$), acetazolamide ($p < 0.0005$) and head down tilt ($p < 0.0005$), whereas no difference ($p = 0.345$) was shown for the phenylephrine group (Table 4.2) .

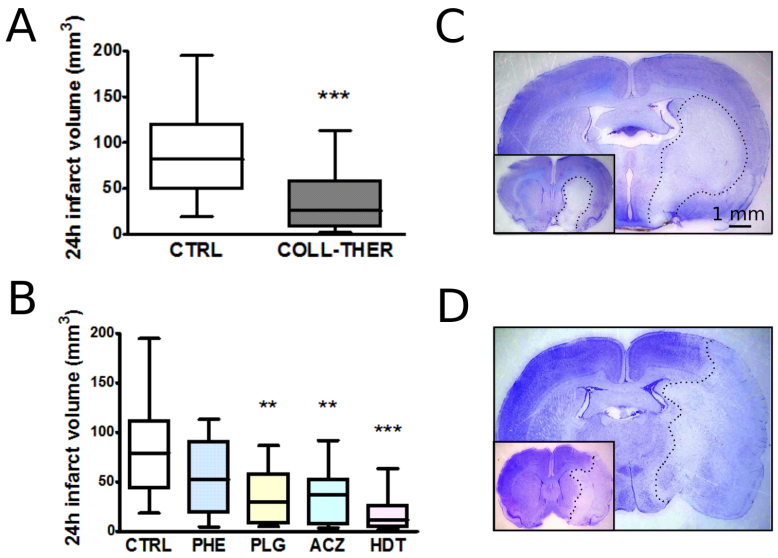

Figure 4.3: Effect of collateral therapeutics on the tissue outcome. **A**. Infarct volume is reduced in treated ($p < 0.001$) compared to control group. **B**. Infarct volume is reduced in animals treated with polygeline ($p < 0.01$), acetazolamide ($p < 0.01$) and head-down tilt ($p < 0.001$) compared to control group. **C**. Representative sections of a subcortical lesion (Bregma -1; Bregma +2). **D**. Representative sections of a corticostriatal lesion (Bregma -1; Bregma +2). ** $p < 0.01$, *** $p < 0.001$ vs CTRL. Unpaired Student's *t*-test was used for two-group analysis. CTRL = control; PHE = phenylephrine; PLG = polygeline; ACZ = acetazolamide; HDT = head-down tilt.

Experimental Group	**Adjusted Mean infarct volume***	**Standard error**	**p-value (vs CTRL)**	**95% Confidence interval**	
				Inferior limit	**Superior limit**
PHE	64.277	12.849	0.345	38.710	89.843
PLG	36.809	10.261	0.001	16.393	57.226
ACZ	32.453	10.253	0.0005	12.053	52.853
HDT	19.876	11.682	0.0005	-3.367	43.118
CTRL	78.091	5.892	-	66.366	89.815

*** Dependent variable**: infarct volume. **Co-variate**: Probe 2 residual perfusion, correlation coefficient = 65,9770, $p < 0.001$.

Table 4.2: Analysis of covariance (ANCOVA) and infarct volume values adjusted for collateral blood flow. Residual perfusion recorded by Probe 2 significantly covaried ($p < 0.001$) with the infarct volumes. On this basis, infarct volumes were adjusted according to the Probe 2 perfusion deficit and their values resulted statistically different compared to control for animals treated with polygeline ($p < 0.001$), acetazolamide ($p < 0.0005$) and head down tilt ($p < 0.0005$), whereas no difference was shown for the phenylephrine group ($p = 0.345$). CTRL = control; PHE = phenylephrine; PLG = polygeline; ACZ = acetazolamide; HDT = head-down tilt.

Neuroscore values were higher, indicating a better neurological outcome, for collateral therapeutics ($p < 0.001$) compared to control group (Figure 4.4-A). When considering single treatments, neuroscore resulted higher in HDT group ($p < 0.001$), while treatment with phenylephrine, polygeline and acetazolamide showed no significant neurological improvement compared to control (Figure 4.4-B).

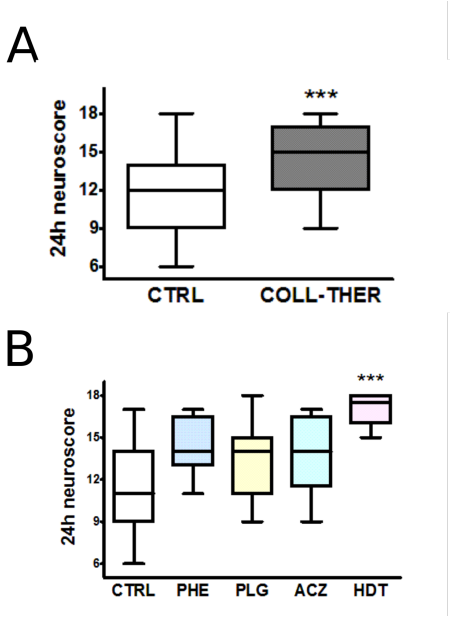

Figure 4.4: Effect of therapeutic strategies on the functional outcome. **A**. Neuroscores are higher (i.e. better outcome) for treated ($p < 0.001$) compared to control animals. **B**. Neuroscores are higher for HDT group ($p < 0.001$) compared to control, whereas no significant improvement was shown in PHE, PLG and ACZ treatment groups. *** $p < 0.001$ vs CTRL. Unpaired Student's *t*-test was used for two-group analysis. CTRL = control; PHE = phenylephrine; PLG = polygeline; ACZ = acetazolamide; HDT = head-down tilt.

4.3.3 Effect of Collateral Therapeutics on Cerebral Hemodynamics

Cerebral perfusion was real-time monitored by multi-site LD throughout the surgical procedure. Representative LD tracings recorded by Probe 1 in the lateral MCA territory and Probe 2 in the ACA-MCA borderzone territory are shown in Figure 4.5. The perfusion parameters considered are also indicated (baseline, residual perfusion after MCAO, maximal perfusion after treatment, reperfusion). In the present study, the perfusion recorded by Probe 2 in the collaterals territory resulted higher compared to Probe 1 for all animals (data not shown).

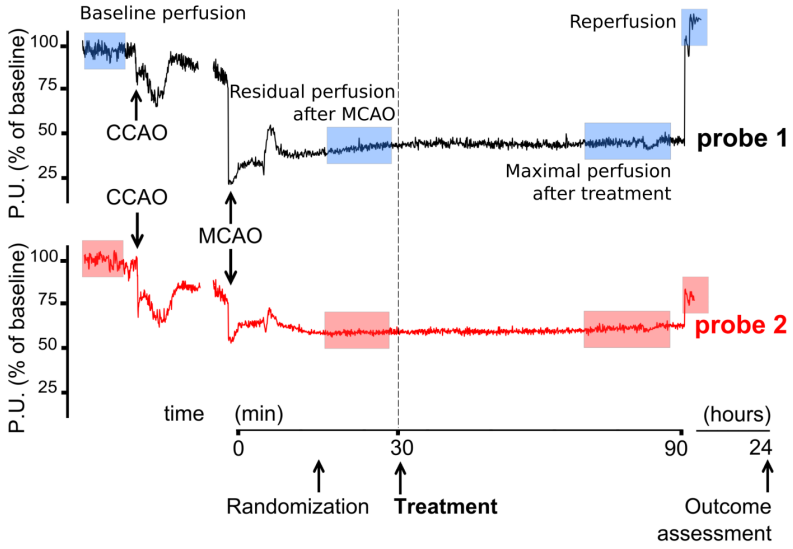

Figure 4.5: Representative multi-site LD tracings. Representative LD tracing recorded by Probe 1 in the lateral MCA territory (upper tracing) and by Probe 2 in the ACA-MCA borderzone territory (lower tracing) are shown along with the experimental design. Cerebral perfusion is real-time monitored throughout the surgical procedure. Baseline perfusion and perfusion drops at both CCAO and MCAO are visible. The residual perfusion recorded by Probe 2 in the collaterals territory resulted higher compared to Probe 1 for all animals in this study. For the animals allocated in a treatment group, the assigned therapeutic strategy is administered after 30 minutes of ischemia and the maximal perfusion after treatment is evaluated. After 90 minutes of ischemia, reperfusion is allowed and confirmed by a recover in cerebral perfusion. At 24 hours post-reperfusion, ischemic outcome is evaluated. P.U. = perfusion units; CCAO = common carotid artery occlusion; MCAO = middle cerebral artery occlusion.

Maximal perfusion after treatment was significantly higher for collateral therapeutics compared to the maximal perfusion recorded in 30-90 minutes of ischemia in control group, for both Probe 1 ($p < 0.05$) and Probe 2 ($p < 0.001$) (Figure 4.6-A). Moreover, perfusion resulted higher in the collaterals territory (Probe 2) compared to the lateral MCA territory (Probe 1), for both control ($p < 0.05$) and collateral therapeutics ($p < 0.0001$) group (Figure 4.6-A). Differently, cerebral perfusion values at reperfusion did not result significantly different between collateral therapeutics and control group, for both probes (Figure 4.6-B). The residual perfusion after MCAO within the first 30 minutes of ischemia and maximal perfusion within 30-90 minutes of ischemia (corresponding to pre-treatment and post-treatment periods for treated animals, respectively) were evaluated in control animals. Perfusion resulted significantly higher during the final 30-90 compared to the initial 0-30 minutes for both Probe 1 ($p < 0.01$) and 2 ($p < 0.01$) (Figure 4.6-C). Notably, perfusion recorded by Probe 2 resulted significantly higher compared to Probe 1 for both 0-30 ($p < 0.001$) and 30-90 ($p < 0.001$) minutes of ischemia (Figure 4.6-C). Analogously, in the collateral therapeutics group, maximal perfusion post-treatment resulted significantly higher for both Probe 1 ($p < 0.001$) and 2 ($p < 0.001$) compared to pre-treatment perfusion. Perfusion recorded by Probe 2 resulted significantly higher compared to Probe 1 for both pre- ($p < 0.001$) and post-treatment ($p < 0.001$) phase.

The maximal residual perfusion after treatment was considered for each treatment and compared to the perfusion after MCAO. For all the therapeutic strategies considered, the maximal residual perfusion after treatment resulted significantly higher compared to pre-treatment values, for both Probe 1 and 2 (see Figure 4.7-A to D). Moreover, perfusion recorded by Probe 2 resulted significantly higher compared to Probe 1 both before and after treatment, for every treatment group, except for HDT group where Probe 2 perfusion was higher than Probe 1 only after treatment (see Figure 4.7-A to D). Representative LD tracings showing the rise in cerebral perfusion after head-down tilt treatment are shown in Figure 4.7-E.

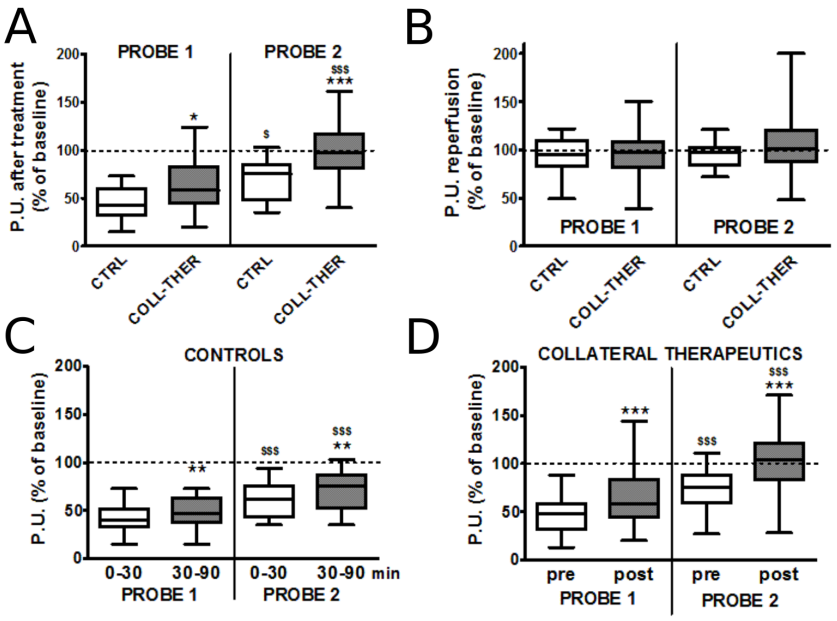

Figure 4.6: Effect of collateral therapeutics on the cerebral perfusion. **A**. Maximal residual perfusion after treatment resulted higher in collateral therapeutics group compared to control, both in Probe 1 ($p < 0.05$) and 2 ($p < 0.001$). Perfusion resulted higher in the collaterals territory (Probe 2) compared to the lateral MCA territory (Probe 1), for both control ($p < 0.05$) and collateral therapeutics ($p < 0.0001$) group. **B**. Cerebral perfusion values at reperfusion were not significantly different between collateral therapeutics and control group for both probes. Unpaired Student's *t*-test was used. **C**. In control group, the maximal perfusion within 30-90 minutes of ischemia resulted significantly higher for both Probe 1 ($p < 0.01$) and 2 ($p < 0.01$) compared to the perfusion after MCAO (0-30 minutes of ischemia). Perfusion recorded by Probe 2 resulted significantly higher compared to Probe 1 for both 0-30 ($p < 0.001$) and 30-90 ($p < 0.001$) minutes of ischemia. **D**. In the collateral therapeutics group, maximal perfusion post-treatment resulted significantly higher for both Probe 1 ($p < 0.001$) and 2 ($p < 0.001$) compared to pre-treatment perfusion. Perfusion recorded by Probe 2 resulted significantly higher compared to Probe 1 for both pre- ($p < 0.001$) and post-treatment ($p < 0.001$) phase. In **A**: * $p < 0.05$, *** $p < 0.001$ vs CTRL for the same Probe; \$ $p < 0.05$, \$\$\$ $p < 0.001$ vs Probe 1 for the same group. Unpaired Student's *t*-test was used. In **C**: ** $p < 0.01$ vs 0-30 min for the same Probe; \$\$\$ $p < 0.001$ vs Probe 1 for the same period of ischemia (0-30 or 30-90 min). Paired Student's *t*-test was used. In **D**: *** $p < 0.001$ vs pre for the same Probe; \$\$\$ $p < 0.001$ vs Probe 1 for the same period of ischemia (pre or post). Paired Student's *t*-test was used. P.U. = perfusion units.

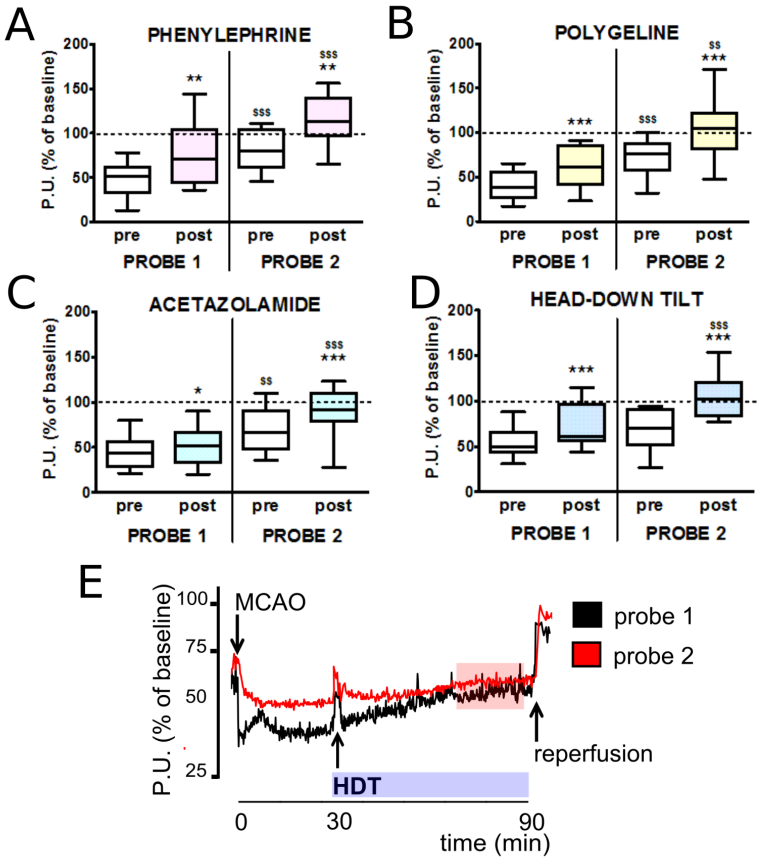

Figure 4.7: Effect of collateral therapeutics (single strategies) on the cerebral perfusion. **A**-**D**. The maximal residual perfusion after treatment recorded by both probes resulted higher compared to the residual perfusion after MCAO for all the single therapeutic strategies considered in this study. Moreover, perfusion recorded by Probe 2 resulted significantly higher compared to Probe 1 both before and after treatment, for every treatment group, except for HDT group where Probe 2 perfusion was higher than Probe 1 only after treatment. **E**. Representative LD tracings for Probe 1 and 2, the rise in cerebral perfusion after treatment is visible for both probes. In **A**-**D**: * $p < 0.05$, ** $p < 0.01$, ** $p < 0.001$ vs pre for the same Probe (Probe 1 or Probe 2); \$\$ $p < 0.01$, \$\$\$ $p < 0.001$ vs Probe 1 for the same period of ischemia (pre or post). Paired Student's *t*-test was used. P.U. = perfusion units; MCAO = middle cerebral artery occlusion; HDT = head-down tilt.

4.3.4 Effect of Collateral Therapeutics on Cardiorespiratory Parameters

Cardiorespiratory parameters (arterial blood pressure, heart rate, breath rate) were monitored throughout the surgical procedure. Arterial blood pressure and heart rate were significantly higher ($p < 0.001$) and lower ($p < 0.05$), respectively, for the PHE group when compared to controls (Figure 4.8). For animals treated with acetazolamide, polygeline and head-down tilt, no significant variations were seen for these parameters.

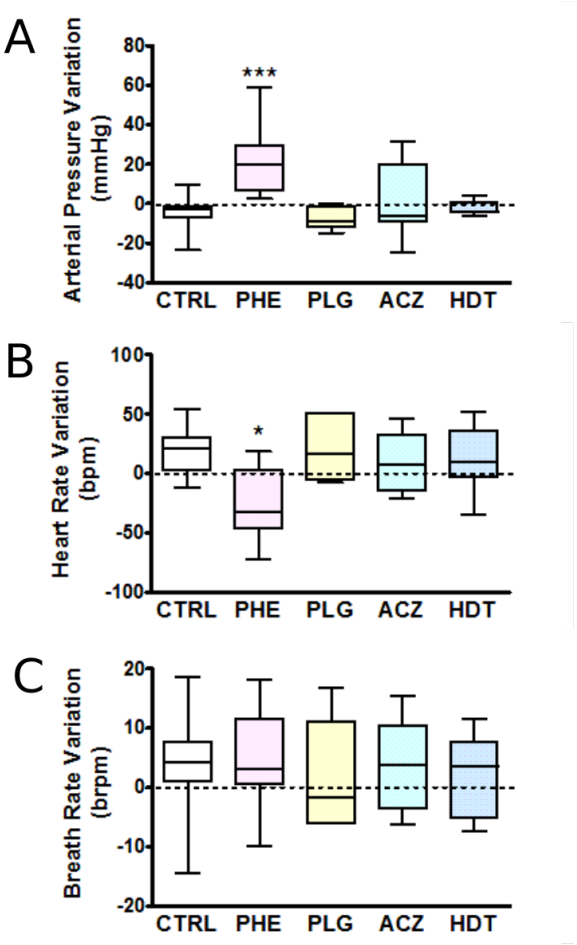

Figure 4.8: Effect of collateral therapeutics on cardiorespiratory parameters. Cardiorespiratory parameters of the four treatment groups were compared to the control group. **A**. Arterial pressure showed no significant variation in treatment groups compared to control, except for PHE group, where it resulted significantly higher ($p < 0.001$). **B**. Heart rate showed no significant variation in treatment groups compared to control, except for PHE group, where resulted significantly higher ($p < 0.05$). **C**. Breath rate showed no significant variation in treatment groups compared to control. * $p < 0.05$, *** $p < 0.001$ vs CTRL.

4.3.5 Treatment-Associated Mortality

In this study, five animals died after treatment administration, representing about 8% of treated animals (n = 60). Three causes of death were identified (Table 4.3):

1. n = 3 rats died of non-procedural SAH (n = 1 treated with acetazolamide, n = 2 treated with phenylephrine); death occured about 45-55 minutes after treatment administration; SAH was confirmed by a 90% drop recorded by both LD probes and visually confirmed after brain extraction.

2. n = 1 rats treated with polygeline died of cardiorespiratory failure; we hypothesized this cause of death because cardiorespiratory alterations preceded cerebral perfusion alterations and no SAH signs were visible after brain extraction.

3. n = 1 rats treated with acetazolamide showed a slow and gradual drop in cerebral perfusion recorded by both LD probes, starting 15-20 minutes after treatment administration; Cardiorespiratory failure and SAH were excluded after evaluation of cerebral perfusion and cardiorespiratory tracings and brain after extraction; thus, we could not define a certain cause of death.

n	**Collateral therapeutic**	**Cause of death**
2	phenylephrine	subarachnoid hemorrhage occurred after initiation of treatment
1	acetazolamide	subarachnoid hemorrhage occurred after initiation of treatment
1	polygeline	cardiorespiratory failure
1	acetazolamide	unknown

Table 4.3: Treatment-related mortality. The number of animals, treatment and cause of death are reported.

4.4 Discussion

We planned this preclinical randomized controlled study to investigate and compare the efficacy and safety of three pharmacological (phenylephrine, polygeline, acetazolamide) and a non-pharmacological (head-down tilt) therapeutic strategies in rats undergoing transient MCAO. Animals were treated 30 minutes after ischemia induction, in order to test the effect of treatments when administered in the hyperacute phase of ischemia, *before* reperfusion.

Therapeutic strategies might act on the collateral circulation through several mechanisms (Cuccione *et al.*, 2015). *Phenylephrine* is a selective α1-adrenergic receptor agonist, which causes systemic vasoconstriction with very limited effects on cerebral vessels. The rise in systemic blood pressure could enhance perfusion through cerebral collateral vessels, as shown in mice after 30% pressure augmentationby phenylephrine infusion (Shin *et al.*, 2008). In small clinical studies, outcome improvement was reported after norepinephrine- o phenylephrine-induced hypertension (Hillis *et al.*, 2003; Koenig *et al.*, 2006; Marzan *et al.*, 2004; Rordorf *et al.*, 2001). In clinical practice, *Polygeline* solution is a colloidal plasma expander used to contrast hypovolemia. Cerebral blood volume augmentation by plasma expansion and hemodiluition could improve cerebral perfusion (Heros and Korosue, 1989), possibly through collateral vessels. Compared to other plasma expanders, such as dextran 70, polygeline has a lower molecular weight, is more rapidly excreted and does not interfere with coagulation, also when injected at high dose. *Acetazolamide* pharmacologically inhibits carbonic anhydrase and consequently augments CO_2 levels (Sullivan *et al.*, 1987), inducing vasodilation, and is used to test hemispheric cerebrovascular reactivity in clinical practice (Kuroda *et al.*, 2001; Ogasawara *et al.*, 2002). A selective arteriolar vasodilation could also enhance collateral blood flow. Pial arteriolar vasodilation and increased cortical perfusion were reported in piglets (Domoki *et al.*, 2008). *Head positioning* could affect collateral recruitment, because of gravitational influences on the pressure gradients in cerebral circulation. Flat head positioning enhanced cerebral perfusion and increased MCA blood flow velocity in stroke patients (Schwarz *et al.*, 2002; Wojner *et al.*, 2002; Wojner-Alexander *et al.*, 2005), whereas a 5° head-down tilt enhanced cerebral perfusion in mice following bilateral CCAO (Nagatani *et al.*, 2012).

In the present study, a composite randomization was considered in order to reach a high (99%) statistical power when comparing the two groups derived from a first randomization (CTRL and COLLTHER), while performing a further explorative analysis, comparing efficacy and safety of each single

therapeutic strategy considered (second randomization: PHE, PLG, ACZ and HDT), with a good statistical power (80%). This statistical design presents advantages from both ethical and economical points of view.

When evaluating the basal characteristics of CTRL and collateral therapeutics groups (first randomization), Probe 2 perfusion after MCAO resulted significantly higher in the treatments group. Since animals were randomized following the randomization list, we assume that this difference occurred by chance in our study. However, ANCOVA analysis to adjust for eventual covariates were also considered. In this regard, Probe 2 perfusion was found to covary (ANCOVA analysis) with infarct volume in this study (and in agreement with our previous work, Riva *et al.* (2012)) and infarct volume adjusted for this covariate were therefore considered.

Again agreement with our previous results (Riva *et al.*, 2012), a strong infarct volume variability emerged, with ischemic lesions ranging from small subcortical to large corticostriatal infarcts. The differential cortical involvement likely reflects the variable performance of the collateral circulation: a better collateral compensation provides a good cortical residual perfusion, sparing, at least partially, the cortical regions. On the contrary, a poor collateral performance is associated with a relevant cortical damage. The subcortical striatal regions are instead constantly involved since vascularised by the lenticulo-striatal arteries, MCA end branches which do not form collaterals with adjacent vascular territories (Zülch, 1981).

When globally considered (CTRL vs COLL-THER group, first randomization), collateral therapeutics administration was associated with improved ischemic outcomes at 24 hours post-reperfusion, i.e. small infarct volumes and better neuroscores. However, when therapeutic strategies were singularly considered (PHE, PLG, ACZ, HDT vs CTRL group, second randomization), differential effects on the ischemic outcome emerged. Phenylephrine showed no significant improvement of ischemic outcome, neither for infarct volume nor for neuroscore. Treatment with acetazolamide and polygeline lead to a significant reduction of infarct volume, but not paralleled by a functional improvement. Head-down tilt is the only therapeutic approach which was associated with both structural and functional improvement in our study. These results were also confirmed for infarct volumes adjusted for Probe 2 perfusion values after ANCOVA analysis.

Cerebral perfusion was continuously monitored using multi-site LDF (Beretta *et al.*, 2013). We assume that the cerebral perfusion drop recorded by Probe 1 in the lateral MCA territory is a direct consequence of MCAO, whereas the perfusion variations recorded by Probe 2 in the ACA-MCA borderzone territory are reflecting the compensatory performance of the leptomeningeal collaterals

connecting the ACA and MCA vascular territories. As expected and in agreement with our previous results (Riva *et al.*, 2012), perfusion recorded after MCAO in the collaterals territory resulted higher than perfusion in the core of the MCA territory, for every animal enrolled in this study.

Treatments were administered 30 minutes after ischemia induction and maximal perfusion after treatment resulted higher when compared to both maximal perfusion in 30-90 minutes of ischemia in control animals and the perfusion recorded before treatment (0-30 minutes) in treated animals. Although maximal perfusion resulted improved in both monitoring sites, the improvement in the collaterals territory (Probe 2) was significantly more marked than in the lateral MCA territory (Probe 1) for any treatment. This supports our hypothesis, according to which the therapeutic strategies considered could acutely enhance cerebral blood flow through collateral vessels.

Interestingly, maximal cerebral perfusion recorded in control animals within 30-90 minutes of ischemia was significantly higher compared to perfusion after MCAO (0-30 minutes), for both Probe 1 and 2. This possibly indicates an endogenous response of the cerebral circulation to ischemia with time, which translates into an improvement of collateral flow also in absence of treatment. In support thereof, Probe 2 perfusion resulted significantly higher than Probe 1.

Polygeline, acetazolamide and head-down tilt caused no significant variation of the cardiorespiratory parameters monitored, indicating that the positive effect is not due to or influenced by cardiorespiratory modifications. Differently, phenylephrine caused an -expected- rise in systemic blood pressure, attributable to the mechanism of action of this therapeutic approach. A reduction in heart rate was also visible for this treatment, in agreement with a previous report (Sleight, 1979).

The mortality associated with treatments administration in this study is about 8% (n = 5 out of 60 treated animals). Two rats died after treatment with phenilephrine, 2 after treatment with acetazolamide and 1 after treatment with polygeline. Identified causes of death are cardiorespiratory failure and non-procedural SAH. Interestingly, no animal died after head-down tilt in this study.

A limit of this work is represented by the intraluminal suture model used. In fact, the mechanical nature of occlusion and reperfusion induction by filament withdrawal prevent us from exploring possible interactions between thrombolytic drug and collateral therapeutics. Although assessment of acute ischemic penumbra, e.g. by diffusion-perfusion mismatch on magnetic resonance imaging, is of strong interest, it was beyond the aim of this study. Further studies exploring the evolution of ischemic penumbra after treatment and also testing these therapeutic approaches in animals with co-morbidities (e.g. hypertension), particularly in the view of hemorrhagic risk, are warranted. Moreover, in order to specifically test the safety of these therapies in the pre-hospital phase, possible harmful effects should

be tested in preclinical models of hemorrhagic stroke.

4.5 Conclusions

In the present preclinical randomized controlled study, the efficacy and safety of four 'collateral therapeutics' was investigated and compared. All strategies enhanced cerebral perfusion and to a greater extent in the collaterals territory compared to the core MCA territory. When globally considered, treatments were shown to improve tissue and functional ischemic outcome at 24 hours post-reperfusion. Differential effects were shown when strategies were singularly considered. Head-down tilt emerged as the strategy with higher translational impact, since associated with both tissue and functional improvement and no mortality. Our results prompt further study of collateral therapeutics for the hyper-acute (even pre-hospital) phase of ischemic stroke, aiming at the extension of the therapeutic window for recanalization therapies.

Chapter 5

General Discussion

Stroke is a multi-factorial pathology and is the first cause of disability (Feigin *et al.*, 2003) and second cause of death worldwide (Lozano *et al.*, 2012). Ischemic stroke, representing 80% of stroke cases, is due to a vascular occlusion causing a sudden drop in cerebral perfusion (Donnan *et al.*, 2008). At present, therapeutic approaches to acute ischemic stroke are limited. Generally, recanalization and neuroprotective therapies are being considered. Recanalization aims at eliminating occlusion and consequently restoring blood flow to the brain, whereas neuroprotective therapies aim at blocking the ischemic cascade by directly targeting the pathological molecular events ongoing in the hypoperfused cerebral tissue. Recanalization by thrombolysis using intravenous rtPA (Alteplase) is the only FDA-approved therapy (NINDS, 1995; Saver *et al.*, 2009). Unfortunately, most patients are not eligible for this therapy because of the restricted time window (4.5 hours from symptoms onset) (Ingall, 2009; Lansberg *et al.*, 2009) and the risk of hemorrhagic transformation. On the other hand, positive results of preclinical neuroprotection studies failed to translate into successful clinical trials (Sutherland *et al.*, 2012).

All therapeutic strategies for acute ischemic stroke aim at saving the "ischemic penumbra", cerebral hypoperfused regions which are not yet permanently damaged by ischemia (in contrast to the ischemic core) and can be potentially saved if reperfusion is timely achieved (Hossmann, 2006). The presence and extension of the ischemic penumbra varies from patient to patient and is being increasingly considered for patient selection for therapy (Davis and Donnan, 2014): beyond the time window, an extended penumbra with potential for salvage encourages therapeutic efforts.

Collateral circulation is a subsidiary vascular network dynamically recruited after vascular occlusion and providing residual perfusion to the ischemic penumbra (Liebeskind, 2003). A good collateral status was associated with larger baseline penumbra and reduced ischemic core (Campbell *et al.*,

2013) and with a more favourable functional outcome and reduced mortality (Bang *et al.*, 2008; Lima *et al.*, 2010; Menon *et al.*, 2011; Miteff *et al.*, 2009) in untreated patients. Also in recanalized patients, a good collateralization protected from infarct growth and hemorrhagic transformation (Bang *et al.*, 2008, 2011b) and was associated with more favourable early and long term outcome (Calleja *et al.*, 2013). Furthermore, modulating collateral blood flow in order to augment or maintain perfusion to the ischemic penumbra could represent a new therapeutic strategy for the hyperacute (even pre-hospital) phase (Liebeskind, 2004, 2010; Shuaib *et al.*, 2011b), particularly if applied before recanalization. Nonetheless, the collateral circulation is frequently neglected in both clinical and preclinical settings.

The present work focused on the collateral circulation in experimental ischemic stroke. In this regard, we explored:

- the relationship between cerebral collateral flow and ischemic penumbra (Chapter 2);
- collateral flow as a predictor of ischemic outcome and stratification factor (Chapter 3);
- strategies for the therapeutic modulation of collateral blood flow (Chapter 4).

Along the development of this research project, we constantly committed ourselves to follow the STAIRS recommendations for standards quality of preclinical stroke research (See Section 1.3.2.1), starting with opting for animal species and experimental stroke model which were best fitting the aims of our work.

In this regard, we considered the intraluminal suture MCAO model in Wistar rats in the view to perform an ischemia of 90 minutes followed by 24 hours of reperfusion. The Wistar strain was chosen among other strains (e.g. Sprague-Dawley, Lewis) and healthy male, young adult animals were used. As an advantage, Wistar lines presenting hypertension (e.g. SHR and spSHR) is available and can be used for future studies in animals with stroke co-morbidities.

Several ischemic stroke models are used in experimental stroke research (see Section 1.3.1). For this study, the occlusion of the MCA, which is the cause of the majority of ischemic stroke cases, was modeled by the insertion of an intraluminal filament to occlude its origin without the need to perform a craniotomy. A mechanical occlusion is thus performed, which can be reverted by filament withdrawal, allowing for controlled time of ischemia and reperfusion.

Rats were considered instead of mice because of their greater size, which made them more appropriate for physiological parameters monitoring and application of neuroimaging techniques (such as MRI), as was done in this study. The monitoring of physiological parameters, among which cerebral blood

flow but also blood pressure, heart and respiratory rate, etc. is strongly recommended, especially in order to discriminate possible indirect neuroprotective effects (Sutherland *et al.*, 2011).

To evaluate the cerebral flow we used an optimized multi-site LDF apparatus (Beretta *et al.*, 2013), which allowed us to monitor cortical perfusion in real time in the lateral MCA territory and in the borderzone territory between ACA and MCA. We assumed that the cerebral perfusion drop recorded by Probe 1 in the lateral MCA territory is a direct consequence of MCAO, whereas the perfusion variations recorded by Probe 2 in the ACA-MCA borderzone territory are reflecting the compensatory performance of the leptomeningeal collaterals connecting the ACA and MCA vascular territories. The advantages of LDF over other techniques for the evaluation of collateral blood flow (e.g. LSCI, TPLSM, see Section 1.2.4) are the real-time monitoring and the possibility to avoid craniotomy, reducing the invasiveness of the approach. On the other hand, a limit of LDF is the lack of spatial resolution, which is in contrast provided by other techniques.

The ischemic outcome was evaluated after 24 hours of reperfusion, both in terms of neurological deficits and tissue lesion. The neurological deficits were assessed using a behavioral and sensory-motor scoring system (Garcia *et al.*, 1995), with the aim to obtain an overall evaluation of the functional damage. However, more specific tasks are being considered and implemented in order to provide a more precise and quantitative assessment. These include plantar test (Hargreaves *et al.*, 1988), sticky-tape test (Sughrue *et al.*, 2006) and corner test (Schallert *et al.*, 1982, 1983) for the evaluation of the hindlimbs, forelimbs and vibrissae sensitive deficits, respectively. These additional tests are going to be included in future experimental campaigns.

The tissue lesion extension was evaluated in terms of infarct volume, expressed in mm^3 and corrected for edema (Leach *et al.*, 1993). The lesion was visualized *in vivo* by T2-weighted MRI (Chapter 3) and *ex-vivo* on coronal brain sections stained with Cresyl violet (Chapter 2 and 4).

Although ischemic outcome evaluation was planned after 24 hours of reperfusion in these studies, longitudinal studies where ischemic outcome is evaluated after longer periods, such as 48h, 7 days or even 1 month are to be planned in the future to confirm outcome stability in time.

In agreement with the fundamental standards for quality (Fisher *et al.*, 2009), we calculated the sample size required to obtain a good statistical power and defined criteria for animal exclusion. We defined and reported exclusion criteria for our studies and excluded animals were subsequently indicated. For the collateral therapeutics study (Chapter 4), animals were randomized according to a randomization list, allocation to experimental groups was concealed and assessment of primary and secondary outcomes was mutually blinded.

Conclusions and Future Perspectives

Taken together, the results of our studies support the importance of monitoring collateral blood flow and its relevance in experimental ischemic stroke, both in the view of ischemic outcome and penumbra prediction and the study of new therapeutic strategies based on the modulation of collateral blood flow.

In the first study (Chapter 2), we showed that a good collateral flow was associated with both reduced post-reperfusion molecular penumbra and ischemic core, i.e. increased areas of preserved tissue. These findings are relevant in the view of the development of strategies acting on the collateral circulation.

In the second study (Chapter 3), we showed how collateral blood flow could be used to *a priori* stratify animals depending on infarct typology (i.e. large hemispheric vs basal ganglia infarct), in agreement with DWI-MRI evaluation (Chauveau *et al.*, 2012). We therefore propose the multi-site LDF approach as an alternative to MRI to predict ischemic outcome and control its variability in preclinical studies.

In the third and last study (Chapter 4), we evaluated four therapeutic strategies that might act on collateral blood flow and showed how they acutely modulated cerebral blood flow, mainly in the collaterals territory, and their differential efficacy on the improvement of 24 hours ischemic outcome, which highlighted head-down tilt as the safest and most efficient among the approaches considered.

The main limitation of the first study (Chapter 2) is the evaluation of a molecular penumbra beyond the acute phase. As discussed in Section 1.1.4, the ischemic penumbra can be evaluated by several modalities, ranging from the assessment of molecular alterations (as done in our study) to neuroimaging techniques. Undoubtedly, the evaluation of the penumbra in the acute phase by imaging techniques such as MRI and its comparison to post-reperfusion molecular penumbra is of foremost interest and will be explored in further studies. In fact, although presenting some limitations, the evaluation of ischemic penumbra in humans relies on neuroimaging techniques, among which PWI-DWI mismatch on MRI is the most commonly used and increasingly improving. Moreover, the evolution of the ischemic penumbra in time can be explored using MRI. Interestingly, penumbra defined by HSP70 expression as also been explored by MRI molecular imaging using targeted nanoliposomes (Agulla *et al.*, 2013). The evaluation of the ischemic penumbra was beyond the aim of the our study of collateral therapeutics (Chapter 4). Nonetheless, exploring both acute (as PWI-DWI mismatch) and post-reperfusion (as HSP70 protein expression) penumbra could provide more information about and further confirm the mechanism of action of putative collateral therapeutic strategies.

A relevant aspect of our studies is the use of male young animals. This is in agreement with the guidelines for preclinical stroke research, suggesting the use of young healthy animals for initial studies. Nonetheless, aged animals and/or with co-morbidities (such as hypertension, diabetes, etc.) are more precisely matching the characteristics of the human population most affected by stroke and should therefore be considered. Moreover, modification in the collateral circulation in both patients (Arsava *et al.*, 2013; Ovbiagele *et al.*, 2007) and animals (Coyle, 1987; Faber *et al.*, 2011; Hecht *et al.*, 2012; Omura-Matsuoka *et al.*, 2011) with advanced age and co-morbidities have been previously reported and might impact on our results. For these reasons, future studies will be performed using aged animals and/or with co-morbidities. Besides, female rats should also be considered and results must be subsequently confirmed in different animal species.

In order to specifically test the safety of therapies acting on the collateral flow in the pre-hospital phase, possible harmful effects should be tested in preclinical models of hemorrhagic stroke, since hemorrhagic transformation of ischemic stroke represents one of the major complications following thrombolytic treatment. Models of both subarachnoid (Bederson *et al.*, 1995; Solomon *et al.*, 1985) and intracerebral hemorrhage (Ma *et al.*, 2011) will thus be incorporated in future studies.

Preclinical stroke research has the potential to directly study collateral blood flow, using different methods and in different controlled experimental conditions and should be therefore exploited to understand the compensatory mechanisms of the collateral circulation during acute ischemic stroke and their potential for the development and translation of new therapeutic strategies, based on the therapeutic modulation of collateral flow.

Bibliography

Adams HP, Bendixen BH, Kappelle LJ, Biller J, Love BB, Gordon DL and Marsh EE. Classification of subtype of acute ischemic stroke. Definitions for use in a multicenter clinical trial. TOAST. Trial of Org 10172 in Acute Stroke Treatment. *Stroke*, 24(1):35–41, 1993.

Agulla J, Brea D, Campos F, Sobrino T, Argibay B, Al-Soufi W, Blanco M, Castillo J and Ramos-Cabrer P. In vivo theranostics at the peri-infarct region in cerebral ischemia. *Theranostics*, 4(1):90–105, 2013.

Albers GW, von Kummer R, Truelsen T, Jensen JK, Ravn GM, GrÃ¸nning BA, Chabriat H, Chang KC, Davalos AE, Ford GA, Grotta J, Kaste M, Schwamm LH, Shuaib A and Investigators D. Safety and efficacy of desmoteplase given 3-9 h after ischaemic stroke in patients with occlusion or high-grade stenosis in major cerebral arteries (DIAS-3): a double-blind, randomised, placebo-controlled phase 3 trial. *Lancet Neurol*, 14(6):575–84, 2015.

Ansar S, Chatzikonstantinou E, Wistuba-Schier A, Mirau-Weber S, Fatar M, Hennerici MG and Meairs S. Characterization of a new model of thromboembolic stroke in C57 black/6J mice. *Transl Stroke Res*, 5(4):526–33, 2014.

Arai K, Jin G, Navaratna D and Lo EH. Brain angiogenesis in developmental and pathological processes: neurovascular injury and angiogenic recovery after stroke. *FEBS J*, 276(17):4644–52, 2009.

Armitage GA, Todd KG, Shuaib A and Winship IR. Laser speckle contrast imaging of collateral blood flow during acute ischemic stroke. *J Cereb Blood Flow Metab*, 30(8):1432–6, 2010.

Arsava EM, Vural A, Akpinar E, Gocmen R, Akcalar S, Oguz KK and Topcuoglu MA. The Detrimental Effect of Aging on Leptomeningeal Collaterals in Ischemic Stroke. *J Stroke Cerebrovasc Dis*, 2013.

Asplund K, Karvanen J, Giampaoli S, Jousilahti P, Niemelä M, Broda G, Cesana G, Dallongeville J, Ducimetriere P, Evans A, Ferrières J, Haas B, Jorgensen T, Tamosiunas A, Vanuzzo D, Wiklund PG, Yarnell J, Kuulasmaa K, Kulathinal S and Project M. Relative risks for stroke by age, sex, and population based on follow-up of 18 European populations in the MORGAM Project. *Stroke*, 40(7):2319–26, 2009.

Astrup J, Symon L, Branston NM and Lassen NA. Cortical evoked potential and extracellular K+ and H+ at critical levels of brain ischemia. *Stroke*, 8(1):51–7, 1977.

Attwell D, Buchan AM, Charpak S, Lauritzen M, Macvicar BA and Newman EA. Glial and neuronal control of brain blood flow. *Nature*, 468(7321):232–43, 2010.

Auer RN and Sutherland GR. Primary intracerebral hemorrhage: pathophysiology. *Can J Neurol Sci*, 32 Suppl 2:S3–12, 2005.

Ayata C, Dunn AK, Gursoy-OZdemir Y, Huang Z, Boas DA and Moskowitz MA. Laser speckle flowmetry for the study of cerebrovascular physiology in normal and ischemic mouse cortex. *J Cereb Blood Flow Metab*, 24(7):744–55, 2004.

Azizyan A, Sanossian N, Mogensen MA and Liebeskind DS. Fluid-attenuated inversion recovery vascular hyperintensities: an important imaging marker for cerebrovascular disease. *AJNR Am J Neuroradiol*, 32(10):1771–5, 2011.

Baird AE, Benfield A, Schlaug G, Siewert B, LÃ¶vblad KO, Edelman RR and Warach S. Enlargement of human cerebral ischemic lesion volumes measured by diffusion-weighted magnetic resonance imaging. *Ann Neurol*, 41(5):581–9, 1997.

Baird AE and Warach S. Magnetic resonance imaging of acute stroke. *J Cereb Blood Flow Metab*, 18(6):583–609, 1998.

Bang OY, Saver JL, Buck BH, Alger JR, Starkman S, Ovbiagele B, Kim D, Jahan R, Duckwiler GR, Yoon SR, Viñuela F, Liebeskind DS and Investigators UC. Impact of collateral flow on tissue fate in acute ischaemic stroke. *J Neurol Neurosurg Psychiatry*, 79(6):625–9, 2008.

Bang OY, Saver JL, Kim SJ, Kim GM, Chung CS, Ovbiagele B, Lee KH and Liebeskind DS. Collateral flow predicts response to endovascular therapy for acute ischemic stroke. *Stroke*, 42(3):693–9, 2011a.

Bang OY, Saver JL, Kim SJ, Kim GM, Chung CS, Ovbiagele B, Lee KH, Liebeskind DS and Collaborators USS. Collateral flow averts hemorrhagic transformation after endovascular therapy for acute ischemic stroke. *Stroke*, 42(8):2235–9, 2011b.

Bar-Shir A, Shemesh N, Nossin-Manor R and Cohen Y. Late stimulation of the sphenopalatine-ganglion in ischemic rats: improvement in N-acetyl-aspartate levels and diffusion weighted imaging characteristics as seen by MR. *J Magn Reson Imaging*, 31(6):1355–63, 2010.

Bardutzky J, Meng X, Bouley J, Duong TQ, Ratan R and Fisher M. Effects of intravenous dimethyl sulfoxide on ischemia evolution in a rat permanent occlusion model. *J Cereb Blood Flow Metab*, 25(8):968–77, 2005a.

Bardutzky J, Shen Q, Henninger N, Bouley J, Duong TQ and Fisher M. Differences in ischemic lesion evolution in different rat strains using diffusion and perfusion imaging. *Stroke*, 36(9):2000–5, 2005b.

Baron JC. Mapping the ischaemic penumbra with PET: implications for acute stroke treatment. *Cerebrovasc Dis*, 9(4):193–201, 1999.

Baron JC, Bousser MG, Rey A, Guillard A, Comar D and Castaigne P. Reversal of focal "misery-perfusion syndrome" by extra-intracranial arterial bypass in hemodynamic cerebral ischemia. A case study with 15O positron emission tomography. *Stroke*, 12(4):454–9, 1981.

Barone FC, Knudsen DJ, Nelson AH, Feuerstein GZ and Willette RN. Mouse strain differences in susceptibility to cerebral ischemia are related to cerebral vascular anatomy. *J Cereb Blood Flow Metab*, 13(4):683–92, 1993.

Baumgartner RW, Baumgartner I, Mattle HP and Schroth G. Transcranial color-coded duplex sonography in the evaluation of collateral flow through the circle of Willis. *AJNR Am J Neuroradiol*, 18(1):127–33, 1997.

Beaulieu C, de Crespigny A, Tong DC, Moseley ME, Albers GW and Marks MP. Longitudinal magnetic resonance imaging study of perfusion and diffusion in stroke: evolution of lesion volume and correlation with clinical outcome. *Ann Neurol*, 46(4):568–78, 1999.

Bederson JB, Germano IM and Guarino L. Cortical blood flow and cerebral perfusion pressure in a new noncraniotomy model of subarachnoid hemorrhage in the rat. *Stroke*, 26(6):1086–91; discussion 1091–2, 1995.

Bederson JB, Pitts LH, Tsuji M, Nishimura MC, Davis RL and Bartkowski H. Rat middle cerebral artery occlusion: evaluation of the model and development of a neurologic examination. *Stroke*, 17(3):472–6, 1986.

Beech JS, Williams SC, Campbell CA, Bath PM, Parsons AA, Hunter AJ and Menon DK. Further characterisation of a thromboembolic model of stroke in the rat. *Brain Res*, 895(1-2):18–24, 2001.

Belayev L, Busto R, Zhao W, Clemens JA and Ginsberg MD. Effect of delayed albumin hemodilution on infarction volume and brain edema after transient middle cerebral artery occlusion in rats. *J Neurosurg*, 87(4):595–601, 1997.

Belayev L, Busto R, Zhao W and Ginsberg MD. Quantitative evaluation of blood-brain barrier permeability following middle cerebral artery occlusion in rats. *Brain Res*, 739(1-2):88–96, 1996.

Belayev L, Zhao W, Pattany PM, Weaver RG, Huh PW, Lin B, Busto R and Ginsberg MD. Diffusion-weighted magnetic resonance imaging confirms marked neuroprotective efficacy of albumin therapy in focal cerebral ischemia. *Stroke*, 29(12):2587–99, 1998.

Beretta S, Cuccione E, Versace A, Carone D, Riva M, Padovano G, Dell'Era V, Cai R, Monza L, Presotto L, Rousseau D, Chauveau F, Paternò G, Pappadà GB, Giussani C, Sganzerla EP and Ferrarese C. Cerebral collateral flow defines topography and evolution of molecular penumbra in experimental ischemic stroke. *Neurobiol Dis*, 74:305–13, 2015.

Beretta S, Riva M, Carone D, Cuccione E, Padovano G, Rodriguez Menendez V, PappadÃ¡ GB, Versace A, Giussani C, Sganzerla EP and Ferrarese C. Optimized system for cerebral perfusion monitoring in the rat stroke model of intraluminal middle cerebral artery occlusion. *J Vis Exp*, (72), 2013.

Berkhemer OA, van Zwam WH, Dippel DW and Investigators MC. Stent-Retriever Thrombectomy for Stroke. *N Engl J Med*, 373(11):1076, 2015.

Berthet K, Lukaszewicz AC, Bousser MG and Payen D. Lower body positive pressure application with an antigravity suit in acute carotid occlusion. *Stroke Res Treat*, 2010, 2010.

Biernaskie J, Corbett D, Peeling J, Wells J and Lei H. A serial MR study of cerebral blood flow changes and lesion development following endothelin-1-induced ischemia in rats. *Magn Reson Med*, 46(4):827–30, 2001.

Bivard A, Spratt N, Levi C and Parsons M. Perfusion computer tomography: imaging and clinical validation in acute ischaemic stroke. *Brain*, 134(Pt 11):3408–16, 2011.

Bonnin P, Leger PL, Deroide N, Fau S, Baud O, Pocard M, Charriaut-Marlangue C and Renolleau S. Impact of intracranial blood-flow redistribution on stroke size during ischemia-reperfusion in 7-day-old rats. *J Neurosci Methods*, 198(1):103–9, 2011.

Bouley J, Fisher M and Henninger N. Comparison between coated vs. uncoated suture middle cerebral artery occlusion in the rat as assessed by perfusion/diffusion weighted imaging. *Neurosci Lett*, 412(3):185–90, 2007.

Bouts MJ, Tiebosch IA, van der Toorn A, Viergever MA, Wu O and Dijkhuizen RM. Early identification of potentially salvageable tissue with MRI-based predictive algorithms after experimental ischemic stroke. *J Cereb Blood Flow Metab*, 33(7):1075–82, 2013.

Braeuninger S and Kleinschnitz C. Rodent models of focal cerebral ischemia: procedural pitfalls and translational problems. *Exp Transl Stroke Med*, 1:8, 2009.

Branston NM, Strong AJ and Symon L. Extracellular potassium activity, evoked potential and tissue blood flow. Relationships during progressive ischaemia in baboon cerebral cortex. *J Neurol Sci*, 32(3):305–21, 1977.

Branston NM, Symon L, Crockard HA and Pasztor E. Relationship between the cortical evoked potential and local cortical blood flow following acute middle cerebral artery occlusion in the baboon. *Exp Neurol*, 45(2):195–208, 1974.

Bremer AM, Yamada K and West CR. Ischemic cerebral edema in primates: effects of acetazolamide, phenytoin, sorbitol, dexamethasone, and methylprednisolone on brain water and electrolytes. *Neurosurgery*, 6(2):149–54, 1980.

Brint S, Jacewicz M, Kiessling M, Tanabe J and Pulsinelli W. Focal brain ischemia in the rat: methods for reproducible neocortical infarction using tandem occlusion of the distal middle cerebral and ipsilateral common carotid arteries. *J Cereb Blood Flow Metab*, 8(4):474–85, 1988.

Broderick JP, Palesch YY, Demchuk AM, Yeatts SD, Khatri P, Hill MD, Jauch EC, Jovin TG, Yan B, Silver FL, von Kummer R, Molina CA, Demaerschalk BM, Budzik R, Clark WM, Zaidat OO, Malisch TW, Goyal M, Schonewille WJ, Mazighi M, Engelter ST, Anderson C, Spilker J, Carrozzella J, Ryckborst KJ, Janis LS, Martin RH, Foster LD, Tomsick TA and Investigators IMoSII. Endovascular therapy after intravenous t-PA versus t-PA alone for stroke. *N Engl J Med*, 368(10):893–903, 2013.

Broughton BR, Reutens DC and Sobey CG. Apoptotic mechanisms after cerebral ischemia. *Stroke*, 40(5):e331–9, 2009.

Brouns R and De Deyn PP. The complexity of neurobiological processes in acute ischemic stroke. *Clin Neurol Neurosurg*, 111(6):483–95, 2009.

Brozici M, van der Zwan A and Hillen B. Anatomy and functionality of leptomeningeal anastomoses: a review. *Stroke*, 34(11):2750–62, 2003.

Brunner F, Tomandl B, Hanken K, Hildebrandt H and Kastrup A. Impact of collateral circulation on early outcome and risk of hemorrhagic complications after systemic thrombolysis. *Int J Stroke*, 9(8):992–8, 2014.

Buchan AM, Xue D and Slivka A. A new model of temporary focal neocortical ischemia in the rat. *Stroke*, 23(2):273–9, 1992.

Busch E, Kräger K and Hossmann KA. Improved model of thromboembolic stroke and rt-PA induced reperfusion in the rat. *Brain Res*, 778(1):16–24, 1997.

Buschmann I, Heil M, Jost M and Schaper W. Influence of inflammatory cytokines on arteriogenesis. *Microcirculation*, 10(3-4):371–9, 2003a.

Buschmann IR, Busch HJ, Mies G and Hossmann KA. Therapeutic induction of arteriogenesis in hypoperfused rat brain via granulocyte-macrophage colony-stimulating factor. *Circulation*, 108(5):610–5, 2003b.

Calamante F, Thomas DL, Pell GS, Wiersma J and Turner R. Measuring cerebral blood flow using magnetic resonance imaging techniques. *J Cereb Blood Flow Metab*, 19(7):701–35, 1999.

Calleja AI, Cortijo E, García-Bermejo P, Gómez RD, Pérez-Fernández S, Del Monte JM, Muñoz MF, Fernández-Herranz R and Arenillas JF. Collateral circulation on perfusion-computed tomography-source images predicts the response to stroke intravenous thrombolysis. *Eur J Neurol*, 20(5):795–802, 2013.

Campbell BC, Christensen S, Tress BM, Churilov L, Desmond PM, Parsons MW, Barber PA, Levi CR, Bladin C, Donnan GA, Davis SM and Investigators E. Failure of collateral blood flow is associated with infarct growth in ischemic stroke. *J Cereb Blood Flow Metab*, 33(8):1168–72, 2013.

Campbell BC, Mitchell PJ and Investigators EI. Endovascular therapy for ischemic stroke. *N Engl J Med*, 372(24):2365–6, 2015a.

Campbell BC, Mitchell PJ, Kleinig TJ, Dewey HM, Churilov L, Yassi N, Yan B, Dowling RJ, Parsons MW, Oxley TJ, Wu TY, Brooks M, Simpson MA, Miteff F, Levi CR, Krause M, Harrington TJ, Faulder KC, Steinfort BS, Priglinger M, Ang T, Scroop R, Barber PA, McGuinness B, Wijeratne T, Phan TG, Chong W, Chandra RV, Bladin CF, Badve M, Rice H, de Villiers L, Ma H, Desmond PM, Donnan GA, Davis SM and Investigators EI. Endovascular therapy for ischemic stroke with perfusion-imaging selection. *N Engl J Med*, 372(11):1009–18, 2015b.

Carmichael ST. Rodent models of focal stroke: size, mechanism, and purpose. *NeuroRx*, 2(3):396–409, 2005.

Caysa H, Metz H, Mäder K and Mueller T. Application of Benchtop-magnetic resonance imaging in a nude mouse tumor model. *J Exp Clin Cancer Res*, 30(1):69, 2011.

Chang TS and Jensen MB. Haemodilution for acute ischaemic stroke. *Cochrane Database Syst Rev*, 8:CD000103, 2014.

Chauveau F, Cho TH, Perez M, Guichardant M, Riou A, Aguettaz P, Picq M, Lagarde M, Berthezène Y, Nighoghossian N and Wiart M. Brain-targeting form of docosahexaenoic acid for experimental stroke treatment: MRI evaluation and anti-oxidant impact. *Curr Neurovasc Res*, 8(2):95–102, 2011.

Chauveau F, Cho TH, Riou A, Langlois JB, Berthezène Y, Nighoghossian N and Wiart M. Does acute behavioral testing reflect successful ischemia in rats with transient middle cerebral artery occlusion? *Int J Stroke*, 7(6):465–72, 2012.

Chen ST, Hsu CY, Hogan EL, Maricq H and Balentine JD. A model of focal ischemic stroke in the rat: reproducible extensive cortical infarction. *Stroke*, 17(4):738–43, 1986.

Cho TH, Aguettaz P, Campuzano O, Charriaut-Marlangue C, Riou A, Berthezène Y, Nighoghossian N, Ovize M, Wiart M and Chauveau F. Pre- and post-treatment with cyclosporine A in a rat model of transient focal cerebral ischaemia with multimodal MRI screening. *Int J Stroke*, 8(8):669–74, 2013.

Chopp M, Li Y, Jiang N, Zhang RL and Prostak J. Antibodies against adhesion molecules reduce apoptosis after transient middle cerebral artery occlusion in rat brain. *J Cereb Blood Flow Metab*, 16(4):578–84, 1996.

Christoforidis GA, Mohammad Y, Kehagias D, Avutu B and Slivka AP. Angiographic assessment of pial collaterals as a prognostic indicator following intra-arterial thrombolysis for acute ischemic stroke. *AJNR Am J Neuroradiol*, 26(7):1789–97, 2005.

Christoforidis GA, Rink C, Kontzialis MS, Mohammad Y, Koch RM, Abduljalil AM, Bergdall VK, Roy S, Khanna S, Slivka AP, Knopp MV and Sen CK. An endovascular canine middle cerebral artery occlusion model for the study of leptomeningeal collateral recruitment. *Invest Radiol*, 46(1):34–40, 2011.

Clayton JA, Chalothorn D and Faber JE. Vascular endothelial growth factor-A specifies formation of native collaterals and regulates collateral growth in ischemia. *Circ Res*, 103(9):1027–36, 2008.

Cortijo E, Calleja AI, García-Bermejo P, Mulero P, Pérez-Fernández S, Reyes J, Muñoz MF, Martínez-Galdámez M and Arenillas J. Relative cerebral blood volume as a marker of durable tissue-at-risk viability in hyperacute ischemic stroke. *Stroke*, 45(1):113–8, 2014.

Coyle P. Different susceptibilities to cerebral infarction in spontaneously hypertensive (SHR) and normotensive Sprague-Dawley rats. *Stroke*, 17(3):520–5, 1986.

Coyle P. Dorsal cerebral collaterals of stroke-prone spontaneously hypertensive rats (SHRSP) and Wistar Kyoto rats (WKY). *Anat Rec*, 218(1):40–4, 1987.

Coyle P and Jokelainen PT. Dorsal cerebral arterial collaterals of the rat. *Anat Rec*, 203(3):397–404, 1982.

Cuccione E, Padovano G, Versace A and Ferrarese A. Cerebral collateral circulation in experimental ischemic stroke. *Exp Transl Stroke Med*. In press, 2015.

Darby DG, Barber PA, Gerraty RP, Desmond PM, Yang Q, Parsons M, Li T, Tress BM and Davis SM. Pathophysiological topography of acute ischemia by combined diffusion-weighted and perfusion MRI. *Stroke*, 30(10):2043–52, 1999.

Davis M, Mendelow AD, Perry RH, Chambers IR and James OF. Experimental stroke and neuroprotection in the aging rat brain. *Stroke*, 26(6):1072–8, 1995.

Davis S and Donnan GA. Time is Penumbra: imaging, selection and outcome. The Johann jacob wepfer award 2014. *Cerebrovasc Dis*, 38(1):59–72, 2014.

Davis SM, Donnan GA, Parsons MW, Levi C, Butcher KS, Peeters A, Barber PA, Bladin C, De Silva DA, Byrnes G, Chalk JB, Fink JN, Kimber TE, Schultz D, Hand PJ, Frayne J, Hankey G, Muir K, Gerraty R, Tress BM, Desmond PM and investigators E. Effects of alteplase beyond 3 h after stroke in the Echoplanar Imaging Thrombolytic Evaluation Trial (EPITHET): a placebo-controlled randomised trial. *Lancet Neurol*, 7(4):299–309, 2008.

Defazio RA, Zhao W, Deng X, Obenaus A and Ginsberg MD. Albumin therapy enhances collateral perfusion after laser-induced middle cerebral artery branch occlusion: a laser speckle contrast flow study. *J Cereb Blood Flow Metab*, 32(11):2012–22, 2012.

del Zoppo GJ, Higashida RT, Furlan AJ, Pessin MS, Rowley HA and Gent M. PROACT: a phase II randomized trial of recombinant pro-urokinase by direct arterial delivery in acute middle cerebral artery stroke. PROACT Investigators. Prolyse in Acute Cerebral Thromboembolism. *Stroke*, 29(1):4–11, 1998.

del Zoppo GJ, Schmid-Schönbein GW, Mori E, Copeland BR and Chang CM. Polymorphonuclear leukocytes occlude capillaries following middle cerebral artery occlusion and reperfusion in baboons. *Stroke*, 22(10):1276–83, 1991.

del Zoppo GJ, Sharp FR, Heiss WD and Albers GW. Heterogeneity in the penumbra. *J Cereb Blood Flow Metab*, 31(9):1836–51, 2011.

Devor A, Sakadžić S, Srinivasan VJ, Yaseen MA, Nizar K, Saisan PA, Tian P, Dale AM, Vinogradov SA, Franceschini MA and Boas DA. Frontiers in optical imaging of cerebral blood flow and metabolism. *J Cereb Blood Flow Metab*, 32(7):1259–76, 2012.

D'Hooge R and De Deyn PP. Applications of the Morris water maze in the study of learning and memory. *Brain Res Brain Res Rev*, 36(1):60–90, 2001.

Dirnagl U. Bench to bedside: the quest for quality in experimental stroke research. *J Cereb Blood Flow Metab*, 26(12):1465–78, 2006.

Dirnagl U and Fisher M. International, multicenter randomized preclinical trials in translational stroke research: it's time to act. *J Cereb Blood Flow Metab*, 32(6):933–5, 2012.

Dirnagl U, Iadecola C and Moskowitz MA. Pathobiology of ischaemic stroke: an integrated view. *Trends Neurosci*, 22(9):391–7, 1999.

Dirnagl U, Kaplan B, Jacewicz M and Pulsinelli W. Continuous measurement of cerebral cortical blood flow by laser-Doppler flowmetry in a rat stroke model. *J Cereb Blood Flow Metab*, 9(5):589–96, 1989.

Dohmen C, Sakowitz OW, Fabricius M, Bosche B, Reithmeier T, Ernestus RI, Brinker G, Dreier JP, Woitzik J, Strong AJ, Graf R and (COSBID) COSoBID. Spreading depolarizations occur in human ischemic stroke with high incidence. *Ann Neurol*, 63(6):720–8, 2008.

Domoki F, Zimmermann A, Tóth-Szuki V, Busija DW and Bari F. Acetazolamide induces indomethacin and ischaemia-sensitive pial arteriolar vasodilation in the piglet. *Acta Paediatr*, 97(3):280–4, 2008.

Donahue J and Wintermark M. Perfusion CT and acute stroke imaging: foundations, applications, and literature review. *J Neuroradiol*, 42(1):21–9, 2015.

Donnan GA, Baron JC, Davis SM and Sharp F. The Ischemic Penumbra. New York: Informa Healthcare USA, 2007.

Donnan GA, Fisher M, Macleod M and Davis SM. Stroke. *Lancet*, 371(9624):1612–23, 2008.

Dreier JP, Woitzik J, Fabricius M, Bhatia R, Major S, Drenckhahn C, Lehmann TN, Sarrafzadeh A, Willumsen L, Hartings JA, Sakowitz OW, Seemann JH, Thieme A, Lauritzen M and Strong AJ. Delayed ischaemic neurological deficits after subarachnoid haemorrhage are associated with clusters of spreading depolarizations. *Brain*, 129(Pt 12):3224–37, 2006.

Duelsner A, Gatzke N, Glaser J, Hillmeister P, Li M, Lee EJ, Lehmann K, Urban D, Meyborg H, Stawowy P, Busjahn A, Nagorka S, Persson AB, Laage R, Schneider A and Buschmann IR. Granulocyte colony-stimulating factor improves cerebrovascular reserve capacity by enhancing collateral growth in the circle of Willis. *Cerebrovasc Dis*, 33(5):419–29, 2012.

Duncan DD and Kirkpatrick SJ. Can laser speckle flowmetry be made a quantitative tool? *J Opt Soc Am A Opt Image Sci Vis*, 25(8):2088–94, 2008.

Dunn AK. Laser speckle contrast imaging of cerebral blood flow. *Ann Biomed Eng*, 40(2):367–77, 2012.

Dunn AK, Bolay H, Moskowitz MA and Boas DA. Dynamic imaging of cerebral blood flow using laser speckle. *J Cereb Blood Flow Metab*, 21(3):195–201, 2001.

Duong TQ. Multimodal MRI of experimental stroke. *Transl Stroke Res*, 3(1):8–15, 2012.

Durukan A and Tatlisumak T. Acute ischemic stroke: overview of major experimental rodent models, pathophysiology, and therapy of focal cerebral ischemia. *Pharmacol Biochem Behav*, 87(1):179–97, 2007.

Durukan A and Tatlisumak T. Animal models of ischemic stroke. *Handb Clin Neurol*, 92:43–66, 2009.

Duverger D and MacKenzie ET. The quantification of cerebral infarction following focal ischemia in the rat: influence of strain, arterial pressure, blood glucose concentration, and age. *J Cereb Blood Flow Metab*, 8(4):449–61, 1988.

Ebinger M, De Silva DA, Christensen S, Parsons MW, Markus R, Donnan GA and Davis SM. Imaging the penumbra - strategies to detect tissue at risk after ischemic stroke. *J Clin Neurosci*, 16(2):178–87, 2009.

Elewa HF, El-Remessy AB, Somanath PR and Fagan SC. Diverse effects of statins on angiogenesis: new therapeutic avenues. *Pharmacotherapy*, 30(2):169–76, 2010.

Emery DJ, Schellinger PD, Selchen D, Douen AG, Chan R, Shuaib A and Butcher KS. Safety and feasibility of collateral blood flow augmentation after intravenous thrombolysis. *Stroke*, 42(4):1135–7, 2011.

Espinosa de Rueda M, Parrilla G, Manzano-Fernández S, García-Villalba B, Zamarro J, Hernández-Fernández F, Sánchez-Vizcaino C, Carreón E, Morales A and Moreno A. Combined Multimodal Computed Tomography Score Correlates With Futile Recanalization After Thrombectomy in Patients With Acute Stroke. *Stroke*, 46(9):2517–22, 2015.

Esposito E, Mandeville ET, Hayakawa K, Singhal AB and Lo EH. Effects of normobaric oxygen on the progression of focal cerebral ischemia in rats. *Exp Neurol*, 249:33–8, 2013.

Faber JE, Zhang H, Lassance-Soares RM, Prabhakar P, Najafi AH, Burnett MS and Epstein SE. Aging causes collateral rarefaction and increased severity of ischemic injury in multiple tissues. *Arterioscler Thromb Vasc Biol*, 31(8):1748–56, 2011.

Feigin VL, Forouzanfar MH, Krishnamurthi R, Mensah GA, Connor M, Bennett DA, Moran AE, Sacco RL, Anderson L, Truelsen T, O'Donnell M, Venketasubramanian N, Barker-Collo S, Lawes CM, Wang W, Shinohara Y, Witt E, Ezzati M, Naghavi M, Murray C, Global Burden of Diseases I, 2010) RFSG and the GBD Stroke Experts Group. Global and regional burden of stroke during 1990-2010: findings from the Global Burden of Disease Study 2010. *Lancet*, 383(9913):245–54, 2014.

Feigin VL, Lawes CM, Bennett DA and Anderson CS. Stroke epidemiology: a review of population-based studies of incidence, prevalence, and case-fatality in the late 20th century. *Lancet Neurol*, 2(1):43–53, 2003.

Fisher M, Feuerstein G, Howells DW, Hurn PD, Kent TA, Savitz SI, Lo EH and Group S. Update of the stroke therapy academic industry roundtable preclinical recommendations. *Stroke*, 40(6):2244–50, 2009.

Fluri F, Schuhmann MK and Kleinschnitz C. Animal models of ischemic stroke and their application in clinical research. *Drug Des Devel Ther*, 9:3445–54, 2015.

Foley LM, Hitchens TK, Barbe B, Zhang F, Ho C, Rao GR and Nemoto EM. Quantitative temporal profiles of penumbra and infarction during permanent middle cerebral artery occlusion in rats. *Transl Stroke Res*, 1(3):220–9, 2010.

Fukuchi K, Kusuoka H, Watanabe Y and Nishimura T. Correlation of sequential MR images of microsphere-induced cerebral ischemia with histologic changes in rats. *Invest Radiol*, 34(11):698–703, 1999.

Furlan A, Higashida R, Wechsler L, Gent M, Rowley H, Kase C, Pessin M, Ahuja A, Callahan F, Clark WM, Silver F and Rivera F. Intra-arterial prourokinase for acute ischemic stroke. The PROACT II study: a randomized controlled trial. Prolyse in Acute Cerebral Thromboembolism. *JAMA*, 282(21):2003–11, 1999.

Furlan AJ, Eyding D, Albers GW, Al-Rawi Y, Lees KR, Rowley HA, Sachara C, Soehngen M, Warach S, Hacke W and Investigators D. Dose Escalation of Desmoteplase for Acute Ischemic Stroke (DEDAS): evidence of safety and efficacy 3 to 9 hours after stroke onset. *Stroke*, 37(5):1227–31, 2006.

Fuxe K, Bjelke B, Andbjer B, Grahn H, Rimondini R and Agnati LF. Endothelin-1 induced lesions of the frontoparietal cortex of the rat. A possible model of focal cortical ischemia. *Neuroreport*, 8(11):2623–9, 1997.

Garcia JH, Wagner S, Liu KF and Hu XJ. Neurological deficit and extent of neuronal necrosis attributable to middle cerebral artery occlusion in rats. Statistical validation. *Stroke*, 26(4):627–34; discussion 635, 1995.

Gerriets T, Li F, Silva MD, Meng X, Brevard M, Sotak CH and Fisher M. The macrosphere model: evaluation of a new stroke model for permanent middle cerebral artery occlusion in rats. *J Neurosci Methods*, 122(2):201–11, 2003.

Giannopoulos S, Katsanos AH, Tsivgoulis G and Marshall RS. Statins and cerebral hemodynamics. *J Cereb Blood Flow Metab*, 32(11):1973–6, 2012.

Giles MF and Rothwell PM. Risk of stroke early after transient ischaemic attack: a systematic review and meta-analysis. *Lancet Neurol*, 6(12):1063–72, 2007.

Ginsberg MD, Palesch YY, Hill MD, Martin RH, Moy CS, Barsan WG, Waldman BD, Tamariz D, Ryckborst KJ, Investigators A and (NETT) NETT. High-dose albumin treatment for acute ischaemic stroke (ALIAS) Part 2: a randomised, double-blind, phase 3, placebo-controlled trial. *Lancet Neurol*, 12(11):1049–58, 2013.

Ginsberg MD, Prado R, Dietrich WD, Busto R and Watson BD. Hyperglycemia reduces the extent of cerebral infarction in rats. *Stroke*, 18(3):570–4, 1987.

Gomis M and Dávalos A. Recanalization and Reperfusion Therapies of Acute Ischemic Stroke: What have We Learned, What are the Major Research Questions, and Where are We Headed? *Front Neurol*, 5:226, 2014.

Goyal M, Demchuk AM and Hill MD. Endovascular therapy for ischemic stroke. *N Engl J Med*, 372(24):2366, 2015.

Grubb RL, Derdeyn CP, Fritsch SM, Carpenter DA, Yundt KD, Videen TO, Spitznagel EL and Powers WJ. Importance of hemodynamic factors in the prognosis of symptomatic carotid occlusion. *JAMA*, 280(12):1055–60, 1998.

Guan Y, Wang Y, Yuan F, Lu H, Ren Y, Xiao T, Chen K, Greenberg DA, Jin K and Yang GY. Effect of suture properties on stability of middle cerebral artery occlusion evaluated by synchrotron radiation angiography. *Stroke*, 43(3):888–91, 2012.

Hacke W, Albers G, Al-Rawi Y, Bogousslavsky J, Davalos A, Eliasziw M, Fischer M, Furlan A, Kaste M, Lees KR, Soehngen M, Warach S and Group DS. The Desmoteplase in Acute Ischemic Stroke Trial (DIAS): a phase II MRI-based 9-hour window acute stroke thrombolysis trial with intravenous desmoteplase. *Stroke*, 36(1):66–73, 2005.

Hacke W, Furlan AJ, Al-Rawi Y, Davalos A, Fiebach JB, Gruber F, Kaste M, Lipka LJ, Pedraza S, Ringleb PA, Rowley HA, Schneider D, Schwamm LH, Leal JS, Söhngen M, Teal PA, Wilhelm-Ogunbiyi K, Wintermark M and Warach S. Intravenous desmoteplase in patients with acute ischaemic stroke selected by MRI perfusion-diffusion weighted imaging or perfusion CT (DIAS-2): a prospective, randomised, double-blind, placebo-controlled study. *Lancet Neurol*, 8(2):141–50, 2009.

Haley EC, Lyden PD, Johnston KC, Hemmen TM and Investigators TiS. A pilot dose-escalation safety study of tenecteplase in acute ischemic stroke. *Stroke*, 36(3):607–12, 2005.

Hammer M, Jovin T, Wahr JA and Heiss WD. Partial occlusion of the descending aorta increases cerebral blood flow in a nonstroke porcine model. *Cerebrovasc Dis*, 28(4):406–10, 2009.

Han JH and Wong KS. Is counterpulsation a potential therapy for ischemic stroke? *Cerebrovasc Dis*, 26(2):97–105, 2008.

Harada H, Wang Y, Mishima Y, Uehara N, Makaya T and Kano T. A novel method of detecting rCBF with laser-Doppler flowmetry without cranial window through the skull for a MCAO rat model. *Brain Res Brain Res Protoc*, 14(3):165–70, 2005.

Hargreaves K, Dubner R, Brown F, Flores C and Joris J. A new and sensitive method for measuring thermal nociception in cutaneous hyperalgesia. *Pain*, 32(1):77–88, 1988.

Hartings JA, Rolli ML, Lu XC and Tortella FC. Delayed secondary phase of peri-infarct depolarizations after focal cerebral ischemia: relation to infarct growth and neuroprotection. *J Neurosci*, 23(37):11602–10, 2003.

Hartkamp MJ, van Der Grond J, van Everdingen KJ, Hillen B and Mali WP. Circle of Willis collateral flow investigated by magnetic resonance angiography. *Stroke*, 30(12):2671–8, 1999.

Hartkamp NS, van Osch MJ, Kappelle J and Bokkers RP. Arterial spin labeling magnetic resonance perfusion imaging in cerebral ischemia. *Curr Opin Neurol*, 27(1):42–53, 2014.

Hata R, Maeda K, Hermann D, Mies G and Hossmann KA. Dynamics of regional brain metabolism and gene expression after middle cerebral artery occlusion in mice. *J Cereb Blood Flow Metab*, 20(2):306–15, 2000a.

Hata R, Maeda K, Hermann D, Mies G and Hossmann KA. Evolution of brain infarction after transient focal cerebral ischemia in mice. *J Cereb Blood Flow Metab*, 20(6):937–46, 2000b.

Hata R, Mies G, Wiessner C and Hossmann KA. Differential expression of c-fos and hsp72 mRNA in focal cerebral ischemia of mice. *Neuroreport*, 9(1):27–32, 1998.

He Z, Yamawaki T, Yang S, Day AL, Simpkins JW and Naritomi H. Experimental model of small deep infarcts involving the hypothalamus in rats: changes in body temperature and postural reflex. *Stroke*, 30(12):2743–51; discussion 2751, 1999.

Hecht N, He J, Kremenetskaia I, Nieminen M, Vajkoczy P and Woitzik J. Cerebral hemodynamic reserve and vascular remodeling in C57/BL6 mice are influenced by age. *Stroke*, 43(11):3052–62, 2012.

Heiss WD. Ischemic penumbra: evidence from functional imaging in man. *J Cereb Blood Flow Metab*, 20(9):1276–93, 2000.

Heiss WD. Best measure of ischemic penumbra: positron emission tomography. *Stroke*, 34(10):2534–5, 2003.

Heiss WD. The ischemic penumbra: correlates in imaging and implications for treatment of ischemic stroke. The Johann Jacob Wepfer award 2011. *Cerebrovasc Dis*, 32(4):307–20, 2011.

Henninger N, Bouley J, Bråtane BT, Bastan B, Shea M and Fisher M. Laser Doppler flowmetry predicts occlusion but not tPA-mediated reperfusion success after rat embolic stroke. *Exp Neurol*, 215(2):290–7, 2009.

Henninger N and Fisher M. Stimulating circle of Willis nerve fibers preserves the diffusion-perfusion mismatch in experimental stroke. *Stroke*, 38(10):2779–86, 2007.

Hermier M, Nighoghossian N, Derex L, Wiart M, Nemoz C, Berthezène Y and Froment JC. Hypointense leptomeningeal vessels at T2*-weighted MRI in acute ischemic stroke. *Neurology*, 65(4):652–3, 2005.

Heros RC and Korosue K. Hemodilution for cerebral ischemia. *Stroke*, 20(3):423–7, 1989.

Hill MD, Martin RH, Palesch YY, Tamariz D, Waldman BD, Ryckborst KJ, Moy CS, Barsan WG, Ginsberg MD, Investigators A and Network NETT. The Albumin in Acute Stroke Part 1 Trial: an exploratory efficacy analysis. *Stroke*, 42(6):1621–5, 2011.

Hillis AE and Baron JC. Editorial: the ischemic penumbra: still the target for stroke therapies? *Front Neurol*, 6:85, 2015.

Hillis AE, Ulatowski JA, Barker PB, Torbey M, Ziai W, Beauchamp NJ, Oh S and Wityk RJ. A pilot randomized trial of induced blood pressure elevation: effects on function and focal perfusion in acute and subacute stroke. *Cerebrovasc Dis*, 16(3):236–46, 2003.

Hoehn-Berlage M, Norris DG, Kohno K, Mies G, Leibfritz D and Hossmann KA. Evolution of regional changes in apparent diffusion coefficient during focal ischemia of rat brain: the relationship of quantitative diffusion NMR imaging to reduction in cerebral blood flow and metabolic disturbances. *J Cereb Blood Flow Metab*, 15(6):1002–11, 1995.

Hossmann KA. Disturbances of cerebral protein synthesis and ischemic cell death. *Prog Brain Res*, 96:161–77, 1993.

Hossmann KA. Viability thresholds and the penumbra of focal ischemia. *Ann Neurol*, 36(4):557–65, 1994.

Hossmann KA. Pathophysiology and therapy of experimental stroke. *Cell Mol Neurobiol*, 26(7-8):1057–83, 2006.

Hossmann KA. Cerebral ischemia: models, methods and outcomes. *Neuropharmacology*, 55(3):257–70, 2008.

Howells DW, Porritt MJ, Rewell SS, O'Collins V, Sena ES, van der Worp HB, Traystman RJ and Macleod MR. Different strokes for different folks: the rich diversity of animal models of focal cerebral ischemia. *J Cereb Blood Flow Metab*, 30(8):1412–31, 2010.

Huang NC, Wei J and Quast MJ. A comparison of the early development of ischemic brain damage in normoglycemic and hyperglycemic rats using magnetic resonance imaging. *Exp Brain Res*, 109(1):33–42, 1996.

Hughes PM, Anthony DC, Ruddin M, Botham MS, Rankine EL, Sablone M, Baumann D, Mir AK and Perry VH. Focal lesions in the rat central nervous system induced by endothelin-1. *J Neuropathol Exp Neurol*, 62(12):1276–86, 2003.

Huh PW, Belayev L, Zhao W, Busto R, Saul I and Ginsberg MD. The effect of high-dose albumin therapy on local cerebral perfusion after transient focal cerebral ischemia in rats. *Brain Res*, 804(1):105–13, 1998.

Humeau A, Fizanne L, Roux J, Asfar P, Cales P and Rousseau D. Linear, nonlinear analyses of laser Doppler flowmetry signals recorded during isoflurane-induced anaesthesia in healthy rats. *Journal of Vascular Research*, 45 (Suppl.2):82, 2008.

Humeau-Heurtier A, Guerreschi E, Abraham P and Mahé G. Relevance of laser Doppler and laser speckle techniques for assessing vascular function: state of the art and future trends. *IEEE Trans Biomed Eng*, 60(3):659–66, 2013.

Hungerhuber E, Zausinger S, Westermaier T, Plesnila N and Schmid-Elsaesser R. Simultaneous bilateral laser Doppler fluxmetry and electrophysiological recording during middle cerebral artery occlusion in rats. *J Neurosci Methods*, 154(1-2):109–15, 2006.

Hunter AJ, Hatcher J, Virley D, Nelson P, Irving E, Hadingham SJ and Parsons AA. Functional assessments in mice and rats after focal stroke. *Neuropharmacology*, 39(5):806–16, 2000.

Höhfeld J, Cyr DM and Patterson C. From the cradle to the grave: molecular chaperones that may choose between folding and degradation. *EMBO Rep*, 2(10):885–90, 2001.

IMS. IMS Study Investigators. Combined intravenous and intra-arterial recanalization for acute ischemic stroke: the Interventional Management of Stroke Study. *Stroke*, 35(4):904–11, 2004.

IMS-II. IMS II Trial Investigators. The Interventional Management of Stroke (IMS) II Study. *Stroke*, 38(7):2127–35, 2007.

Ingall TJ. Intravenous thrombolysis for acute ischemic stroke: time is prime. *Stroke*, 40(6):2264–5, 2009.

Iqbal S. A comprehensive study of the anatomical variations of the circle of willis in adult human brains. *J Clin Diagn Res*, 7(11):2423–7, 2013.

Jäger HR and Grieve JP. Advances in non-invasive imaging of intracranial vascular disease. *Ann R Coll Surg Engl*, 82(1):1–5, 2000.

Jansen O, Schellinger P, Fiebach J, Hacke W and Sartor K. Early recanalisation in acute ischaemic stroke saves tissue at risk defined by MRI. *Lancet*, 353(9169):2036–7, 1999.

Jauch EC, Saver JL, Adams HP, Bruno A, Connors JJ, Demaerschalk BM, Khatri P, McMullan PW, Qureshi AI, Rosenfield K, Scott PA, Summers DR, Wang DZ, Wintermark M, Yonas H, Council AHAS, Nursing CoC, Disease CoPV and Cardiology CoC. Guidelines for the early management of patients with acute ischemic stroke: a guideline for healthcare professionals from the American Heart Association/American Stroke Association. *Stroke*, 44(3):870–947, 2013.

Jung S, Gilgen M, Slotboom J, El-Koussy M, Zubler C, Kiefer C, Luedi R, Mono ML, Heldner MR, Weck A, Mordasini P, Schroth G, Mattle HP, Arnold M, Gralla J and Fischer U. Factors that determine penumbral tissue loss in acute ischaemic stroke. *Brain*, 136(Pt 12):3554–60, 2013.

Kahle MP and Bix GJ. Successfully Climbing the "STAIRs": Surmounting Failed Translation of Experimental Ischemic Stroke Treatments. *Stroke Res Treat*, 2012:374098, 2012.

Karatas H, Erdener SE, Gursoy-Ozdemir Y, Gurer G, Soylemezoglu F, Dunn AK and Dalkara T. Thrombotic distal middle cerebral artery occlusion produced by topical FeCl(3) application: a novel model suitable for intravital microscopy and thrombolysis studies. *J Cereb Blood Flow Metab*, 31(6):1452–60, 2011.

Kaschka IN, Kloska SP, Struffert T, Engelhorn T, Gölitz P, Kurka N, Köhrmann M, Schwab S and Doerfler A. Clot Burden and Collaterals in Anterior Circulation Stroke: Differences Between Single-Phase CTA and Multi-phase 4D-CTA. *Clin Neuroradiol*, 2014.

Khurana D, Kaul S, Bornstein NM and Group IS. Implant for augmentation of cerebral blood flow trial 1: a pilot study evaluating the safety and effectiveness of the Ischaemic Stroke System for treatment of acute ischaemic stroke. *Int J Stroke*, 4(6):480–5, 2009.

Kidwell CS, Alger JR and Saver JL. Beyond mismatch: evolving paradigms in imaging the ischemic penumbra with multimodal magnetic resonance imaging. *Stroke*, 34(11):2729–35, 2003.

Kidwell CS, Jahan R, Gornbein J, Alger JR, Nenov V, Ajani Z, Feng L, Meyer BC, Olson S, Schwamm LH, Yoo AJ, Marshall RS, Meyers PM, Yavagal DR, Wintermark M, Guzy J, Starkman S, Saver JL and Investigators MR. A trial of imaging selection and endovascular treatment for ischemic stroke. *N Engl J Med*, 368(10):914–23, 2013.

Kidwell CS, Saver JL, Mattiello J, Starkman S, Vinuela F, Duckwiler G, Gobin YP, Jahan R, Vespa P, Kalafut M and Alger JR. Thrombolytic reversal of acute human cerebral ischemic injury shown by diffusion/perfusion magnetic resonance imaging. *Ann Neurol*, 47(4):462–9, 2000.

Kim HY, Singhal AB and Lo EH. Normobaric hyperoxia extends the reperfusion window in focal cerebral ischemia. *Ann Neurol*, 57(4):571–5, 2005.

Kim SJ, Ha YS, Ryoo S, Noh HJ, Ha SY, Bang OY, Kim GM, Chung CS and Lee KH. Sulcal effacement on fluid attenuation inversion recovery magnetic resonance imaging in hyperacute stroke: association with collateral flow and clinical outcomes. *Stroke*, 43(2):386–92, 2012.

Kim Y, Sin DS, Park HY, Park MS and Cho KH. Relationship between flow diversion on transcranial Doppler sonography and leptomeningeal collateral circulation in patients with middle cerebral artery occlusive disorder. *J Neuroimaging*, 19(1):23–6, 2009.

Kinoshita T, Ogawa T, Kado H, Sasaki N and Okudera T. CT angiography in the evaluation of intracranial occlusive disease with collateral circulation: comparison with MR angiography. *Clin Imaging*, 29(5):303–6, 2005.

Kinouchi H, Sharp FR, Chan PH, Koistinaho J, Sagar SM and Yoshimoto T. Induction of c-fos, junB, c-jun, and hsp70 mRNA in cortex, thalamus, basal ganglia, and hippocampus following middle cerebral artery occlusion. *J Cereb Blood Flow Metab*, 14(5):808–17, 1994.

Kinouchi H, Sharp FR, Hill MP, Koistinaho J, Sagar SM and Chan PH. Induction of 70-kDa heat shock protein and hsp70 mRNA following transient focal cerebral ischemia in the rat. *J Cereb Blood Flow Metab*, 13(1):105–15, 1993a.

Kinouchi H, Sharp FR, Koistinaho J, Hicks K, Kamii H and Chan PH. Induction of heat shock hsp70 mRNA and HSP70 kDa protein in neurons in the 'penumbra' following focal cerebral ischemia in the rat. *Brain Res*, 619(1-2):334–8, 1993b.

Kirsch JR, Traystman RJ and Hurn PD. Anesthetics and cerebroprotection: experimental aspects. *Int Anesthesiol Clin*, 34(4):73–93, 1996.

Kläsner B, Lumenta DB, Pruneau D, Zausinger S and Plesnila N. Therapeutic window of bradykinin B2 receptor inhibition after focal cerebral ischemia in rats. *Neurochem Int*, 49(5):442–7, 2006.

Kleinschnitz C, Braeuninger S, Pham M, Austinat M, Nölte I, Renné T, Nieswandt B, Bendszus M and Stoll G. Blocking of platelets or intrinsic coagulation pathway-driven thrombosis does not prevent cerebral infarctions induced by photothrombosis. *Stroke*, 39(4):1262–8, 2008.

Knauth M, von Kummer R, Jansen O, Hähnel S, Dörfler A and Sartor K. Potential of CT angiography in acute ischemic stroke. *AJNR Am J Neuroradiol*, 18(6):1001–10, 1997.

Koenig MA, Geocadin RG, de Grouchy M, Glasgow J, Vimal S, Restrepo L and Wityk RJ. Safety of induced hypertension therapy in patients with acute ischemic stroke. *Neurocrit Care*, 4(1):3–7, 2006.

Koizumi J, Yoshida Y, Nakazawa T and Ooneda G. Experimental studies of ischemic brain edema. I. A new experimental model of cerebral embolism in which recirculation can introduced into the ischemic area. *Jpn J Stoke*, 8(1):1–8, 1986.

Krieger DW and Yenari MA. Therapeutic hypothermia for acute ischemic stroke: what do laboratory studies teach us? *Stroke*, 35(6):1482–9, 2004.

Krupiński J, Kałuza J, Kumar P, Kumar S and Wang JM. Some remarks on the growth-rate and angiogenesis of microvessels in ischemic stroke. Morphometric and immunocytochemical studies. *Patol Pol*, 44(4):203–9, 1993.

Krupinski J, Kaluza J, Kumar P, Kumar S and Wang JM. Role of angiogenesis in patients with cerebral ischemic stroke. *Stroke*, 25(9):1794–8, 1994.

Krupinski J, Stroemer P, Slevin M, Marti E, Kumar P and Rubio F. Three-dimensional structure and survival of newly formed blood vessels after focal cerebral ischemia. *Neuroreport*, 14(8):1171–6, 2003.

Kuroda S, Houkin K, Kamiyama H, Mitsumori K, Iwasaki Y and Abe H. Long-term prognosis of medically treated patients with internal carotid or middle cerebral artery occlusion: can acetazolamide test predict it? *Stroke*, 32(9):2110–6, 2001.

Kuwabara Y, Ichiya Y, Sasaki M, Yoshida T and Masuda K. Time dependency of the acetazolamide effect on cerebral hemodynamics in patients with chronic occlusive cerebral arteries. Early steal phenomenon demonstrated by [15O]H2O positron emission tomography. *Stroke*, 26(10):1825–9, 1995.

Lansberg MG, Bluhmki E and Thijs VN. Efficacy and safety of tissue plasminogen activator 3 to 4.5 hours after acute ischemic stroke: a metaanalysis. *Stroke*, 40(7):2438–41, 2009.

Lansberg MG, Cereda CW, Mlynash M, Mishra NK, Inoue M, Kemp S, Christensen S, Straka M, Zaharchuk G, Marks MP, Bammer R, Albers GW, Investigators D, for Understanding Stroke Evolution 2 (DEFUSE 2) Study PIE, Investigators D and for Understanding Stroke Evolution 2 DEFUSE 2 Study PIE. Response to endovascular reperfusion is not time-dependent in patients with salvageable tissue. *Neurology*, 2015.

Lansberg MG, Lee J, Christensen S, Straka M, De Silva DA, Mlynash M, Campbell BC, Bammer R, Olivot JM, Desmond P, Davis SM, Donnan GA and Albers GW. RAPID automated patient selection for reperfusion therapy: a pooled analysis of the Echoplanar Imaging Thrombolytic Evaluation Trial (EPITHET) and the

Diffusion and Perfusion Imaging Evaluation for Understanding Stroke Evolution (DEFUSE) Study. *Stroke*, 42(6):1608–14, 2011.

Lansberg MG, O'Brien MW, Tong DC, Moseley ME and Albers GW. Evolution of cerebral infarct volume assessed by diffusion-weighted magnetic resonance imaging. *Arch Neurol*, 58(4):613–7, 2001.

Lansberg MG, Straka M, Kemp S, Mlynash M, Wechsler LR, Jovin TG, Wilder MJ, Lutsep HL, Czartoski TJ, Bernstein RA, Chang CW, Warach S, Fazekas F, Inoue M, Tipirneni A, Hamilton SA, Zaharchuk G, Marks MP, Bammer R, Albers GW and investigators Ds. MRI profile and response to endovascular reperfusion after stroke (DEFUSE 2): a prospective cohort study. *Lancet Neurol*, 11(10):860–7, 2012.

Lay CC, Davis MF, Chen-Bee CH and Frostig RD. Mild sensory stimulation completely protects the adult rodent cortex from ischemic stroke. *PLoS One*, 5(6):e11270, 2010.

Lay CC, Davis MF, Chen-Bee CH and Frostig RD. Mild sensory stimulation reestablishes cortical function during the acute phase of ischemia. *J Neurosci*, 31(32):11495–504, 2011.

Leach MJ, Swan JH, Eisenthal D, Dopson M and Nobbs M. BW619C89, a glutamate release inhibitor, protects against focal cerebral ischemic damage. *Stroke*, 24(7):1063–7, 1993.

Lee MJ, Bang OY, Kim SJ, Kim GM, Chung CS, Lee KH, Ovbiagele B, Liebeskind DS and Saver JL. Role of statin in atrial fibrillation-related stroke: an angiographic study for collateral flow. *Cerebrovasc Dis*, 37(2):77–84, 2014.

Lee RM. Morphology of cerebral arteries. *Pharmacol Ther*, 66(1):149–73, 1995.

Legos JJ, Lenhard SC, Haimbach RE, Schaeffer TR, Bentley RG, McVey MJ, Chandra S, Irving EA, Parsons AA and Barone FC. SB 234551 selective ET(A) receptor antagonism: perfusion/diffusion MRI used to define treatable stroke model, time to treatment and mechanism of protection. *Exp Neurol*, 212(1):53–62, 2008.

Leigh R, Urrutia VC, Llinas RH, Gottesman RF, Krakauer JW and Hillis AE. A comparison of two methods for MRI classification of at-risk tissue and core infarction. *Front Neurol*, 5:155, 2014.

Leist M and Nicotera P. Apoptosis, excitotoxicity, and neuropathology. *Exp Cell Res*, 239(2):183–201, 1998.

Leoni RF, Paiva FF, Kang BT, Henning EC, Nascimento GC, Tannús A, De Araújo DB and Silva AC. Arterial spin labeling measurements of cerebral perfusion territories in experimental ischemic stroke. *Transl Stroke Res*, 3(1):44–55, 2012.

Letourneur A, Roussel S, Toutain J, Bernaudin M and Touzani O. Impact of genetic and renovascular chronic arterial hypertension on the acute spatiotemporal evolution of the ischemic penumbra: a sequential study with MRI in the rat. *J Cereb Blood Flow Metab*, 31(2):504–13, 2011.

Levi H, Schoknecht K, Prager O, Chassidim Y, Weissberg I, Serlin Y and Friedman A. Stimulation of the sphenopalatine ganglion induces reperfusion and blood-brain barrier protection in the photothrombotic stroke model. *PLoS One*, 7(6):e39636, 2012.

Li F, Omae T and Fisher M. Spontaneous hyperthermia and its mechanism in the intraluminal suture middle cerebral artery occlusion model of rats. *Stroke*, 30(11):2464–70; discussion 2470–1, 1999.

Li L, Ke Z, Tong KY and Ying M. Evaluation of cerebral blood flow changes in focal cerebral ischemia rats by using transcranial Doppler ultrasonography. *Ultrasound Med Biol*, 36(4):595–603, 2010.

Liebeskind DS. Collateral circulation. *Stroke*, 34(9):2279–84, 2003.

Liebeskind DS. Collateral therapeutics for cerebral ischemia. *Expert Rev Neurother*, 4(2):255–65, 2004.

Liebeskind DS. Collaterals in acute stroke: beyond the clot. *Neuroimaging Clin N Am*, 15(3):553–73, x, 2005a.

Liebeskind DS. Neuroprotection from the collateral perspective. *IDrugs*, 8(3):222–8, 2005b.

Liebeskind DS. Of mice and men: essential considerations in the translation of collateral therapeutics. *Stroke*, 39(12):e187–8; author reply e189, 2008.

Liebeskind DS. Reperfusion for acute ischemic stroke: arterial revascularization and collateral therapeutics. *Curr Opin Neurol*, 23(1):36–45, 2010.

Liebeskind DS. Collateral perfusion: time for novel paradigms in cerebral ischemia. *Int J Stroke*, 7(4):309–10, 2012.

Liebeskind DS. Trials of endovascular therapies or collaterals? *Int J Stroke*, 8(4):258–9, 2013.

Liebeskind DS and Alexandrov AV. Advanced multimodal CT/MRI approaches to hyperacute stroke diagnosis, treatment, and monitoring. *Ann N Y Acad Sci*, 1268:1–7, 2012.

Liebeskind DS, Cotsonis GA, Saver JL, Lynn MJ, Cloft HJ, Chimowitz MI and Investigators WASIDW. Collateral circulation in symptomatic intracranial atherosclerosis. *J Cereb Blood Flow Metab*, 31(5):1293–301, 2011.

Liebeskind DS and Sanossian N. How well do blood flow imaging and collaterals on angiography predict brain at risk? *Neurology*, 79(13 Suppl 1):S105–9, 2012.

Liebeskind DS, Tomsick TA, Foster LD, Yeatts SD, Carrozzella J, Demchuk AM, Jovin TG, Khatri P, von Kummer R, Sugg RM, Zaidat OO, Hussain SI, Goyal M, Menon BK, Al Ali F, Yan B, Palesch YY, Broderick JP and Investigators II. Collaterals at Angiography and Outcomes in the Interventional Management of Stroke (IMS) III Trial. *Stroke*, 45(3):759–64, 2014.

Lima FO, Furie KL, Silva GS, Lev MH, Camargo EC, Singhal AB, Harris GJ, Halpern EF, Koroshetz WJ, Smith WS, Yoo AJ and Nogueira RG. The pattern of leptomeningeal collaterals on CT angiography is a strong predictor of long-term functional outcome in stroke patients with large vessel intracranial occlusion. *Stroke*, 41(10):2316–22, 2010.

Lin W, Xiong L, Han J, Leung TW, Soo YO, Chen X and Wong KS. External counterpulsation augments blood pressure and cerebral flow velocities in ischemic stroke patients with cerebral intracranial large artery occlusive disease. *Stroke*, 43(11):3007–11, 2012.

Liu S, Zhen G, Meloni BP, Campbell K and Winn HR. RODENT STROKE MODEL GUIDELINES FOR PRECLINICAL STROKE TRIALS (1ST EDITION). *J Exp Stroke Transl Med*, 2(2):2–27, 2009.

Liu W, Xu G, Yue X, Wang X, Ma M, Zhang R, Wang H, Zhou C and Liu X. Hyperintense vessels on FLAIR: a useful non-invasive method for assessing intracerebral collaterals. *Eur J Radiol*, 80(3):786–91, 2011.

Liu Y, Belayev L, Zhao W, Busto R, Belayev A and Ginsberg MD. Neuroprotective effect of treatment with human albumin in permanent focal cerebral ischemia: histopathology and cortical perfusion studies. *Eur J Pharmacol*, 428(2):193–201, 2001.

Liu Y, Karonen JO, Vanninen RL, Nuutinen J, Koskela A, Soimakallio S and Aronen HJ. Acute ischemic stroke: predictive value of 2D phase-contrast MR angiography–serial study with combined diffusion and perfusion MR imaging. *Radiology*, 231(2):517–27, 2004.

Longa EZ, Weinstein PR, Carlson S and Cummins R. Reversible middle cerebral artery occlusion without craniectomy in rats. *Stroke*, 20(1):84–91, 1989.

Lozano R, Naghavi M, Foreman K, Lim S, Shibuya K, Aboyans V, Abraham J, Adair T, Aggarwal R, Ahn SY, Alvarado M, Anderson HR, Anderson LM, Andrews KG, Atkinson C, Baddour LM, Barker-Collo S, Bartels DH, Bell ML, Benjamin EJ, Bennett D, Bhalla K, Bikbov B, Bin Abdulhak A, Birbeck G, Blyth F, Bolliger I, Boufous S, Bucello C, Burch M, Burney P, Carapetis J, Chen H, Chou D, Chugh SS, Coffeng LE, Colan SD, Colquhoun S, Colson KE, Condon J, Connor MD, Cooper LT, Corriere M, Cortinovis M, de Vaccaro KC, Couser W, Cowie BC, Criqui MH, Cross M, Dabhadkar KC, Dahodwala N, De Leo D, Degenhardt L, Delossantos A, Denenberg J, Des Jarlais DC, Dharmaratne SD, Dorsey ER, Driscoll T, Duber H, Ebel B, Erwin PJ, Espindola P, Ezzati M, Feigin V, Flaxman AD, Forouzanfar MH, Fowkes FG, Franklin R, Fransen M, Freeman MK, Gabriel SE, Gakidou E, Gaspari F, Gillum RF, Gonzalez-Medina D, Halasa YA, Haring D, Harrison JE, Havmoeller R, Hay RJ, Hoen B, Hotez PJ, Hoy D, Jacobsen KH, James SL, Jasrasaria R, Jayaraman S, Johns N, Karthikeyan G, Kassebaum N, Keren A, Khoo JP, Knowlton LM, Kobusingye O, Koranteng A, Krishnamurthi R, Lipnick M, Lipshultz SE, Ohno SL *et al.* Global and regional mortality from 235 causes of death for 20 age groups in 1990 and 2010: a systematic analysis for the Global Burden of Disease Study 2010. *Lancet*, 380(9859):2095–128, 2012.

Lu A, Ran R, Parmentier-Batteur S, Nee A and Sharp FR. Geldanamycin induces heat shock proteins in brain and protects against focal cerebral ischemia. *J Neurochem*, 81(2):355–64, 2002.

Lu H, Wang Y, He X, Yuan F, Lin X, Xie B, Tang G, Huang J, Tang Y, Jin K, Chen S and Yang GY. Netrin-1 hyperexpression in mouse brain promotes angiogenesis and long-term neurological recovery after transient focal ischemia. *Stroke*, 43(3):838–43, 2012.

Ma H, Parsons MW, Christensen S, Campbell BC, Churilov L, Connelly A, Yan B, Bladin C, Phan T, Barber AP, Read S, Hankey GJ, Markus R, Wijeratne T, Grimley R, Mahant N, Kleinig T, Sturm J, Lee A, Blacker D, Gerraty R, Krause M, Desmond PM, McBride SJ, Carey L, Howells DW, Hsu CY, Davis SM, Donnan GA and investigators E. A multicentre, randomized, double-blinded, placebo-controlled Phase III study to investigate EXtending the time for Thrombolysis in Emergency Neurological Deficits (EXTEND). *Int J Stroke*, 7(1):74–80, 2012.

Ma Q, Khatibi NH, Chen H, Tang J and Zhang JH. History of preclinical models of intracerebral hemorrhage. *Acta Neurochir Suppl*, 111:3–8, 2011.

Maas MB, Lev MH, Ay H, Singhal AB, Greer DM, Smith WS, Harris GJ, Halpern E, Kemmling A, Koroshetz WJ and Furie KL. Collateral vessels on CT angiography predict outcome in acute ischemic stroke. *Stroke*, 40(9):3001–5, 2009.

Macrae IM. Preclinical stroke research–advantages and disadvantages of the most common rodent models of focal ischaemia. *Br J Pharmacol*, 164(4):1062–78, 2011.

Manning NW, Campbell BC, Oxley TJ and Chapot R. Acute ischemic stroke: time, penumbra, and reperfusion. *Stroke*, 45(2):640–4, 2014.

Marinoni M, Ginanneschi A, Forleo P and Amaducci L. Technical limits in transcranial Doppler recording: inadequate acoustic windows. *Ultrasound Med Biol*, 23(8):1275–7, 1997.

Markus R, Reutens DC, Kazui S, Read S, Wright P, Chambers BR, Sachinidis JI, Tochon-Danguy HJ and Donnan GA. Topography and temporal evolution of hypoxic viable tissue identified by 18F-fluoromisonidazole positron emission tomography in humans after ischemic stroke. *Stroke*, 34(11):2646–52, 2003.

Marzan AS, Hungerbühler HJ, Studer A, Baumgartner RW and Georgiadis D. Feasibility and safety of norepinephrine-induced arterial hypertension in acute ischemic stroke. *Neurology*, 62(7):1193–5, 2004.

Matkowskyj KA, Schonfeld D and Benya RV. Quantitative immunohistochemistry by measuring cumulative signal strength using commercially available software photoshop and matlab. *J Histochem Cytochem*, 48(2):303–12, 2000.

Matsumori Y, Northington FJ, Hong SM, Kayama T, Sheldon RA, Vexler ZS, Ferriero DM, Weinstein PR and Liu J. Reduction of caspase-8 and -9 cleavage is associated with increased c-FLIP and increased binding of Apaf-1 and Hsp70 after neonatal hypoxic/ischemic injury in mice overexpressing Hsp70. *Stroke*, 37(2):507–12, 2006.

McAuliffe M, Lalonde F, McGarry D, Gandler W, Csaky K and Trus B. Medical Image Processing, Analysis and Visualization in clinical research, 2001.

McCabe C, Gallagher L, Gsell W, Graham D, Dominiczak AF and Macrae IM. Differences in the evolution of the ischemic penumbra in stroke-prone spontaneously hypertensive and Wistar-Kyoto rats. *Stroke*, 40(12):3864–8, 2009.

Mcilvoy LH. The effect of hypothermia and hyperthermia on acute brain injury. *AACN Clin Issues*, 16(4):488–500, 2005.

McVerry F, Liebeskind DS and Muir KW. Systematic review of methods for assessing leptomeningeal collateral flow. *AJNR Am J Neuroradiol*, 33(3):576–82, 2012.

Meng X, Fisher M, Shen Q, Sotak CH and Duong TQ. Characterizing the diffusion/perfusion mismatch in experimental focal cerebral ischemia. *Ann Neurol*, 55(2):207–12, 2004.

Menon BK, Smith EE, Modi J, Patel SK, Bhatia R, Watson TW, Hill MD, Demchuk AM and Goyal M. Regional leptomeningeal score on CT angiography predicts clinical and imaging outcomes in patients with acute anterior circulation occlusions. *AJNR Am J Neuroradiol*, 32(9):1640–5, 2011.

Meschia JF, Bushnell C, Boden-Albala B, Braun LT, Bravata DM, Chaturvedi S, Creager MA, Eckel RH, Elkind MS, Fornage M, Goldstein LB, Greenberg SM, Horvath SE, Iadecola C, Jauch EC, Moore WS, Wilson JA, Council AHAS, Nursing CoC, Stroke, Cardiology CoC, Biology CoFG, Translational and Hypertension Co. Guidelines for the primary prevention of stroke: a statement for healthcare professionals from the American Heart Association/American Stroke Association. *Stroke*, 45(12):3754–832, 2014.

Metz GA. Behavioral testing in rodent models of stroke. In: Rodent Models of Stroke, 199–212. Springer, 2010.

Micieli G, Marcheselli S and Tosi PA. Safety and efficacy of alteplase in the treatment of acute ischemic stroke. *Vasc Health Risk Manag*, 5(1):397–409, 2009.

Mies G. Neuroprotective effect of sumatriptan, a 5-HT(1D) receptor agonist, in focal cerebral ischemia of rat brain. *J Stroke Cerebrovasc Dis*, 7(4):242–9, 1998.

Mies G, Iijima T and Hossmann KA. Correlation between peri-infarct DC shifts and ischaemic neuronal damage in rat. *Neuroreport*, 4(6):709–11, 1993.

Mies G, Ishimaru S, Xie Y, Seo K and Hossmann KA. Ischemic thresholds of cerebral protein synthesis and energy state following middle cerebral artery occlusion in rat. *J Cereb Blood Flow Metab*, 11(5):753–61, 1991.

Minematsu K, Fisher M, Li L and Sotak CH. Diffusion and perfusion magnetic resonance imaging studies to evaluate a noncompetitive N-methyl-D-aspartate antagonist and reperfusion in experimental stroke in rats. *Stroke*, 24(12):2074–81, 1993.

Miteff F, Levi CR, Bateman GA, Spratt N, McElduff P and Parsons MW. The independent predictive utility of computed tomography angiographic collateral status in acute ischaemic stroke. *Brain*, 132(Pt 8):2231–8, 2009.

Mohanan A, Deshpande S, Jamadarkhana PG, Kumar P, Gupta RC, Chauthaiwale V and Dutt C. Delayed intervention in experimental stroke with TRC051384–a small molecule HSP70 inducer. *Neuropharmacology*, 60(6):991–9, 2011.

Moseley ME, Cohen Y, Mintorovitch J, Chileuitt L, Shimizu H, Kucharczyk J, Wendland MF and Weinstein PR. Early detection of regional cerebral ischemia in cats: comparison of diffusion- and T2-weighted MRI and spectroscopy. *Magn Reson Med*, 14(2):330–46, 1990a.

Moseley ME, Kucharczyk J, Mintorovitch J, Cohen Y, Kurhanewicz J, Derugin N, Asgari H and Norman D. Diffusion-weighted MR imaging of acute stroke: correlation with T2-weighted and magnetic susceptibility-enhanced MR imaging in cats. *AJNR Am J Neuroradiol*, 11(3):423–9, 1990b.

Moskowitz MA, Lo EH and Iadecola C. The science of stroke: mechanisms in search of treatments. *Neuron*, 67(2):181–98, 2010.

Muir KW and Santosh C. Imaging of acute stroke and transient ischaemic attack. *J Neurol Neurosurg Psychiatry*, 76 Suppl 3:iii19–iii28, 2005.

Murray CJ, Vos T, Lozano R, Naghavi M, Flaxman AD, Michaud C, Ezzati M, Shibuya K, Salomon JA, Abdalla S, Aboyans V, Abraham J, Ackerman I, Aggarwal R, Ahn SY, Ali MK, Alvarado M, Anderson HR, Anderson LM, Andrews KG, Atkinson C, Baddour LM, Bahalim AN, Barker-Collo S, Barrero LH, Bartels DH, Basáñez MG, Baxter A, Bell ML, Benjamin EJ, Bennett D, Bernabé E, Bhalla K, Bhandari B, Bikbov B, Bin Abdulhak A, Birbeck G, Black JA, Blencowe H, Blore JD, Blyth F, Bolliger I, Bonaventure A, Boufous S, Bourne R, Boussinesq M, Braithwaite T, Brayne C, Bridgett L, Brooker S, Brooks P, Brugha TS, Bryan-Hancock C, Bucello C, Buchbinder R, Buckle G, Budke CM, Burch M, Burney P, Burstein R, Calabria B, Campbell B, Canter CE, Carabin H, Carapetis J, Carmona L, Cella C, Charlson F, Chen H, Cheng AT, Chou D, Chugh SS, Coffeng LE, Colan SD, Colquhoun S, Colson KE, Condon J, Connor MD, Cooper LT, Corriere M, Cortinovis M, de Vaccaro KC, Couser W, Cowie BC, Criqui MH, Cross M, Dabhadkar KC, Dahiya M, Dahodwala N, Damsere-Derry J, Danaei G, Davis A, De Leo D, Degenhardt L, Dellavalle R, Delossantos A, Denenberg J, Derrett S, Des Jarlais DC, Dharmaratne SD *et al.* Disability-adjusted life years (DALYs) for 291 diseases and injuries in 21 regions, 1990-2010: a systematic analysis for the Global Burden of Disease Study 2010. *Lancet*, 380(9859):2197–223, 2012.

Nagatani K, Nawashiro H, Takeuchi S, Otani N, Wada K and Shima K. Effects of a head-down tilt on cerebral blood flow in mice during bilateral common carotid artery occlusion. *Asian J Neurosurg*, 7(4):171–3, 2012.

Nakagomi S, Kiryu-Seo S and Kiyama H. Endothelin-converting enzymes and endothelin receptor B messenger RNAs are expressed in different neural cell species and these messenger RNAs are coordinately induced in neurons and astrocytes respectively following nerve injury. *Neuroscience*, 101(2):441–9, 2000.

NC3Rs. National Center for Replacement, Refinement & Reduction of Animals in Research. Determining the source of variability within experimental stroke models. London, UK. Available at: `https://www.nc3rs.org.uk/determining-source-variability-within-experimental-stroke-models`. Accessed August, 2015.

Neumann-Haefelin T, Wittsack HJ, Wenserski F, Siebler M, Seitz RJ, Mödder U and Freund HJ. Diffusion- and perfusion-weighted MRI. The DWI/PWI mismatch region in acute stroke. *Stroke*, 30(8):1591–7, 1999.

Nicoli F, Lafaye de Micheaux P and Girard N. Perfusion-weighted imaging-derived collateral flow index is a predictor of MCA M1 recanalization after i.v. thrombolysis. *AJNR Am J Neuroradiol*, 34(1):107–14, 2013.

Nicoli F, Scalzo F, Saver JL, Pautot F, Mitulescu A, Chaibi Y, Girard N, Salamon N, Liebeskind DS and Investigators US. The combination of baseline magnetic resonance perfusion-weighted imaging-derived tissue volume with severely prolonged arterial-tissue delay and diffusion-weighted imaging lesion volume is predictive of MCA-M1 recanalization in patients treated with endovascular thrombectomy. *Neuroradiology*, 56(2):117–27, 2014.

Nimmagadda A, Park HP, Prado R and Ginsberg MD. Albumin therapy improves local vascular dynamics in a rat model of primary microvascular thrombosis: a two-photon laser-scanning microscopy study. *Stroke*, 39(1):198–204, 2008.

NINDS. Tissue plasminogen activator for acute ischemic stroke. The National Institute of Neurological Disorders and Stroke rt-PA Stroke Study Group. *N Engl J Med*, 333(24):1581–7, 1995.

Nishimura N, Rosidi NL, Iadecola C and Schaffer CB. Limitations of collateral flow after occlusion of a single cortical penetrating arteriole. *J Cereb Blood Flow Metab*, 30(12):1914–27, 2010.

Nishimura N, Schaffer CB, Friedman B, Lyden PD and Kleinfeld D. Penetrating arterioles are a bottleneck in the perfusion of neocortex. *Proc Natl Acad Sci U S A*, 104(1):365–70, 2007.

Noor R, Wang CX, Todd K, Elliott C, Wahr J and Shuaib A. Partial intra-aortic occlusion improves perfusion deficits and infarct size following focal cerebral ischemia. *J Neuroimaging*, 20(3):272–6, 2010.

O'Collins VE, Macleod MR, Donnan GA, Horky LL, van der Worp BH and Howells DW. 1,026 experimental treatments in acute stroke. *Ann Neurol*, 59(3):467–77, 2006.

O'Donnell MJ, Xavier D, Liu L, Zhang H, Chin SL, Rao-Melacini P, Rangarajan S, Islam S, Pais P, McQueen MJ, Mondo C, Damasceno A, Lopez-Jaramillo P, Hankey GJ, Dans AL, Yusoff K, Truelsen T, Diener HC, Sacco RL, Ryglewicz D, Czlonkowska A, Weimar C, Wang X, Yusuf S and investigators I. Risk factors for ischaemic and intracerebral haemorrhagic stroke in 22 countries (the INTERSTROKE study): a case-control study. *Lancet*, 376(9735):112–23, 2010.

Ogasawara K, Ogawa A and Yoshimoto T. Cerebrovascular reactivity to acetazolamide and outcome in patients with symptomatic internal carotid or middle cerebral artery occlusion: a xenon-133 single-photon emission computed tomography study. *Stroke*, 33(7):1857–62, 2002.

Oliff HS, Coyle P and Weber E. Rat strain and vendor differences in collateral anastomoses. *J Cereb Blood Flow Metab*, 17(5):571–6, 1997.

Oliff HS, Marek P, Miyazaki B and Weber E. The neuroprotective efficacy of MK-801 in focal cerebral ischemia varies with rat strain and vendor. *Brain Res*, 731(1-2):208–12, 1996.

Olivot JM, Mlynash M, Thijs VN, Purushotham A, Kemp S, Lansberg MG, Wechsler L, Gold GE, Bammer R, Marks MP and Albers GW. Geography, structure, and evolution of diffusion and perfusion lesions in Diffusion and perfusion imaging Evaluation For Understanding Stroke Evolution (DEFUSE). *Stroke*, 40(10):3245–51, 2009.

Omura-Matsuoka E, Yagita Y, Sasaki T, Terasaki Y, Oyama N, Sugiyama Y, Todo K, Sakoda S and Kitagawa K. Hypertension impairs leptomeningeal collateral growth after common carotid artery occlusion: restoration by antihypertensive treatment. *J Neurosci Res*, 89(1):108–16, 2011.

Orset C, Macrez R, Young AR, Panthou D, Angles-Cano E, Maubert E, Agin V and Vivien D. Mouse model of in situ thromboembolic stroke and reperfusion. *Stroke*, 38(10):2771–8, 2007.

Ostergaard L, Weisskoff RM, Chesler DA, Gyldensted C and Rosen BR. High resolution measurement of cerebral blood flow using intravascular tracer bolus passages. Part I: Mathematical approach and statistical analysis. *Magn Reson Med*, 36(5):715–25, 1996.

Ovbiagele B, Saver JL, Starkman S, Kim D, Ali LK, Jahan R, Duckwiler GR, Viñuela F, Pineda S and Liebeskind DS. Statin enhancement of collateralization in acute stroke. *Neurology*, 68(24):2129–31, 2007.

Park HP, Nimmagadda A, DeFazio RA, Busto R, Prado R and Ginsberg MD. Albumin therapy augments the effect of thrombolysis on local vascular dynamics in a rat model of arteriolar thrombosis: a two-photon laser-scanning microscopy study. *Stroke*, 39(5):1556–62, 2008.

Parsons MW, Miteff F, Bateman GA, Spratt N, Loiselle A, Attia J and Levi CR. Acute ischemic stroke: imaging-guided tenecteplase treatment in an extended time window. *Neurology*, 72(10):915–21, 2009.

Parthasarathy AB, Tom WJ, Gopal A, Zhang X and Dunn AK. Robust flow measurement with multi-exposure speckle imaging. *Opt Express*, 16(3):1975–89, 2008.

Paxinos G and Watson C. The Rat Brain in Stereotaxic Coordinates. 6th ed. Academic Press. San Diego, 2007.

Powers WJ, Derdeyn CP, Biller J, Coffey CS, Hoh BL, Jauch EC, Johnston KC, Johnston SC, Khalessi AA, Kidwell CS, Meschia JF, Ovbiagele B, Yavagal DR and Council AHAS. 2015 American Heart Association/American Stroke Association Focused Update of the 2013 Guidelines for the Early Management of Patients With Acute Ischemic Stroke Regarding Endovascular Treatment: A Guideline for Healthcare Professionals From the American Heart Association/American Stroke Association. *Stroke*, 46(10):3020–35, 2015.

Prado R, Ginsberg MD, Dietrich WD, Watson BD and Busto R. Hyperglycemia increases infarct size in collaterally perfused but not end-arterial vascular territories. *J Cereb Blood Flow Metab*, 8(2):186–92, 1988.

Qureshi AI, El-Gengaihi A, Hussein HM, Suri MF and Liebeskind DS. Occurence and variability in acute formation of leptomeningeal collaterals in proximal middle cerebral artery occlusion. *J Vasc Interv Neurol*, 1(3):70–2, 2008.

Qureshi AI, Harris-Lane P, Kirmani JF, Janjua N, Divani AA, Mohammad YM, Suarez JI and Montgomery MO. Intra-arterial reteplase and intravenous abciximab in patients with acute ischemic stroke: an open-label, dose-ranging, phase I study. *Neurosurgery*, 59(4):789–96; discussion 796–7, 2006.

Qureshi AI, Pande RU, Kim SH, Hanel RA, Kirmani JF and Yahia AM. Third generation thrombolytics for the treatment of ischemic stroke. *Curr Opin Investig Drugs*, 3(12):1729–32, 2002.

Rajdev S, Hara K, Kokubo Y, Mestril R, Dillmann W, Weinstein PR and Sharp FR. Mice overexpressing rat heat shock protein 70 are protected against cerebral infarction. *Ann Neurol*, 47(6):782–91, 2000.

Regli F, Yamaguchi T and Waltz AG. Effects of acetazolamide on cerebral ischemia and infarction after experimental occlusion of middle cerebral artery. *Stroke*, 2(5):456–60, 1971.

Reid E, Graham D, Lopez-Gonzalez MR, Holmes WM, Macrae IM and McCabe C. Penumbra detection using PWI/DWI mismatch MRI in a rat stroke model with and without comorbidity: comparison of methods. *J Cereb Blood Flow Metab*, 32(9):1765–77, 2012.

Ribo M, Flores A, Rubiera M, Pagola J, Sargento-Freitas J, Rodriguez-Luna D, Coscojuela P, Maisterra O, Piñeiro S, Romero FJ, Alvarez-Sabin J and Molina CA. Extending the time window for endovascular procedures according to collateral pial circulation. *Stroke*, 42(12):3465–9, 2011.

Riva M, Pappadà GB, Papadakis M, Cuccione E, Carone D, Menendez VR, Sganzerla EP and Beretta S. Hemodynamic monitoring of intracranial collateral flow predicts tissue and functional outcome in experimental ischemic stroke. *Exp Neurol*, 233(2):815–20, 2012.

Robinson MJ, Macrae IM, Todd M, Reid JL and McCulloch J. Reduction of local cerebral blood flow to pathological levels by endothelin-1 applied to the middle cerebral artery in the rat. *Neurosci Lett*, 118(2):269–72, 1990.

Robinson RG, Shoemaker WJ, Schlumpf M, Valk T and Bloom FE. Effect of experimental cerebral infarction in rat brain on catecholamines and behaviour. *Nature*, 255(5506):332–4, 1975.

Rordorf G, Koroshetz WJ, Ezzeddine MA, Segal AZ and Buonanno FS. A pilot study of drug-induced hypertension for treatment of acute stroke. *Neurology*, 56(9):1210–3, 2001.

Sakoh M, Ostergaard L, RÃ¸hl L, Smith DF, Simonsen CZ, SÃ¸rensen JC, Poulsen PV, Gyldensted C, Sakaki S and Gjedde A. Relationship between residual cerebral blood flow and oxygen metabolism as predictive of ischemic tissue viability: sequential multitracer positron emission tomography scanning of middle cerebral artery occlusion during the critical first 6 hours after stroke in pigs. *J Neurosurg*, 93(4):647–57, 2000.

Sanossian N, Saver JL, Alger JR, Kim D, Duckwiler GR, Jahan R, Vinuela F, Ovbiagele B and Liebeskind DS. Angiography reveals that fluid-attenuated inversion recovery vascular hyperintensities are due to slow flow, not thrombus. *AJNR Am J Neuroradiol*, 30(3):564–8, 2009.

Sargento-Freitas J, Pagola J, Rubiera M, Flores A, Silva F, Rodriguez-Luna D, Pineiro S, Alvarez-Sabín J, Molina CA and Ribo M. Preferential effect of premorbid statins on atherothrombotic strokes through collateral circulation enhancement. *Eur Neurol*, 68(3):171–6, 2012.

Saver JL, Gornbein J, Grotta J, Liebeskind D, Lutsep H, Schwamm L, Scott P and Starkman S. Number needed to treat to benefit and to harm for intravenous tissue plasminogen activator therapy in the 3- to 4.5-hour window: joint outcome table analysis of the ECASS 3 trial. *Stroke*, 40(7):2433–7, 2009.

Saver JL, Smith EE, Fonarow GC, Reeves MJ, Zhao X, Olson DM, Schwamm LH and Investigators GSSCa. The "golden hour" and acute brain ischemia: presenting features and lytic therapy in ¿30,000 patients arriving within 60 minutes of stroke onset. *Stroke*, 41(7):1431–9, 2010.

Schaefer PW, Barak ER, Kamalian S, Gharai LR, Schwamm L, Gonzalez RG and Lev MH. Quantitative assessment of core/penumbra mismatch in acute stroke: CT and MR perfusion imaging are strongly correlated when sufficient brain volume is imaged. *Stroke*, 39(11):2986–92, 2008.

Schaffer CB, Friedman B, Nishimura N, Schroeder LF, Tsai PS, Ebner FF, Lyden PD and Kleinfeld D. Two-photon imaging of cortical surface microvessels reveals a robust redistribution in blood flow after vascular occlusion. *PLoS Biol*, 4(2):e22, 2006.

Schallert T. Behavioral tests for preclinical intervention assessment. *NeuroRx*, 3(4):497–504, 2006.

Schallert T, Upchurch M, Lobaugh N, Farrar SB, Spirduso WW, Gilliam P, Vaughn D and Wilcox RE. Tactile extinction: distinguishing between sensorimotor and motor asymmetries in rats with unilateral nigrostriatal damage. *Pharmacol Biochem Behav*, 16(3):455–62, 1982.

Schallert T, Upchurch M, Wilcox RE and Vaughn DM. Posture-independent sensorimotor analysis of inter-hemispheric receptor asymmetries in neostriatum. *Pharmacol Biochem Behav*, 18(5):753–9, 1983.

Schellinger PD, Fiebach JB and Hacke W. Imaging-based decision making in thrombolytic therapy for ischemic stroke: present status. *Stroke*, 34(2):575–83, 2003.

Schirmer SH, van Royen N, Moerland PD, Fledderus JO, Henriques JP, van der Schaaf RJ, Vis MM, Baan J, Koch KT, Horrevoets AJ, Hoefer IE and Piek JJ. Local cytokine concentrations and oxygen pressure are related to maturation of the collateral circulation in humans. *J Am Coll Cardiol*, 53(23):2141–7, 2009.

Schlaug G, Benfield A, Baird AE, Siewert B, Lövblad KO, Parker RA, Edelman RR and Warach S. The ischemic penumbra: operationally defined by diffusion and perfusion MRI. *Neurology*, 53(7):1528–37, 1999.

Schmid-Elsaesser R, Zausinger S, Hungerhuber E, Baethmann A and Reulen HJ. A critical reevaluation of the intraluminal thread model of focal cerebral ischemia: evidence of inadvertent premature reperfusion and subarachnoid hemorrhage in rats by laser-Doppler flowmetry. *Stroke*, 29(10):2162–70, 1998a.

Schmid-Elsaesser R, Zausinger S, Hungerhuber E, Baethmann A and Reulen HJ. A critical reevaluation of the intraluminal thread model of focal cerebral ischemia: evidence of inadvertent premature reperfusion and subarachnoid hemorrhage in rats by laser-Doppler flowmetry. *Stroke*, 29(10):2162–70, 1998b.

Schneider UC, Schilling L, Schroeck H, Nebe CT, Vajkoczy P and Woitzik J. Granulocyte-macrophage colony-stimulating factor-induced vessel growth restores cerebral blood supply after bilateral carotid artery occlusion. *Stroke*, 38(4):1320–8, 2007.

Schwarz S, Georgiadis D, Aschoff A and Schwab S. Effects of body position on intracranial pressure and cerebral perfusion in patients with large hemispheric stroke. *Stroke*, 33(2):497–501, 2002.

Scremin OU. Cerebral Vascular System, 1165–93. 3rd ed. In Paxinos, G. (Ed.), The Rat Nervous System. Elsevier Academic Press. London, 2004.

Shapira S, Sapir M, Wengier A, Grauer E and Kadar T. Aging has a complex effect on a rat model of ischemic stroke. *Brain Res*, 925(2):148–58, 2002.

Sharp FR, Lu A, Tang Y and Millhorn DE. Multiple molecular penumbras after focal cerebral ischemia. *J Cereb Blood Flow Metab*, 20(7):1011–32, 2000.

Sharp FR, Zhan X and Liu DZ. Heat shock proteins in the brain: role of Hsp70, Hsp 27, and HO-1 (Hsp32) and their therapeutic potential. *Transl Stroke Res*, 4(6):685–92, 2013.

Shen F, Fan Y, Su H, Zhu Y, Chen Y, Liu W, Young WL and Yang GY. Adeno-associated viral vector-mediated hypoxia-regulated VEGF gene transfer promotes angiogenesis following focal cerebral ischemia in mice. *Gene Ther*, 15(1):30–9, 2008.

Shen Q, Meng X, Fisher M, Sotak CH and Duong TQ. Pixel-by-pixel spatiotemporal progression of focal ischemia derived using quantitative perfusion and diffusion imaging. *J Cereb Blood Flow Metab*, 23(12):1479–88, 2003.

Sheperd AP and Öberg PA. Laser-Doppler Blood Flowmetry., 1990.

Shigeno T, Teasdale GM, McCulloch J and Graham DI. Recirculation model following MCA occlusion in rats. Cerebral blood flow, cerebrovascular permeability, and brain edema. *J Neurosurg*, 63(2):272–7, 1985.

Shih AY, Friedman B, Drew PJ, Tsai PS, Lyden PD and Kleinfeld D. Active dilation of penetrating arterioles restores red blood cell flux to penumbral neocortex after focal stroke. *J Cereb Blood Flow Metab*, 29(4):738–51, 2009.

Shin HK, Nishimura M, Jones PB, Ay H, Boas DA, Moskowitz MA and Ayata C. Mild induced hypertension improves blood flow and oxygen metabolism in transient focal cerebral ischemia. *Stroke*, 39(5):1548–55, 2008.

Shuaib A, Bornstein NM, Diener HC, Dillon W, Fisher M, Hammer MD, Molina CA, Rutledge JN, Saver JL, Schellinger PD, Shownkeen H and Investigators ST. Partial aortic occlusion for cerebral perfusion augmentation: safety and efficacy of NeuroFlo in Acute Ischemic Stroke trial. *Stroke*, 42(6):1680–90, 2011a.

Shuaib A, Butcher K, Mohammad AA, Saqqur M and Liebeskind DS. Collateral blood vessels in acute ischaemic stroke: a potential therapeutic target. *Lancet Neurol*, 10(10):909–21, 2011b.

Sleight P. Reflex control of the heart. *Am J Cardiol*, 44(5):889–94, 1979.

Smit EJ, Vonken EJ, van Seeters T, Dankbaar JW, van der Schaaf IC, Kappelle LJ, van Ginneken B, Velthuis BK and Prokop M. Timing-invariant imaging of collateral vessels in acute ischemic stroke. *Stroke*, 44(8):2194–9, 2013.

Solomon RA, Antunes JL, Chen RY, Bland L and Chien S. Decrease in cerebral blood flow in rats after experimental subarachnoid hemorrhage: a new animal model. *Stroke*, 16(1):58–64, 1985.

STAIRs. Stroke Therapy Academic Industry Roundtable. Recommendations for standards regarding preclinical neuroprotective and restorative drug development. *Stroke*, 30(12):2752–8, 1999.

Straka M, Albers GW and Bammer R. Real-time diffusion-perfusion mismatch analysis in acute stroke. *J Magn Reson Imaging*, 32(5):1024–37, 2010.

Stroke-Trials-Registry. Dallas: UT Southwestern Medical Center, 1997. Available at: `http://www.strokecenter.org/trials/`. Accessed August, 2015.

Ström JO, Ingberg E, Theodorsson A and Theodorsson E. Method parameters' impact on mortality and variability in rat stroke experiments: a meta-analysis. *BMC Neurosci*, 14:41, 2013.

Strong AJ, Bezzina EL, Anderson PJ, Boutelle MG, Hopwood SE and Dunn AK. Evaluation of laser speckle flowmetry for imaging cortical perfusion in experimental stroke studies: quantitation of perfusion and detection of peri-infarct depolarisations. *J Cereb Blood Flow Metab*, 26(5):645–53, 2006.

Sughrue ME, Mocco J, Komotar RJ, Mehra A, D'Ambrosio AL, Grobelny BT, Penn DL and Connolly ES. An improved test of neurological dysfunction following transient focal cerebral ischemia in rats. *J Neurosci Methods*, 151(2):83–9, 2006.

Sugiyama Y, Yagita Y, Oyama N, Terasaki Y, Omura-Matsuoka E, Sasaki T and Kitagawa K. Granulocyte colony-stimulating factor enhances arteriogenesis and ameliorates cerebral damage in a mouse model of ischemic stroke. *Stroke*, 42(3):770–5, 2011.

Sullivan HG, Kingsbury TB, Morgan ME, Jeffcoat RD, Allison JD, Goode JJ and McDonnell DE. The rCBF response to Diamox in normal subjects and cerebrovascular disease patients. *J Neurosurg*, 67(4):525–34, 1987.

Sutherland BA, Minnerup J, Balami JS, Arba F, Buchan AM and Kleinschnitz C. Neuroprotection for ischaemic stroke: translation from the bench to the bedside. *Int J Stroke*, 7(5):407–18, 2012.

Sutherland BA, Papadakis M, Chen RL and Buchan AM. Cerebral blood flow alteration in neuroprotection following cerebral ischaemia. *J Physiol*, 589(Pt 17):4105–14, 2011.

Swanson RA, Morton MT, Tsao-Wu G, Savalos RA, Davidson C and Sharp FR. A semiautomated method for measuring brain infarct volume. *J Cereb Blood Flow Metab*, 10(2):290–3, 1990.

Symon L, Branston NM, Strong AJ and Hope TD. The concepts of thresholds of ischaemia in relation to brain structure and function. *J Clin Pathol Suppl (R Coll Pathol)*, 11:149–54, 1977.

Takasawa M, Beech JS, Fryer TD, Hong YT, Hughes JL, Igase K, Jones PS, Smith R, Aigbirhio FI, Menon DK, Clark JC and Baron JC. Imaging of brain hypoxia in permanent and temporary middle cerebral artery occlusion in the rat using 18F-fluoromisonidazole and positron emission tomography: a pilot study. *J Cereb Blood Flow Metab*, 27(4):679–89, 2007.

Tamaki M, Kidoguchi K, Mizobe T, Koyama J, Kondoh T, Sakurai T, Kohmura E, Yokono K and Umetani K. Carotid artery occlusion and collateral circulation in C57Black/6J mice detected by synchrotron radiation microangiography. *Kobe J Med Sci*, 52(5):111–8, 2006.

Tamura A, Graham DI, McCulloch J and Teasdale GM. Focal cerebral ischaemia in the rat: 1. Description of technique and early neuropathological consequences following middle cerebral artery occlusion. *J Cereb Blood Flow Metab*, 1(1):53–60, 1981.

Tan IY, Demchuk AM, Hopyan J, Zhang L, Gladstone D, Wong K, Martin M, Symons SP, Fox AJ and Aviv RI. CT angiography clot burden score and collateral score: correlation with clinical and radiologic outcomes in acute middle cerebral artery infarct. *AJNR Am J Neuroradiol*, 30(3):525–31, 2009.

Taninishi H, Jung JY, Izutsu M, Wang Z, Sheng H and Warner DS. A blinded randomized assessment of laser Doppler flowmetry efficacy in standardizing outcome from intraluminal filament MCAO in the rat. *J Neurosci Methods*, 241:111–20, 2015.

Terpolilli NA, Kim SW, Thal SC, Kataoka H, Zeisig V, Nitzsche B, Klaesner B, Zhu C, Schwarzmaier S, Meissner L, Mamrak U, Engel DC, Drzezga A, Patel RP, Blomgren K, Barthel H, Boltze J, Kuebler WM and Plesnila N. Inhalation of nitric oxide prevents ischemic brain damage in experimental stroke by selective dilatation of collateral arterioles. *Circ Res*, 110(5):727–38, 2012a.

Terpolilli NA, Moskowitz MA and Plesnila N. Nitric oxide: considerations for the treatment of ischemic stroke. *J Cereb Blood Flow Metab*, 32(7):1332–46, 2012b.

Thrift AG, Donnan GA and McNeil JJ. Epidemiology of intracerebral hemorrhage. *Epidemiol Rev*, 17(2):361–81, 1995.

Todo K, Kitagawa K, Sasaki T, Omura-Matsuoka E, Terasaki Y, Oyama N, Yagita Y and Hori M. Granulocyte-macrophage colony-stimulating factor enhances leptomeningeal collateral growth induced by common carotid artery occlusion. *Stroke*, 39(6):1875–82, 2008.

Troidl K and Schaper W. Arteriogenesis versus angiogenesis in peripheral artery disease. *Diabetes Metab Res Rev*, 28 Suppl 1:27–9, 2012.

Tudela R, Soria G, Pérez-De-Puig I, Ros D, Pavía J and Planas A. Infarct volume prediction using apparent diffusion coefficient maps during middle cerebral artery occlusion and soon after reperfusion in the rat. *Brain Res*, 1583:169–78, 2014.

Türeyen K, Vemuganti R, Sailor KA and Dempsey RJ. Ideal suture diameter is critical for consistent middle cerebral artery occlusion in mice. *Neurosurgery*, 56(1 Suppl):196–200; discussion 196–200, 2005.

van Laar PJ, Hendrikse J, Klijn CJ, Kappelle LJ, van Osch MJ and van der Grond J. Symptomatic carotid artery occlusion: flow territories of major brain-feeding arteries. *Radiology*, 242(2):526–34, 2007.

VANDER EECKEN HM. [Morphological significance of leptomeningeal anastomoses confined to the territory of cerebral arteries]. *Acta Neurol Psychiatr Belg*, 54(7):525–32, 1954.

Wang RY, Wang PS and Yang YR. Effect of age in rats following middle cerebral artery occlusion. *Gerontology*, 49(1):27–32, 2003.

Wang Z, Luo W, Zhou F, Li P and Luo Q. Dynamic change of collateral flow varying with distribution of regional blood flow in acute ischemic rat cortex. *J Biomed Opt*, 17(12):125001, 2012.

Warlow C, Sudlow C, Dennis M, Wardlaw J and Sandercock P. Stroke. *Lancet*, 362(9391):1211–24, 2003.

Watson BD, Dietrich WD, Busto R, Wachtel MS and Ginsberg MD. Induction of reproducible brain infarction by photochemically initiated thrombosis. *Ann Neurol*, 17(5):497–504, 1985.

Wei L, Erinjeri JP, Rovainen CM and Woolsey TA. Collateral growth and angiogenesis around cortical stroke. *Stroke*, 32(9):2179–84, 2001.

Weinstein PR, Hong S and Sharp FR. Molecular identification of the ischemic penumbra. *Stroke*, 35(11 Suppl 1):2666–70, 2004.

Weishaupt D, Köchli VD and Marincek B. How does MRI work?: an introduction to the physics and function of magnetic resonance imaging. Springer Science & Business Media, 2008.

Wessels T, Bozzato A, Mull M and Klötzsch C. Intracranial collateral pathways assessed by contrast-enhanced three-dimensional transcranial color-coded sonography. *Ultrasound Med Biol*, 30(11):1435–40, 2004.

Wheeler HM, Mlynash M, Inoue M, Tipirneni A, Liggins J, Zaharchuk G, Straka M, Kemp S, Bammer R, Lansberg MG, Albers GW and Investigators D. Early diffusion-weighted imaging and perfusion-weighted imaging lesion volumes forecast final infarct size in DEFUSE 2. *Stroke*, 44(3):681–5, 2013.

Willats L and Calamante F. The 39 steps: evading error and deciphering the secrets for accurate dynamic susceptibility contrast MRI. *NMR Biomed*, 26(8):913–31, 2013.

Winship IR, Armitage GA, Ramakrishnan G, Dong B, Todd KG and Shuaib A. Augmenting collateral blood flow during ischemic stroke via transient aortic occlusion. *J Cereb Blood Flow Metab*, 34(1):61–71, 2014.

Wintermark M, Flanders AE, Velthuis B, Meuli R, van Leeuwen M, Goldsher D, Pineda C, Serena J, van der Schaaf I, Waaijer A, Anderson J, Nesbit G, Gabriely I, Medina V, Quiles A, Pohlman S, Quist M, Schnyder P, Bogousslavsky J, Dillon WP and Pedraza S. Perfusion-CT assessment of infarct core and penumbra: receiver operating characteristic curve analysis in 130 patients suspected of acute hemispheric stroke. *Stroke*, 37(4):979–85, 2006.

Woitzik J and Schilling L. Control of completeness and immediate detection of bleeding by a single laser-Doppler flow probe during intravascular middle cerebral artery occlusion in rats. *J Neurosci Methods*, 122(1):75–8, 2002.

Wojner AW, El-Mitwalli A and Alexandrov AV. Effect of head positioning on intracranial blood flow velocities in acute ischemic stroke: a pilot study. *Crit Care Nurs Q*, 24(4):57–66, 2002.

Wojner-Alexander AW, Garami Z, Chernyshev OY and Alexandrov AV. Heads down: flat positioning improves blood flow velocity in acute ischemic stroke. *Neurology*, 64(8):1354–7, 2005.

Wu B, Wang X, Guo J, Xie S, Wong EC, Zhang J, Jiang X and Fang J. Collateral circulation imaging: MR perfusion territory arterial spin-labeling at 3T. *AJNR Am J Neuroradiol*, 29(10):1855–60, 2008.

Yamauchi H, Fukuyama H, Nagahama Y, Nabatame H, Nakamura K, Yamamoto Y, Yonekura Y, Konishi J and Kimura J. Evidence of misery perfusion and risk for recurrent stroke in major cerebral arterial occlusive diseases from PET. *J Neurol Neurosurg Psychiatry*, 61(1):18–25, 1996.

Yanagisawa M, Kurihara H, Kimura S, Goto K and Masaki T. A novel peptide vasoconstrictor, endothelin, is produced by vascular endothelium and modulates smooth muscle Ca2+ channels. *J Hypertens Suppl*, 6(4):S188–91, 1988.

Yoneda Y, Tokui K, Hanihara T, Kitagaki H, Tabuchi M and Mori E. Diffusion-weighted magnetic resonance imaging: detection of ischemic injury 39 minutes after onset in a stroke patient. *Ann Neurol*, 45(6):794–7, 1999.

Zacharek A, Chen J, Cui X, Yang Y and Chopp M. Simvastatin increases notch signaling activity and promotes arteriogenesis after stroke. *Stroke*, 40(1):254–60, 2009.

Zaro-Weber O, Moeller-Hartmann W, Heiss WD and Sobesky J. The performance of MRI-based cerebral blood flow measurements in acute and subacute stroke compared with 15O-water positron emission tomography: identification of penumbral flow. *Stroke*, 40(7):2413–21, 2009.

Zarow GJ, Karibe H, States BA, Graham SH and Weinstein PR. Endovascular suture occlusion of the middle cerebral artery in rats: effect of suture insertion distance on cerebral blood flow, infarct distribution and infarct volume. *Neurol Res*, 19(4):409–16, 1997.

Zhan X, Kim C and Sharp FR. Very brief focal ischemia simulating transient ischemic attacks (TIAs) can injure brain and induce Hsp70 protein. *Brain Res*, 1234:183–97, 2008.

Zhang H, Prabhakar P, Sealock R and Faber JE. Wide genetic variation in the native pial collateral circulation is a major determinant of variation in severity of stroke. *J Cereb Blood Flow Metab*, 30(5):923–34, 2010.

Zhang L, Zhang RL, Wang Y, Zhang C, Zhang ZG, Meng H and Chopp M. Functional recovery in aged and young rats after embolic stroke: treatment with a phosphodiesterase type 5 inhibitor. *Stroke*, 36(4):847–52, 2005.

Zhang Z, Zhang RL, Jiang Q, Raman SB, Cantwell L and Chopp M. A new rat model of thrombotic focal cerebral ischemia. *J Cereb Blood Flow Metab*, 17(2):123–35, 1997.

Zhao H, Mayhan WG and Sun H. A modified suture technique produces consistent cerebral infarction in rats. *Brain Res*, 1246:158–66, 2008.

Zülch K. Cerebrovascular pathology and pathogenesis as a basis of neuroradiological diagnosis. *Handbuch der medizinischen Radiologie*, 14:1–192, 1981.

Publications and Communications

Publications:

• *PhD period*

Cuccione E, Padovano G, Versace A, Ferrarese C, Beretta S. Cerebral collateral circulation in experimental ischemic stroke. Review. *Exp Transl Stroke Med*, *in press*.

Beretta S*, **Cuccione E***, Versace A, Carone D, Riva M, Padovano G, Dell'Era V, Cai R, Monza L, Presotto L, Rousseau D, Chauveau F, Paternò G, Pappadà GB, Giussani C, Sganzerla EP, Ferrarese C. Cerebral collateral flow defines topography and evolution of molecular penumbra in experimental ischemic stroke. *Neurobiol Dis* 2015 Feb;74:305-13. * These authors equally contributed to this work.

Beretta S, Riva M, Carone D, **Cuccione E**, Padovano G, Rodriguez Menendez V, Pappadá GB, Versace A, Giussani C, Sganzerla EP, Ferrarese C. Optimized system for cerebral perfusion monitoring in the rat stroke model of intraluminal middle cerebral artery occlusion. *J Vis Exp* 2013 Feb 17;(72).

• *Previous*

Riva M, Pappadà GB, Papadakis M, **Cuccione E**, Carone D, Menendez VR, Sganzerla EP, Beretta S. Hemodynamic monitoring of intracranial collateral flow predicts tissue and functional outcome in experimental ischemic stroke. *Exp Neurol* 2012 Feb;233(2):815-20.

• *Other publications*

Carone D, Librizzi L, Cattalini A, Sala G, Conti E, **Cuccione E**, Versace A, Cai R, Monza L, de Curtis M, Ferrarese C, Beretta S. Pravastatin acute neuroprotective effects depend on blood brain barrier integrity in experimental cerebral ischemia. *Brain Res* 2015 Jul 30;1615:31-41.

Communications:

• *PhD period*

Beretta S, **Cuccione E**, Versace A, Carone D, Riva M, Padovano G, Dell'Era V, Cai R, Monza L, Presotto L, Rousseau D, Chauveau F, Giussani C, Sganzerla EP, Ferrarese C. Cerebral collateral flow defines topography and evolution of molecular penumbra in experimental ischemic stroke. BIS 2014, Rome (Abstract, Poster). *Participation to the conference.*

Cuccione E, Beretta S, Padovano G, Versace A, Cai R, Dell'Era V, Rodriguez Menendez v, Riva M, Carone D, Ferrarese C. Topographical and morphological patterns of post reperfusion molecular penumbra. 8th International Symposium on Neuroprotection and Neurorepair 2014, Magdeburg (Abstract, Poster). *Participation to the conference.*

Beretta S, **Cuccione E**, Versace, A, Carone D, Riva M, Padovano, G, Dell'Era V, Cai R, Monza L, Presotto L, Rousseau D, Chauveau F, Giussani C, Sganzerla EP, Ferrarese C. Intracranial collateral flow defines the boundaries of molecular penumbra in experimental ischemic stroke. 8th International Symposium on Neuroprotection and Neurorepair 2014, Magdeburg (Abstract, Poster).

Carone D, Beretta S, **Cuccione E**, Versace A, Riva M, Padovano G, Dell'Era V, Cai R, Presotto L, Paternò G, Pappadà GB, Giussani C, Sganzerla EP, Ferrarese C. Therapeutic modulation of intracranial collateral flow improves outcome in experimental ischemic stroke. 8th International Symposium on Neuroprotection and Neurorepair 2014, Magdeburg (Abstract, Poster).

Beretta, S, Riva M, **Cuccione E**, Carone D, Padovano G, Versace A, Rodriguez Menendez V, Pappadà GB, Sganzerla EP, Papadakis M, Ferrarese C. Intracranial collateral flow in experimental ischemic stroke. From hemodynamic monitoring to collateral therapeutics. BIS 2012, Rome (Abstract, Oral Presentation).

• *Previous*

Beretta S, Riva M, Pappadà GB, Papadakis M, **Cuccione E**, Carone D, Rodriguez Menendez V, Sganzerla EP, Ferrarese C. Hemodynamic monitoring of intracranial collateral flow predicts tissue and functional outcome in experimental ischemic stroke. 7th International Symposium on Neuroprotection and Neurorepair 2012, Potsdam (Abstract, Oral Presentation).